REVISION SUMMARY

Section	Changes	Reason for Change
Part 2: Final Safety Analysis Report		
Tables 2.0-202 & 2.2-203	Revised table data, added % Difference column, deleted note (c)	EPRI 2013 GMM is current source for values
Figures 2.0-201 thru 2.0-204, 2.0-206, 2.0-207, 2.5.2-230 thru 2.5.2-258, 2.5.2-274 thru 2.5.2-320	Revised	EPRI 2013 GMM is current source for values
2.5.2.1.1.1.2, 2.5.2.2.4.3, 2.5.2.4.1, 2.5.2.4.5.1, 2.5.2.6.2	Changed reference from EPRI 2004 to EPRI 2013	EPRI 2013 GMM is current source
2.5.2.4.4	Revised to account for EPRI 2013	EPRI 2013 GMM is current source
2.5.2.4.5.1	Editorial	Changes for consistency
2.5.2.6.2, 2.5.2.6.2.2	Revised values throughout to reflect EPRI 2013 GMM	EPRI 2013 GMM is current source for values
2.5.2.6.2.2, 2.5.2.6.2.3	Revised to reflect inclusion of FWSC in calculation of V/H envelope	Reflect inclusion of FWSC in calculation of V/H envelope
Tables 2.5.2-216 thru 2.5.2-219, 2.5.2-221 thru 2.5.2-228	Revised table data	EPRI 2013 GMM is current source for values
2.5.4.5.1	Added information to describe the excavation	Revised response to RAI 03.07.01-7
2.5.4.7.4, 2.5.4.8.2, 2.5.4.10.3	Added description of input rock motions sources	EPRI 2013 GMM is current source
2.5.5.2.3.b, 2.5.5.2.4.b	Included EPRI 2013 in description and corrected description of maximum horizontal acceleration location in slope stability analysis discussion	EPRI 2013 GMM is current source and correction to text
Figure 2.5.4-250	Added note specifying source of input rock motions	EPRI 2013 GMM is current source
Section 2.5 References	Added references 2.5-407 thru 2.5-409	EPRI 2013 GMM is current source and NRC letter endorses use of 2013 GMM
3.7.1.1.4.1.1, 3.7.1.1.4.1.2	Clarified depth of soil column in several figures and updated values per EPRI 2013 GMM	EPRI 2013 GMM is current source

REVISION SUMMARY

Section	Changes	Reason for Change
3.7.1.1.4.2.1, 3.7.1.1.4.2.2, 3.7.1.1.5.1; Tables 3.7.1-201 thru 3.7.1-219	Updated values per EPRI 2013 GMM	EPRI 2013 GMM is current source for values
Figures 3.7.1-201 thru 3.7.1-294	Replaced	EPRI 2013 GMM is current source for figures
Part 7: Departures Report		
Variances, VAR 2.0-4	Revised Request	EPRI 2013 GMM is current source

NAPS COL 2.0-1-A
NAPS ESP VAR 2.0-4

Table 2.0-202 Comparison of the ESP Horizontal SSE Design Response Spectrum for the Top of Zone III-IV and Unit 3 Horizontal GMRS

Freq. (Hz)	GMRS SA[(a)] (g)	ESP SA[(b)] ~~(c)~~ (g)	Controlling ESP or GMRS ~~(c)~~	% Difference
100.00	0.551	0.555	ESP	-0.7
50.00	1.142	1.20	ESP	-4.4
30.00	1.192	1.47	ESP	-18.9
25.00	1.170	1.48	ESP	-20.7
20.00	1.146	1.45	ESP	-20.7
10.00	0.776	0.945	ESP	-17.9
8.00	0.629	0.717	ESP	-12.3
6.00	0.485	0.481	GMRS	0.8
5.00	0.413	0.376	GMRS	9.8
4.00	0.334	0.287	GMRS	16.5
3.00	0.252	0.214	GMRS	17.6
2.50	0.207	0.179	GMRS	15.7
2.00	0.171	0.142	GMRS	20.3
1.00	0.079	0.0677	GMRS	16.4
0.80	0.066	0.0576	GMRS	14.4
0.60	0.051	0.0488	GMRS	4.0
0.50	0.042	0.0429	ESP	-1.4
0.40	0.034	0.0343	ESP	-1.3
0.30	0.025	0.0233	GMRS	8.1
0.20	0.017	0.0130	GMRS	29.3
0.10	0.008	0.00382	GMRS	119.7

(a) Values from Table 2.5.2-228
(b) Values from SSAR Table 2.5-27A
~~(c) " " denotes not applicable: SA(g) value was not calculated for the ESPA SSAR~~

NAPS COL 2.0-1-A
NAPS ESP VAR 2.0-4

Table 2.0-203 Comparison of the ESP Vertical SSE Design Response Spectrum for the Top of Zone III-IV and Unit 3 Vertical GMRS

Freq. (Hz)	GMRS SA[(a)] (g)	ESP SA[(b)] ~~(c)~~ (g)	Controlling ESP or GMRS ~~(c)~~	% Difference
100.00	0.551	0.555	ESP	-0.7
50.00	1.316	1.33	ESP	-1.0
30.00	1.117	1.38	ESP	-19.1
25.00	1.030	1.29	ESP	-20.1
20.00	0.946	1.20	ESP	-21.1
10.00	0.582	0.708	ESP	-17.8
8.00	0.471	0.537	ESP	-12.2
6.00	0.364	0.360	GMRS	1.0
5.00	0.310	0.282	GMRS	9.8
4.00	0.251	0.215	GMRS	16.6
3.00	0.189	0.160	GMRS	18.0
2.50	0.155	0.134	GMRS	16.0
2.00	0.128	0.106	GMRS	20.9
1.00	0.059	0.0507	GMRS	16.5
0.80	0.049	0.0432	GMRS	14.4
0.60	0.038	0.0366	GMRS	4.0
0.50	0.032	0.0321	ESP	-1.1
0.40	0.025	0.0257	ESP	-1.2
0.30	0.019	0.0174	GMRS	8.5
0.20	0.013	0.00973	GMRS	29.4
0.10	0.006	0.00286	GMRS	120.1

(a) Values from Table 2.5.2-228
(b) Values from SSAR Table 2.5-27A
~~(c) " " denotes not applicable: SA(g) value was not calculated for the ESPA SSAR~~

NAPS COL 2.0-1-A
NAPS DEP 3.7-1

Figure 2.0-201 Comparison of Horizontal CSDRS with Unit 3 FIRS for RB/FB and CB

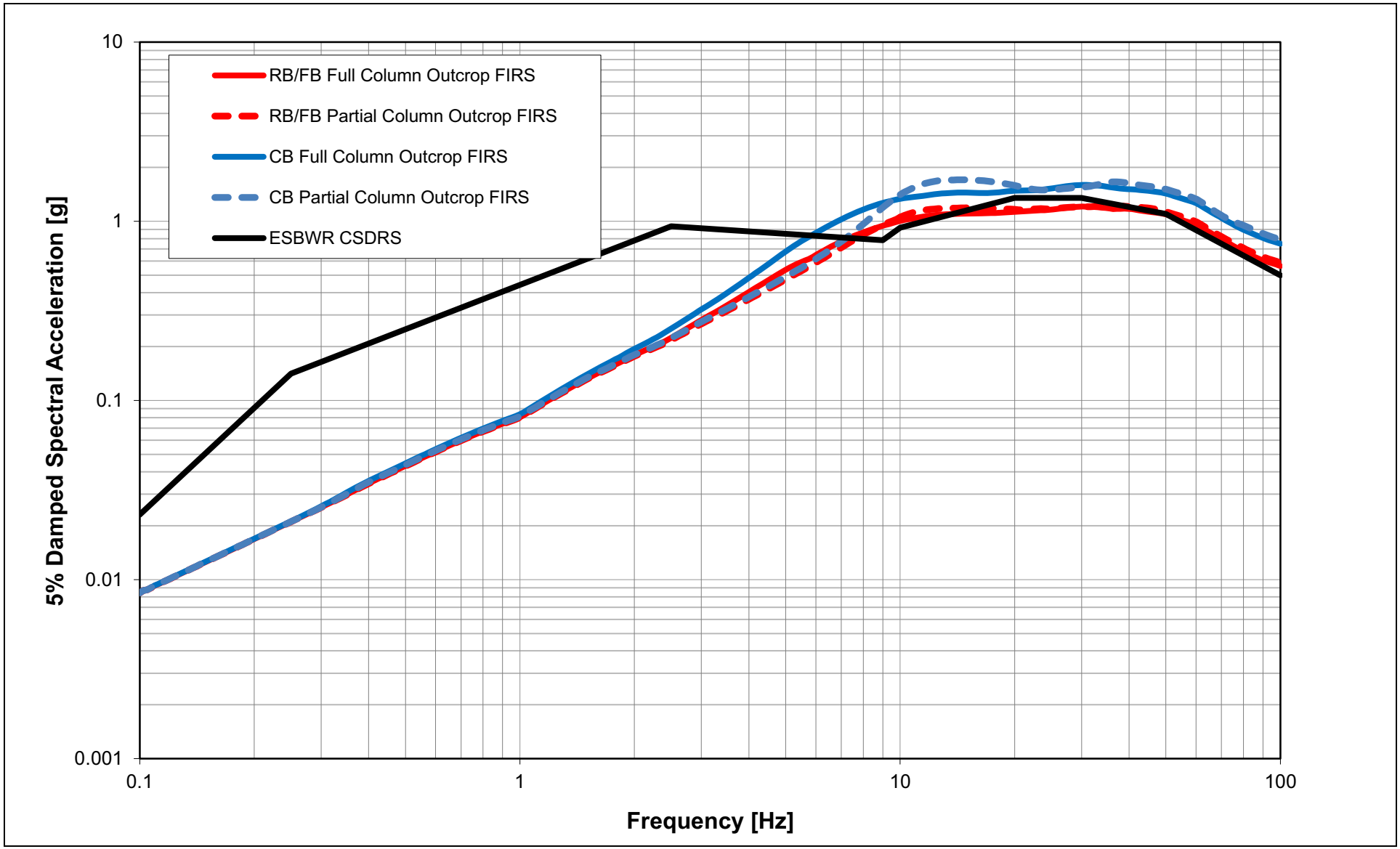

NAPS COL 2.0-1-A
NAPS DEP 3.7-1

Figure 2.0-202 Comparison of Vertical CSDRS with Unit 3 FIRS for RB/FB and CB

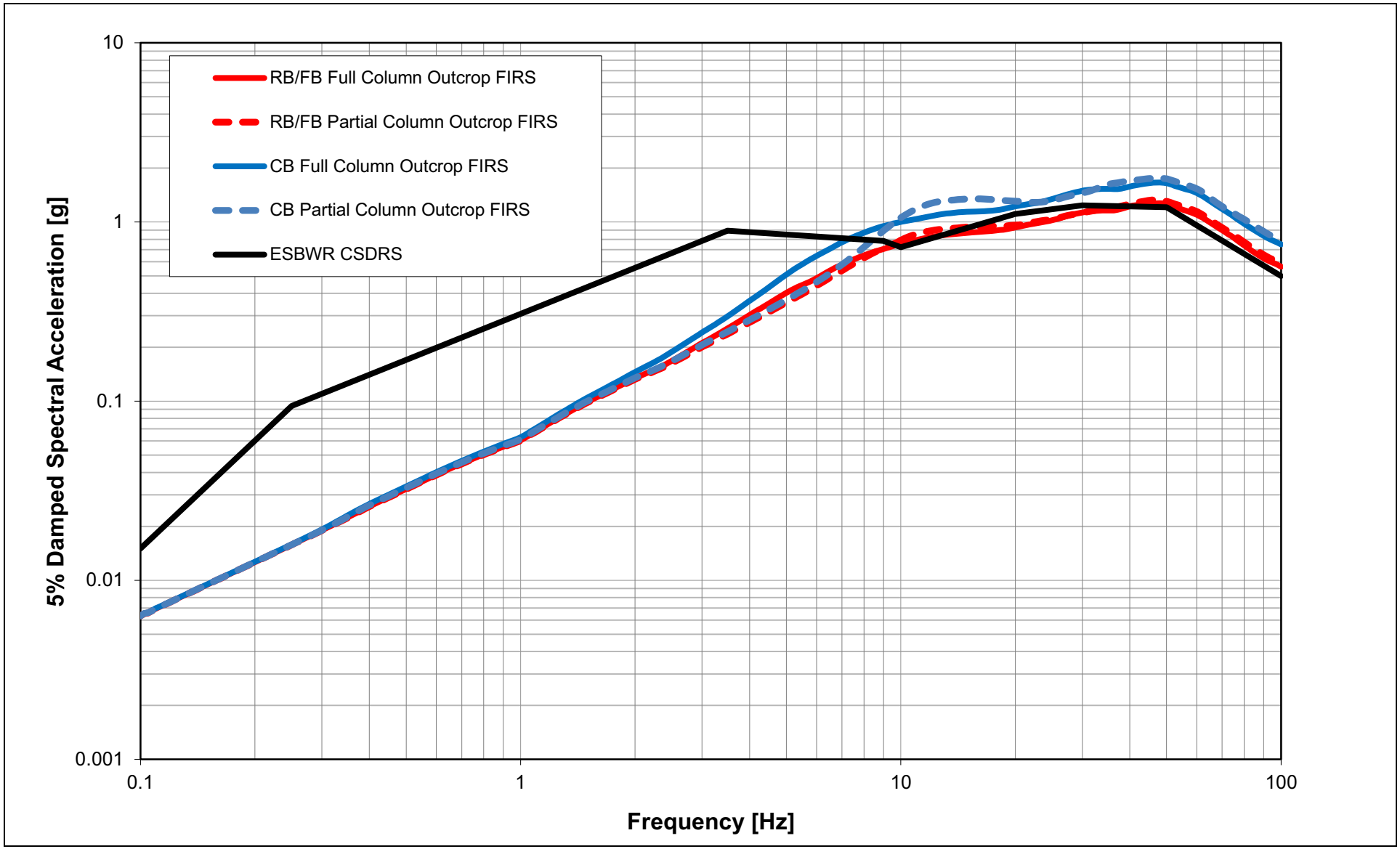

NAPS COL 2.0-1-A
NAPS DEP 3.7-1

Figure 2.0-203 Comparison of Horizontal CSDRS with Unit 3 FIRS for the FWSC

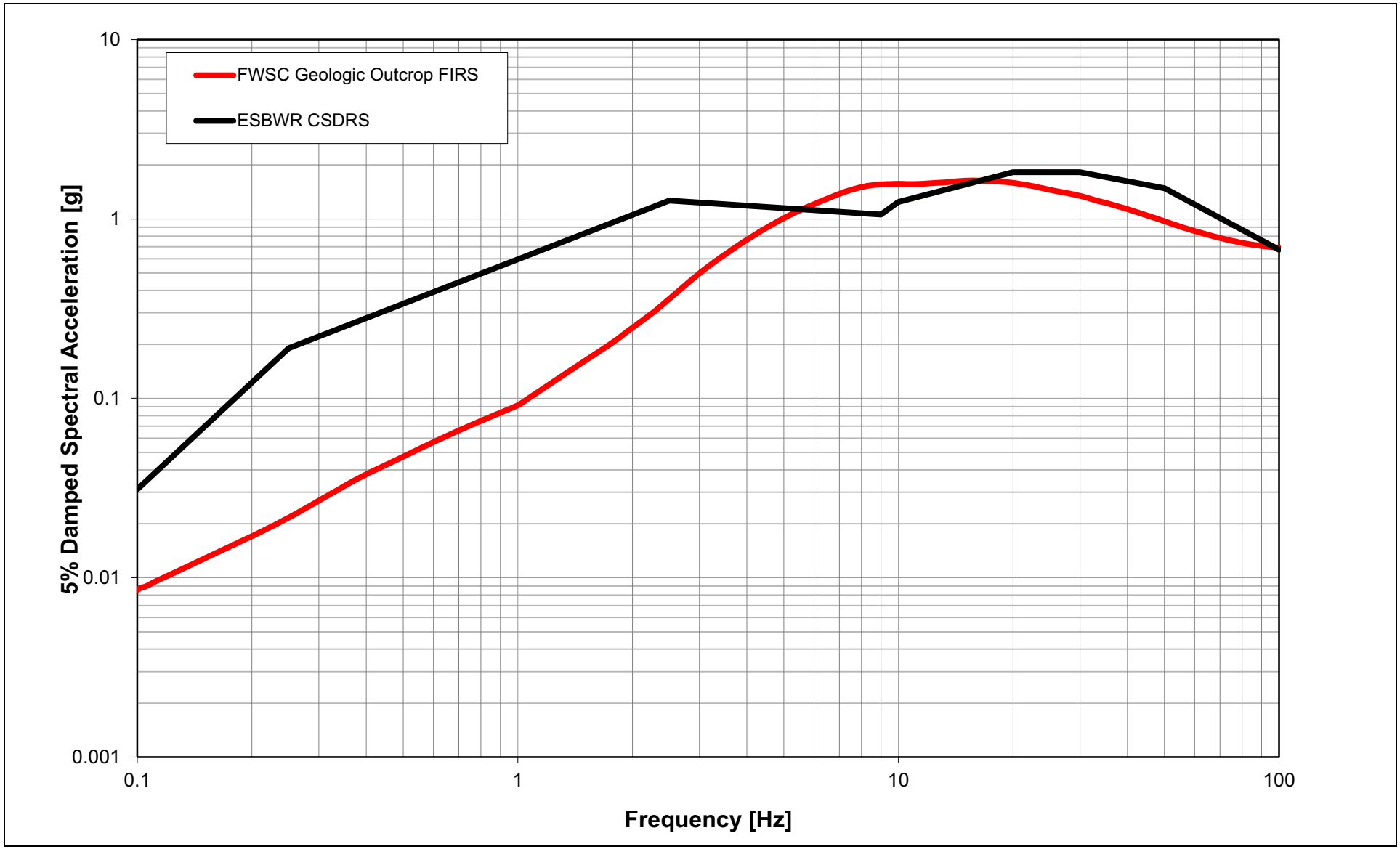

NAPS COL 2.0-1-A
NAPS DEP 3.7-1

Figure 2.0-204 Comparison of Vertical CSDRS with Unit 3 FIRS for the FWSC

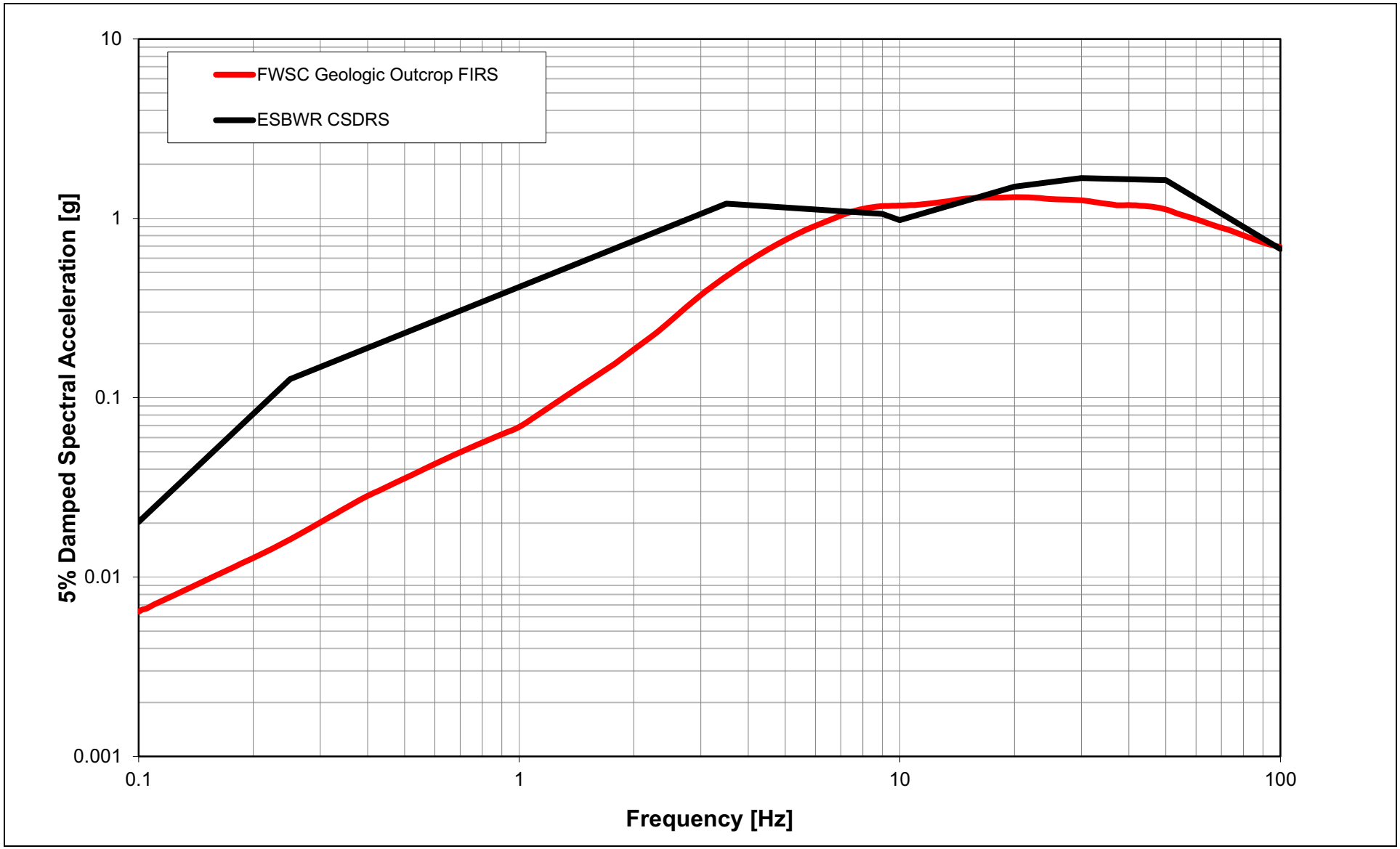

NAPS COL 2.0-1-A
NAPS ESP VAR 2.0-4

Figure 2.0-206 Comparison of the ESP Horizontal SSE Design Response Spectrum for the Top of Zone III-IV and Unit 3 Horizontal GMRS

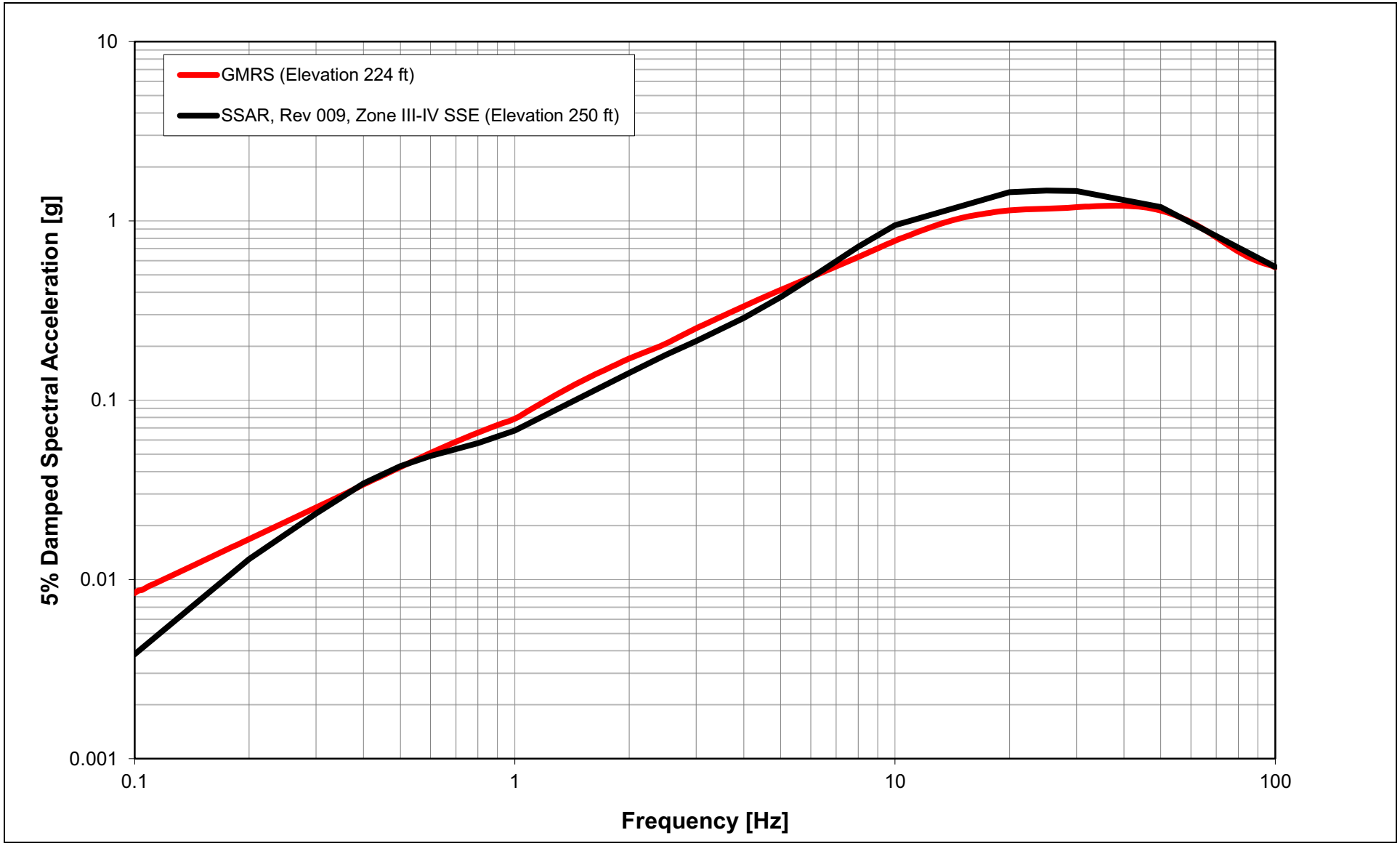

NAPS COL 2.0-1-A
NAPS ESP VAR 2.0-4

Figure 2.0-207 Comparison of the ESP Vertical SSE Design Response Spectrum for the Top of Zone III-IV and Unit 3 Vertical GMRS

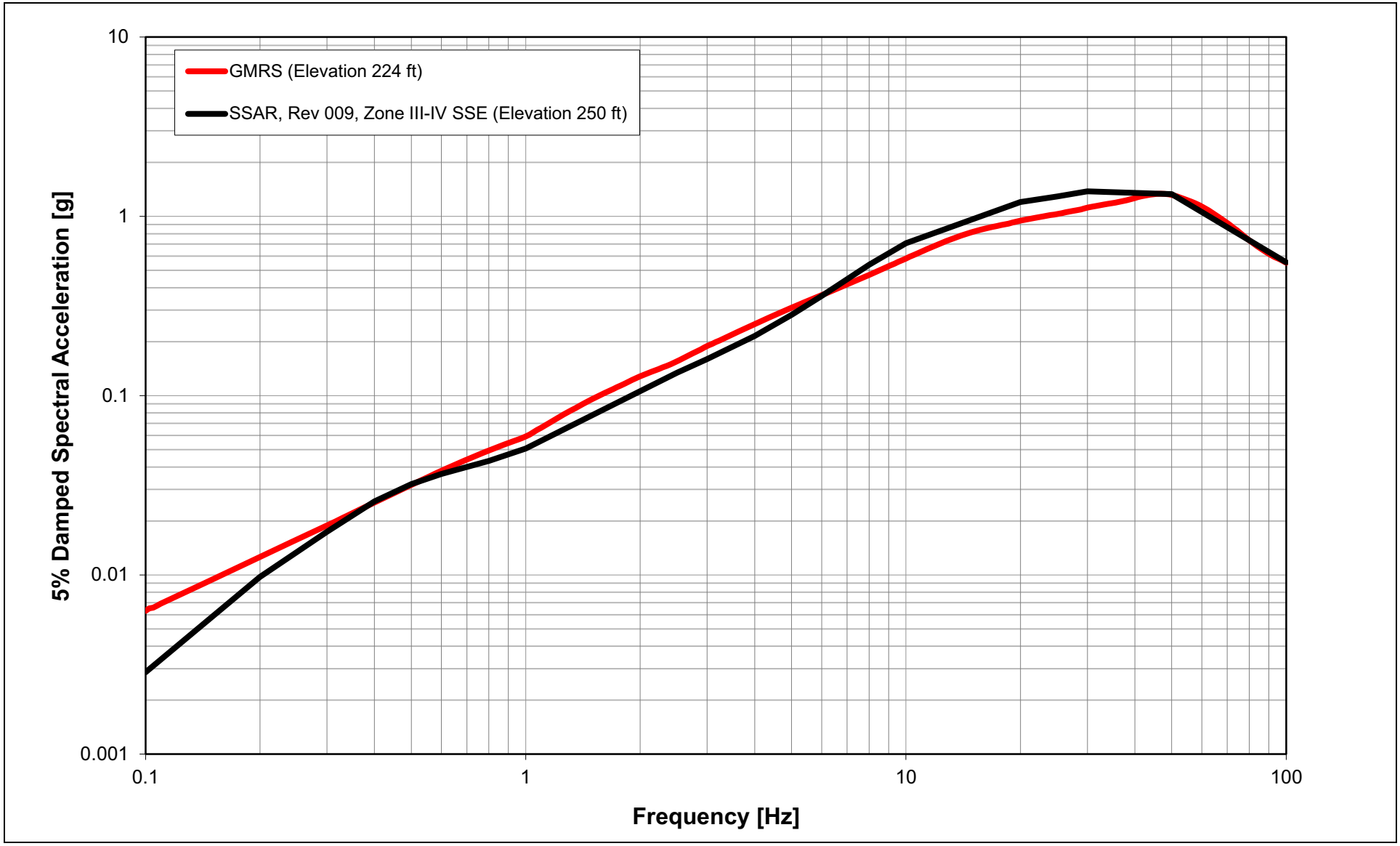

The USGS and GSC catalogs each represent a synthesis of catalog information from many sources into simple one-line catalog entries of date, time, location, and selected estimate(s) of earthquake size. In that process, some information important to the use of the earthquake catalog for the CEUS SSC Project may not have been retained. Therefore, during the development of the CEUS SSC earthquake catalog an extensive review of original catalog sources was performed as part of the catalog compilation. In addition, numerous special studies of individual earthquakes, earthquake sequences, and specific geographic areas were reviewed and the information compiled as part of the CEUS SSC earthquake catalog development. A number of these studies included information on important parameters (e.g., moment magnitudes) that is not included in the more regional catalogs.

In the process of catalog compilation from multiple sources, close attention was paid to the inclusion of duplicate entries for some earthquakes, as well as the possible inclusion of nontectonic events (e.g., quarry blasts, collapses, and explosions) that had been purposely excluded from other catalogs.

2.5.2.1.1.1.2 Uniformity of Catalog Processing

An important goal of catalog compilation is to use an earthquake size measure that is consistent with the GMPEs that are used to compute seismic hazards. Most recent GMPEs applicable to the CEUS, such as EPRI ~~(2004) (Reference 2.5-224)~~ (2013) (Reference 2.5-407), use the moment magnitude scale, **M**, as the earthquake size measure, and it is expected that the next generation of ground motion models (GMMs) will continue to use the moment magnitude scale. Unfortunately, however, this is not the magnitude scale that has been used for routine earthquake monitoring and catalog compilation in the CEUS. The recent practice for many seismic hazard analyses in the CEUS, including EPRI-SOG and NSHMP, has been to estimate earthquake occurrence rates in terms of body-wave magnitude, m_b, and then use magnitude conversion relationships to convert to **M** as part of the ground motion estimation. This magnitude conversion introduces an additional source of magnitude uncertainty, particularly since many of the catalog magnitude entries are themselves converted from other size measures, such as shaking intensity used for pre-instrumental earthquakes.

The EPRI-SOG project (Reference 2.5-248) developed techniques to produce a catalog with a uniform size measure that is appropriate for an

unbiased estimation of earthquake occurrence rates for use in a seismic hazard assessment. These techniques were used in the EPRI-SOG study to develop a uniform catalog of the m_b scale. Recent use of the EPRI-SOG SSC has been combined with a GMPE model based on **M** (i.e., ~~Reference 2.5-224~~ (EPRI 2013), requiring magnitude conversion within a PSHA. During the CEUS SSC Project, a goal of the catalog development efforts was to use the same techniques to produce a catalog of uniform **M** values that have properly accounted for the uncertainty in size estimation. As **M**-based GMPEs remain to be used in current PSHAs, development of **M**-based seismicity and source recurrence rates eliminates the need for magnitude conversion as part of the hazard calculation and avoids propagation of unnecessary conversion-associated uncertainty through the hazard analysis. To achieve this goal, the CEUS SSC Report presented the updated magnitude scale conversions, which are developed from a variety of earthquake size measures to moment magnitude. See CEUS SSC Report, Table 3.3-1.

An equally important task was to obtain the original size measures for catalog entries in order to use a direct conversion to moment magnitude, rather than introduce additional uncertainty by converting previously converted size estimates. Take for example in the GSC catalog where a number of the magnitudes are designated local magnitude, M_L, yet many of these earthquakes occurred in the pre-instrumental period. Examination of the magnitude entries suggests that they were, in fact, converted from maximum intensity, I_0, using the Gutenberg and Richter (1956) (Reference 2.5-255) relationship. Therefore, the original source for the catalog of intensity data was obtained References 2.5-256 and 2.5-257) and the I_0 values for these earthquakes were entered into the catalog in order to make a direct conversion from I_0 to **M**.

2.5.2.1.1.1.3 Catalog Review

An important element of the CEUS SSC earthquake catalog development was the review by seismologists with extensive knowledge and experience in catalog compilation. The result of the review contributed to enhance the methodologies used to develop the final CEUS SSC earthquake catalog. One result of the review was to recommend the use of original earthquake information sources as much as possible in general preference to relying only on catalog compilations, yet still recognizing that some compilations, like the CEUS SSC earthquake

small to account for the Holocene rate of paleoseismicity (Calais et al., 2005 (Reference 2.5-320); Smalley et al., 2005 (Reference 2.5-321)). To account for uncertainty in the future rate of earthquakes in the NMFS RLME, the CEUS SSC model allows for alternatives (at very low weights) in which some or all of the fault segments of the NMFS are inactive. A detailed discussion of the recurrence of large earthquakes in the NMFS RLME source is presented in CEUS SSC Report, Section 6.1.5.4.

The Mmax distribution for the NMFS RLME source is based on the estimated magnitudes of the earthquakes in the 1811-1812 sequence. The CEUS SSC model equally weights the estimates from Bakun and Hopper (2004) (Reference 2.5-322), Johnston (2004, personal communication, as cited in Reference 2.5-223)), and Hough and Page (2011) (Reference 2.5-323), which are **M** 7.2 to **M** 7.8, **M** 7.5 to **M** 7.9, and **M** 6.5 to **M** 6.9, respectively. The resulting Mmax distribution for the NMFS RLME source in the CEUS SSC model ranges from **M** 6.7 to **M** 7.9 (see Table 2.5.2-213).

All other uncertainties identified in the NMFS logic tree (see Figure 2.5.2-227) are included in the North Anna 3 site hazard calculation exactly as detailed in the CEUS SSC Report, with the exception of seismogenic depth, which is simplified from the distribution listed in Table 2.5.2-210 to a single value of 15 km. Given the distance of the NMFS RLME source to the site, this simplification is judged to be adequate for the Unit 3 PSHA.

2.5.2.2.4.3 **Wabash Valley**

Liquefaction features within the southern Illinois basin provide evidence for at least eight Holocene to latest Pleistocene earthquakes, which are estimated to be between approximately **M** 6 and **M** 7.8 (Obermeier et al., 1991 (Reference 2.5-324); Munson et al., 1997 (Reference 2.5-325); Pond and Martin, 1997 (Reference 2.5-326); Obermeier, 1998 (Reference 2.5-327); McNulty and Obermeier, 1999 (Reference 2.5-328); Tuttle et al., 1999 (Reference 2.5-329)). The proximity of the two largest paleoearthquakes (referred to in the literature as “Vincennes” and “Skelton”) to the strongest historical events in the Wabash Valley area suggests that this is a source of repeating large-magnitude earthquakes. The Wabash Valley area is therefore modeled as an RLME source in the CEUS SSC model.

At its closest approach, this RLME source extends to within approximately 780 km of the site (see Figure 2.5.2-218). Sensitivity calculations to assess hazard contributions from distant RLME sources, however, found that this source contributes 0.4 percent of the total 1 Hz hazard at the 10^{-4} hazard level. When combined with contributions from two other distant sources (SLR and IBEB), these three zones exceed 1 percent of the total hazard.

The tectonic features responsible for large-magnitude earthquakes in Wabash Valley are not known. The geometry of the Wabash Valley RLME therefore captures a range of potentially causative structures, neotectonic deformation, and inferred energy centers for the two largest paleoearthquakes in the region. Further uncertainty specified by the CEUS SSC Report related to the style, orientation, and focal depth of Wabash Valley earthquakes is detailed in Table 2.5.2-210. For the Unit 3 PSHA, earthquakes within the Wabash Valley source are represented as point sources using the EPRI ~~(2004) (Reference 2.5-224)~~ (2013) correction factors for rupture distance.

Estimates of the magnitudes of the Vincennes and Skelton paleoearthquakes range from **M** 7.0-7.8 and **M** 6.3-7.3, respectively (see the CEUS SSC Report, Section 6.1.9.3). The difference in magnitude between these two paleoearthquakes is assumed to reflect both aleatory uncertainty and epistemic uncertainty in the estimation of the characteristic Wabash Valley RLME magnitude. As a result, the modeled maximum magnitude for this RLME source is broadly distributed from **M** 6.75 to **M** 7.5 (see Table 2.5.2-214).

2.5.2.2.5 Post-CEUS SSC Studies

This section describes geologic and seismic investigations of the site region and provides information that can be used to evaluate and potentially update the CEUS SSC model relevant to the Unit 3 PSHA. Specifically, these studies include ongoing investigations of the 2011 Mineral earthquake that occurred in or near the CVSZ and the geologic investigations of the ETSZ.

2.5.2.2.5.1 Investigations of the 2011 Mineral Earthquake

The **M** 5.8 Mineral earthquake, as described in Sections 2.5.1.1.7 and 2.5.2.1.3, occurred southwest of the Unit 3 site and near the town of Mineral (Figure 2.5.2-228). A series of aftershocks highlighted the rupture plane of the Mineral earthquake, which was previously unrecognized at

Illinois Basin Extended Basement Zone (IBEB) - The IBEB zone encompasses faults within Precambrian basement and the Paleozoic Illinois Basin as well as a zone of liquefaction features thought to be associated with four moderate events (approximately **M** 6.20 to 6.30). The largest event to have occurred in the IBEB zone was the 1898 E[**M**] 5.5 event in southern Illinois. Larger earthquakes have occurred in the zone (E[**M**] ≥ 6.5), but they are characterized by the Wabash Valley RLME. Seismicity is sparse in the northern part of the IBEB zone, increasing regularly to the south (see Figure 2.5.2-229). Hypocentral depths range from shallow (less than 5 km) to deep (up to 27 km), with shallower earthquakes slightly more common. Earthquakes do not define linear trends or areas of concentrated seismicity. Seismicity is relatively evenly distributed and dense compared with surrounding regions not characterized as RLME sources. Several structures and processes have been posited as sources of earthquakes in the IBEB zone, but they remain poorly understood.

2.5.2.4 Probabilistic Seismic Hazard Analysis and Controlling Earthquakes

This section details the PSHA for Unit 3. In accordance with the guidance of RG 1.206 and RG 1.208, Section 2.5.2.4.1 describes the starting point for the PSHA, which is the 2012 CEUS SSC Report. Relevant new geologic and seismic information that post-dates completion of the CEUS SSC model is discussed in Section 2.5.2.4.2. Related updates to the CEUS SSC model based on this new information are discussed in Section 2.5.2.4.3. GMPEs used in the PSHA are detailed in Section 2.5.2.4.4. The results of the PSHA, including mean and fractile seismic hazard curves, the relative contribution of individual seismic sources, uniform hazard response spectra, and details on the controlling earthquakes are presented in Section 2.5.2.4.5.

2.5.2.4.1 CEUS SSC Model Implementation

The CEUS SSC model is the starting point used for probabilistic seismic hazard calculations at Unit 3. As discussed in Section 2.5.2.2, the CEUS SSC model is the most recent seismic source characterization specifically designed for PSHAs of nuclear facilities, developed using the SSHAC Study Level 3 methodology (References 2.5-281, 2.5-282, and 2.5-283) to ensure that uncertainty is represented in a manner consistent with NRC regulations.

For Unit 3, seismic hazard was calculated using source parameters from the CEUS SSC model. Simplifications to the CEUS SSC model were made for this calculation, and included:

- The exclusion of distributed seismicity sources and RLME sources that do not contribute significantly to hazard at the site (Section 2.5.2.2, Tables 2.5.2-206 and 2.5.2-210).
- The truncation of seismicity within distributed seismicity sources at 1,000 km from the site (Sections 2.5.2.2.2 and 2.5.2.2.3).
- Collapsing seismogenic depth in the New Madrid RLME logic tree to a single value of 15 km (with a corresponding weight of 1.0) (Section 2.5.2.2.4.2).
- The exclusion of sense of slip (described as a future rupture characteristic in the CEUS SSC Report, Table 5.4-2; Table 2.5.2-210), since current GMPEs (EPRI, ~~2004; 2006~~ 2013) do not consider this parameter.
- Rupture strike and dip (described as a future rupture characteristic in the CEUS SSC Report, Table 5.4-2; Table 2.5.2-210) were included for the Charleston and New Madrid RLME sources, but were not considered for other sources. A sensitivity study performed for the CEUS SSC model (Reference 2.5-223, p. 9-8) demonstrated that representing earthquakes as point sources, using EPRI (~~2004~~ 2013) correction factors for rupture distance, is an acceptable approximation.
- Depth distributions (described as a future rupture characteristic in the CEUS SSC Report, Table 5.4-2; Table 2.5.2-210) were collapsed to a single value for background sources.

Further modifications to the CEUS SSC model motivated by the updated earthquake catalog and site investigations are discussed in detail below.

2.5.2.4.2 New Information and New Seismic Source Characterizations

Sources of new information that potentially require updates to the CEUS SSC model include the updated earthquake catalog (Section 2.5.2.1) and geologic investigations of the site.

The published CEUS SSC earthquake catalog extends through 2008. For the Unit 3 PSHA, this catalog was updated through mid-December of 2011, as described in Section 2.5.2.1. As discussed in Section 2.5.2.3,

The Mmax assessment resulted in a minor revision to the lower bound of the Mmax distribution for ECC-AM seismotectonic source zone (see Table 2.5.2-215). No other Mmax values are affected in zones that hosted the Mineral earthquake. Had the E[**M**] 6.1 Cape Ann event occurred with a 100 percent probability in the ECC-AM, then there would have been no modification to any Mmax value. The occurrence of the Mineral earthquake shifts the lower part of the distribution to the right, enough to shift the lowest magnitude in the discretized distribution (weight 0.101; associated with the intersection between the curve and the lowest horizontal line) from **M** 6.0 to 6.1. One could even argue that this 0.1 unit shift is an artifact of the one-decimal round-off and that the true difference would be on the order of 0.02 magnitude units if one used two decimals to characterize the discretized magnitude distributions.

2.5.2.4.4 Ground Motion Prediction Equations

~~Ground-motions were estimated using hard-rock GMPEs from EPRI (2004) with aleatory uncertainties from EPRI (2006). These equations were developed for hard-rock conditions (shear-wave velocities V_S of 9200 ft/s). Separate sets of equations are used for "general, non-rift" sources typical of the CEUS, and for "non-general rift" sources, such as the Charleston seismic zone and the New Madrid seismic zone. These GMPEs were developed following a SSHAC (1997) (Reference 2.5-281) Level 3 process and are well-documented regarding the underlying models, parameters, and weights assigned to alternative interpretations. For "general, non-rift" sources, 9 alternative equations are used with weights. For "non-general rift" sources, 12 alternative equations are used with weights. For each equation, 6 alternative logarithmic standard deviations are used with weights to quantify aleatory uncertainty are used. The mid-Continent equations were not used from EPRI (2004), because the site lies well within the mid-Continent region specified therein.~~

~~Ground-motions are available for 7 spectral frequencies from EPRI (2004). These spectral frequencies are PGA (equivalent to 100 Hz), 25 Hz, 10 Hz, 5 Hz, 2.5 Hz, 1 Hz, and 0.5 Hz. All ground motion equations represent spectral acceleration at 5 percent of critical damping, and this damping applies to all spectral amplitude results presented here.~~

Starting around 2004, earthquake ground motions and their aleatory uncertainties for nuclear facilities in the CEUS were routinely estimated

using hard-rock GMPEs from EPRI (2004) (Reference 2.5-224). The aleatory uncertainties from were subsequently updated by EPRI (2006) (Reference 2.5-225). This combined EPRI (2004, 2006) earthquake GMM was developed for hard-rock conditions (shear-wave velocities V_S of 9200 ft/s). Separate sets of equations were used for "general, non-rift" sources typical of the CEUS, and for "non-general rift" sources, such as the Charleston seismic zone and the New Madrid seismic zone. These GMPEs were developed following a SSHAC (1997) (Reference 2.5-281) Level 3 process and are well-documented regarding the underlying models, parameters, and weights assigned to alternative interpretations. For “general, non-rift” sources, 9 alternative equations are used with weights. For “non-general rift” sources, 12 alternative equations are used with weights. For each equation, 6 alternative logarithmic standard deviations are used with weights to quantify aleatory uncertainty.

EPRI (2013) performed a detailed review and update of the EPRI (2004, 2006) GMM. Considering current NRC guidance for updating an accepted existing hazard model, contained in NUREG-2117, Practical Implementation Guidelines for SSHAC Level 3 and 4 Hazard Studies (Reference 2.5-283), the study used an enhanced SSHAC Level 2 assessment process. EPRI (2013) considered both new CEUS GMPEs and additional information on observed ground motions in developing refined GMPEs and specifying epistemic and aleatory uncertainties. The functional structure of the EPRI (2013) GMM is similar to that of EPRI (2004, 2006), including the specification of two separate regional models (Midcontinent and Gulf Coast), although the boundary between these regions was slightly modified from its definition in EPRI (2004).

For the PSHA presented herein, the 9 general, non-rift EPRI (2013) GMM relationships for the Midcontinent region were applied to all background seismic sources, and the 12 non-general, rift EPRI (2013) GMM relationships for the Midcontinent region were applied to all RLME sources.

Ground motion relationships are available for 7 spectral frequencies from EPRI (2013). These spectral frequencies are PGA (equivalent to 100 Hz), 25 Hz, 10 Hz, 5 Hz, 2.5 Hz, 1 Hz, and 0.5 Hz. All ground motion equations represent response spectral acceleration at 5 percent of critical damping, and this damping applies to all spectral amplitude results presented here.

NEI (2013) (Reference 2.5-409) presents the industry's responses to the NRC's review of EPRI (2013), including errata pages to EPRI (2013). These "errata" included text clarifications and the correction of a typographical error in one of the ground motion equations in Chapter 7. The correction to the equation makes it consistent with the content of EPRI (2013) Appendix G, Hazard Input Document (HID). As the HID was used in the PSHA presented in this FSAR, there is no impact from the errata indicated in NEI (2013). The EPRI (2013) GMM was endorsed by the NRC (2013) (Reference 2.5-408) as an acceptable ground motion attenuation model for use by CEUS plants in developing plant-specific ground motion response spectra.

2.5.2.4.5 Updated Probabilistic Seismic Hazard Analysis and Deaggregation

The following sections describe the updated PSHA and the deaggregation results for the site.

2.5.2.4.5.1 Seismic Sources

The analysis here is an updated calculation of rock seismic hazard using the CEUS SSC seismic source characterizations, the ~~EPRI (2004) ground motion model with the revised sigmas of EPRI (2006)~~ EPRI (2013) GMM, and updated seismicity files that include the effect of recent seismicity on background sources. The cumulative absolute velocity (CAV) filter is not applied in this calculation and no site amplification factors are used, so the results are consistent with hard-rock conditions (shear-wave velocities of 9200 ft/s). The methodology for seismic hazard calculations is well established in the technical literature (e.g., McGuire, 2004 (Reference 2.5-378)).

Seismic source inputs to the hazard calculations consist of background sources (large regions representing earthquakes not associated with specific tectonic structures, i.e., Mmax Zones and Seismotectonic Zones) and RLME sources (those representing the potential occurrence of Repeated Large Magnitude Earthquakes). Specific background sources that are documented in the CEUS SSC Report and that are included in the hazard calculations consist of the following:

Atlantic Highly Extended Crust (AHEX)

Extended Continental Crust-Atlantic Margin (ECC-AM)*

Mesozoic Extended-wide (MESE-W)*

Mesozoic Extended-narrow (MESE-N)*

Non-Mesozoic Extended-narrow (NMESE-N)*

Non-Mesozoic Extended-wide (NMESE-W)

Paleozoic Extended Crust-narrow (PEZ-N)*

Paleozoic Extended Crust-wide (PEZ-W)*

Study Region (Study_R)*

Midcontinent-Craton (MiDC-A)*

Midcontinent-Craton (MiDC-B)*

Midcontinent-Craton (MiDC-C)

Midcontinent-Craton (MiDC-D)

Illinois Basin Extended Basement (IBEB)

St. Lawrence Rift (SLR)*

* indicates seismicity file was updated, as discussed below.

This list represents all background sources that lie within 322 km (200 miles) of the site, which is consistent with the recommendation in RG 1.208, Section 1.1.1 regarding the identification of seismic sources. BEB and SLR are well beyond this 322 km (200 miles) distance but were included because sensitivity studies indicated that the hazard from these two sources, when combined with the hazard from the Wabash Valley RLME, amounts to 1 percent of total hazard at the 10^{-4} amplitude for 1 Hz spectral acceleration. Sources are truncated so that only distributed seismicity within 1,000 km is considered in the analysis. All background sources are represented with gridded seismicity at 5 km depth consisting of 24 sets of rates and *b*-value parameters for each source. These parameters consist of 8 equally likely realizations of parameters (Reference 2.5-223, pages 5-35 and 5-36) for each of three smoothing models (Reference 2.5-223, page 5-37 and cases A, B, and E in Table 5.3.2-1). Each background source also has a distribution of maximum magnitude (Reference 2.5-223, Tables 6.3.2-1 and 7.4.2-1) with a minimum magnitude of 5.0. All magnitudes in this calculation are moment magnitudes (**M**).

For background sources identified with an asterisk in the above list, seismicity parameters were recalculated using an updated earthquake catalog, because the earthquake catalog from the CEUS SSC study included earthquakes only through 2008. This catalog was updated using

the same procedures documented in the CEUS SSC Report, to identify earthquakes occurring in the CEUS between January 1, 2009, and mid-December, 2011 (see Section 2.5.2.1). Updated rate- and *b*-value files were calculated for the 24 cases described above, using the same spatial smoothing assumptions, for each background source. In addition, the Mmax distribution for each background source was examined and compared to additional earthquakes that occurred in that source, to determine if the Mmax distribution should be modified based on the additional seismicity. With the exception of the seismotectonic zone ECC-AM, as discussed earlier, it was determined that the original Mmax distributions of all background sources remain valid.

RLMEs represent additional sources of seismic hazard that are added to the hazard from the background sources discussed above. RLME sources that are included in the hazard calculations consist of the following:

- Charleston—regional source
- Charleston—local source
- Charleston—narrow source
- New Madrid fault system—Reelfoot Thrust (cluster model)
- New Madrid fault system—New Madrid North fault (cluster model)
- New Madrid fault system—New Madrid South fault (cluster model)
- Reelfoot Thrust alone
- Wabash Valley

These RLME sources have distributions representing the frequency of occurrence of large earthquakes, and the potential sizes of those earthquakes. In the CEUS SSC Report the Charleston magnitudes and annual frequencies are documented in Section 6.1.2.4 and Tables 6.1.2-4 and 6.1.2-5. The NMFS includes a model of earthquake clusters and the frequency of occurrence of those clusters, wherein all three New Madrid faults cause earthquakes in a short period of time (effectively simultaneously). In the CEUS SSC Report the magnitudes and annual frequencies of the NMFS earthquakes are documented in Section 6.1.5.3 and Tables 6.1.5-5 through 6.1.5-7.

In the CEUS SSC Report, Section 6.1.5.1, the NMFS cluster model is given a weight of 0.9. A second model is that the NMFS cluster is in a period of quiescence (not in a cluster sequence), but that the Reelfoot

Thrust alone is active (weight of 0.05). A third model is that all faults are quiescent and the NMFS does not produce large earthquakes (weight of 0.05). A discussion of the cluster model, as well as the alternatives, can be found in the CEUS SSC Report, Section 6.1.5.1.

The Wabash Valley RLME is approximately 800 km from the site and only contributes ~0.4 percent to the total hazard at 1 Hz spectral amplitude corresponding to 10^{-4}. However, this hazard, when combined with the contributions from distant background sources IBEB and SLR, exceeds 1 percent of total hazard at this amplitude. (Contributions at higher spectral frequencies, and at lower annual frequencies of exceedance, would be lower). Therefore the Wabash Valley RLME is included in the analysis. Magnitudes and annual frequencies for this RLME are documented in the CEUS SSC Report, Section 6.1.9.3 and Table 6.1.9-2.

Other RLMEs (e.g., the Eastern Rift Margin, Marianna, and Commerce) are much farther from the site, have lower annual frequencies, and/or lower characteristic magnitudes, and, therefore, would contribute even less hazard. These RLMEs would not exceed 1 percent of total hazard and were not included in the analysis.

Seismic source characteristics relevant to seismic hazard described in the CEUS SSC Report were modeled, including the correlation of the activity of seismic sources, as represented in logic trees published therein. This applies to both the background sources and RLME sources.

The 9 general, non-rift ~~mid-Continent ground motion models~~ Midcontinent GMMs from EPRI (~~2004~~ 2013) were applied to background seismic sources, and the 12 non-general rift ~~mid-Continent ground motion models~~ Midcontinent GMMs from EPRI (~~2004~~ 2013) were applied to the Charleston, NMFS, and Wabash Valley sources. For the background sources the point source (epicenter) to rupture adjustment ("random epicenters" model) from EPRI (~~2004~~ 2013) was implemented. For the Charleston and NMFS sources, earthquake sources were explicitly modeled as ruptures on faults, so the point source to rupture adjustment was not used. The correlation of ground motion equations between background (general, non-rift) sources and RLME (non-general, rift) sources was modeled, as described in EPRI (~~2004~~ 2013).

2.5.2.4.5.2 Seismic Hazard Results

Mean and fractile rock hazard curves for 7 frequencies (0.5, 1, 2.5, 5, 10, 25 Hz and PGA) are shown in Figures 2.5.2-230 through 2.5.2-236. The

2.5.2.6.1.6 FWSC Geologic Outcrop Horizontal FIRS

Figure 2.5.2-306 shows the plot of the $UHRS_{sH}(f\,|10^{-4})$ and $UHRS_{sH}(f\,|10^{-5})$ for the FWSC geologic outcrop at the elevation of 282 ft. The same figure shows the corresponding DRS, as developed in application of Equations 2.5.2.6-1 through 2.5.2.6-3. This DRS is the FWSC Geologic Outcrop Horizontal FIRS, as shown in Figure 2.5.2-312 and tabulated in Table 2.5.2-227.

2.5.2.6.1.7 Horizontal GMRS

Figure 2.5.2-299 shows the plot of the $UHRS_{sH}(f\,|10^{-4})$ and $UHRS_{sH}(f\,|10^{-5})$ for the RB/FB geologic outcrop at the elevation of 224 ft. The same figure shows the corresponding DRS, as developed in application of Equations 2.5.2.6-1 through 2.5.2.6-3.

Similarly, Figure 2.5.2-305 shows the plot of the $UHRS_{sH}(f\,|10^{-4})$ and $UHRS_{sH}(f\,|10^{-5})$ for the CB geologic outcrop at the same elevation of 224 ft. The same figure shows the corresponding DRS, as developed in application of Equations 2.5.2.6-1 through 2.5.2.6-3.

Given the proximity of the RB/FB and CB structures and consideration of marginal conservatism, the GMRS, as shown in Figure 2.5.2-313 and tabulated in Table 2.5.2-228, is the envelope of the two DRS shown in Figures 2.5.2-299 and 2.5.2-305.

2.5.2.6.2 Vertical DRS

As presented in RG 1.208, a vertical response spectrum is developed by combining the appropriate horizontal response spectrum and the most up-to-date V/H response spectral ratios appropriate for the site. That is,

$$DRS_V(f) = DRS_H(f) \times V/H(f) \qquad (2.5.2.6\text{-}4)$$

While appropriate V/H ratios for CEUS rock and soil sites are best determined from the most up-to-date attenuation relations, there are currently, however, no CEUS GMPEs that predict vertical ground motions. Again, as presented in RG 1.208, for CEUS rock sites—with V_{S30} of at least 9,200 ft/s—appropriate V/H ratios are provided in Reference 2.5-385. For CEUS soil sites, NUREG/CR-6728, Appendix J (Reference 2.5-385) outlines a procedure to determine a WUS-to-CEUS transfer function that may be used to modify the WUS V/H ratios.

Appendix J of the NUREG describes a procedure by which V/H functions can be estimated for CEUS sites where there is little empirical data. The NUREG procedure is to consider the wealth of empirical horizontal and

vertical ground motion data for WUS, as well as known differences in relevant crustal characterizations of WUS and CEUS, as a guide for developing transfer functions that can be used to scale accepted CEUS V/H functions for application to a given CEUS location. As discussed in the NUREG, this approach was used to develop the NUREG-recommended hard rock CEUS V/H functions (Reference 2.5-385, Figure 4-39 and Table 4-5). Since the Unit 3 site is not a hard rock site (i.e., explicitly, shear-wave velocity of 9,200 ft/s), then the effects of lower shear-wave velocity on V/H should be considered.

The following equation indicates an implementation of the NUREG procedure used here:

$$V/H_{CEUS,soil} = V/H_{CEUS,rock} \times f\,(\text{rock-to-soil}) \times f\,(\text{WUS-to-CEUS}) \qquad (2.5.2.6\text{-}5)$$

where:

$V/H_{CEUS,rock}$ = the appropriate hard rock CEUS V/H from the NUREG

f (rock-to-soil) = transfer function for converting rock V/H to soil V/H

f (WUS-to-CEUS) = transfer function for converting WUS V/H to CEUS V/H

Given the dearth of CEUS observations of horizontal or vertical ground motions, the NUREG procedure is necessarily approximating in nature. In development and use of the f (rock-to-soil) transfer function, the characterization of “rock” and “soil” ground motions using readily available WUS relationships has often been generic, intended to capture dominant vertical ground motion characteristics that are distinctly different on rock versus weaker material. Current methodologies, however, allow for more explicit distinction in the specification of V_{S30}, as discussed below. The f (WUS-to-CEUS) transfer function is intended to capture the most relevant distinction between WUS and CEUS ground motions. As presented in the NUREG, even the $V/H_{CEUS,rock}$ function entails significant modeling assumptions and approximations, e.g., the dependence of V/H observed on magnitude and distance uses only three discrete bins of rock peak ground acceleration (PGA) values as a proxy for magnitude and distance dependency (Reference 2.5-385, Figure 4-39 and Table 4-5).

For the development of vertical FIRS and GMRS in this section, each of the three elements of the right side of Equation 2.5.2.6-5 are estimated, as appropriate for the Unit 3 site, in order to develop an estimate of an

appropriate V/H for the application of Equation 2.5.2.6-4.

$V/H_{CEUS,rock}$

Figure 2.5.2-314 plots WUS rock and CEUS rock V/H ratios from the NUREG (Reference 2.5-385). The CEUS rock V/H from the NUREG gives the $V/H_{CEUS,rock}$ of Equation 2.5.2.6-5, as a function of the appropriate hard rock PGA. Given the hard rock PSHA results in Table 2.5.2-217, the 10^{-4} and 10^{-5} PGA values are ~~0.259g and 0.847g~~ 0.271g and 0.854g, respectively. Applying RG 1.208 DRS Equations 2.5.2.6-1 through 2.5.2.6-3, an equivalent hard rock DRS PGA would be ~~0.401g~~ 0.407g. Consequently, the appropriate NUREG CEUS rock V/H function, to be used as $V/H_{CEUS,rock}$, is the middle V/H ratio relationship, specified for 0.2g < PGA ≤ 0.5g.

***f* (rock-to-soil)**

To estimate the transfer function for converting rock V/H to soil V/H, the WUS V/H model of Gülerce and Abrahamson (2011) (Reference 2.5-388), referred to here as the "GA11" model, is used. This model is a function of magnitude, distance, V_{S30}, and various fault parameters, as discussed further, below.

The *f* (rock-to-soil) transfer function takes the following form:

$$f\text{ (rock-to-soil)} = V/H_{WUS,soil}/V/H_{WUS,rock} \qquad (2.5.2.6\text{-}6)$$

where "soil" corresponds to the appropriate V_{S30} for the FIRS/GMRS soil profile horizon of interest, and "rock" is for a V_{S30} of 9,200 ft/s.

The magnitude and distance dependence of the V/H GA11 model is addressed by considering the controlling earthquakes given in Table 2.5.2-218 for high-frequency and low-frequency at MAFE of 10^{-4} and 10^{-5}.

For the purpose of developing the *f* (rock-to-soil) transfer function of Equation 2.5.2.6-6, the fact that the current EPRI (~~2004~~ 2013) GMPEs are not dependent on most fault parameters, and that the application of V/H considers the PSHA contribution of multiple seismic sources, the fault parameters used with the GA11 model are kept generic: e.g., strike-slip fault, dip 90 degrees, no hanging wall/foot wall.

***f* (WUS-to-CEUS)**

The purpose of this transfer function is to basically adjust the *f* (rock-to-soil) transfer function to be appropriate for CEUS, since what

was developed above from GA11 is based on WUS GMPE data and models. As discussed in the NUREG, as well as EPRI (1993) (Reference 2.5-387), development of such regional transfer functions require significant modeling and analyses to obtain for even generic CEUS transfer functions.

As in other recent SSAR and FSAR documents in the NRC Reading Room that use the NUREG (Reference 2.5-385) procedure, a simplified approach is considered here in estimating the *f* (WUS-to-CEUS) transfer function. Similar to what is seen in ground motions, WUS V/H functions tend to peak at a lower frequency than CEUS V/H functions. This can be seen in Figure 2.5.2-314. As discussed in the NUREG, this high-frequency shift is generally attributed to the lower kappa (κ) values (shallow crustal damping factor) in CEUS than WUS. To affect this frequency shift – similar to considering the peak in WUS rock V/H at ~16 to 17 Hz in Figure 2.5.2-314 shifted to the peak in CEUS rock V/H at ~60 Hz – one needs simply to scale the frequencies of the *f* (rock-to-soil) = $V/H_{WUS,soil}/V/H_{WUS,rock}$ function by the ratio of the peak frequencies in Figure 2.5.2-314. The scaling factor of (62.5/16.7) is used, where the numerator and denominator values are taken at the frequencies (in Hz) of the CEUS and WUS V/H peaks, respectively, as given in the NUREG Tables 4.5 and 4.4, respectively, and shown in Figure 2.5.2-314. Therefore, two of the terms on the right-side of Equation 2.5.2.6-5 become

$$f\text{ (rock-to-soil) x }f\text{ (WUS-to-CEUS)} = (V/H_{WUS,soil}/V/H_{WUS,rock})_{frequency\text{-}shifted} \quad (2.5.2.6\text{-}7)$$

Or, to combine Equations 2.5.2.6-4, 2.5.2.6-5, and 2.5.2.6-7

$$DRS_V(f) = DRS_H(f) \times V/H_{CEUS,rock} \times (V/H_{WUS,soil} / V/H_{WUS,rock})_{frequency\text{-}shifted} \quad (2.5.2.6\text{-}8)$$

$V/H_{CEUS,soil}$

Finally, to implement Equation 2.5.2.6-5, it remains only to multiply the appropriate CEUS rock V/H ($V/H_{CEUS,rock}$) by the frequency-shifted $V/H_{WUS,soil}$ / $V/H_{WUS,rock}$ of Equation 2.5.2.6-7.

2.5.2.6.2.1 RB/FB and CB Vertical FIRS

In the development of the $DRS_V(f)$ from Equation 2.5.2.6-8 for each of these FIRS, the corresponding $DRS_H(f)$ are given as the various horizontal FIRS in Sections 2.5.2.6.1.1 through 2.5.2.6.1.4.

As presented earlier, the appropriate $V/H_{CEUS,rock}$ for all of the FIRS, as well as the GMRS, is the middle CEUS hard rock V/H ratio relationship, specified for $0.2g < PGA \leq 0.5g$, given by the NUREG (Reference 2.5-385).

The remaining term of Equation 2.5.2.6-8 is the frequency-shifted version of the ratio $V/H_{WUS,soil} / V/H_{WUS,rock}$, where the numerator and denominator are given by the GA11 V/H model. In the determination of the "soil" and "rock" V/H_{WUS} ratios, the four magnitude-distance pairs of controlling earthquakes (10^{-4} and 10^{-5}, HF and LF), given in Table 2.5.2-218, are considered. For the denominator $V/H_{WUS,rock}$ the V_{S30} is fixed to 9,200 ft/s. For the numerator $V/H_{WUS,soil}$ the V_{S30} is set to the value corresponding to the FIRS soil column and horizon:

Soil Column	Elev. (ft)	V_{S30}
RB/FB Column	241	6,078 ft/s
RB/FB Column	224	6,783 ft/s
CB Column	241	6,068 ft/s
CB Column	224	7,553 ft/s

One of the aspects of the GA11 model is that for V_{S30} greater than about 5,000 ft/s, the V/H ratio does not change. Therefore, for the RB/FB and CB columns at the elevations above $(V/H_{WUS,soil} / V/H_{WUS,rock})_{frequency\text{-}shifted}$ is simply unity, and the applicable V/H ratio $V/_{HCEUS,soil}$ is just equal to $V/H_{CEUS,rock}$, the middle CEUS hard rock V/H ratio relationship, specified for 0.2g < PGA ≤ 0.5g, given by the NUREG (Reference 2.5-385). See Figure 2.5.2-314.

Upon application of Equation 2.5.2.6-4, the V/H ratios and corresponding $FIRS_V(f)$ for the RB/FB Full Column Outcrop, CB Full Column Outcrop, RB/FB Partial Column Outcrop, and CB Partial Outcrop are tabulated in Table 2.5.2-222, 2.5.2-223, 2.5.2-224, and 2.5.2-225, respectively, and the $FIRS_V(f)$ are shown in Figures 2.5.2-307, 2.5.2-308, 2.5.2-309, and 2.5.2-310, respectively.

2.5.2.6.2.2 Vertical PBSRS for RB/FB and CB

In the development of the $DRS_V(f)$ from Equation 2.5.2.6-8 for the PBSRS for RB/FB and CB, the corresponding $DRS_H(f)$ is given as the horizontal PBSRS in Section 2.5.2.6.1.5.

As presented earlier, the appropriate $V/H_{CEUS,rock}$ for all of the FIRS, as well as the GMRS and PBSRS, is the middle CEUS hard rock V/H ratio relationship, specified for 0.2g < PGA ≤ 0.5g, given by NUREG/CR-6728.

The remaining term of Equation 2.5.2.6-8 is the frequency-shifted version of the ratio $V/H_{WUS,soil}$ /$V/H_{WUS,rock}$, where the numerator and denominator are given by the GA11 V/H model. In the determination of the "soil" and "rock" V/H_{WUS} ratios, the four magnitude-distance pairs of controlling earthquakes (10^{-4} and 10^{-5}, HF and LF), given in Table 2.5.2-218, are considered. For the denominator $V/H_{WUS,rock}$ the V_{S30} is fixed to 5,000 ft/s—equivalent to using V_{S30} fixed to 9,200 ft/s, as discussed earlier. For the numerator $V/H_{WUS,soil}$ the V_{S30} is set to the pair of values corresponding to the soil columns and finished grade horizon considered for the PBSRS:

Soil Column	Elevation (ft)	V_{S30}
RB/FB Column	290 {finished grade}	3,423 ft/s
CB Column	290 {finished grade}	2,439 ft/s

Considering the V_{S30} of 2,439 ft/s, Figure 2.5.2-315 shows the four magnitude-distance versions of the ratio $V/H_{WUS,soil}$ /$V/H_{WUS,rock}$, where they are very similar, with the envelope being given by the **M** ~~6.2~~ 6.1 at a distance of ~~17~~ 15 km. Figure 2.5.2-316 shows the four frequency-shifted versions of the ratio $V/H_{WUS,soil}$ /$V/H_{WUS,rock}$.

Shown in Figure 2.5.2-317, the $V/H_{CEUS,rock}$ has been multiplied by each of the four frequency-shifted versions of the ratio $V/H_{WUS,soil}$ / $V/H_{WUS,rock}$ to give V/H ratios considering the V_{S30} of 2,439 ft/s. As a comparison, this figure also shows $V/H_{CEUS,rock}$ and the often-considered V/H ratio from RG 1.60. For frequencies less than about 2.5 Hz, the V/H ratio developed here is slightly greater than that given by RG 1.60. For frequencies above about 3.5 Hz the RG 1.60 V/H ratio is 1.0, while the V/H ratio developed here initially decreases between about 3.5 Hz and 7.5 Hz, then increases to a V/H ratio greater than 1.0 between about 40 and 85 Hz. The high frequency V/H exceedance of 1.0 reflects the character of the $V/H_{CEUS,rock}$ for moderate to high ground motions. The lower value dip in the V/H ratio between about 2 and 20 Hz is addressed further below.

Similar to the process above for determining $V/H_{CEUS,soil}$ ratios for a V_{S30} of 2,439 ft/s (743 m/s) in Figure 2.5.2-317, Figure 2.5.2-318 shows a similar plot of $V/H_{CEUS,soil}$ ratios for the second V_{S30} of 3,423 ft/s (1.043 m/s). This second V/H ratio is equal to or slightly higher than that for the V_{S30} of 2,439 ft/s, except for slightly lower V/H values in the peak range of 35 to 75 Hz.

For the purpose a single V/H ratio for application to the PBSRS $DRS_H(f)$, Figure 2.5.2-319 shows an *initial* $V/H_{CEUS,soil}$ ratio for the PBSRS, based on the envelope of all eight $V/H_{CEUS,soil}$ ratios presented above.

As initially described earlier in this section regarding Figure 2.5.2-317, the initial PBSRS V/H in Figure 2.5.2-319 has a dip in V/H values between 4.5 and 20 Hz, which could be considered an unconservative or WUS-biased character. Analogous to what was done in the NUREG for the CEUS V/H rock ratios, as compared to the WUS V/H rock ratios (see Figure 2.5.2-314) the V/H values in this dip were raised and enveloped with the FWSC $V/H_{CEUS,soil}$ (discussed in Section 2.5.2.6.2.3) to give the *final* V/H ratio for the PBSRS for RB/FB and CB, shown in Figure 2.5.2-320. As seen in Figure 2.5.2-320, the final $V/H_{CEUS,soil}$ ratio for the PBSRS for RB/FB and CB is very similar to $V/H_{CEUS,rock}$.

Upon application of Equation 2.5.2.6-4, the V/H ratio and corresponding $PBSRS_V(f)$ for the PBSRS for CB/FB and CB are tabulated in Table 2.5.2-226 and the $PBSRS_V(f)$ is shown in Figure 2.5.2-311.

2.5.2.6.2.3 FWSC Geologic Outcrop Vertical FIRS

In the development of the $DRS_V(f)$ from Equation 2.5.2.6-8 for the FWSC FIRS, the corresponding $DRS_H(f)$ is given as the horizontal FIRS in the earlier Section 2.5.2.6.1.6.

As presented in Section 2.5.2.6.2, the appropriate $V/H_{CEUS,rock}$ for all of the FIRS, as well as the GMRS, is the middle CEUS hard rock V/H ratio relationship, specified for 0.2g < PGA ≤ 0.5g, given by NUREG/CR-6728.

The remaining term of Equation 2.5.2.6-8 is the frequency-shifted version of the ratio $V/H_{WUS,soil}$ /$V/H_{WUS,rock}$, where the numerator and denominator are given by the GA11 V/H model. In the determination of the "soil" and "rock" V/H_{WUS} ratios, the four magnitude-distance pairs of controlling earthquakes (10^{-4} and 10^{-5}, HF and LF), given in Table 2.5.2-218, are considered. For the denominator $V/H_{WUS,rock}$ the V_{S30} is fixed to 5,000 ft/s, equivalent to using V_{S30} fixed to 9,200 ft/s, as

discussed earlier. For the numerator $V/H_{WUS,soil}$ the V_{S30} is set to the value corresponding to the FIRS soil column and horizon:

Soil Column	Elev. (ft)	V_{S30}
FWSC Column	282	2,124 ft/s

Following the same procedure as detailed in Section 2.5.2.6.2.2 for the PBSRS, a similar $V/H_{CEUS,soil}$ for the FWSC Geologic Outcrop FIRS was determined~~, therefore, the~~. The envelope of the $V/H_{CEUS,soil}$ for FWSC and $V/H_{CEUS,soil}$ for PBSRS is used as the final PBSRS $V/H_{CEUS,soil}$. The final PBSRS $V/H_{CEUS,soil}$ is also used for the FWSC Geologic Outcrop FIRS.

Upon application of Equation 2.5.2.6-4, the V/H ratio and corresponding $FIRS_V(f)$ for the FWSC Geologic Outcrop are tabulated in Table 2.5.2-227 and the $FIRS_V(f)$ is shown in Figure 2.5.2-312.

2.5.2.6.2.4 Vertical GMRS

In the development of the $DRS_V(f)$ from Equation 2.5.2.6-8 for the GMRS, the corresponding $DRS_H(f)$ is given as the horizontal GMRS in Section 2.5.2.6.1.7.

As presented in Section 2.5.2.6.2, the appropriate $V/H_{CEUS,rock}$ for all of the FIRS, as well as the GMRS, is the middle CEUS hard rock V/H ratio relationship, specified for 0.2g < PGA ≤ 0.5g, given by NUREG/CR-6728.

The remaining term of Equation 2.5.2.6-8 is the frequency-shifted version of the ratio $V/H_{WUS,soil}/V/H_{WUS,rock}$, where the numerator and denominator are given by the GA11 V/H model. In the determination of the "soil" and "rock" V/H_{WUS} ratios, the four magnitude-distance pairs of controlling earthquakes (10^{-4} and 10^{-5}, HF and LF), given in Table 2.5.2-218, are considered. For the denominator $V/H_{WUS,rock}$ the V_{S30} is fixed to 9,200 ft/s. For the numerator $V/H_{WUS,soil}$ the V_{S30} is set to the pair of values corresponding to the soil columns and horizon considered for the GMRS:

Soil Column	Elev. (ft)	V_{S30}
RB/FB Column	224	6,783 ft/s
CB Column	224	7,553 ft/s

One of the aspects of the GA11 model is that for V_{S30} greater than about 5,000 ft/s, the V/H ratio does not change. Therefore, for the RB/FB and CB columns at the elevation above ($V/H_{WUS,soil}$/

NAPS COL 2.0-27-A
NAPS ESP VAR 2.0-4

Table 2.5.2-216 Total Mean Rock Hazard for 7 Spectral Frequencies

Horizontal Rock Spectral Acceleration[1], g	0.5 Hz	1 Hz	2.5 Hz	5 Hz	10 Hz	25 Hz	PGA
0.0005	2.42E-02	4.77E-02	7.68E-02	7.82E-02	7.18E-02	5.99E-02	4.94E-02
0.001	1.38E-02	2.85E-02	5.15E-02	5.40E-02	4.94E-02	3.97E-02	3.08E-02
0.005	2.88E-03	6.11E-03	1.32E-02	1.58E-02	1.59E-02	1.32E-02	9.04E-03
0.01	1.07E-03	2.44E-03	5.99E-03	8.33E-03	9.30E-03	8.23E-03	5.09E-03
0.015	5.09E-04	1.25E-03	3.51E-03	5.55E-03	6.69E-03	6.20E-03	3.56E-03
0.03	1.12E-04	3.28E-04	1.28E-03	2.58E-03	3.63E-03	3.65E-03	1.83E-03
0.05	3.35E-05	1.13E-04	5.72E-04	1.38E-03	2.17E-03	2.32E-03	1.06E-03
0.075	1.32E-05	4.88E-05	2.92E-04	7.98E-04	1.38E-03	1.55E-03	6.59E-04
0.1	7.09E-06	2.71E-05	1.77E-04	5.26E-04	9.71E-04	1.13E-03	4.56E-04
0.15	3.03E-06	1.18E-05	8.42E-05	2.80E-04	5.67E-04	6.99E-04	2.59E-04
0.3	7.02E-07	2.73E-06	2.10E-05	8.23E-05	1.98E-04	2.73E-04	8.46E-05
0.5	2.22E-07	8.53E-07	6.85E-06	2.95E-05	8.06E-05	1.22E-04	3.22E-05
0.75	8.33E-08	3.15E-07	2.63E-06	1.20E-05	3.64E-05	5.99E-05	1.35E-05
1	3.96E-08	1.48E-07	1.28E-06	6.08E-06	1.98E-05	3.46E-05	6.92E-06
1.5	1.29E-08	4.72E-08	4.31E-07	2.16E-06	7.78E-06	1.49E-05	2.45E-06
3	1.47E-09	5.17E-09	5.21E-08	2.91E-07	1.25E-06	2.86E-06	3.11E-07
5	2.36E-10	7.98E-10	8.55E-09	5.29E-08	2.63E-07	6.88E-07	5.07E-08
7.5	4.70E-11	1.54E-10	1.72E-09	1.17E-08	6.51E-08	1.92E-07	9.82E-09
10	1.37E-11	4.39E-11	5.01E-10	3.64E-09	2.21E-08	7.11E-08	2.73E-09

1. 5% critical damping

NAPS COL 2.0-27-A
NAPS ESP VAR 2.0-4

Table 2.5.2-217 Horizontal Rock Spectral Accelerations from the PSHA for MAFEs of 10^{-4}, 10^{-5}, and 10^{-6}

	5% Critically-Damped Spectral Acceleration, g		
Spectral Frequency	**10^{-4}**	**10^{-5}**	**10^{-6}**
PGA (100 Hz)	0.271	0.854	2.03
25 Hz	0.560	1.77	4.37
10 Hz	0.442	1.35	3.23
5.0 Hz	0.269	0.811	1.96
2.5 Hz	0.137	0.421	1.10
1.0 Hz	0.0531	0.162	0.466
0.5 Hz	0.0315	0.0853	0.254

PSHA: probabilistic seismic hazard analysis
MAFE: mean annual frequency of exceedance
PGA: peak ground acceleration
~~UHRS: uniform hazard response spectrum~~

NAPS COL 2.0-27-A
NAPS ESP VAR 2.0-4

Table 2.5.2-218 Mean Magnitude and Distance for LF and HF Response Spectra for Three MAFEs

MAFE >	**10^{-4}**	**10^{-5}**	**10^{-6}**
Low Frequency **M**	7.1	6.4	6.7
Low Frequency R (km)	340	21	16
High Frequency **M**	5.9	6.1	6.4
High Frequency R (km)	22	15	13

LF: low frequency, 1 to 2.5 Hz
HF: high frequency, 5 to 10 Hz
MAFE: mean annual frequency of exceedance
M: moment magnitude
R: distance (kilometers)

NAPS COL 2.0-27-A
NAPS ESP VAR 2.0-4

Table 2.5.2-219 Horizontal Rock UHRS (g) for MAFEs of 10^{-4}, 10^{-5}, and 10^{-6}

Spectral Frequency, Hz	10^{-4} HF	10^{-4} LF	10^{-5} HF	10^{-5} LF	10^{-6} HF	10^{-6} LF
100	2.71E-01	1.34E-01	8.54E-01	6.36E-01	2.03E+00	1.52E+00
90	2.93E-01	1.45E-01	9.23E-01	6.91E-01	2.20E+00	1.65E+00
80	3.32E-01	1.66E-01	1.05E+00	7.87E-01	2.50E+00	1.88E+00
70	3.90E-01	1.96E-01	1.23E+00	9.33E-01	2.95E+00	2.23E+00
60	4.63E-01	2.35E-01	1.46E+00	1.12E+00	3.52E+00	2.66E+00
50	5.30E-01	2.71E-01	1.67E+00	1.29E+00	4.04E+00	3.07E+00
45	5.54E-01	2.85E-01	1.75E+00	1.35E+00	4.24E+00	3.23E+00
40	5.70E-01	2.95E-01	1.80E+00	1.40E+00	4.37E+00	3.34E+00
35	5.76E-01	3.02E-01	1.82E+00	1.43E+00	4.44E+00	3.41E+00
30	5.74E-01	3.05E-01	1.81E+00	1.43E+00	4.44E+00	3.43E+00
25	5.60E-01	3.04E-01	1.77E+00	1.42E+00	4.37E+00	3.39E+00
20	5.51E-01	2.98E-01	1.72E+00	1.37E+00	4.21E+00	3.28E+00
15	5.19E-01	2.86E-01	1.60E+00	1.26E+00	3.87E+00	3.03E+00
12.5	4.88E-01	2.75E-01	1.50E+00	1.17E+00	3.60E+00	2.84E+00
10	4.42E-01	2.59E-01	1.35E+00	1.05E+00	3.23E+00	2.57E+00
9	4.13E-01	2.51E-01	1.26E+00	9.94E-01	3.01E+00	2.43E+00
8	3.81E-01	2.41E-01	1.16E+00	9.30E-01	2.78E+00	2.29E+00
7	3.47E-01	2.30E-01	1.05E+00	8.59E-01	2.53E+00	2.12E+00
6	3.09E-01	2.17E-01	9.36E-01	7.81E-01	2.25E+00	1.94E+00
5	2.69E-01	2.00E-01	8.11E-01	6.94E-01	1.96E+00	1.74E+00

NAPS COL 2.0-27-A
NAPS ESP VAR 2.0-4

Table 2.5.2-219 Horizontal Rock UHRS (g) for MAFEs of 10^{-4}, 10^{-5}, and 10^{-6} *(continued)*

Spectral Frequency, Hz	10^{-4} HF	10^{-4} LF	10^{-5} HF	10^{-5} LF	10^{-6} HF	10^{-6} LF
4	2.20E-01	1.80E-01	6.67E-01	5.98E-01	1.65E+00	1.52E+00
3	1.67E-01	1.54E-01	5.09E-01	4.87E-01	1.30E+00	1.26E+00
2.5	1.37E-01	1.37E-01	4.21E-01	4.21E-01	1.10E+00	1.10E+00
2	1.08E-01	1.15E-01	3.36E-01	3.50E-01	8.99E-01	9.37E-01
1.5	7.52E-02	8.65E-02	2.39E-01	2.63E-01	6.59E-01	7.28E-01
1.25	5.86E-02	7.02E-02	1.88E-01	2.14E-01	5.27E-01	6.02E-01
1	4.24E-02	5.31E-02	1.38E-01	1.62E-01	3.92E-01	4.66E-01
0.9	3.63E-02	4.97E-02	1.18E-01	1.49E-01	3.39E-01	4.32E-01
0.8	3.04E-02	4.58E-02	9.95E-02	1.35E-01	2.87E-01	3.94E-01
0.7	2.48E-02	4.14E-02	8.15E-02	1.20E-01	2.37E-01	3.51E-01
0.6	1.95E-02	3.67E-02	6.44E-02	1.03E-01	1.89E-01	3.05E-01
0.5	1.45E-02	3.15E-02	4.84E-02	8.53E-02	1.44E-01	2.54E-01
0.4	1.16E-02	2.52E-02	3.87E-02	6.82E-01	1.15E-01	2.03E-01
0.3	8.71E-03	1.89E-02	2.91E-02	5.12E-02	8.63E-02	1.52E-01
0.2	5.81E-03	1.26E-02	1.94E-02	3.41E-02	5.75E-02	1.02E-01
0.167	4.85E-03	1.05E-02	1.62E-02	2.85E-02	4.80E-02	8.48E-02
0.125	3.63E-03	7.88E-03	1.21E-02	2.13E-02	3.59E-02	6.35E-02
0.1	2.90E-03	6.30E-03	9.69E-03	1.71E-02	2.88E-02	5.08E-02

NAPS COL 2.0-27-A
NAPS ESP VAR 2.0-4

Table 2.5.2-219 Horizontal Rock UHRS (g) for MAFEs of 10^{-4}, 10^{-5}, and 10^{-6} *(continued)*

LF: low frequency, 1 to 2.5 Hz
HF: high frequency, 5 to 10 Hz
MAFE: mean annual frequency of exceedance
UHRS: uniform hazard response spectrum/a

NAPS COL 2.0-27-A

Table 2.5.2-220 V_{S30} Values[1] for RB/FB, CB, and FWSC Soil Columns

V_{S30} (fps)	RB/FB Soil Column	CB Soil Column	FWSC Soil Column
Elevation 290 ft (Finished Grade)	3,423	2,439	
Elevation 282 ft (FIRS elevation for FWSC)			2,124
Elevation 241 ft (FIRS elevation for CB)	6,078	6,068	
Elevation 224 ft (FIRS elevation for RB/FB)	6,783	7,553	

1 V_{S30}: Travel-time averaged shear-wave velocity in the top 30 meters of the soil column

NAPS COL 2.0-27-A
NAPS ESP VAR 2.0-4

Table 2.5.2-221 Input Hard Rock Motions and Associated Parameters

Rock Motion	Magnitude (M)	Distance (R, km)	Duration (sec)	Effective Strain Ratio
LF 10^{-4}	7.1	340	26.3	0.61
HF 10^{-4}	5.9	22	2.4	0.49
LF 10^{-5}	6.4	21	5.1	0.54
HF 10^{-5}	6.1	15	5.1	0.51

NAPS COL 2.0-27-A
NAPS DEP 3.7-1

Table 2.5.2-222 Horizontal and Vertical RB/FB Full Column Outcrop FIRS

Frequency (Hz)	$FIRS_H(f)$ (g)	V/H(*f*)	$FIRS_V(f)$ (g)
100	0.563	1.000	0.563
90	0.605	1.038	0.627
80	0.677	1.090	0.739
70	0.795	1.131	0.899
60	0.953	1.151	1.097
50	1.093	1.152	1.260
45	1.131	1.113	1.259
40	1.173	1.042	1.223
35	1.184	0.981	1.161
30	1.207	0.937	1.131
25	1.162	0.880	1.023
20	1.129	0.826	0.932
15	1.105	0.788	0.871
12.5	1.086	0.771	0.838
10	1.005	0.750	0.754
9	0.943	0.750	0.707
8	0.868	0.750	0.651
7	0.771	0.750	0.578
6	0.647	0.750	0.485
5	0.536	0.750	0.402
4	0.403	0.750	0.302
3	0.281	0.750	0.211
2.5	0.224	0.750	0.168
2	0.179	0.750	0.134
1.5	0.132	0.750	0.099

NAPS COL 2.0-27-A
NAPS DEP 3.7-1

Table 2.5.2-222 Horizontal and Vertical RB/FB Full Column Outcrop FIRS *(continued)*

Frequency (Hz)	$FIRS_H(f)$ (g)	V/H(*f*)	$FIRS_V(f)$ (g)
1.25	0.107	0.750	0.080
1	0.081	0.750	0.060
0.9	0.074	0.750	0.056
0.8	0.067	0.750	0.050
0.7	0.060	0.750	0.045
0.6	0.052	0.750	0.039
0.5	0.043	0.750	0.032
0.4	0.034	0.750	0.026
0.3	0.025	0.750	0.019
0.2	0.017	0.750	0.013
0.167	0.014	0.750	0.011
0.125	0.011	0.750	0.008
0.1	0.008	0.750	0.006

NAPS COL 2.0-27-A
NAPS DEP 3.7-1

Table 2.5.2-223 Horizontal and Vertical CB Full Column Outcrop FIRS

Frequency (Hz)	$FIRS_H(f)$ (g)	V/H(*f*)	$FIRS_V(f)$ (g)
100	0.749	1.000	0.749
90	0.807	1.038	0.837
80	0.896	1.090	0.977
70	1.044	1.131	1.181
60	1.261	1.151	1.452
50	1.429	1.152	1.647
45	1.479	1.113	1.646
40	1.512	1.042	1.576
35	1.561	0.981	1.531
30	1.594	0.937	1.493
25	1.526	0.880	1.343
20	1.481	0.826	1.223
15	1.447	0.788	1.140
12.5	1.421	0.771	1.096
10	1.334	0.750	1.001
9	1.264	0.750	0.948
8	1.163	0.750	0.872
7	1.026	0.750	0.770
6	0.861	0.750	0.646
5	0.679	0.750	0.509
4	0.483	0.750	0.363
3	0.322	0.750	0.241
2.5	0.252	0.750	0.189
2	0.194	0.750	0.145
1.5	0.140	0.750	0.105

NAPS COL 2.0-27-A
NAPS DEP 3.7-1

Table 2.5.2-223 Horizontal and Vertical CB Full Column Outcrop FIRS *(continued)*

Frequency (Hz)	$FIRS_H(f)$ (g)	V/H(*f*)	$FIRS_V(f)$ (g)
1.25	0.112	0.750	0.084
1	0.084	0.750	0.063
0.9	0.077	0.750	0.058
0.8	0.070	0.750	0.052
0.7	0.062	0.750	0.046
0.6	0.053	0.750	0.040
0.5	0.045	0.750	0.033
0.4	0.036	0.750	0.027
0.3	0.026	0.750	0.019
0.2	0.017	0.750	0.013
0.167	0.014	0.750	0.011
0.125	0.011	0.750	0.008
0.1	0.008	0.750	0.006

NAPS COL 2.0-27-A
NAPS DEP 3.7-1

Table 2.5.2-224 Horizontal and Vertical RB/FB Partial Column Outcrop FIRS

Frequency (Hz)	$FIRS_H(f)$ (g)	V/H(*f*)	$FIRS_V(f)$ (g)
100	0.586	1.000	0.586
90	0.632	1.038	0.656
80	0.708	1.090	0.772
70	0.821	1.131	0.929
60	0.992	1.151	1.143
50	1.130	1.152	1.302
45	1.185	1.113	1.320
40	1.208	1.042	1.259
35	1.223	0.981	1.199
30	1.202	0.937	1.126
25	1.170	0.880	1.030
20	1.165	0.826	0.962
15	1.190	0.788	0.938
12.5	1.174	0.771	0.905
10	1.053	0.750	0.790
9	0.953	0.750	0.715
8	0.841	0.750	0.631
7	0.713	0.750	0.535
6	0.587	0.750	0.440
5	0.474	0.750	0.355
4	0.367	0.750	0.275
3	0.267	0.750	0.200
2.5	0.217	0.750	0.163
2	0.176	0.750	0.132
1.5	0.131	0.750	0.098

NAPS COL 2.0-27-A
NAPS DEP 3.7-1

Table 2.5.2-224 Horizontal and Vertical RB/FB Partial Column Outcrop FIRS *(continued)*

Frequency (Hz)	$FIRS_H(f)$ (g)	V/H(*f*)	$FIRS_V(f)$ (g)
1.25	0.106	0.750	0.079
1	0.080	0.750	0.060
0.9	0.074	0.750	0.055
0.8	0.067	0.750	0.050
0.7	0.060	0.750	0.045
0.6	0.052	0.750	0.039
0.5	0.043	0.750	0.032
0.4	0.034	0.750	0.026
0.3	0.025	0.750	0.019
0.2	0.017	0.750	0.013
0.167	0.014	0.750	0.011
0.125	0.011	0.750	0.008
0.1	0.008	0.750	0.006

NAPS COL 2.0-27-A
NAPS DEP 3.7-1

Table 2.5.2-225 Horizontal and Vertical CB Partial Column Outcrop FIRS

Frequency (Hz)	$FIRS_H(f)$ (g)	V/H(*f*)	$FIRS_V(f)$ (g)
100	0.788	1.000	0.788
90	0.853	1.038	0.885
80	0.948	1.090	1.034
70	1.079	1.131	1.221
60	1.330	1.151	1.532
50	1.510	1.152	1.740
45	1.569	1.113	1.747
40	1.630	1.042	1.699
35	1.647	0.981	1.615
30	1.548	0.937	1.450
25	1.498	0.880	1.319
20	1.584	0.826	1.308
15	1.705	0.788	1.344
12.5	1.679	0.771	1.295
10	1.407	0.750	1.055
9	1.192	0.750	0.894
8	0.966	0.750	0.724
7	0.770	0.750	0.578
6	0.616	0.750	0.462
5	0.491	0.750	0.368
4	0.378	0.750	0.284
3	0.275	0.750	0.206
2.5	0.223	0.750	0.167
2	0.180	0.750	0.135
1.5	0.133	0.750	0.100

NAPS COL 2.0-27-A
NAPS DEP 3.7-1

Table 2.5.2-225 Horizontal and Vertical CB Partial Column Outcrop FIRS *(continued)*

Frequency (Hz)	$FIRS_H(f)$ (g)	V/H(*f*)	$FIRS_V(f)$ (g)
1.25	0.108	0.750	0.081
1	0.081	0.750	0.061
0.9	0.075	0.750	0.056
0.8	0.068	0.750	0.051
0.7	0.061	0.750	0.045
0.6	0.052	0.750	0.039
0.5	0.044	0.750	0.033
0.4	0.035	0.750	0.026
0.3	0.025	0.750	0.019
0.2	0.017	0.750	0.013
0.167	0.014	0.750	0.011
0.125	0.011	0.750	0.008
0.1	0.008	0.750	0.006

NAPS COL 2.0-27-A
NAPS DEP 3.7-1

Table 2.5.2-226 Horizontal and Vertical PBSRS for RB/FB and CB

Frequency (Hz)	PBSRS $_H(f)$ (g)	V/H(f)	PBSRS $_V(f)$ (g)
100	0.894	1.000	0.894
90	0.949	1.038	0.984
80	1.040	1.090	1.134
70	1.182	1.131	1.337
60	1.382	1.151	1.592
50	1.557	1.152	1.794
45	1.692	1.113	1.884
40	1.835	1.042	1.913
35	1.865	0.981	1.829
30	1.887	0.937	1.767
25	1.829	0.880	1.610
20	1.866	0.826	1.540
15	1.929	0.788	1.520
12.5	1.962	0.771	1.513
10	1.905	0.750	1.428
9	1.809	0.750	1.357
8	1.666	0.750	1.250
7	1.476	0.750	1.107
6	1.256	0.750	0.942
5	0.994	0.750	0.746
4	0.679	0.750	0.509
3	0.402	0.750	0.302
2.5	0.297	0.750	0.223
2	0.217	0.750	0.163
1.5	0.151	0.750	0.113

NAPS COL 2.0-27-A
NAPS DEP 3.7-1

Table 2.5.2-226 Horizontal and Vertical PBSRS for RB/FB and CB *(continued)*

Frequency (Hz)	PBSRS $_H(f)$ (g)	V/H(f)	PBSRS $_V(f)$ (g)
1.25	0.119	0.750	0.089
1	0.089	0.750	0.066
0.9	0.081	0.750	0.061
0.8	0.073	0.750	0.055
0.7	0.065	0.750	0.049
0.6	0.056	0.750	0.042
0.5	0.047	0.750	0.035
0.4	0.037	0.750	0.028
0.3	0.027	0.750	0.020
0.2	0.017	0.750	0.013
0.167	0.014	0.750	0.011
0.125	0.011	0.750	0.008
0.1	0.009	0.750	0.006

NAPS COL 2.0-27-A
NAPS DEP 3.7-1

Table 2.5.2-227 Horizontal and Vertical FWSC Geologic Outcrop FIRS

Frequency (Hz)	$FIRS_H(f)$ (g)	V/H(*f*)	$FIRS_V(f)$ (g)
100	0.691	1.000	0.691
90	0.708	1.038	0.734
80	0.735	1.090	0.802
70	0.783	1.131	0.886
60	0.859	1.151	0.989
50	0.972	1.152	1.120
45	1.047	1.113	1.166
40	1.136	1.042	1.184
35	1.228	0.981	1.204
30	1.345	0.937	1.260
25	1.454	0.880	1.280
20	1.590	0.826	1.313
15	1.636	0.788	1.289
12.5	1.586	0.771	1.223
10	1.570	0.750	1.177
9	1.558	0.750	1.169
8	1.506	0.750	1.130
7	1.381	0.750	1.036
6	1.210	0.750	0.908
5	1.010	0.750	0.758
4	0.766	0.750	0.575
3	0.497	0.750	0.373
2.5	0.358	0.750	0.269
2	0.247	0.750	0.186
1.5	0.162	0.750	0.122

NAPS COL 2.0-27-A
NAPS DEP 3.7-1

Table 2.5.2-227 Horizontal and Vertical FWSC Geologic Outcrop FIRS *(continued)*

Frequency (Hz)	$FIRS_H(f)$ (g)	V/H(*f*)	$FIRS_V(f)$ (g)
1.25	0.125	0.750	0.094
1	0.092	0.750	0.069
0.9	0.083	0.750	0.062
0.8	0.075	0.750	0.056
0.7	0.066	0.750	0.050
0.6	0.057	0.750	0.043
0.5	0.047	0.750	0.035
0.4	0.038	0.750	0.028
0.3	0.027	0.750	0.020
0.2	0.017	0.750	0.013
0.167	0.014	0.750	0.011
0.125	0.011	0.750	0.008
0.1	0.009	0.750	0.006

NAPS COL 2.0-27-A
NAPS ESP VAR 2.0-4

Table 2.5.2-228 Horizontal and Vertical GMRS

Frequency (Hz)	$GMRS_H(f)$ (g)	V/H(*f*)	$GMRS_V(f)$ (g)
100	0.551	1.000	0.551
90	0.597	1.038	0.619
80	0.673	1.090	0.734
70	0.810	1.131	0.916
60	0.985	1.151	1.134
50	1.142	1.152	1.316
45	1.194	1.113	1.329
40	1.216	1.042	1.267
35	1.213	0.981	1.189
30	1.192	0.937	1.117
25	1.170	0.880	1.030
20	1.146	0.826	0.946
15	1.041	0.788	0.820
12.5	0.928	0.771	0.715
10	0.776	0.750	0.582
9	0.702	0.750	0.526
8	0.629	0.750	0.471
7	0.556	0.750	0.417
6	0.485	0.750	0.364
5	0.413	0.750	0.310
4	0.334	0.750	0.251
3	0.252	0.750	0.189
2.5	0.207	0.750	0.155
2	0.171	0.750	0.128
1.5	0.128	0.750	0.096
1.25	0.104	0.750	0.078

NAPS COL 2.0-27-A
NAPS ESP VAR 2.0-4

Table 2.5.2-228 Horizontal and Vertical GMRS *(continued)*

Frequency (Hz)	$GMRS_H(f)$ (g)	V/H(*f*)	$GMRS_V(f)$ (g)
1	0.079	0.750	0.059
0.9	0.073	0.750	0.054
0.8	0.066	0.750	0.049
0.7	0.059	0.750	0.044
0.6	0.051	0.750	0.038
0.5	0.042	0.750	0.032
0.4	0.034	0.750	0.025
0.3	0.025	0.750	0.019
0.2	0.017	0.750	0.013
0.167	0.014	0.750	0.011
0.125	0.010	0.750	0.008
0.1	0.008	0.750	0.006

NAPS COL 2.0-27-A
NAPS ESP VAR 2.0-4

Figure 2.5.2-230 Mean and Fractile Rock Hazard Curves for 0.5 Hz

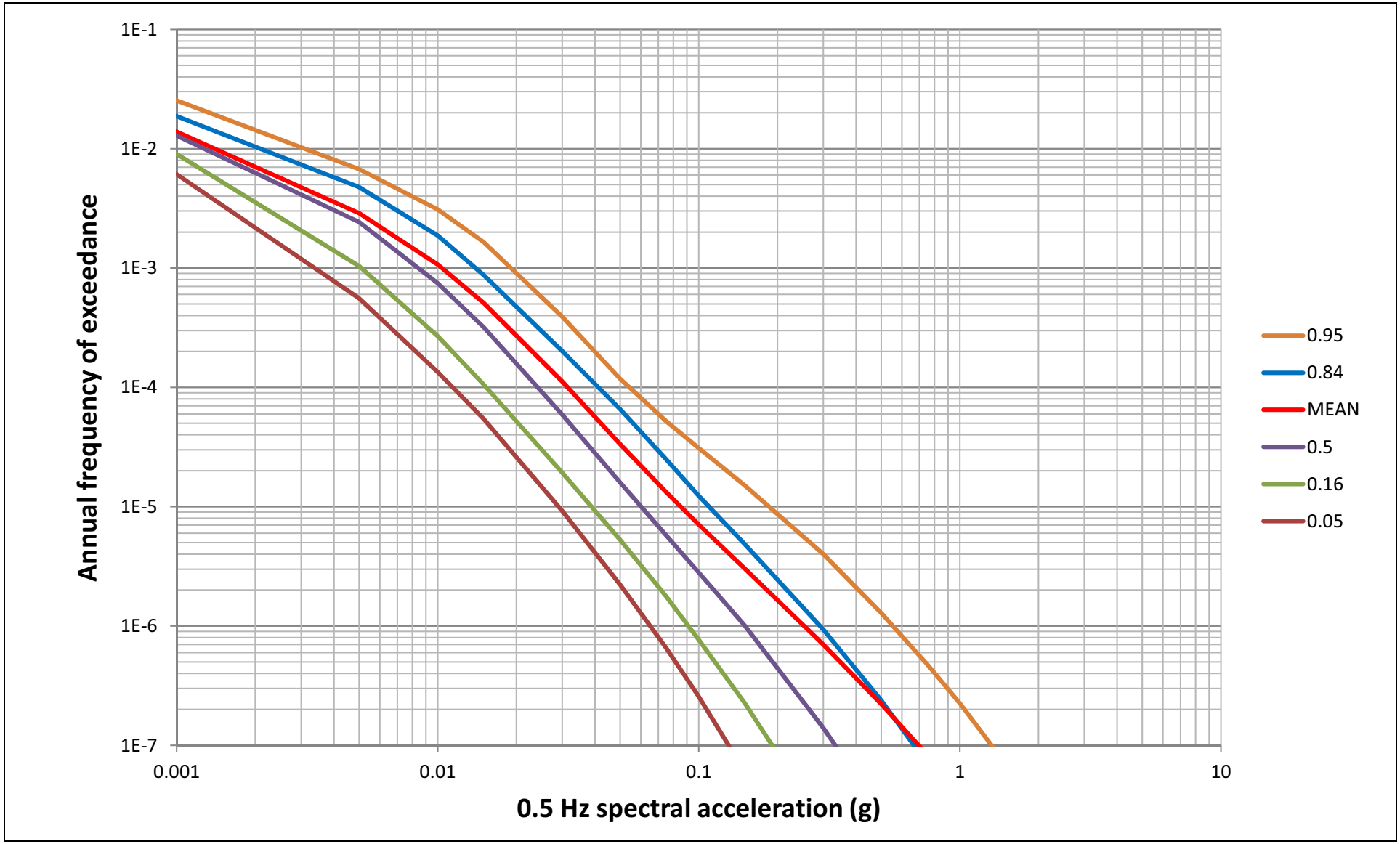

NAPS COL 2.0-27-A
NAPS ESP VAR 2.0-4

Figure 2.5.2-231 Mean and Fractile Rock Hazard Curves for 1 Hz

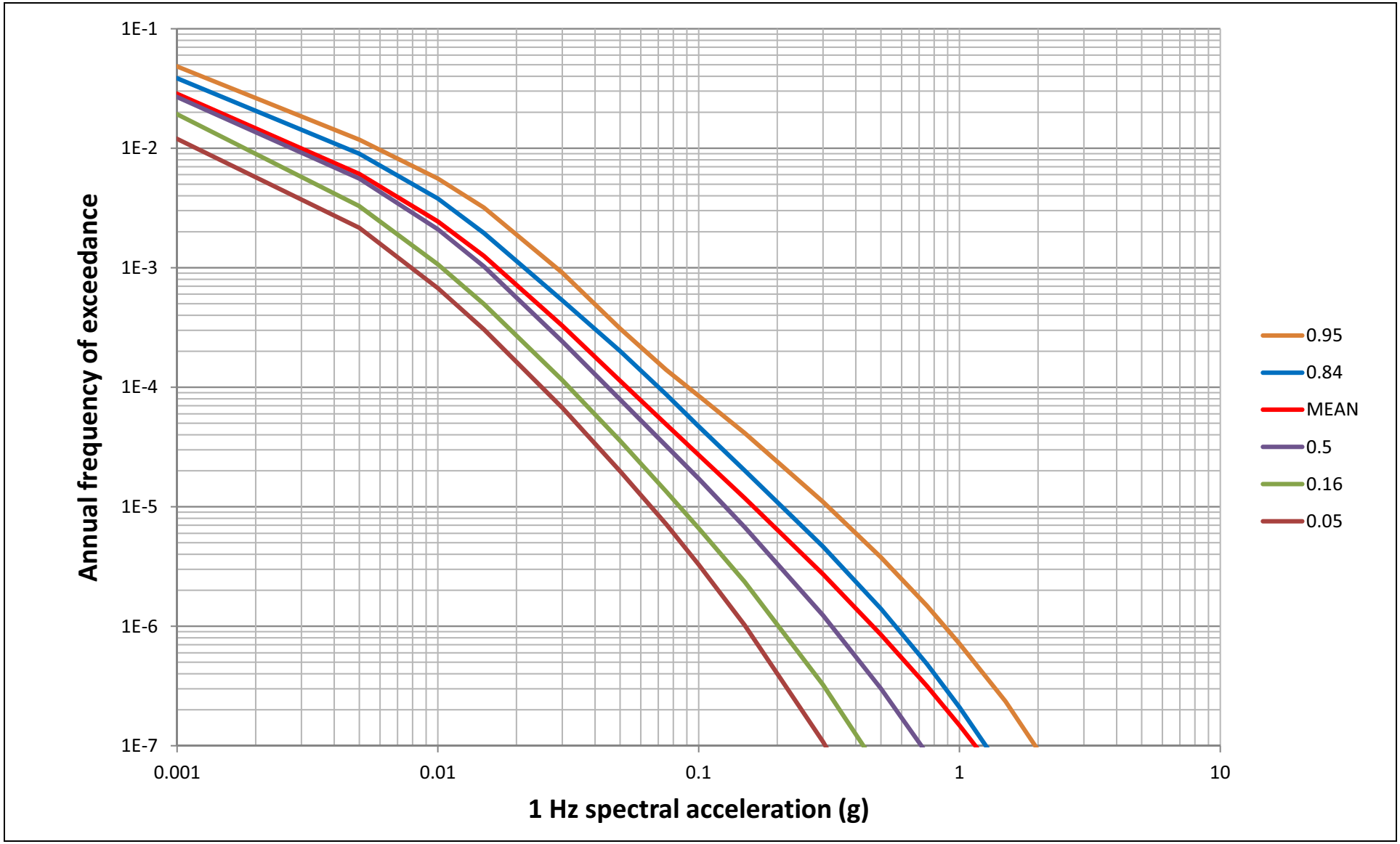

NAPS COL 2.0-27-A
NAPS ESP VAR 2.0-4

Figure 2.5.2-232 Mean and Fractile Rock Hazard Curves for 2.5 Hz

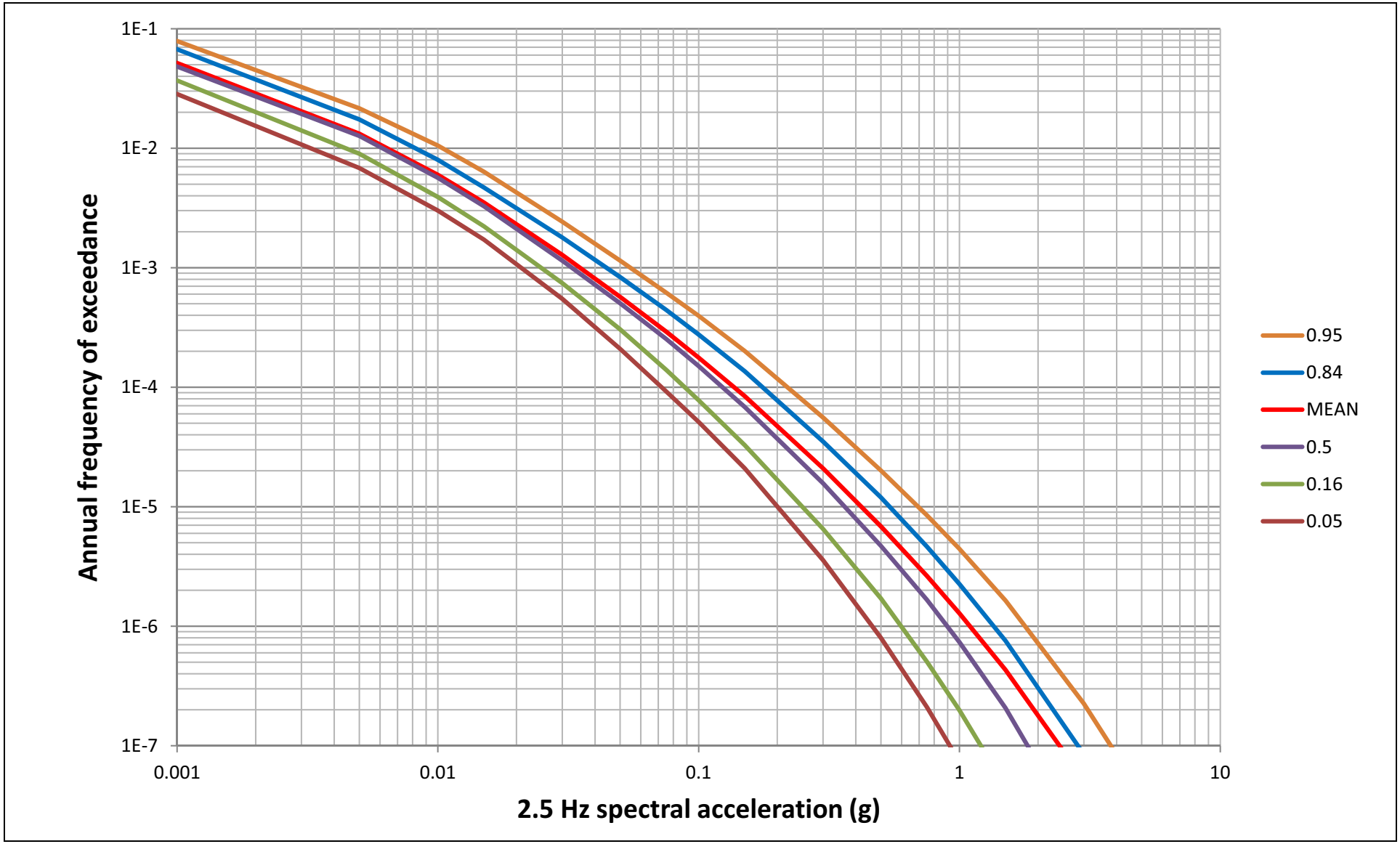

NAPS COL 2.0-27-A
NAPS ESP VAR 2.0-4

Figure 2.5.2-233 Mean and Fractile Rock Hazard Curves for 5 Hz

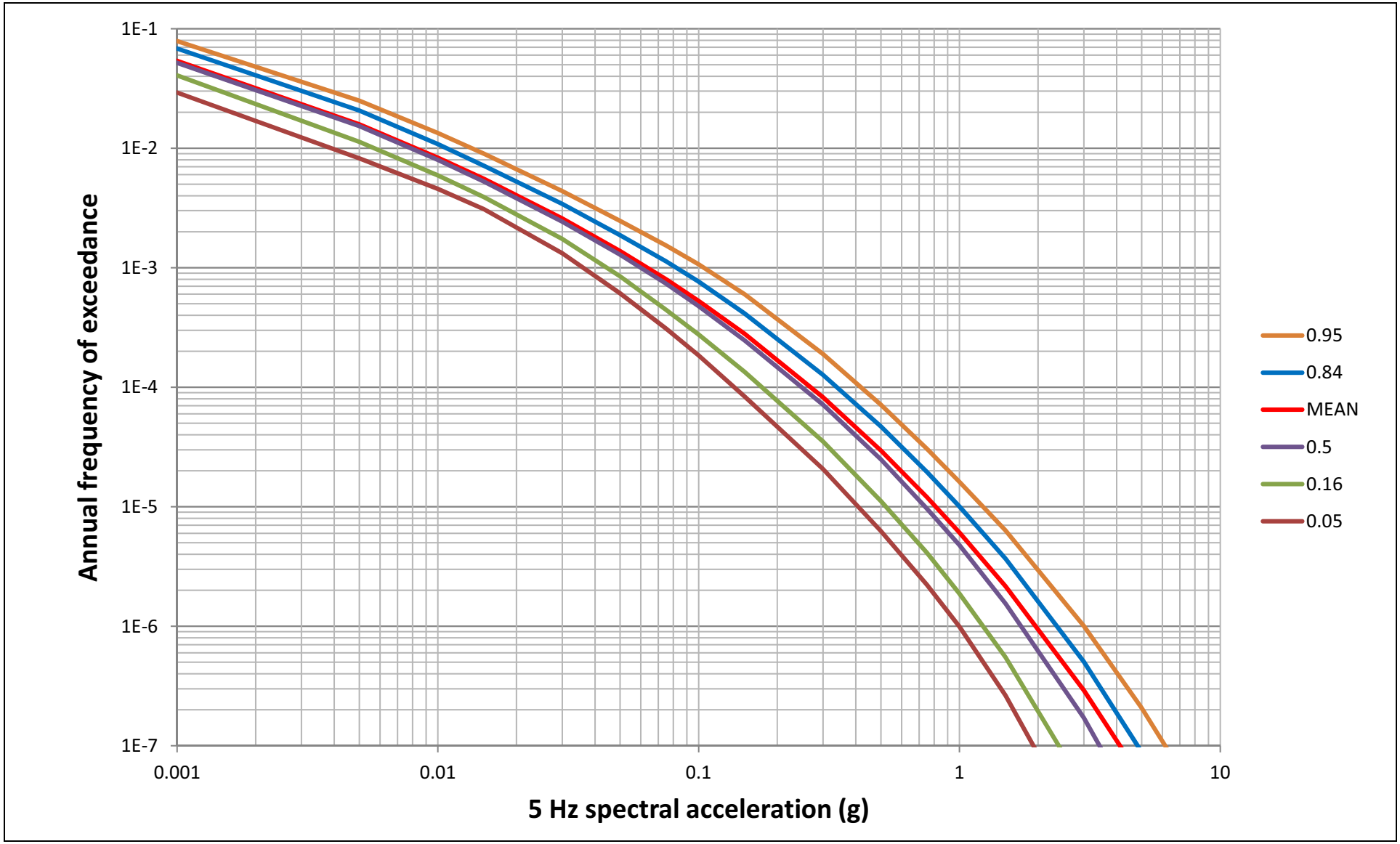

NAPS COL 2.0-27-A
NAPS ESP VAR 2.0-4

Figure 2.5.2-234 Mean and Fractile Rock Hazard Curves for 10 Hz

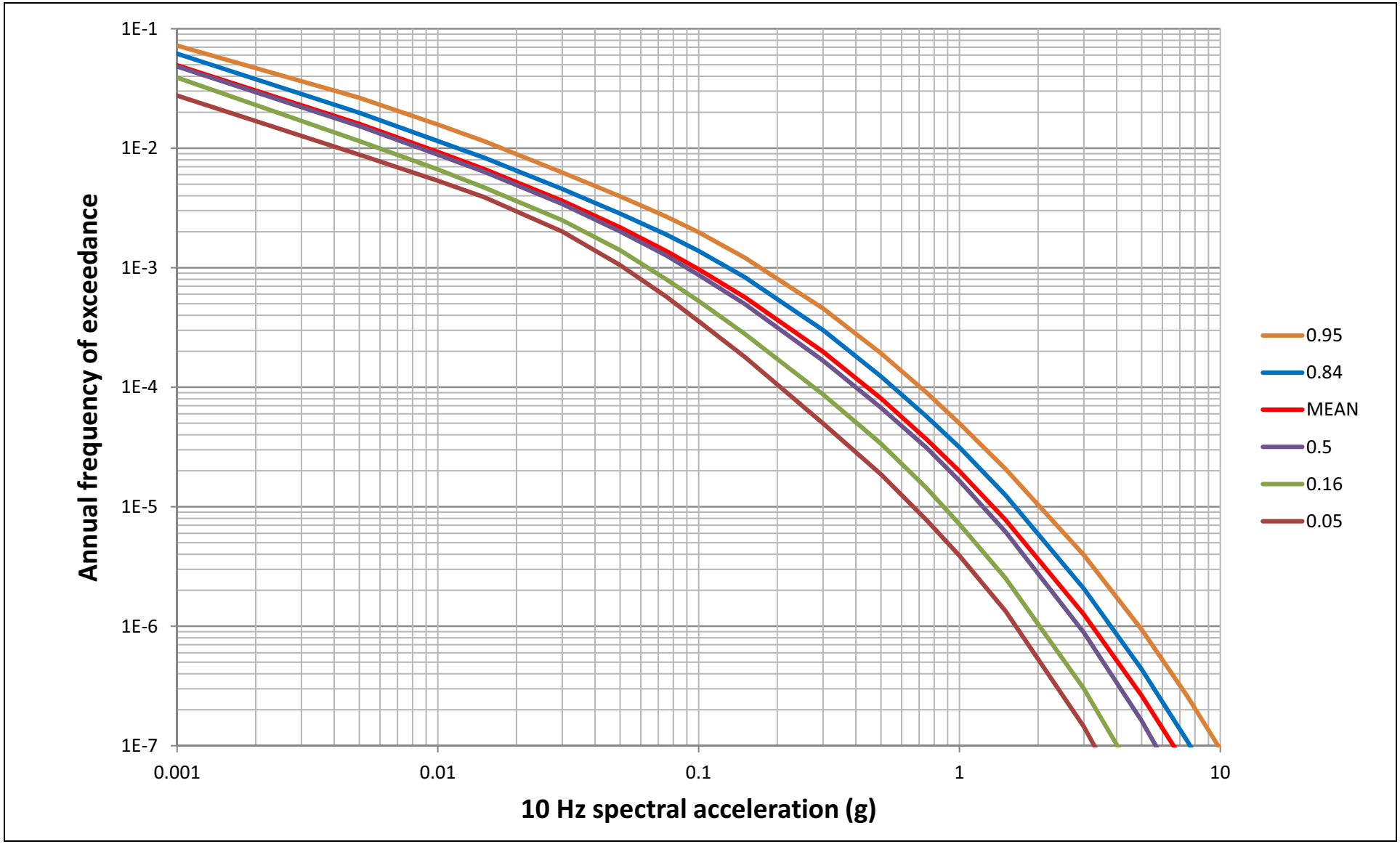

NAPS COL 2.0-27-A
NAPS ESP VAR 2.0-4

Figure 2.5.2-235 Mean and Fractile Rock Hazard Curves for 25 Hz

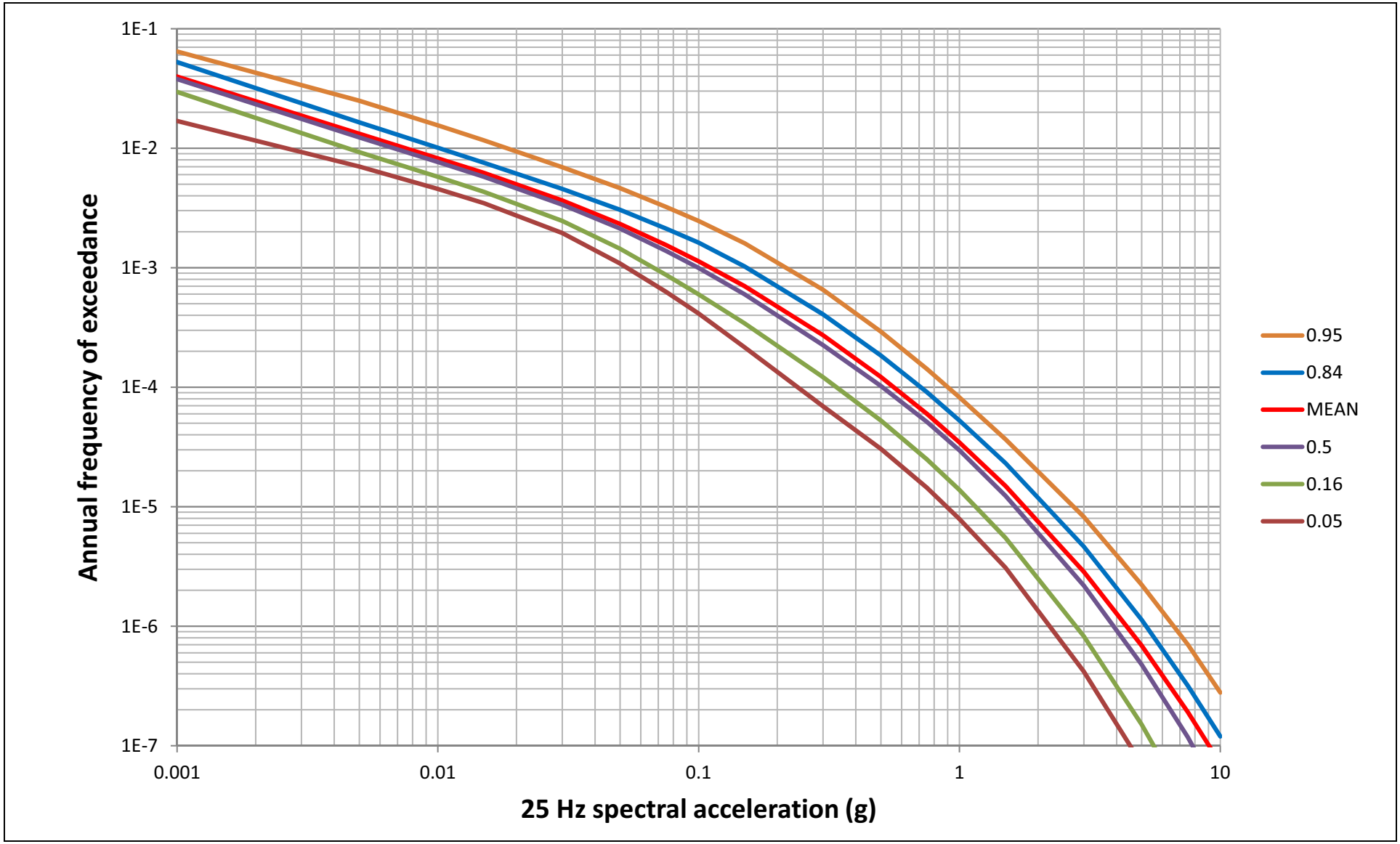

NAPS COL 2.0-27-A
NAPS ESP VAR 2.0-4

Figure 2.5.2-236 Mean and Fractile Rock Hazard Curves for PGA

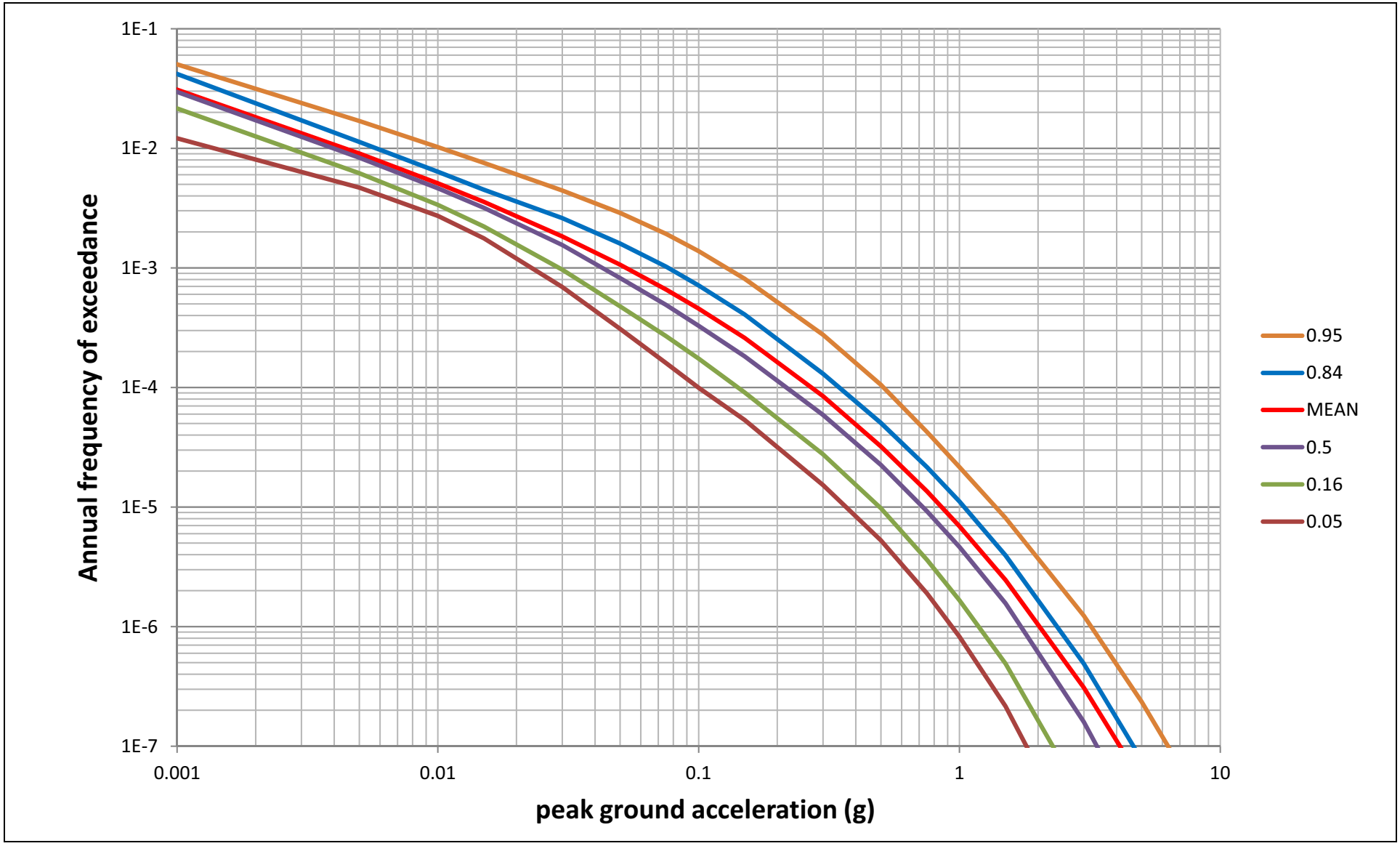

NAPS COL 2.0-27-A
NAPS ESP VAR 2.0-4

Figure 2.5.2-237 1 Hz Mean Rock Hazard from Background, Charleston, New Madrid and Wabash Valley

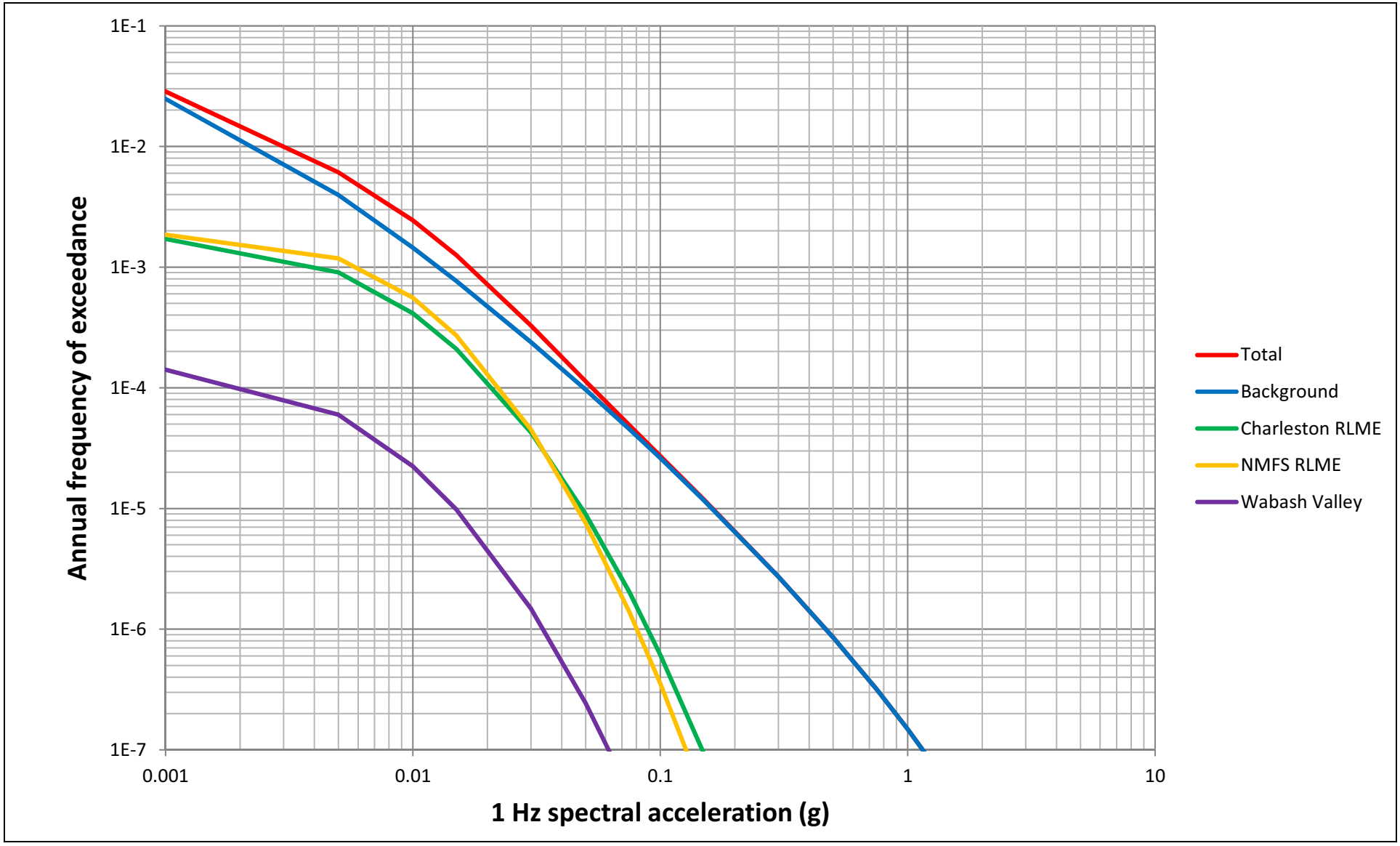

NAPS COL 2.0-27-A
NAPS ESP VAR 2.0-4

Figure 2.5.2-238 10 Hz Mean Rock Hazard from Background, Charleston, New Madrid and Wabash Valley

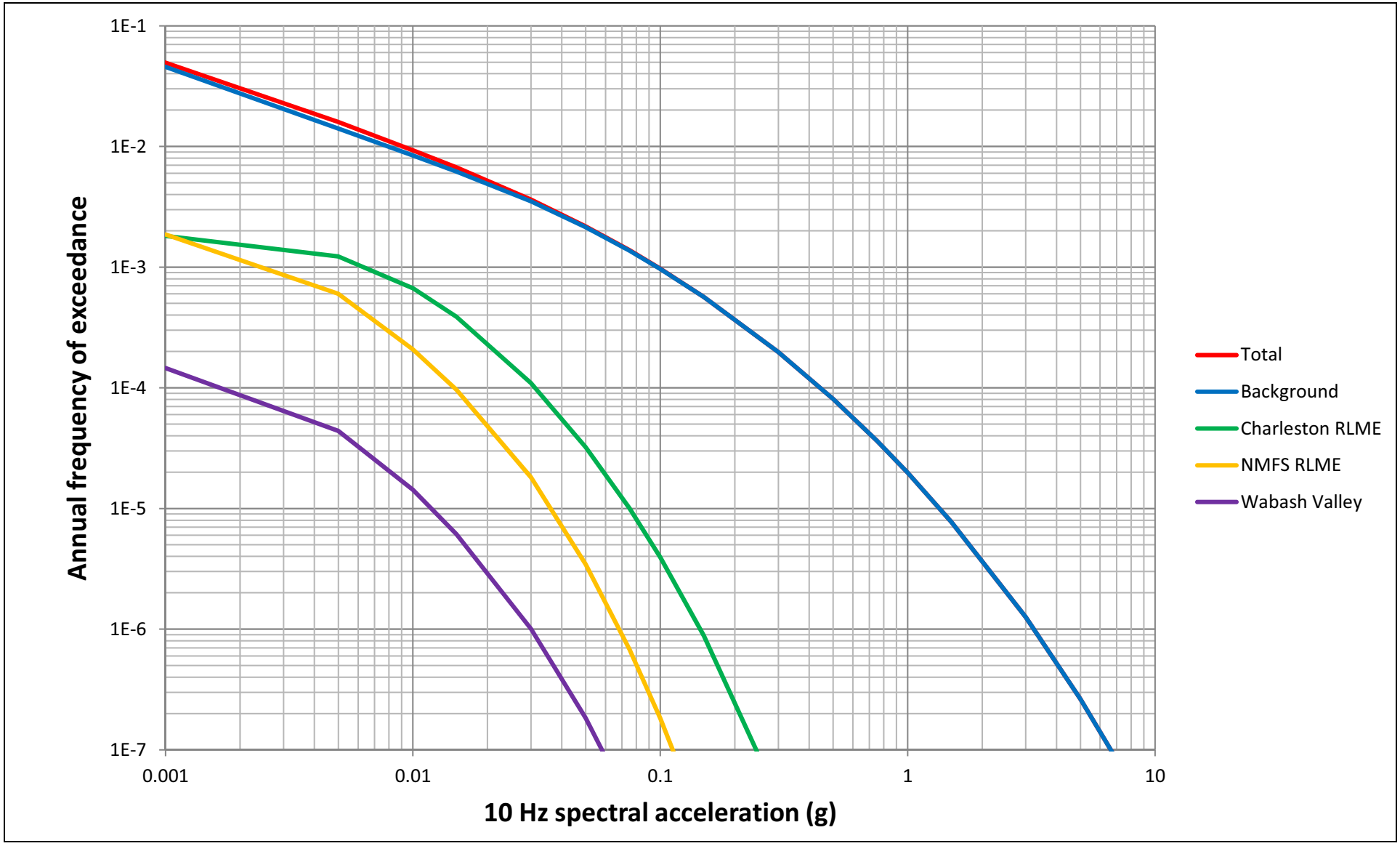

NAPS COL 2.0-27-A
NAPS ESP VAR 2.0-4

Figure 2.5.2-239 1 Hz Mean Rock Hazard from Individual Weighted Background Sources

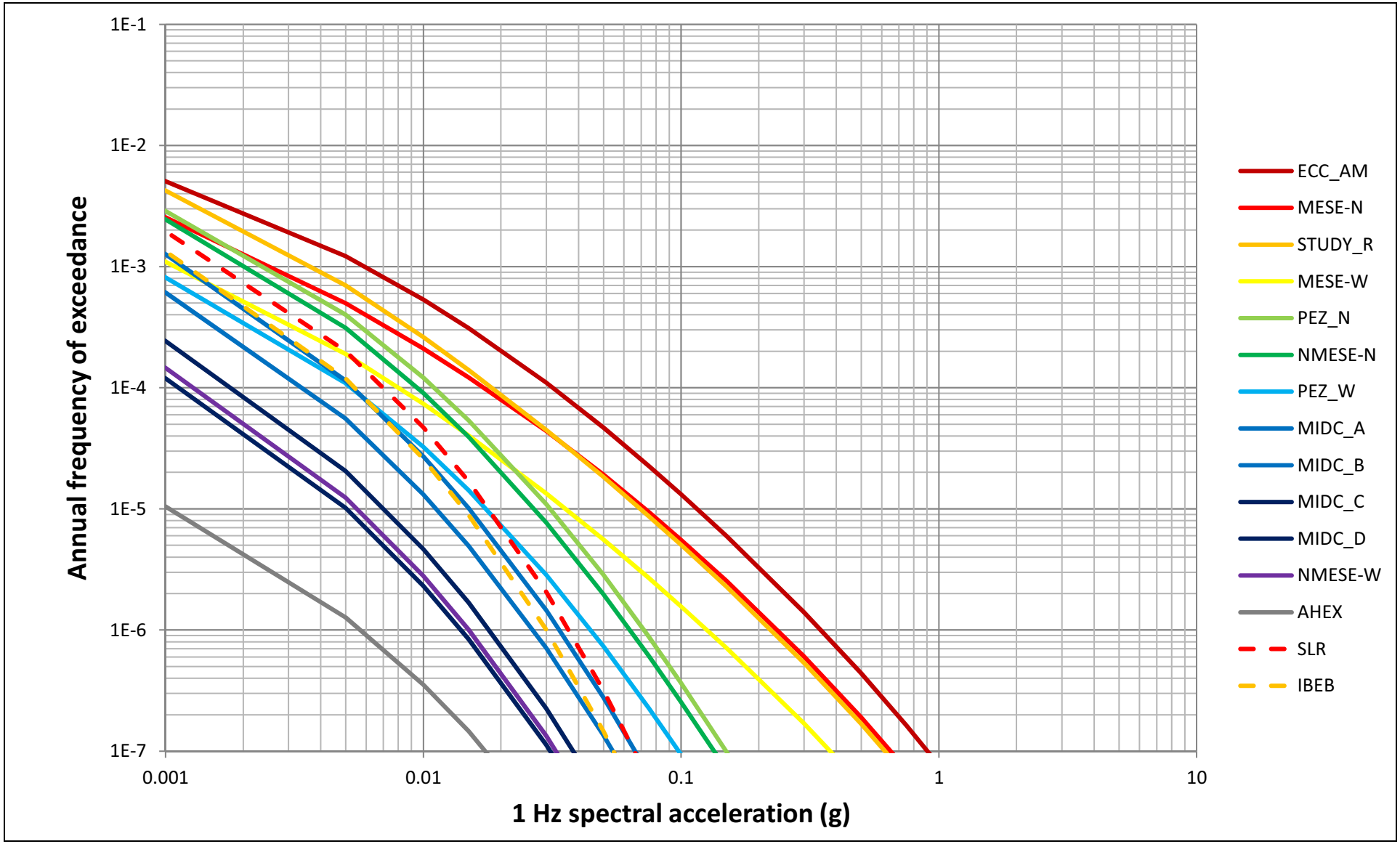

NAPS COL 2.0-27-A
NAPS ESP VAR 2.0-4

Figure 2.5.2-240 10 Hz Mean Rock Hazard from Individual Weighted Background Sources

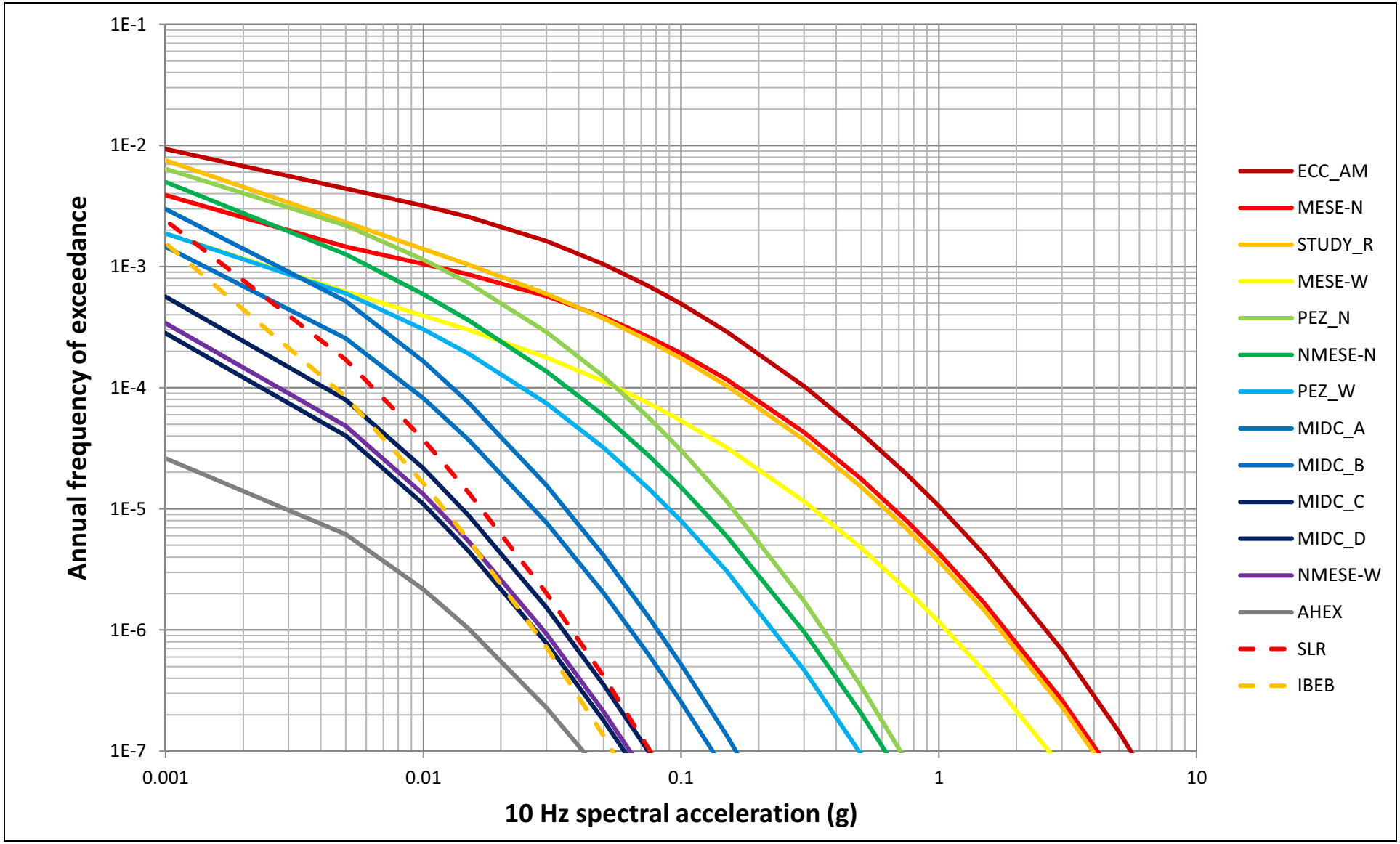

NAPS COL 2.0-27-A
NAPS ESP VAR 2.0-4

Figure 2.5.2-241 1 Hz Mean Rock Hazard from Individual Weighted Charleston Sources

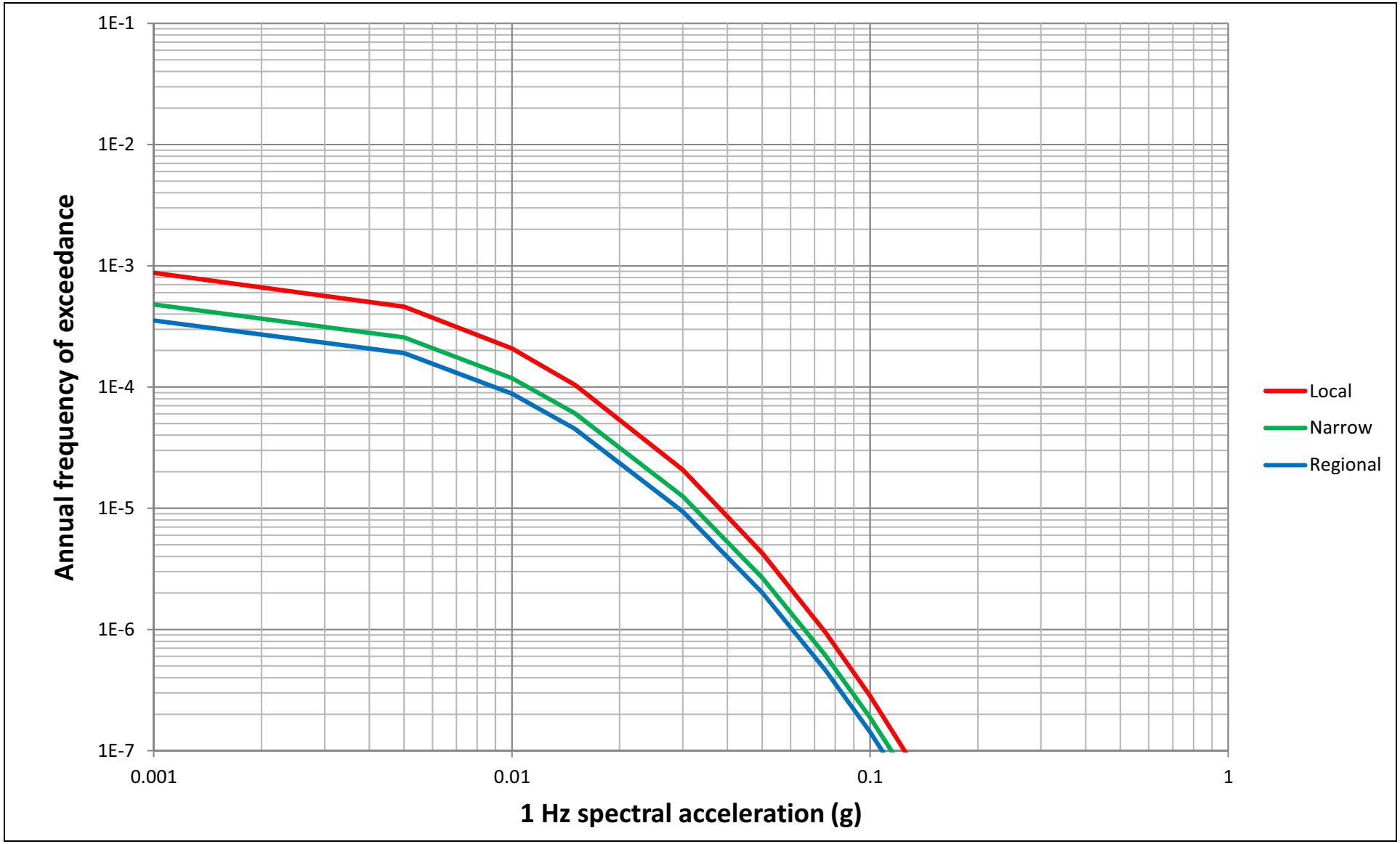

NAPS COL 2.0-27-A
NAPS ESP VAR 2.0-4

Figure 2.5.2-242 10 Hz Mean Rock Hazard from Individual Weighted Charleston Sources

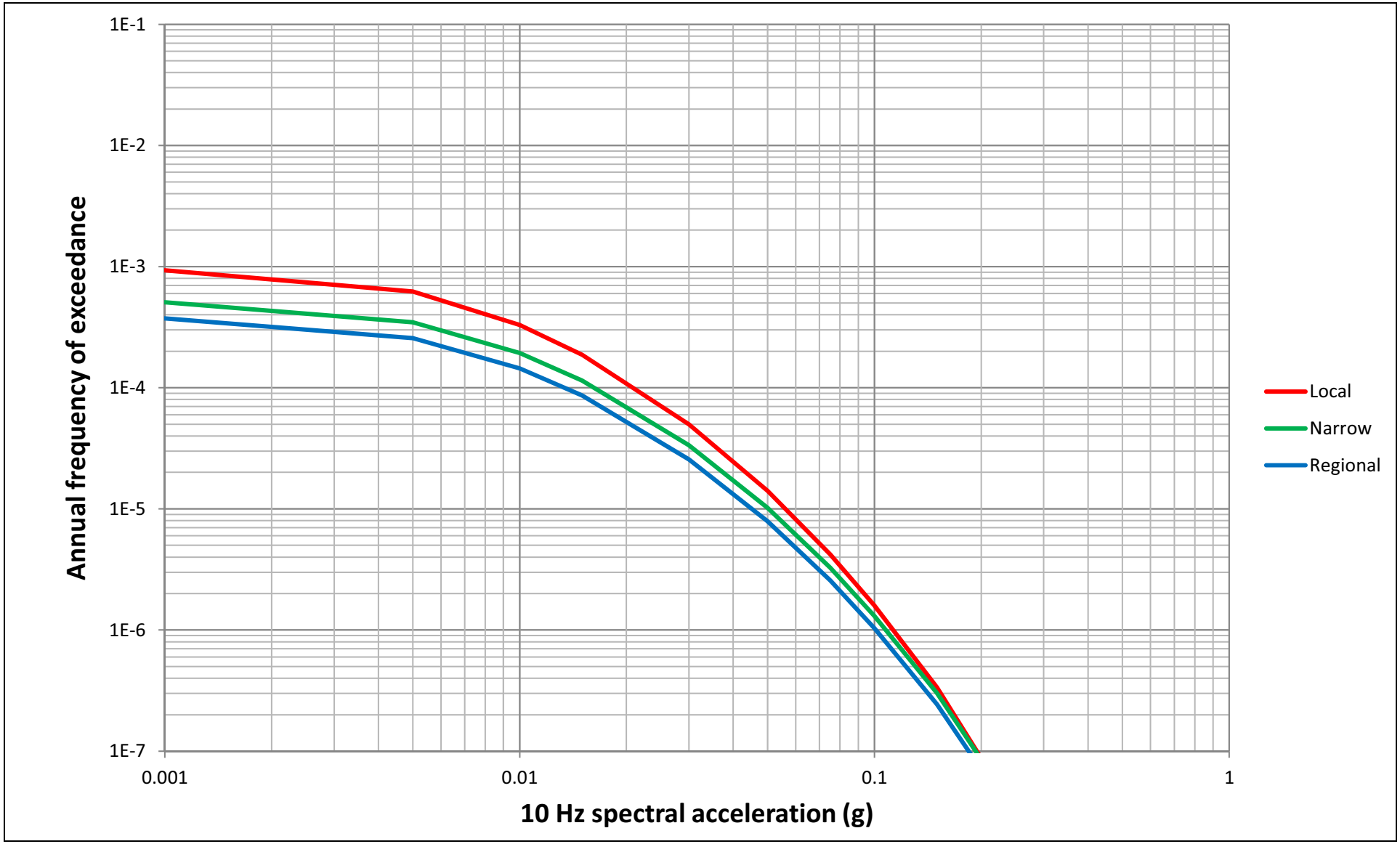

NAPS COL 2.0-27-A
NAPS ESP VAR 2.0-4

Figure 2.5.2-243 Unweighted Sensitivity to the 9 EPRI (Background) Ground Motion Prediction Equations (GMPE), 1 Hz

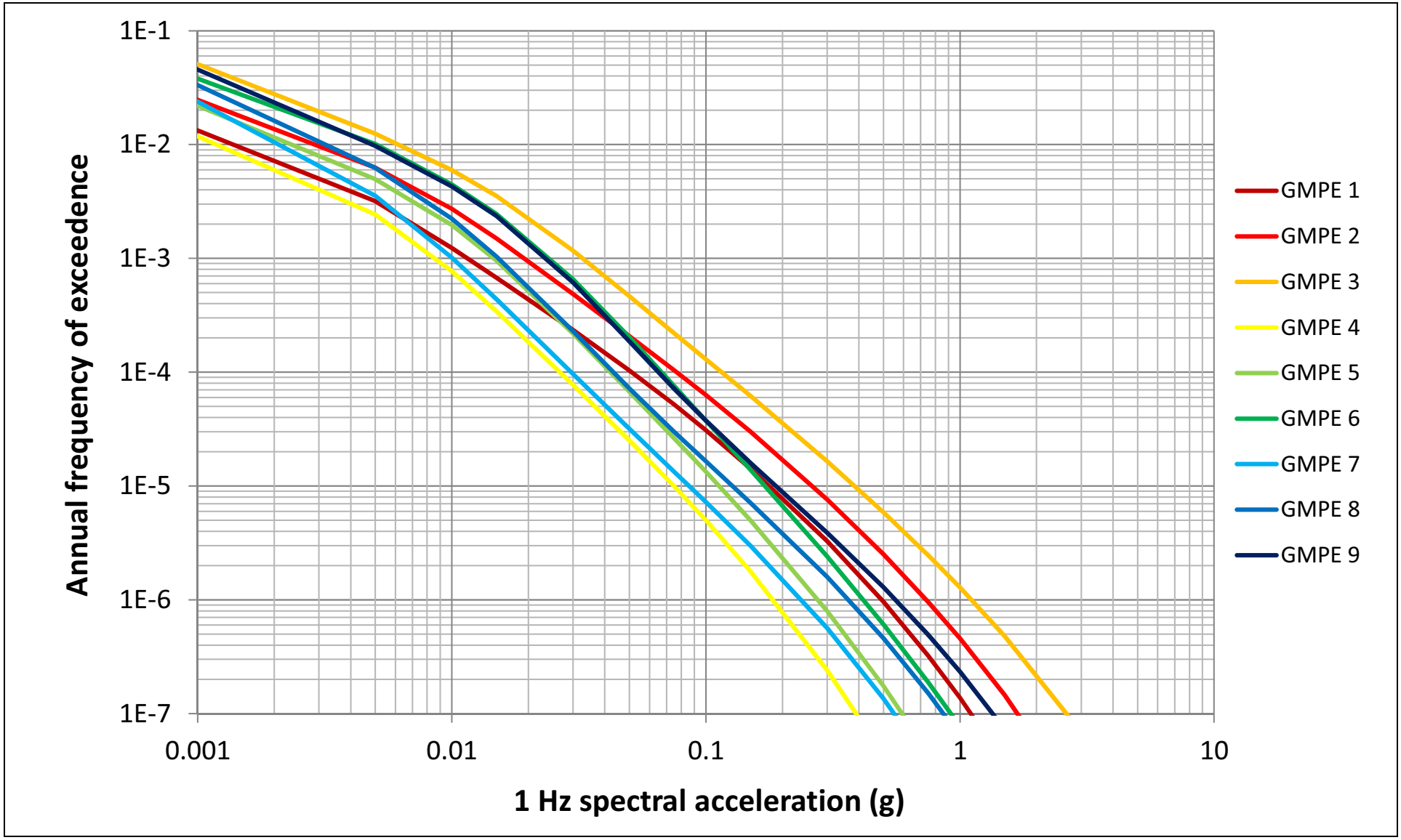

NAPS COL 2.0-27-A
NAPS ESP VAR 2.0-4

Figure 2.5.2-244 Unweighted Sensitivity to the 9 EPRI (Background) Ground Motion Prediction Equations (GMPE), 10 Hz

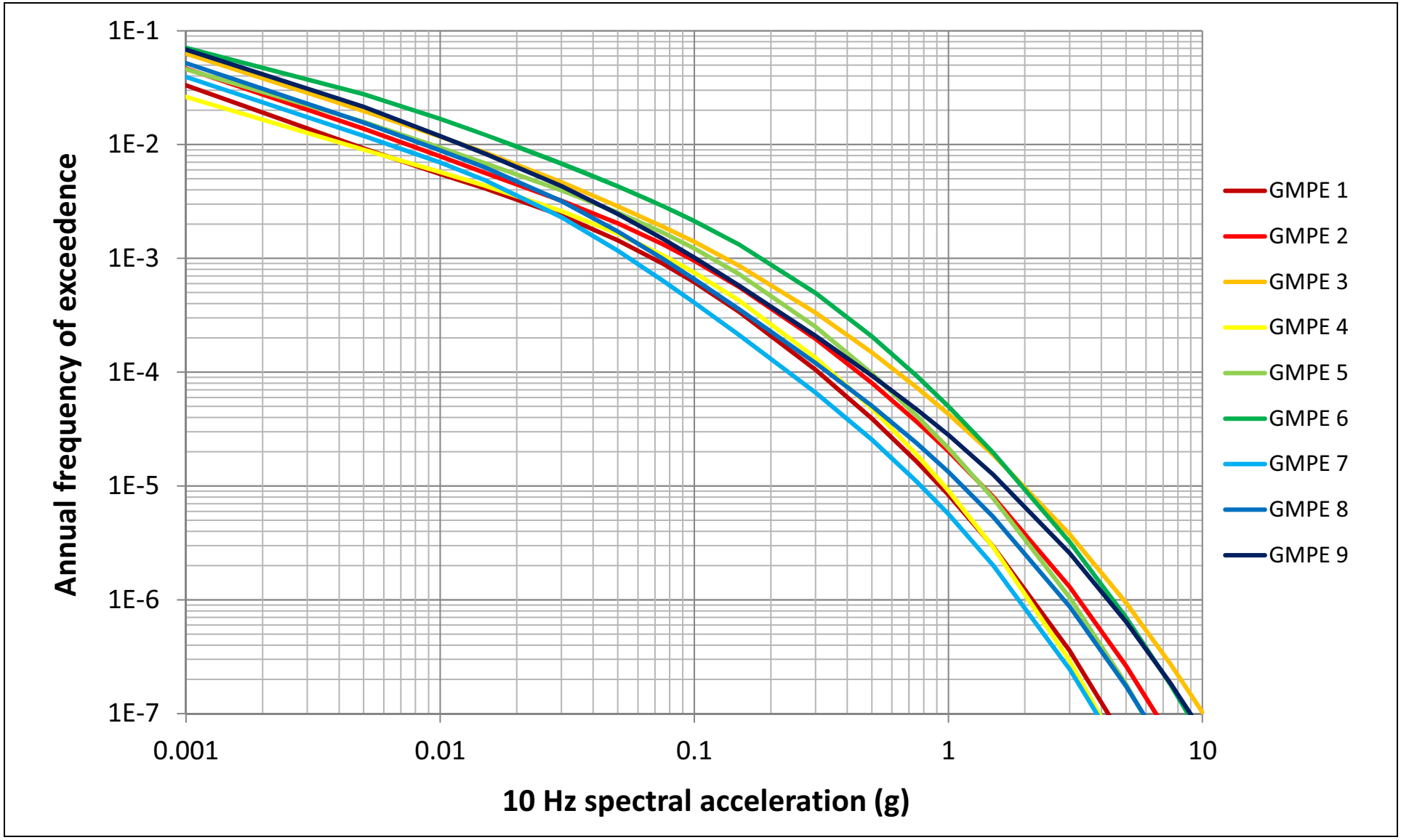

NAPS COL 2.0-27-A
NAPS ESP VAR 2.0-4

Figure 2.5.2-245 Unweighted Sensitivity to the 12 EPRI (RLME) Ground Motion Prediction Equations (GMPE), 1 Hz

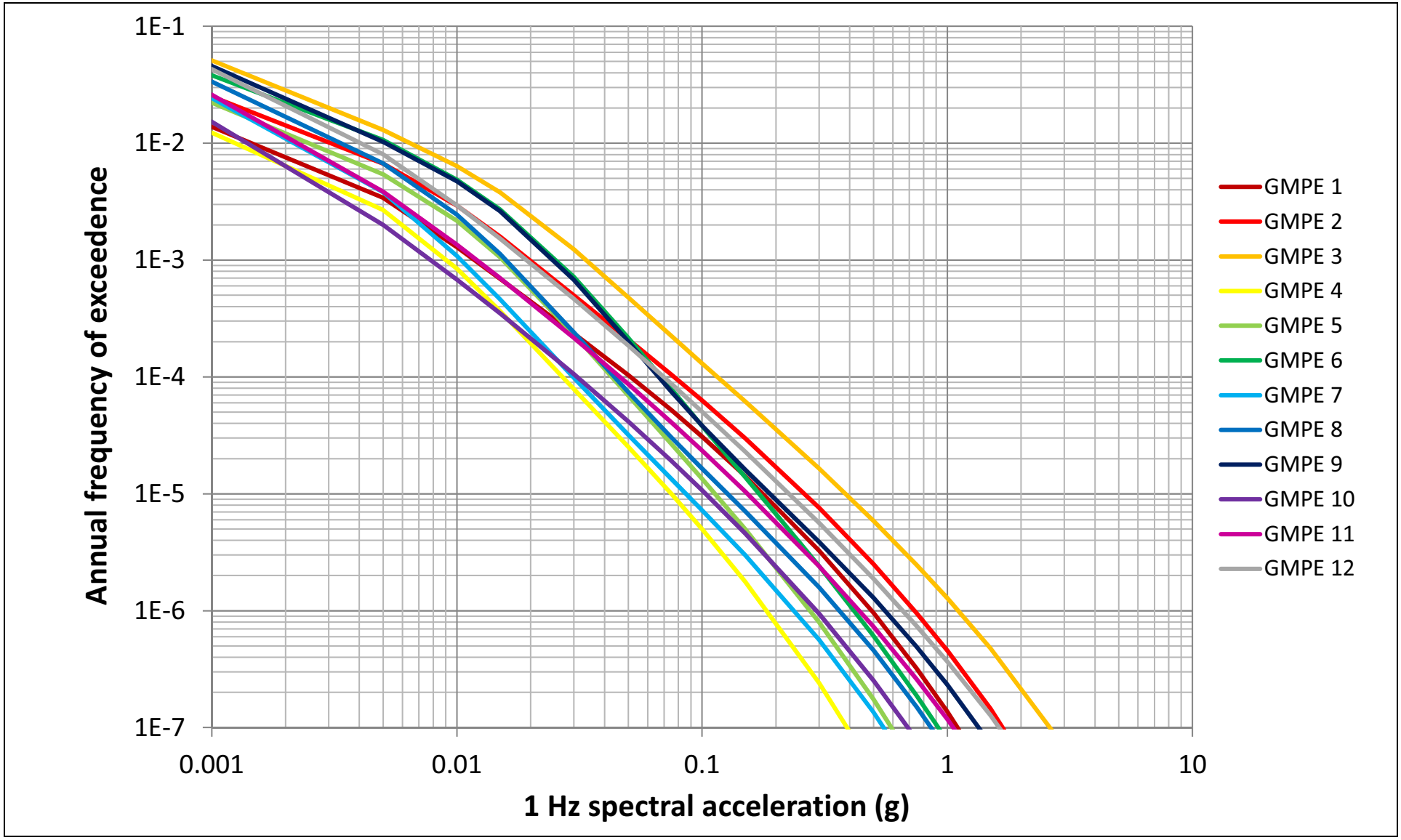

NAPS COL 2.0-27-A
NAPS ESP VAR 2.0-4

Figure 2.5.2-246 Unweighted Sensitivity to the 12 EPRI (RLME) Ground Motion Prediction Equations (GMPE), 10 Hz

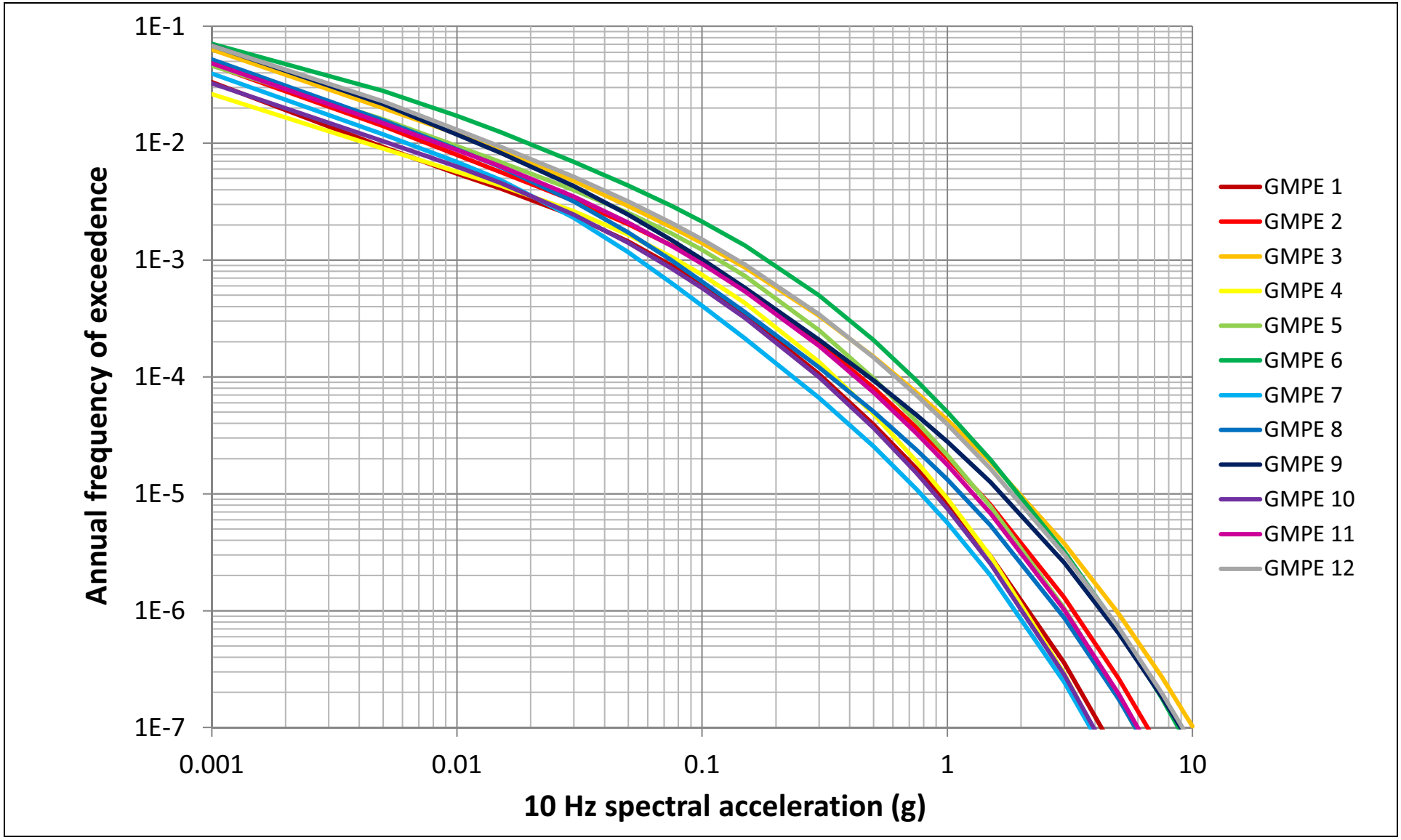

NAPS COL 2.0-27-A
NAPS ESP VAR 2.0-4

Figure 2.5.2-247 1 Hz Median Rock Hazard from Background, Charleston, New Madrid and Wabash Valley

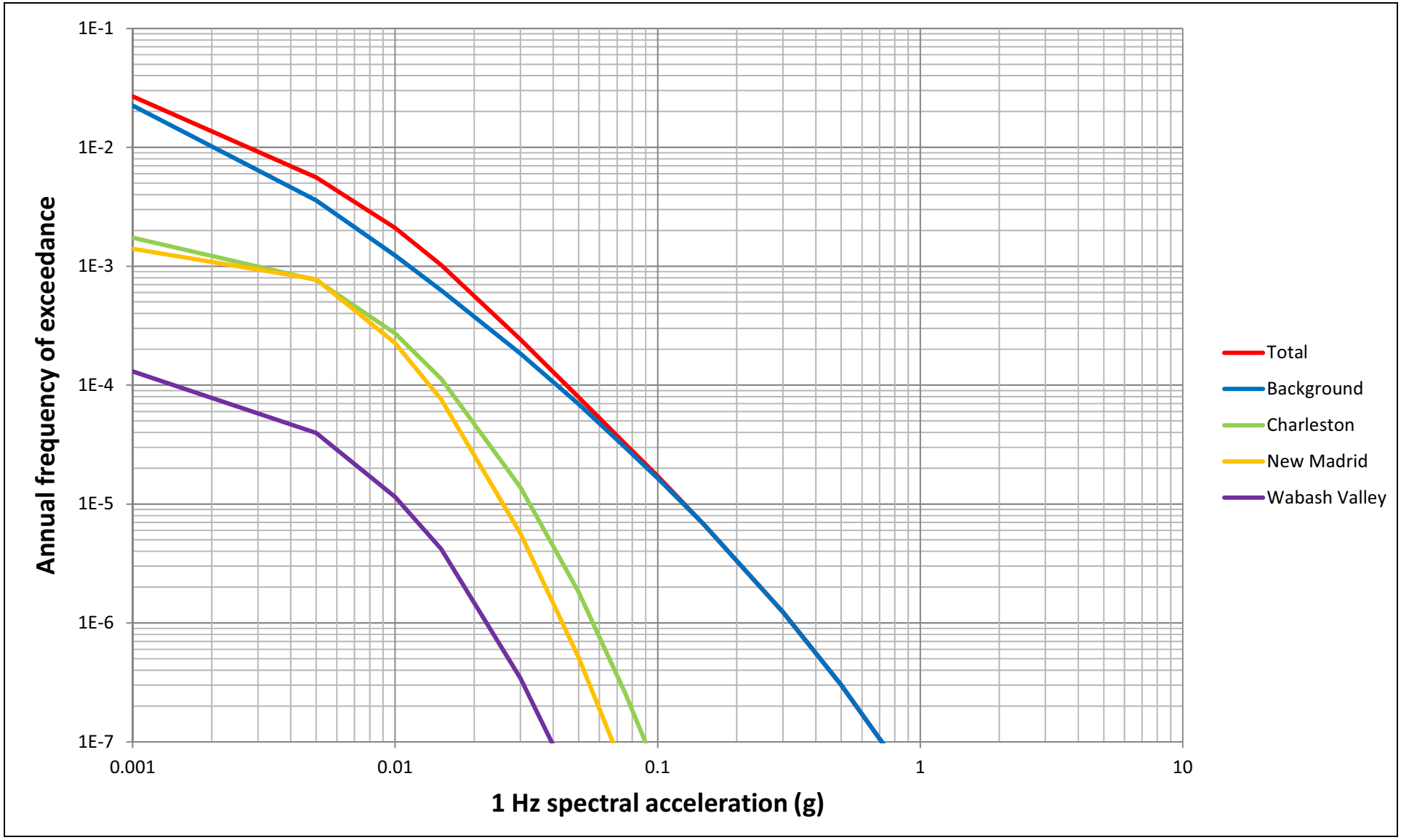

NAPS COL 2.0-27-A
NAPS ESP VAR 2.0-4

Figure 2.5.2-248 10 Hz Median Rock Hazard from Background, Charleston, New Madrid and Wabash Valley

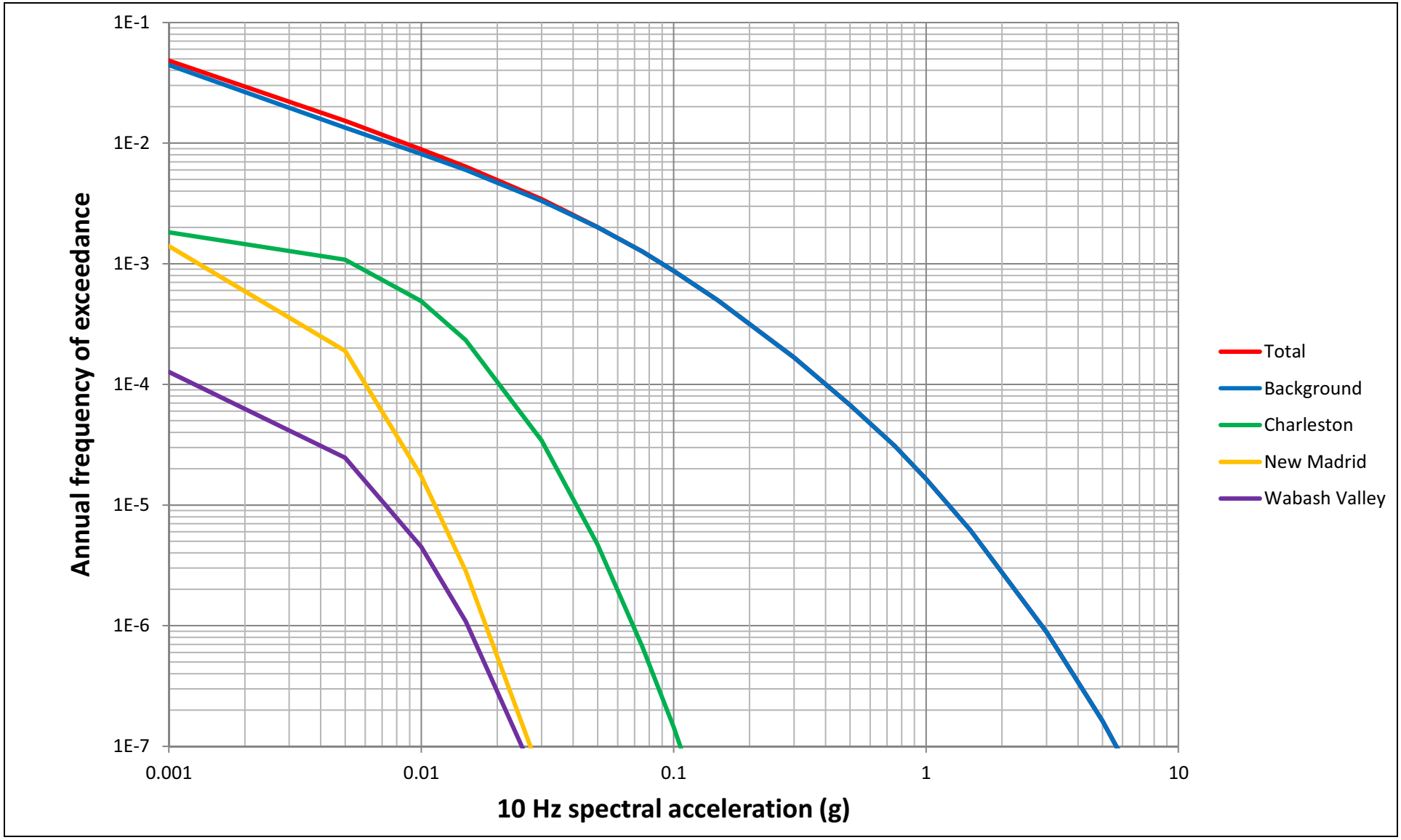

NAPS COL 2.0-27-A
NAPS ESP VAR 2.0-4

Figure 2.5.2-249 Mean Total Rock Hazard Curves for 7 Spectral Frequencies

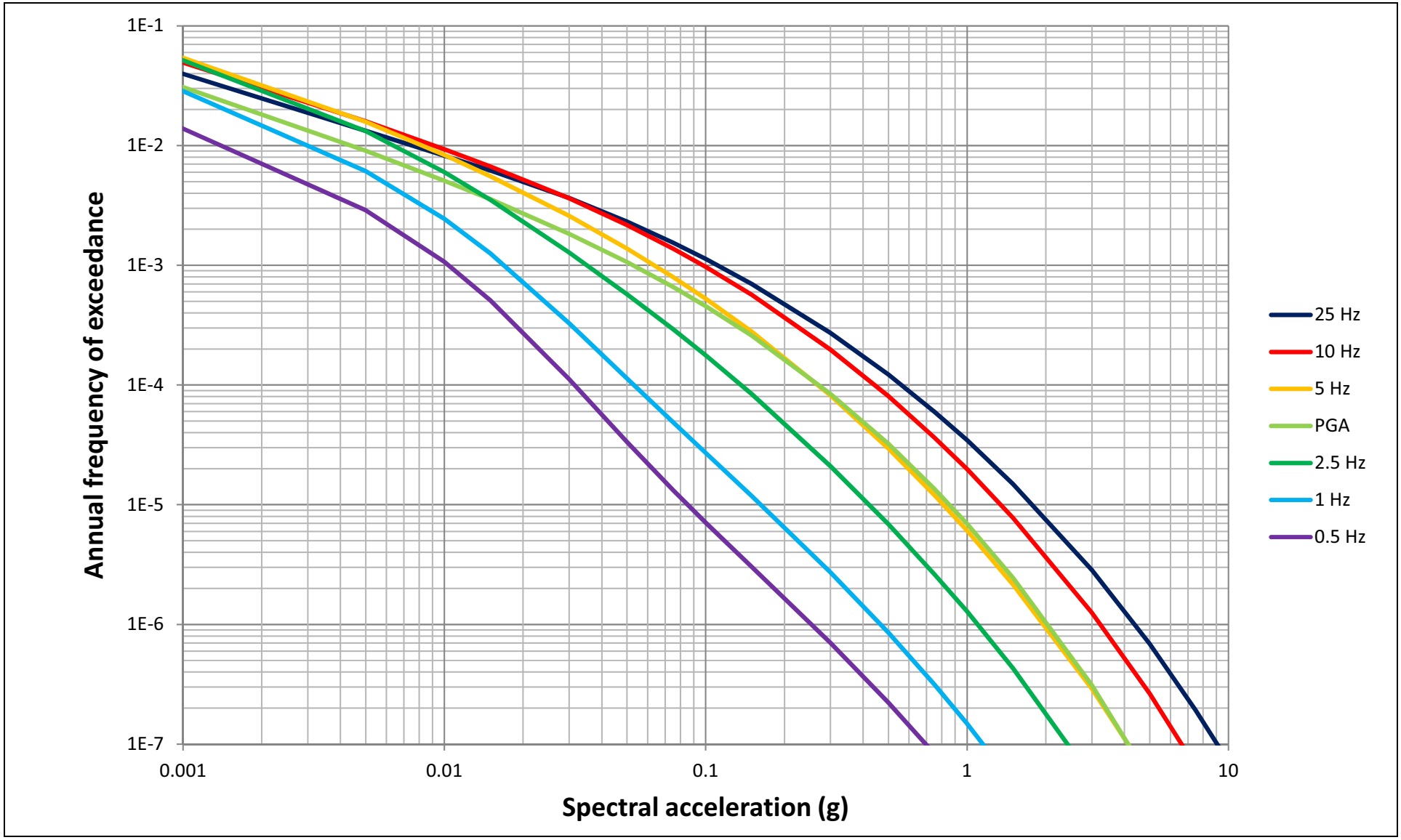

NAPS COL 2.0-27-A
NAPS ESP VAR 2.0-4

Figure 2.5.2-250 Mean 10^{-4} Deaggregation Plot for 1 and 2.5 Hz (LF)

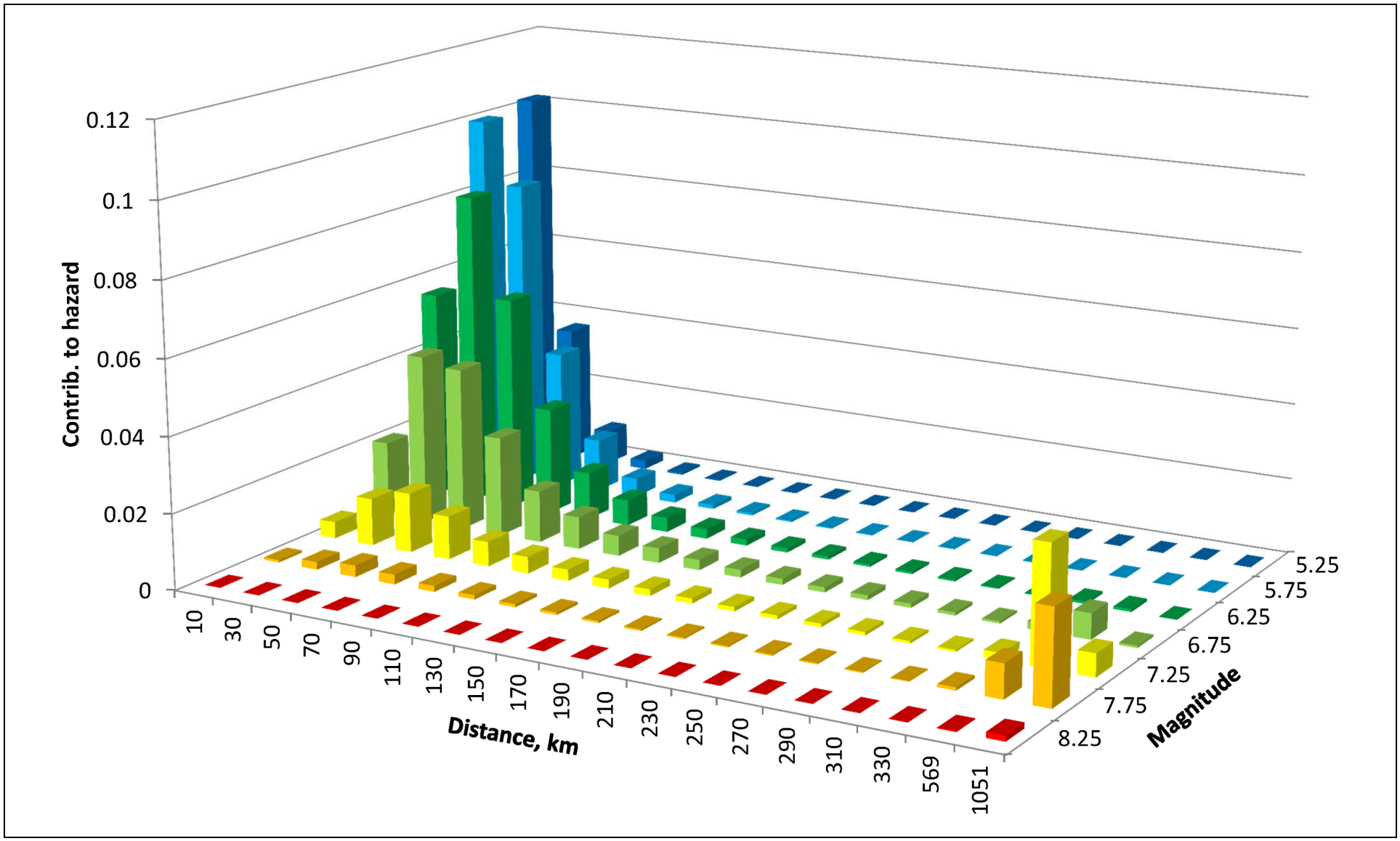

NAPS COL 2.0-27-A
NAPS ESP VAR 2.0-4

Figure 2.5.2-251 Mean 10^{-4} Deaggregation Plot for 5 and 10 Hz (HF)

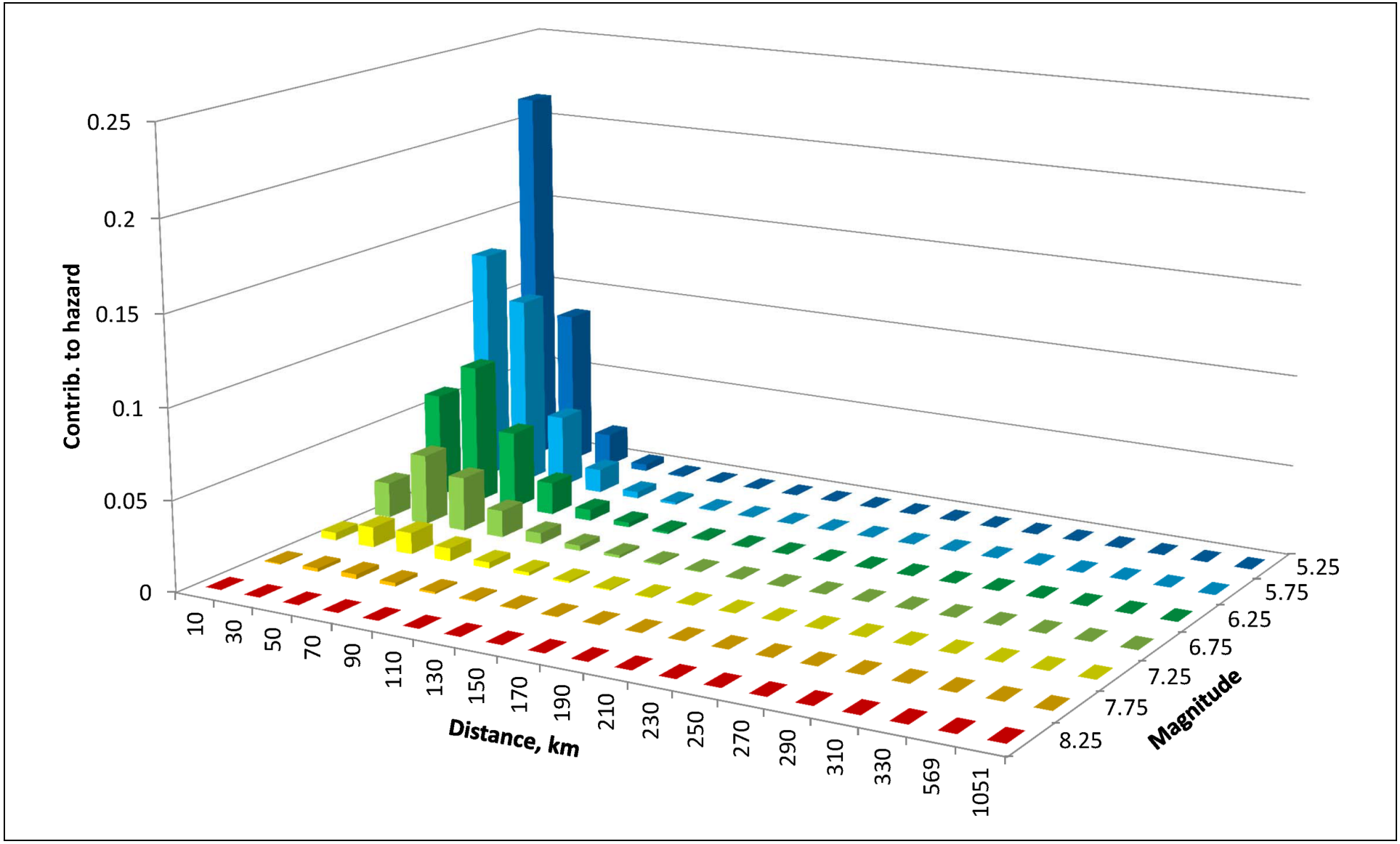

NAPS COL 2.0-27-A
NAPS ESP VAR 2.0-4

Figure 2.5.2-252 Mean 10^{-5} Deaggregation Plot for 1 and 2.5 Hz (LF)

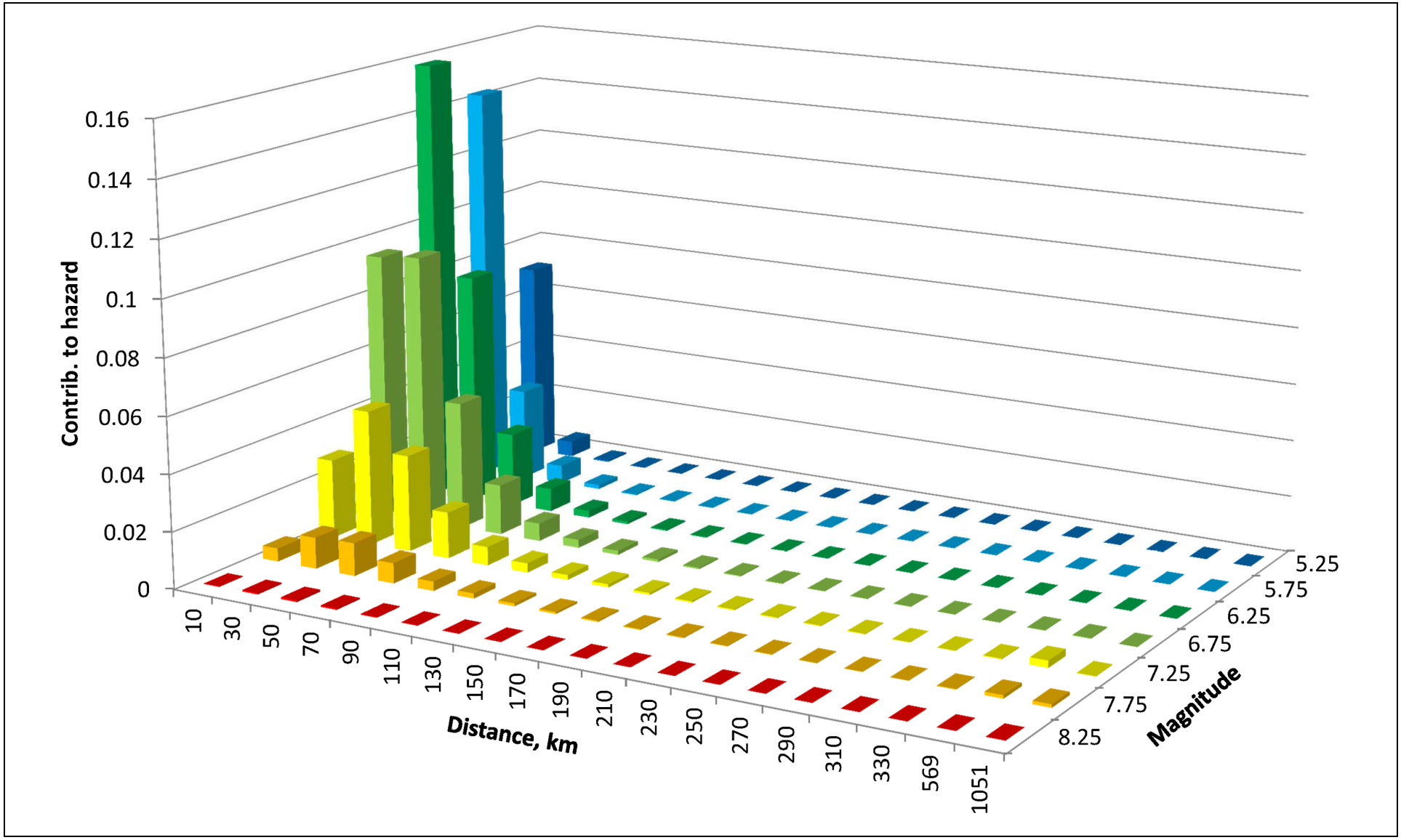

NAPS COL 2.0-27-A
NAPS ESP VAR 2.0-4

Figure 2.5.2-253 Mean 10^{-5} Deaggregation Plot for 5 and 10 Hz (HF)

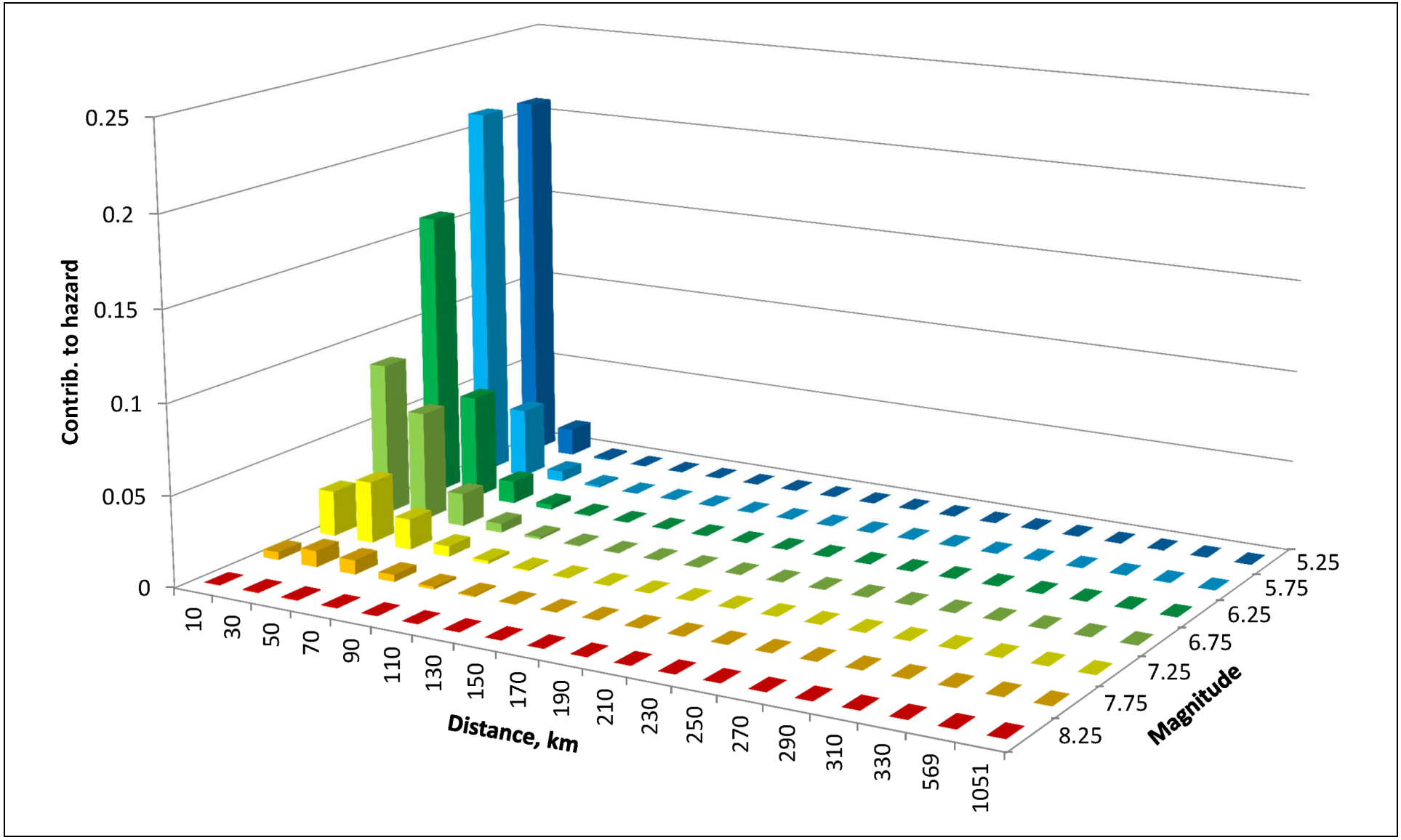

NAPS COL 2.0-27-A
NAPS ESP VAR 2.0-4

Figure 2.5.2-254 Mean 10^{-6} Deaggregation Plot for 1 and 2.5 Hz (LF)

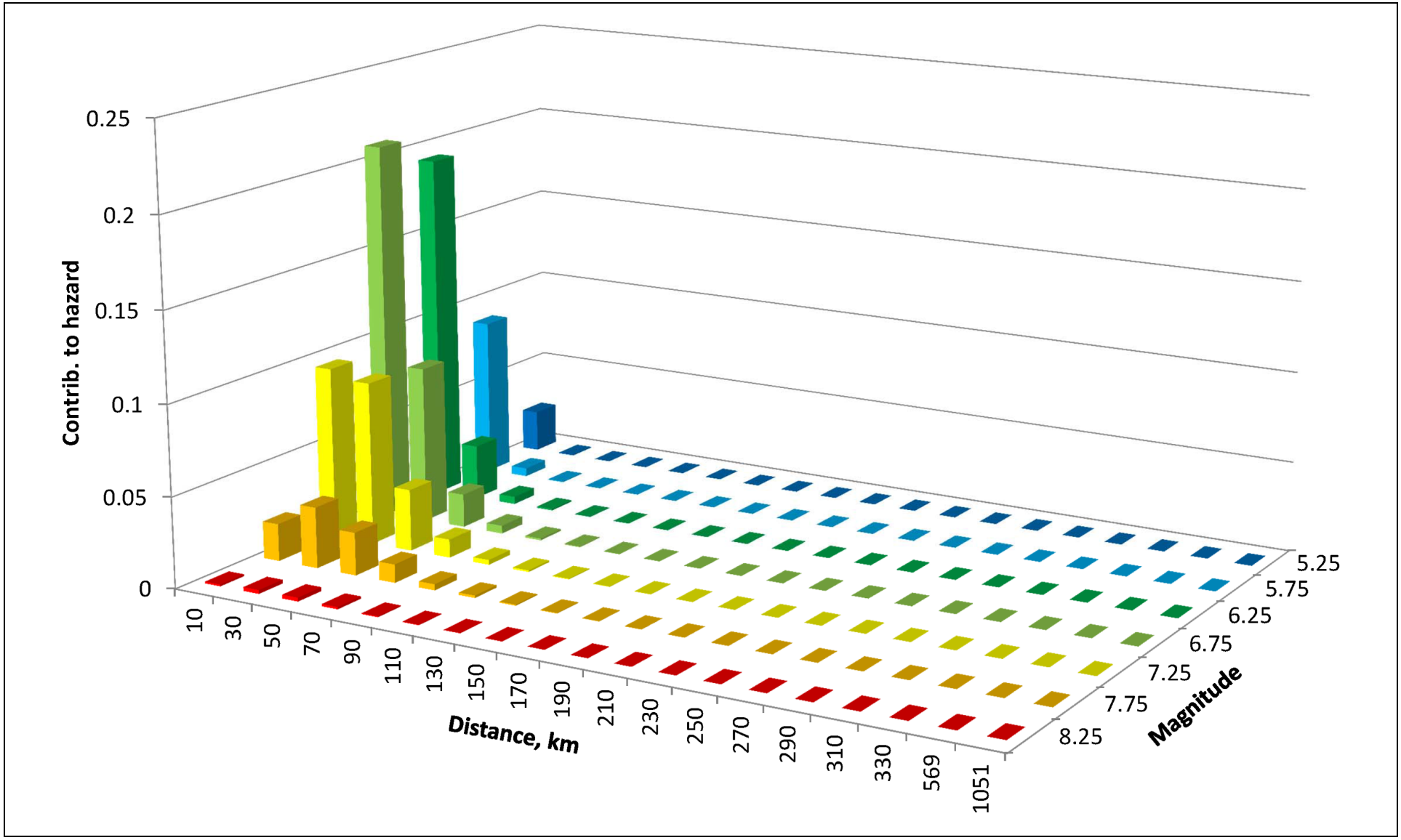

NAPS COL 2.0-27-A
NAPS ESP VAR 2.0-4

Figure 2.5.2-255 Mean 10^{-6} Deaggregation Plot for 5 and 10 Hz (HF)

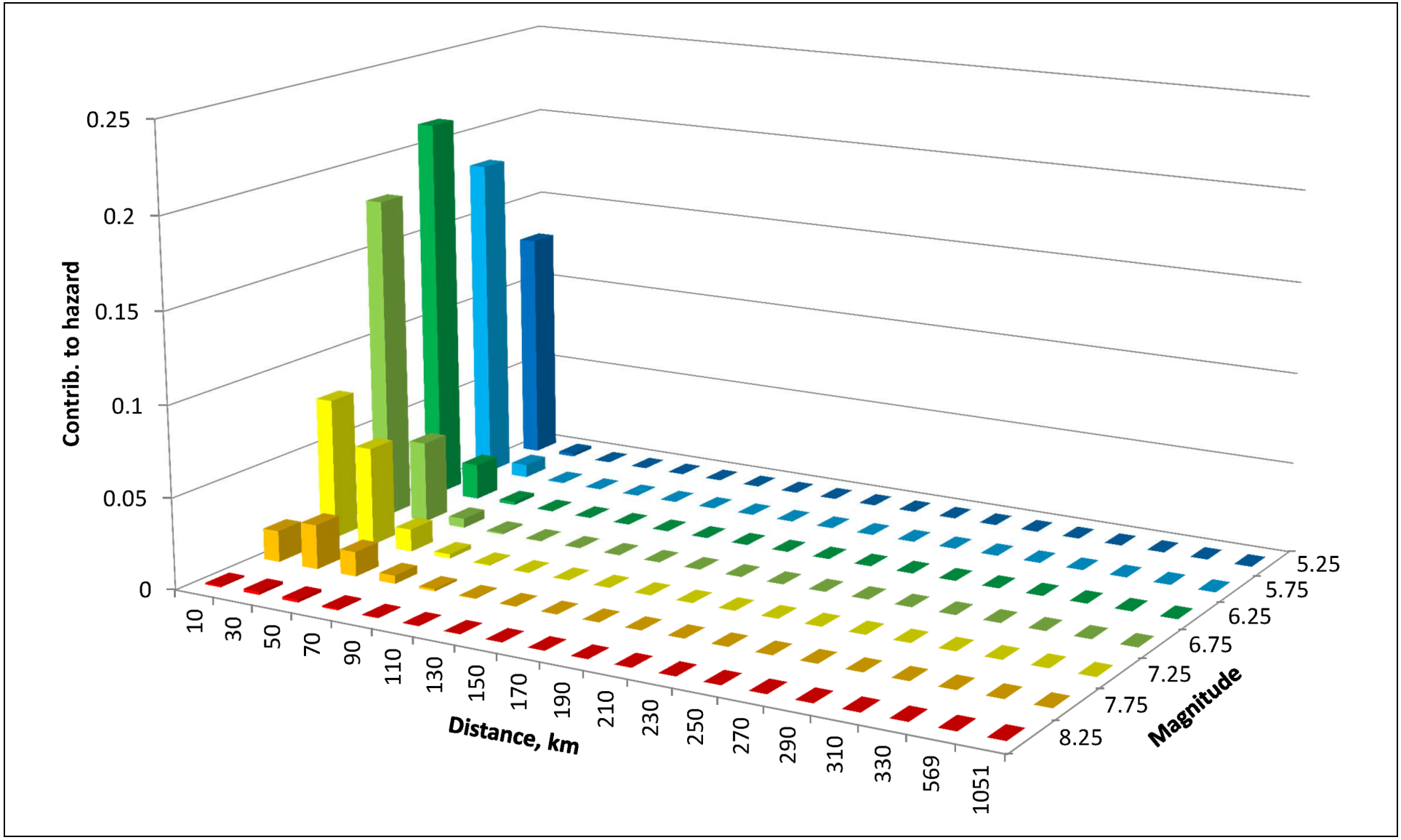

NAPS COL 2.0-27-A
NAPS ESP VAR 2.0-4

Figure 2.5.2-256 High and Low Frequency Mean UHRS for MAFEs of 10^{-4}, 10^{-5} and 10^{-6}

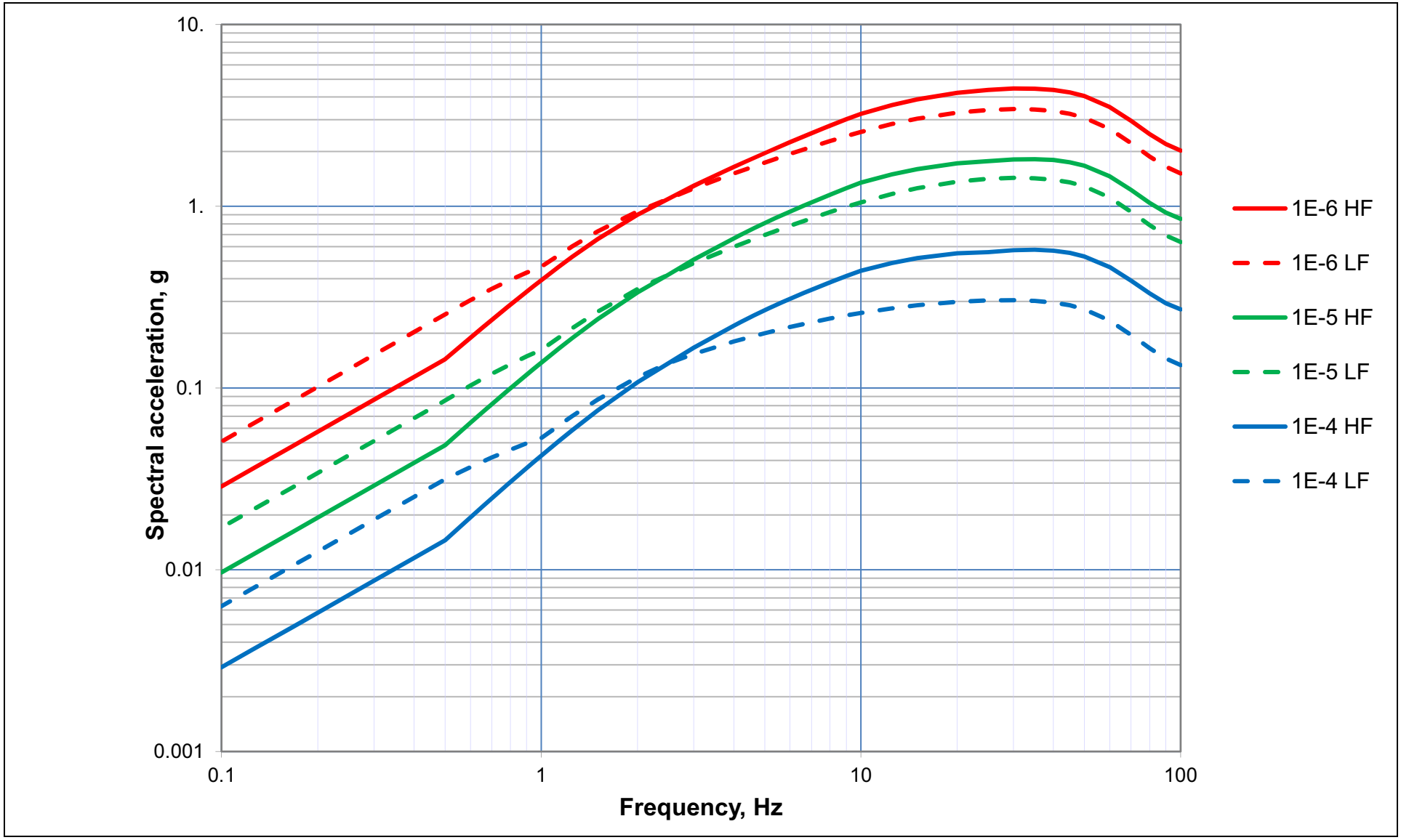

NAPS COL 2.0-27-A
NAPS ESP VAR 2.0-4

Figure 2.5.2-257 Mean Rock UHRS for MAFEs of 10^{-4}, 10^{-5} and 10^{-6}

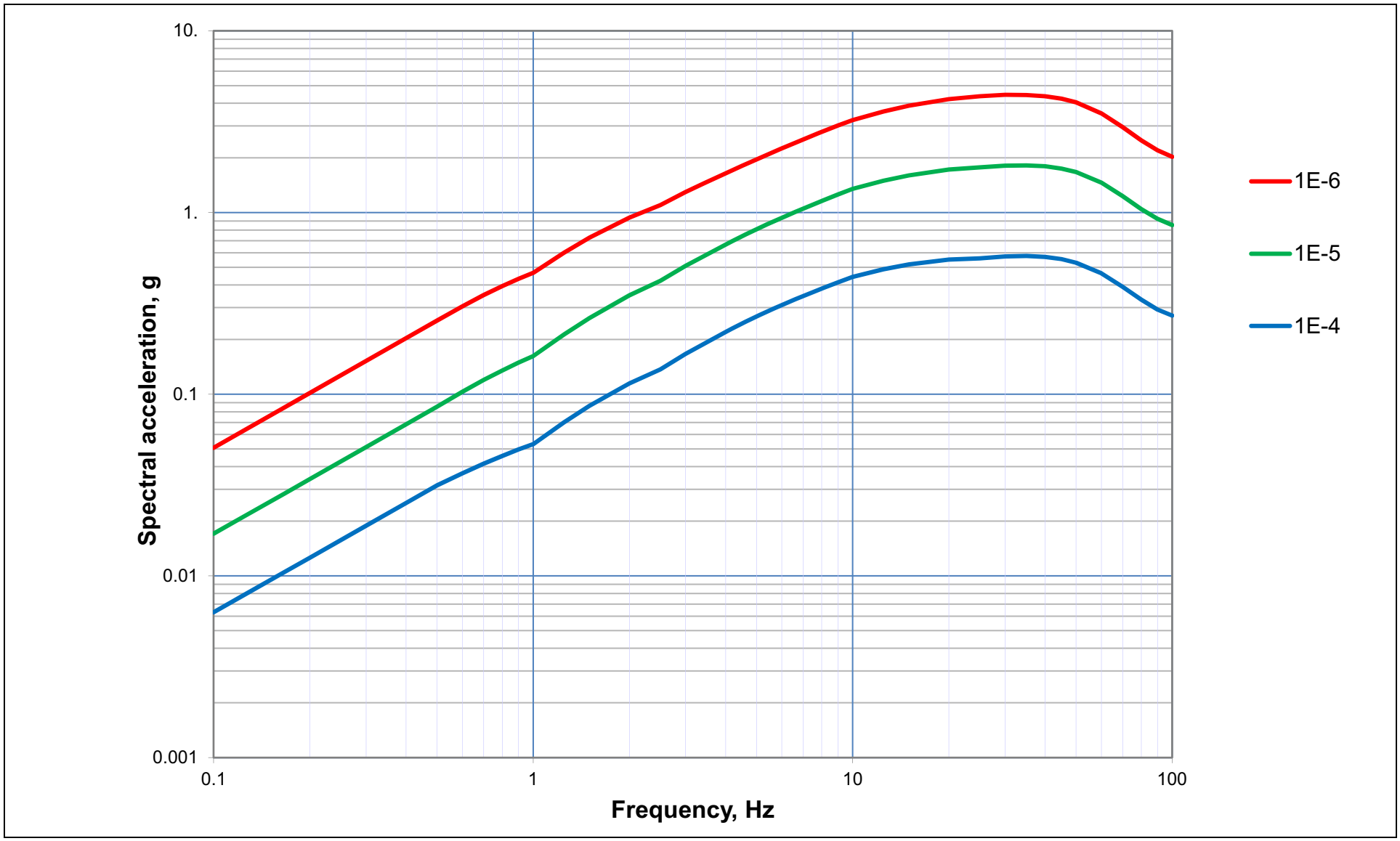

NAPS COL 2.0-27-A
NAPS ESP VAR 2.0-4

Figure 2.5.2-258 Median Rock UHRS for MAFEs of 10^{-4}, 10^{-5} and 10^{-6}

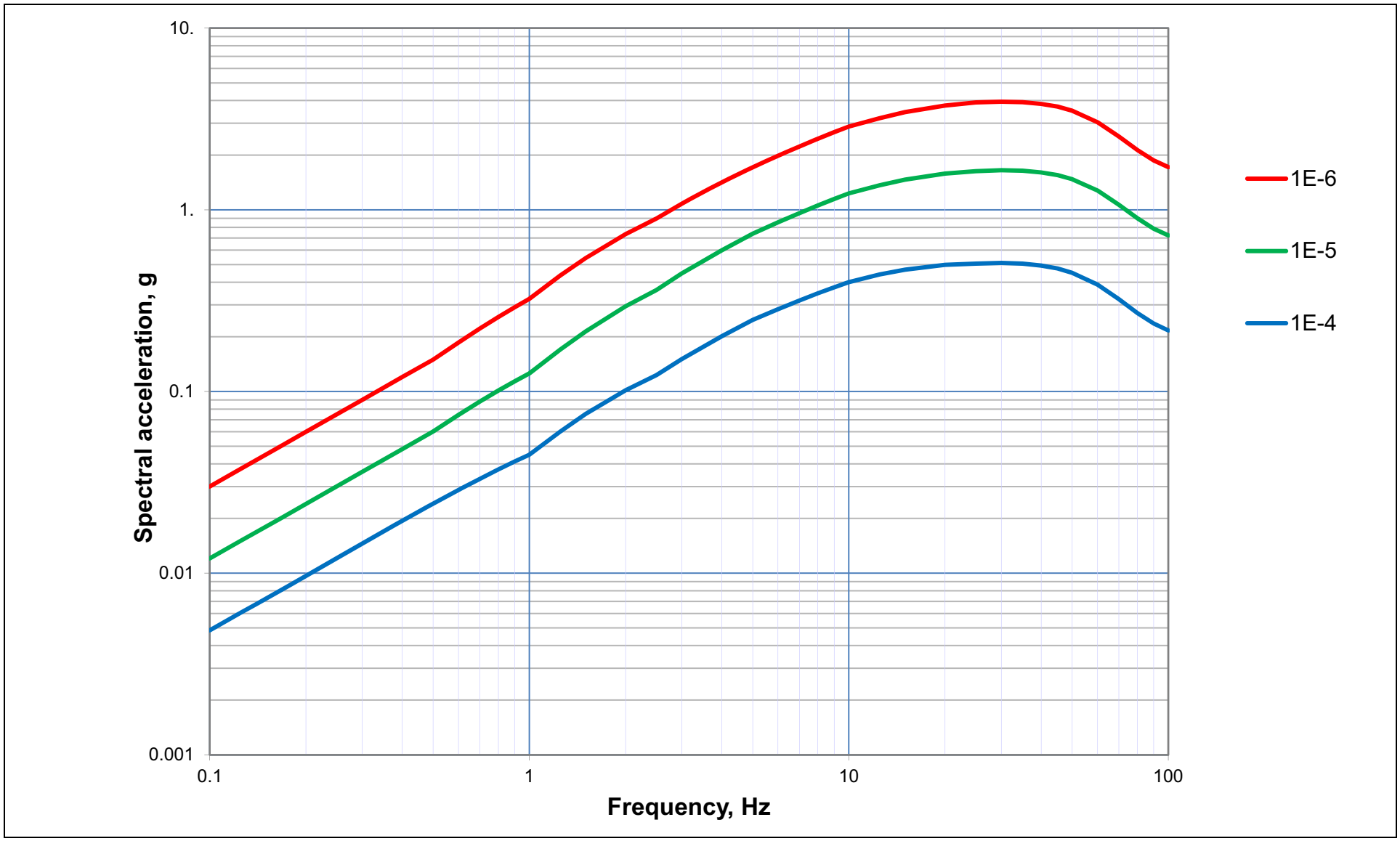

NAPS COL 2.0-27-A
NAPS ESP VAR 2.0-4

Figure 2.5.2-274 High Frequency (HF) and Low Frequency (LF) Hard Rock Input Ground Motion Spectra

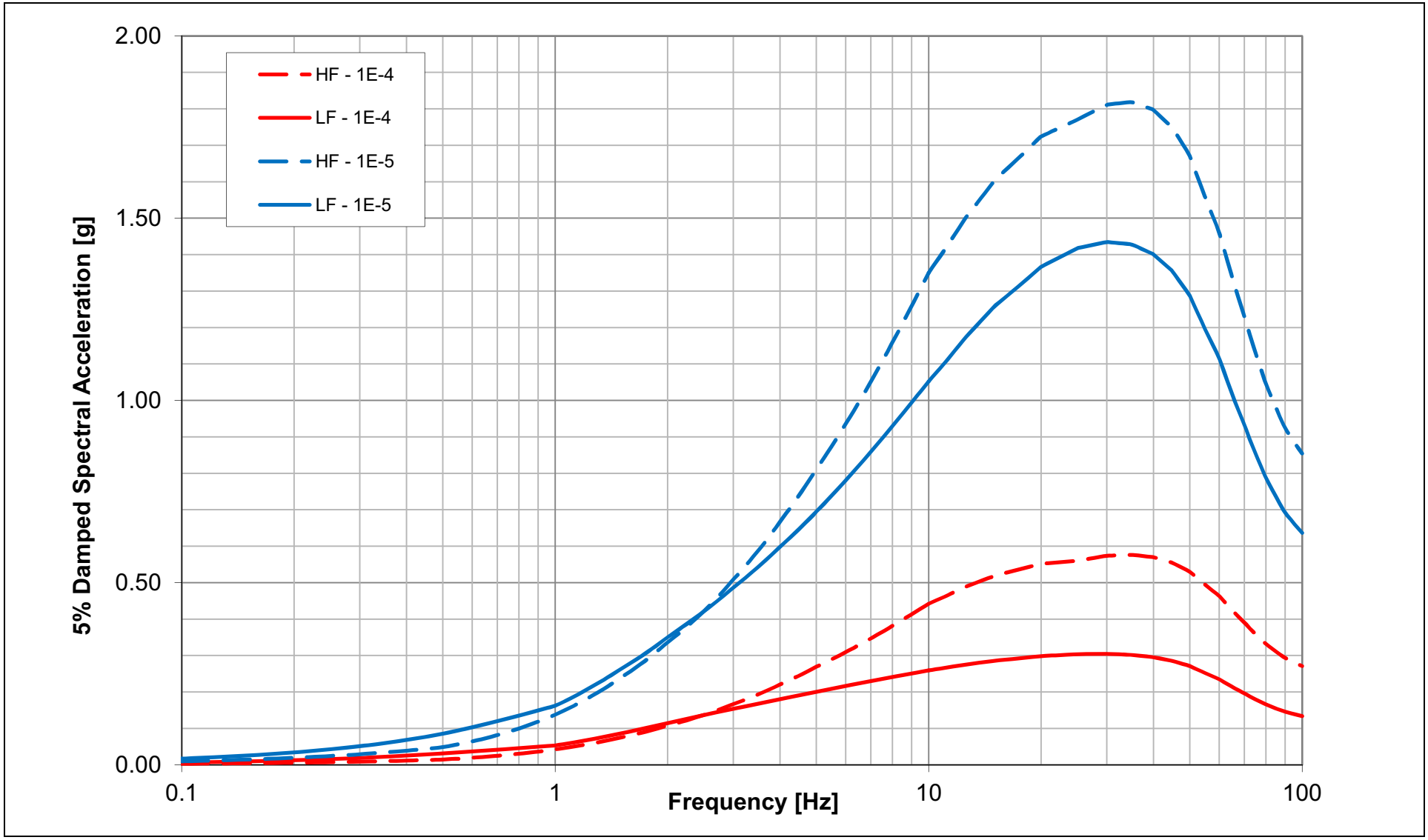

NAPS COL 2.0-27-A **Figure 2.5.2-275 Log-Mean Strain Profiles in RB/FB Soil Column Subject to 10^{-4} and 10^{-5} HF and LF Input Hard Rock Ground Motions**

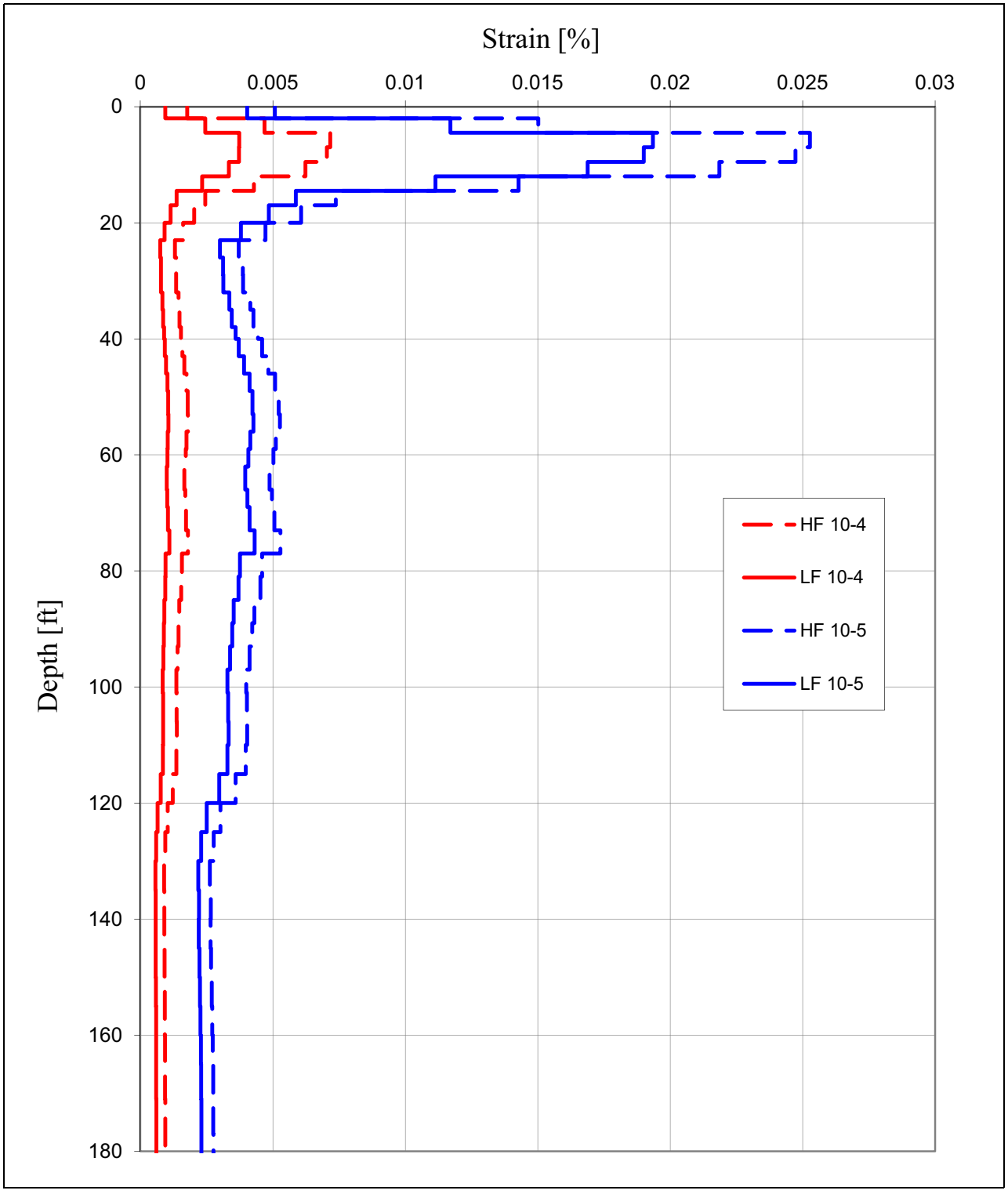

NOTE: Depth of zero corresponds to the finished grade at Elevation 290 ft.

NAPS COL 2.0-27-A **Figure 2.5.2-276 Log-Mean Low Strain and Strain-Compatible Shear Wave Velocity Profiles for RB/FB Soil Column Subject to 10^{-4} and 10^{-5} HF and LF Input Hard Rock Ground Motions**

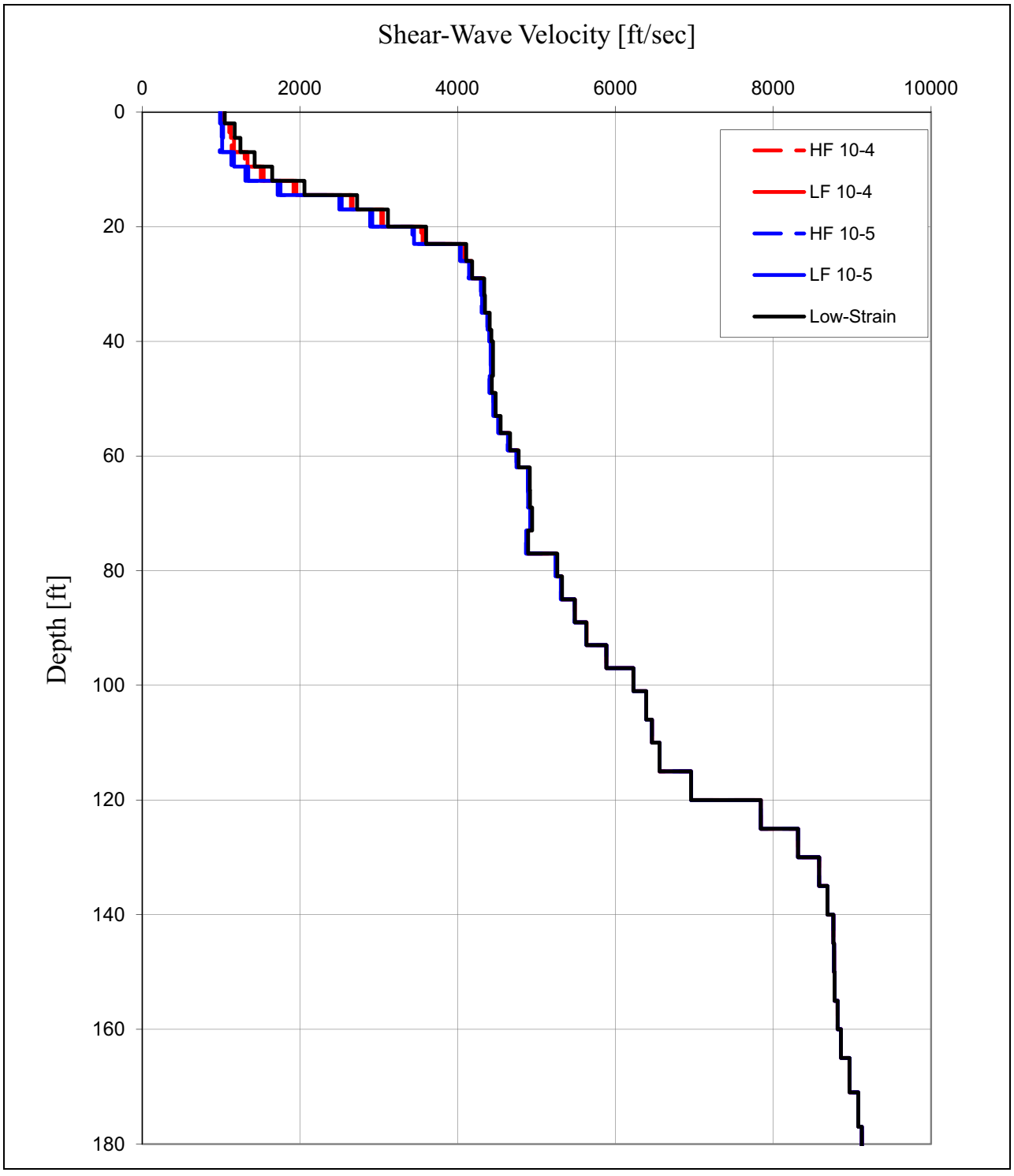

NOTE: Depth of zero corresponds to the finished grade at Elevation 290 ft.

NAPS COL 2.0-27-A **Figure 2.5.2-277 Log-Mean Low Strain and Strain-Compatible Damping Profiles for RB/FB Soil Column Subject to 10^{-4} and 10^{-5} HF and LF Input Hard Rock Ground Motions**

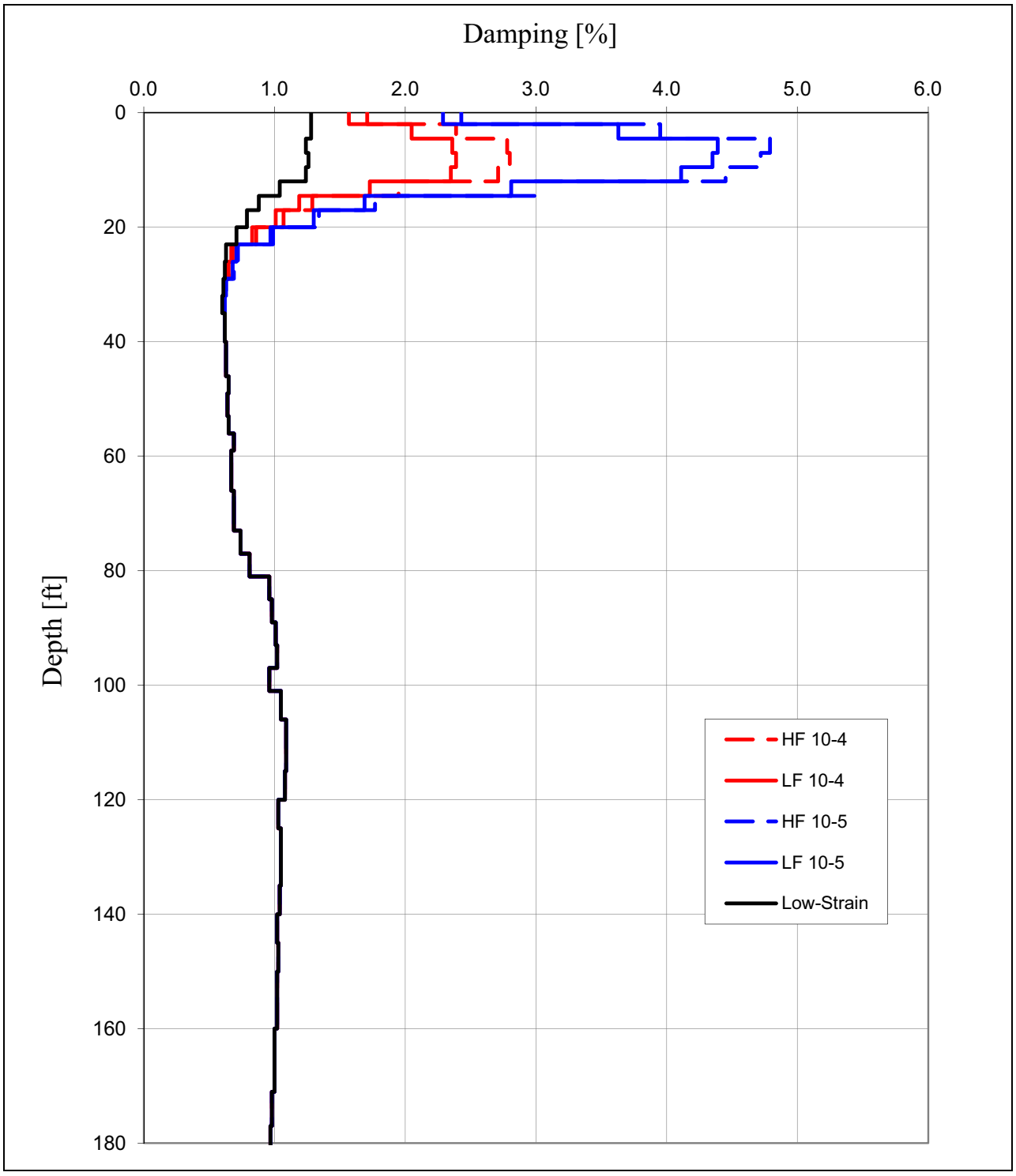

NOTE: Depth of zero corresponds to the finished grade at Elevation 290 ft.

NAPS COL 2.0-27-A **Figure 2.5.2-278 Mean Full Column Outcrop ARS Amplification Factors for RB/FB Soil Column at 10^{-4} Hazard Level Input Ground Motion**

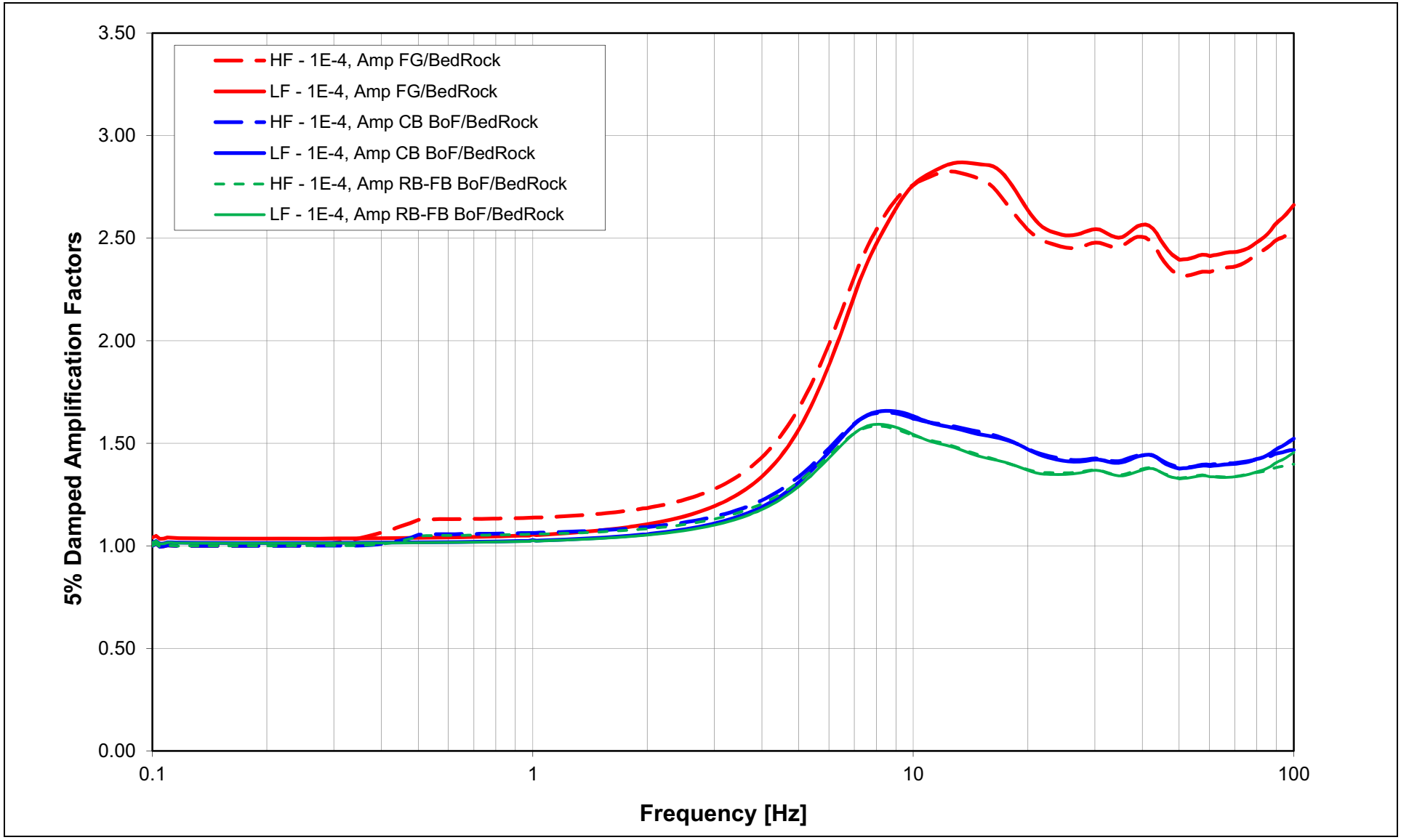

NAPS COL 2.0-27-A **Figure 2.5.2-279 Mean Full Column Outcrop ARS Amplification Factors for RB/FB Soil Column at 10^{-5} Hazard Level Input Ground Motion**

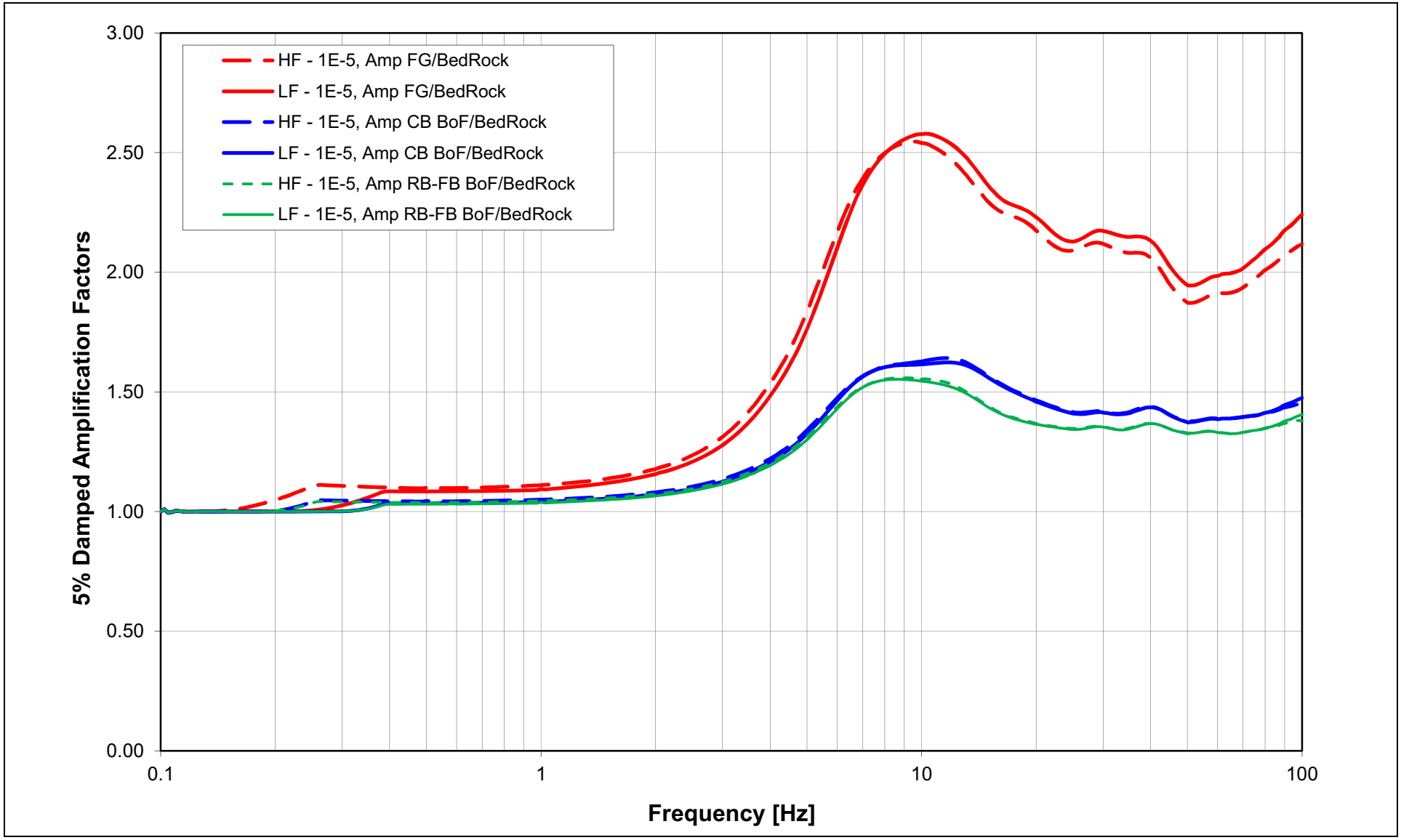

NAPS COL 2.0-27-A **Figure 2.5.2-280 Mean Full Column Outcrop ARS for RB/FB Soil Column at 10^{-4} Hazard Level Input Ground Motion**

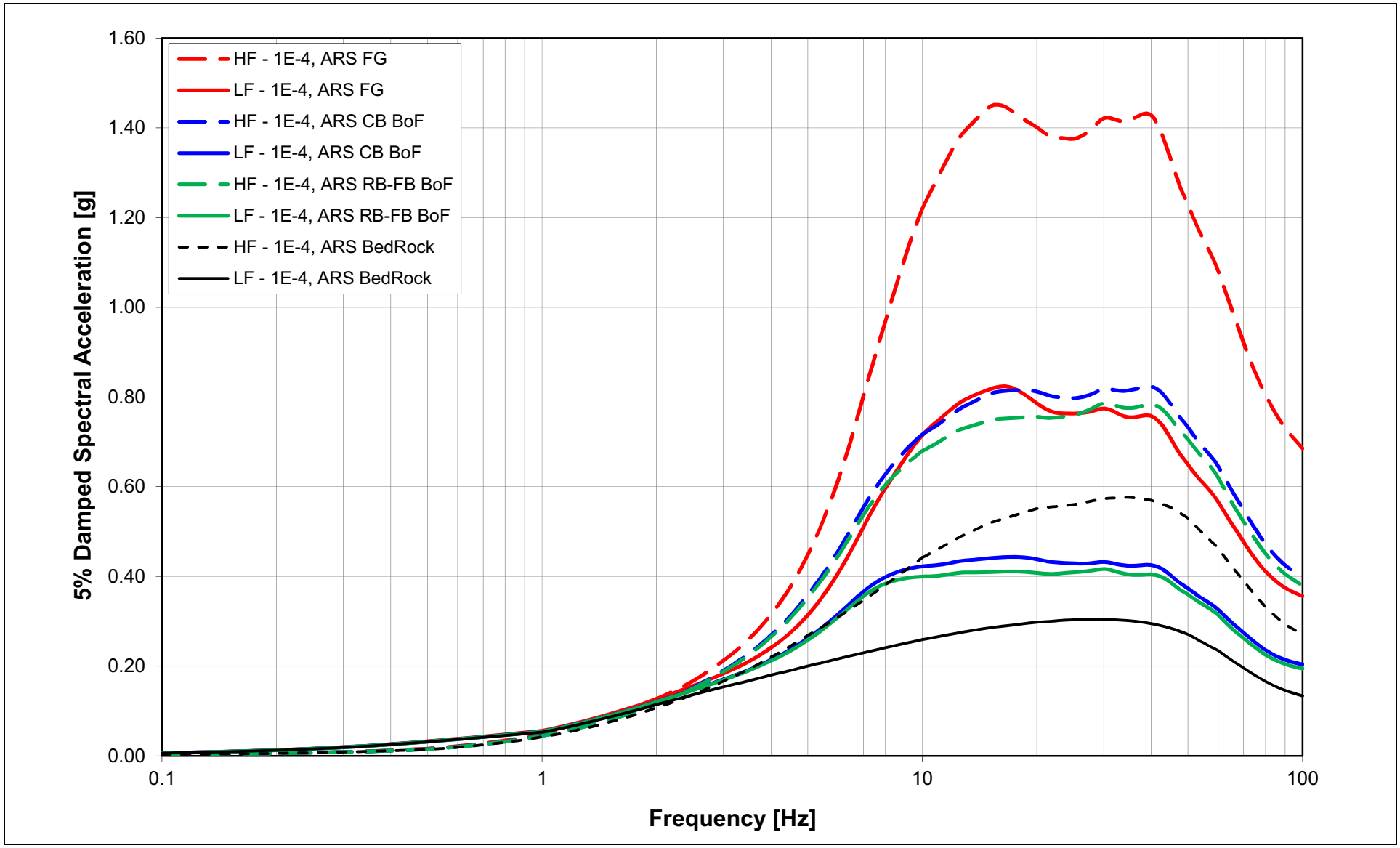

NAPS COL 2.0-27-A **Figure 2.5.2-281 Mean Full Column Outcrop ARS for RB/FB Soil Column at 10^{-5} Hazard Level Input Ground Motion**

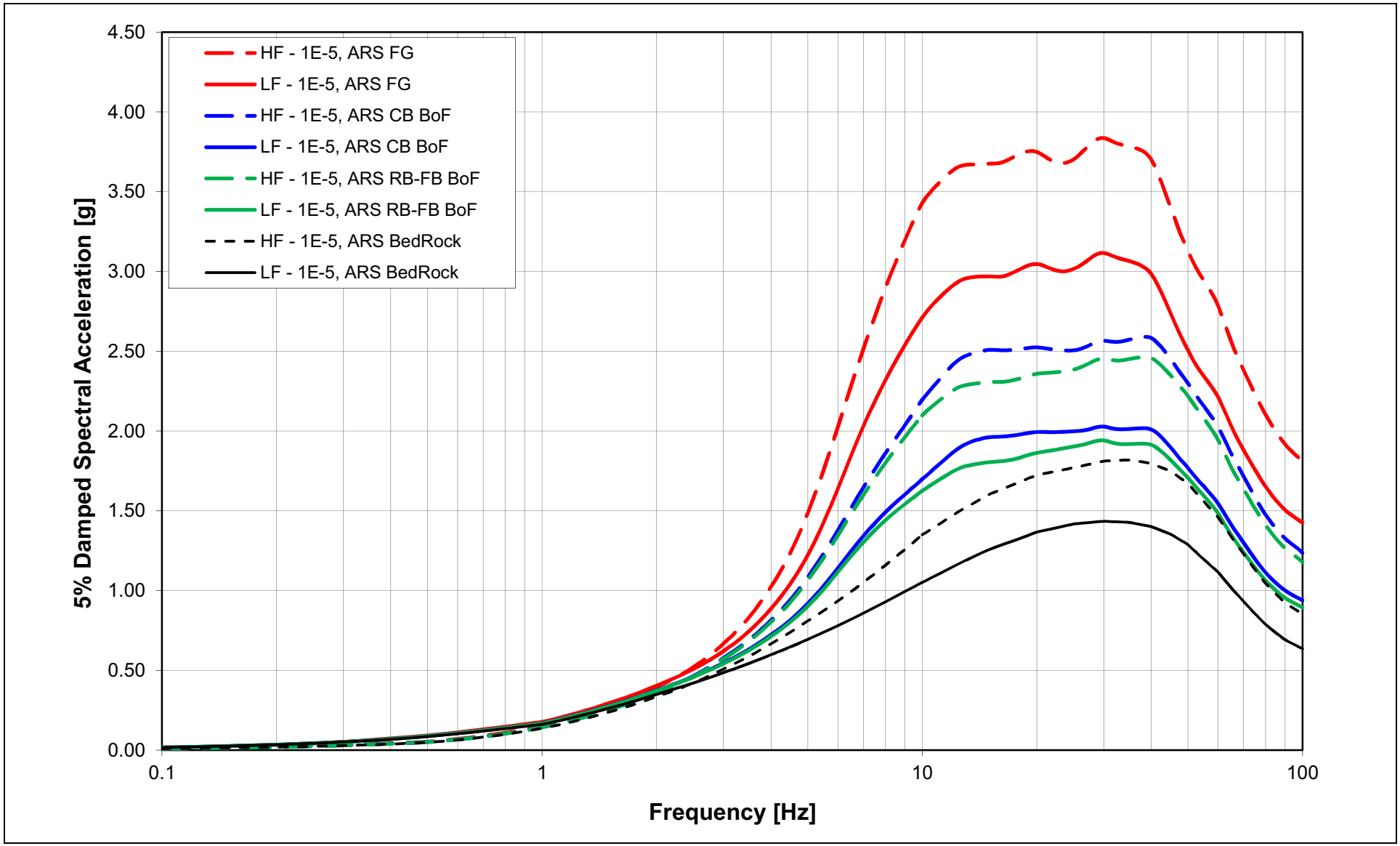

NAPS COL 2.0-27-A **Figure 2.5.2-282 Mean Partial Column Outcrop ARS Amplification Factors for RB/FB Soil Column at 10^{-4} Hazard Level Input Ground Motion**

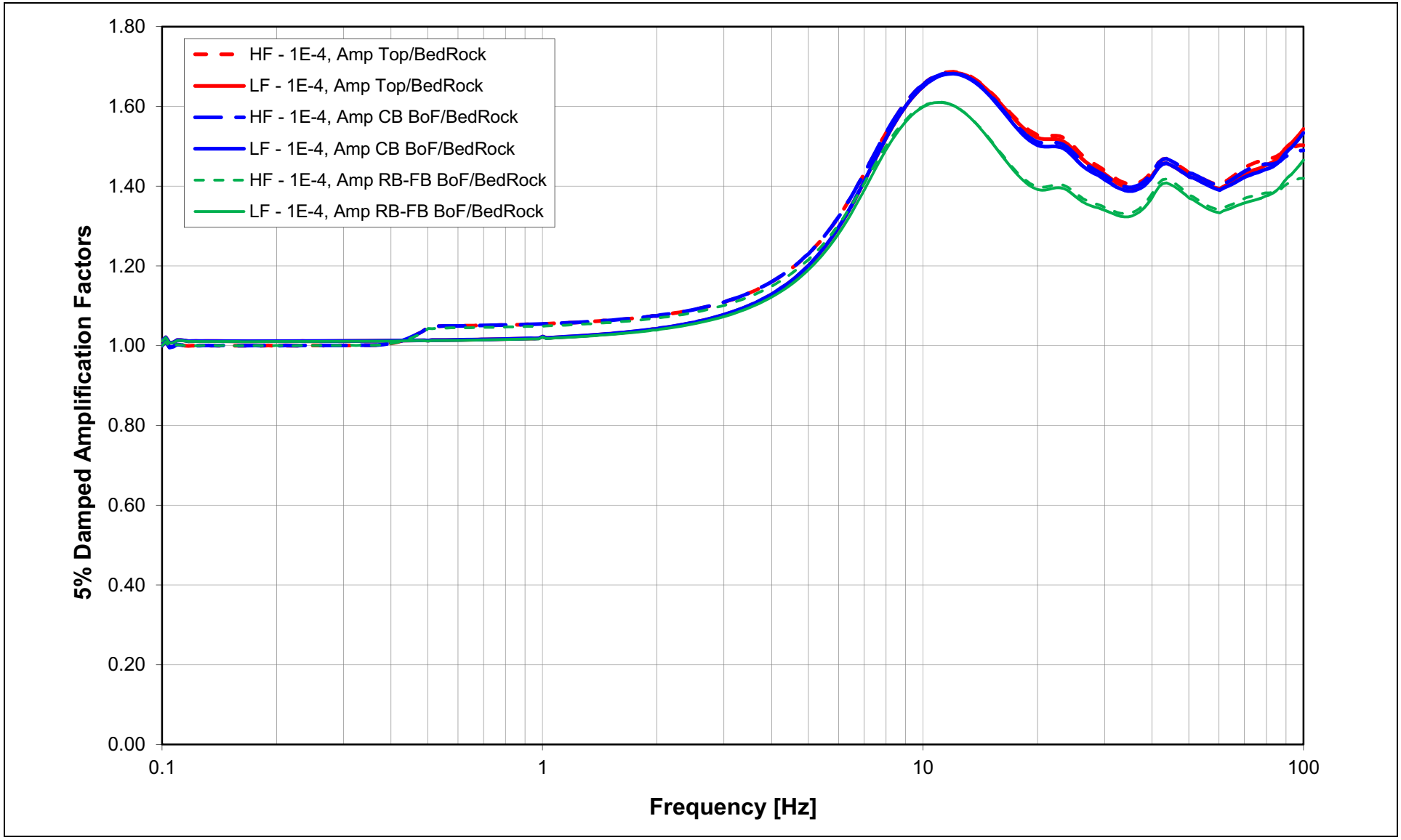

NAPS COL 2.0-27-A **Figure 2.5.2-283 Mean Partial Column Outcrop ARS Amplification Factors for RB/FB Soil Column at 10^{-5} Hazard Level Input Ground Motion**

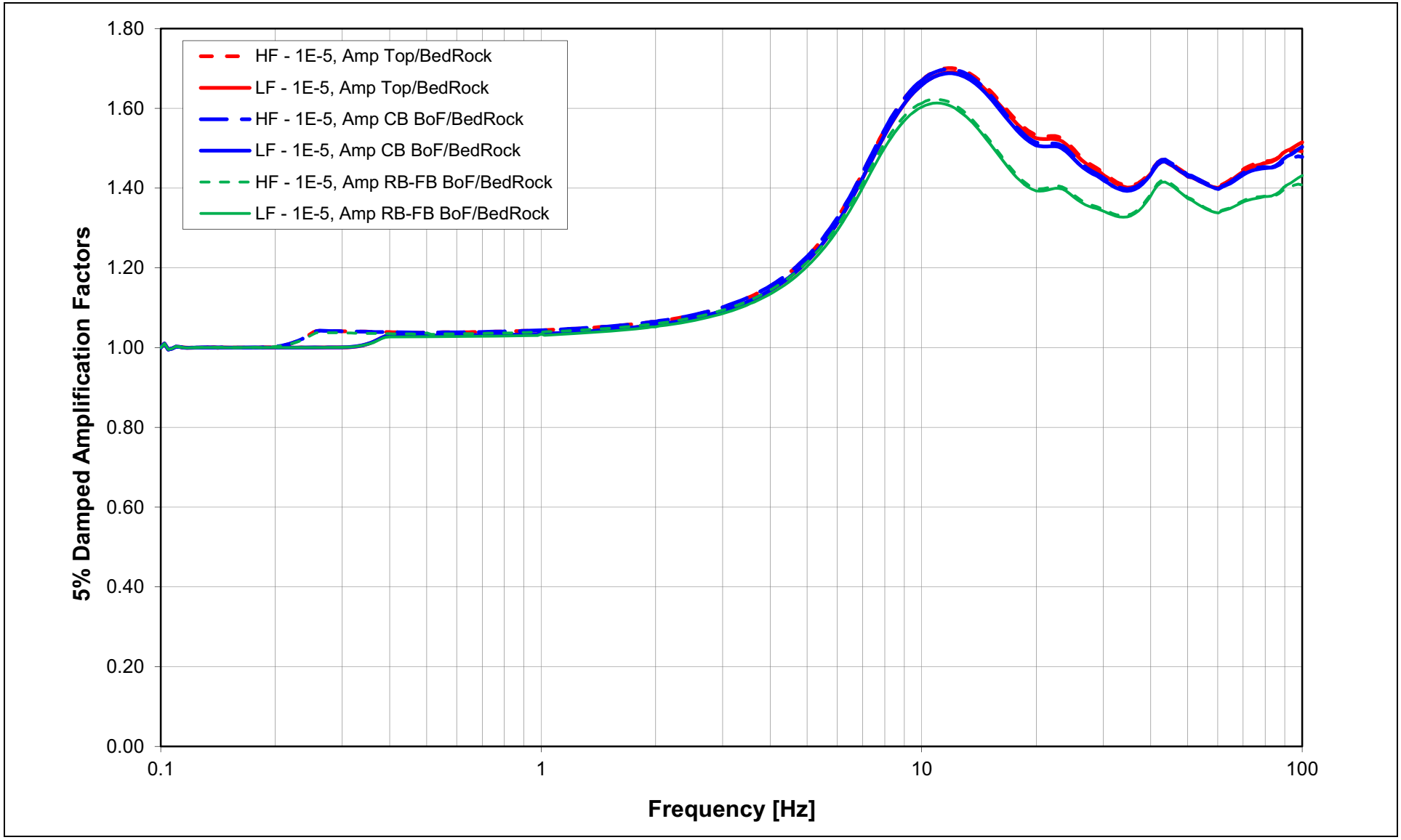

NAPS COL 2.0-27-A **Figure 2.5.2-284 Mean Partial Column Outcrop ARS for RB/FB Soil Column at 10^{-4} Hazard Level Input Ground Motion**

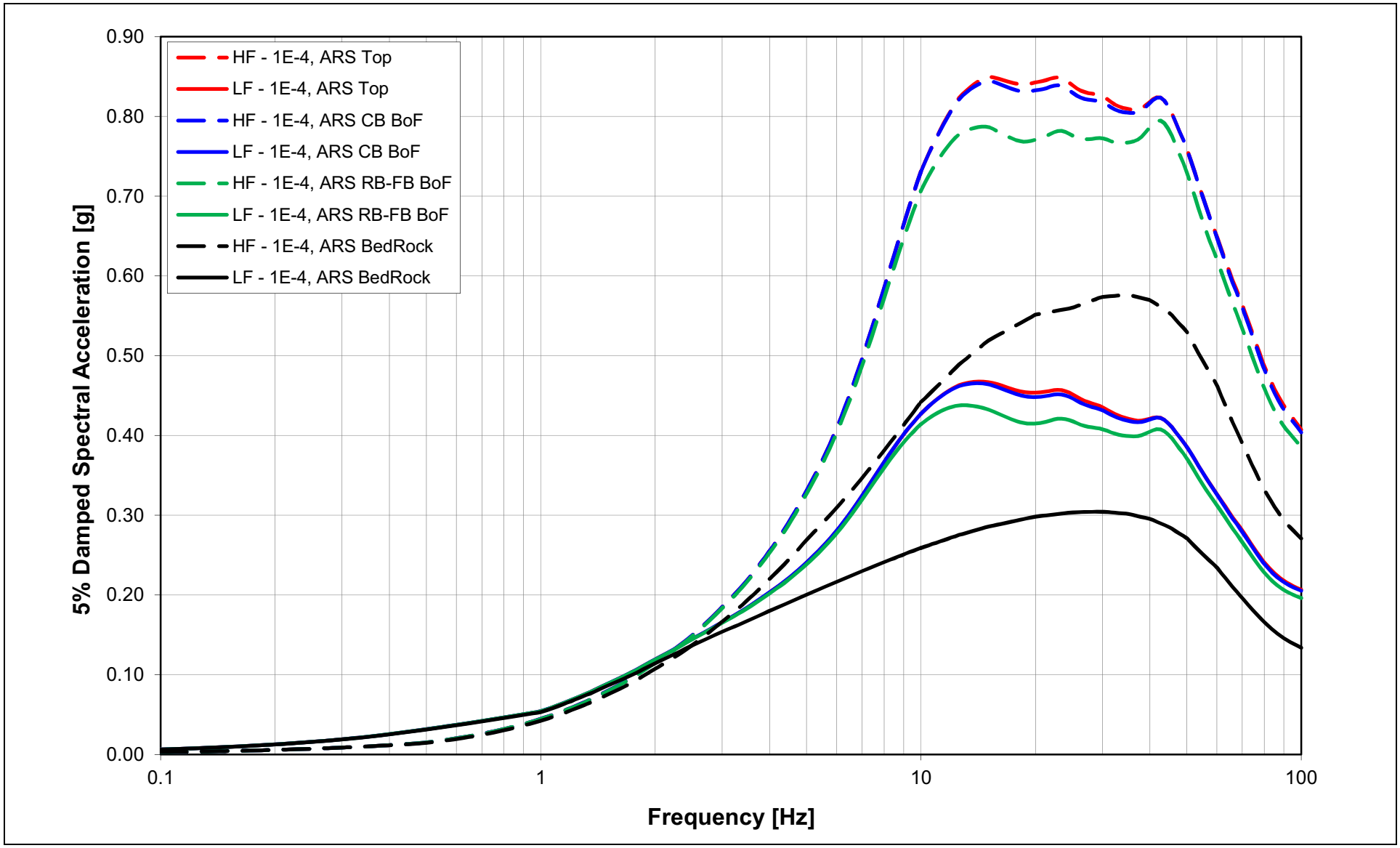

NAPS COL 2.0-27-A **Figure 2.5.2-285 Mean Partial Column Outcrop ARS for RB/FB Soil Column at 10^{-5} Hazard Level Input Ground Motion**

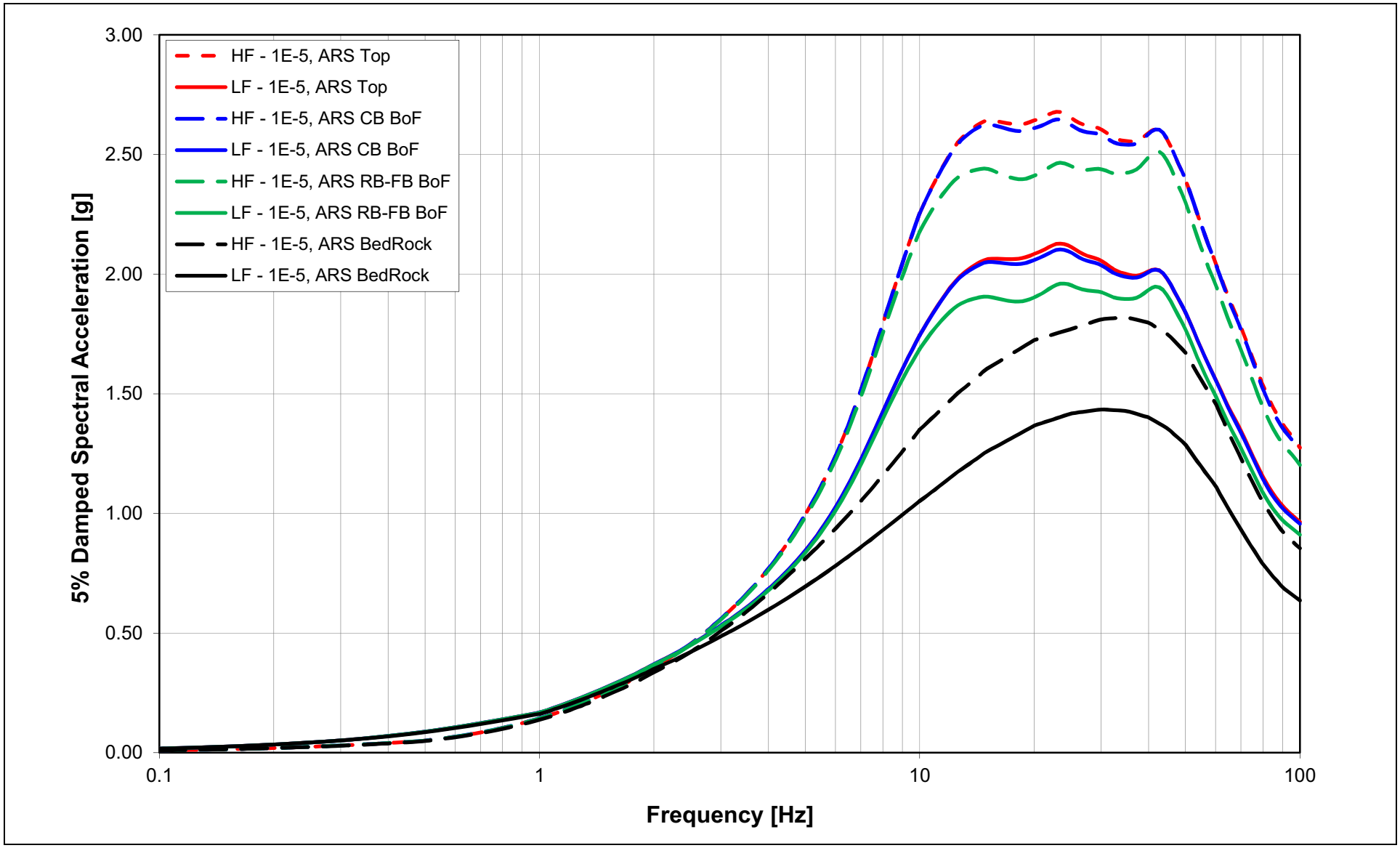

NAPS COL 2.0-27-A **Figure 2.5.2-286 Mean Geologic Outcrop ARS Amplification Factors for RB/FB Soil Column at 10^{-4} Hazard Level Input Ground Motion**

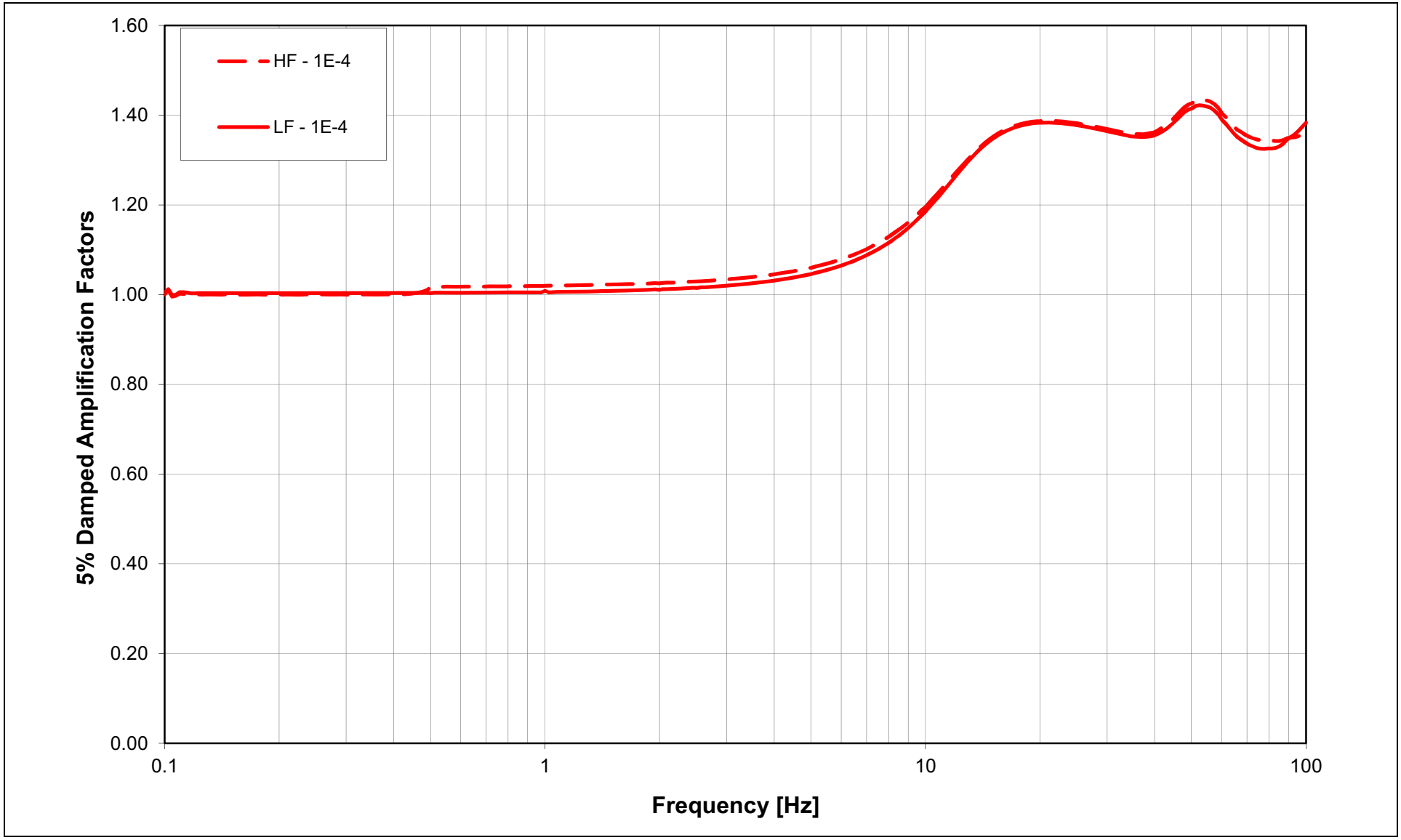

NAPS COL 2.0-27-A **Figure 2.5.2-287 Mean Geologic Outcrop ARS Amplification Factors for RB/FB Soil Column at 10^{-5} Hazard Level Input Ground Motion**

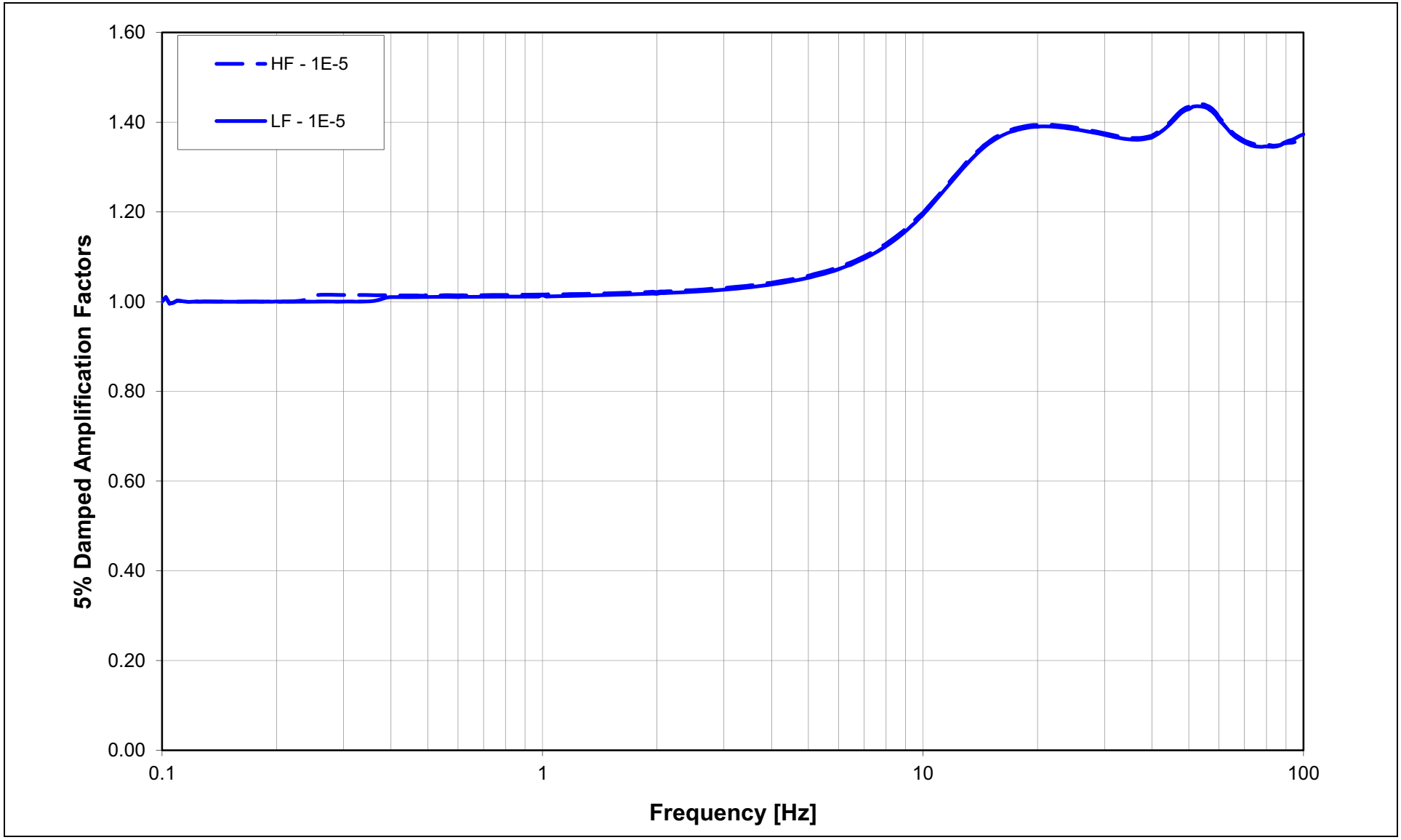

NAPS COL 2.0-27-A **Figure 2.5.2-288 Mean Geologic Outcrop ARS for RB/FB Soil Column at 10^{-4} Hazard Level Input Ground Motion**

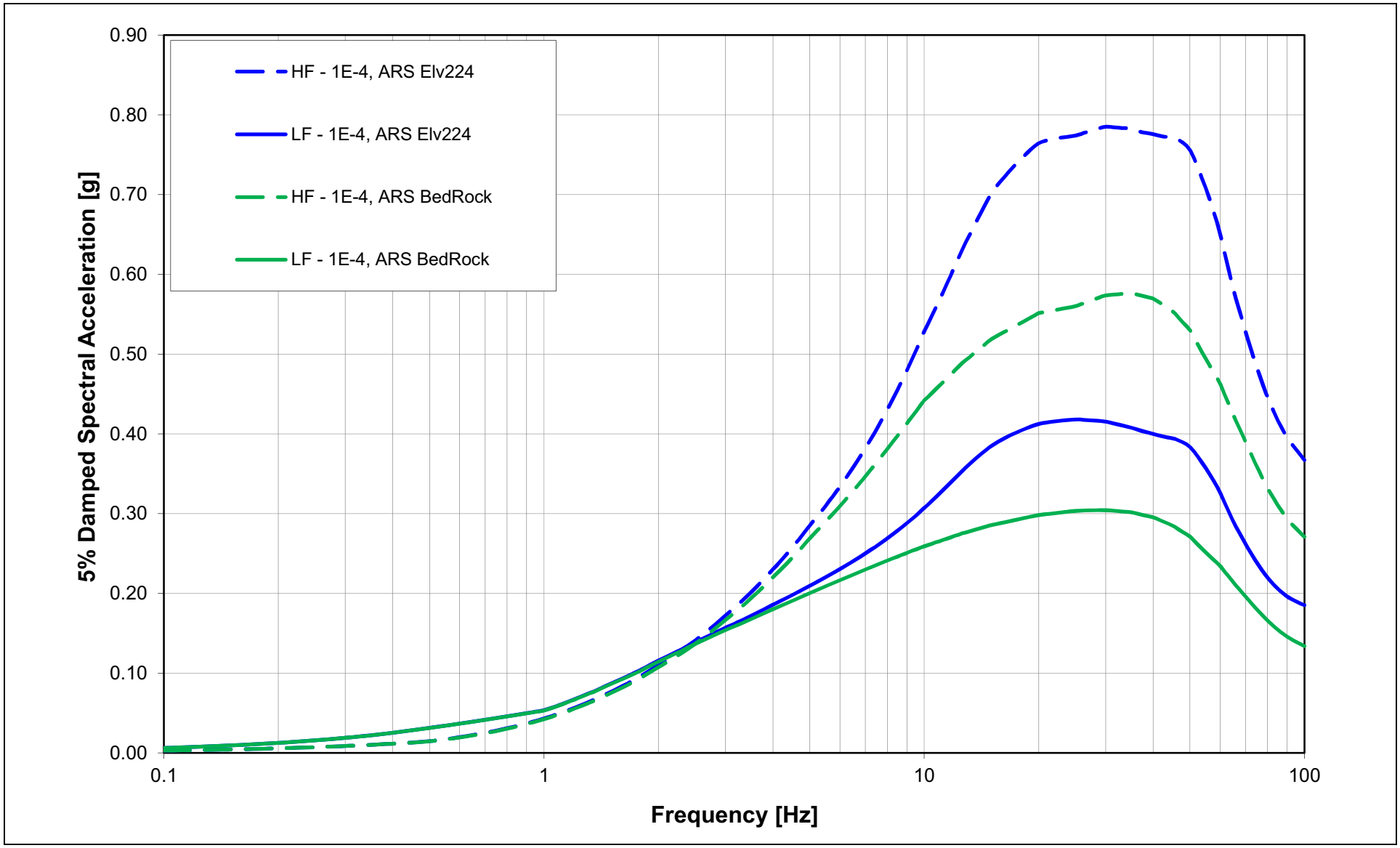

NAPS COL 2.0-27-A **Figure 2.5.2-289 Mean Geologic Outcrop ARS for RB/FB Soil Column at 10^{-5} Hazard Level Input Ground Motion**

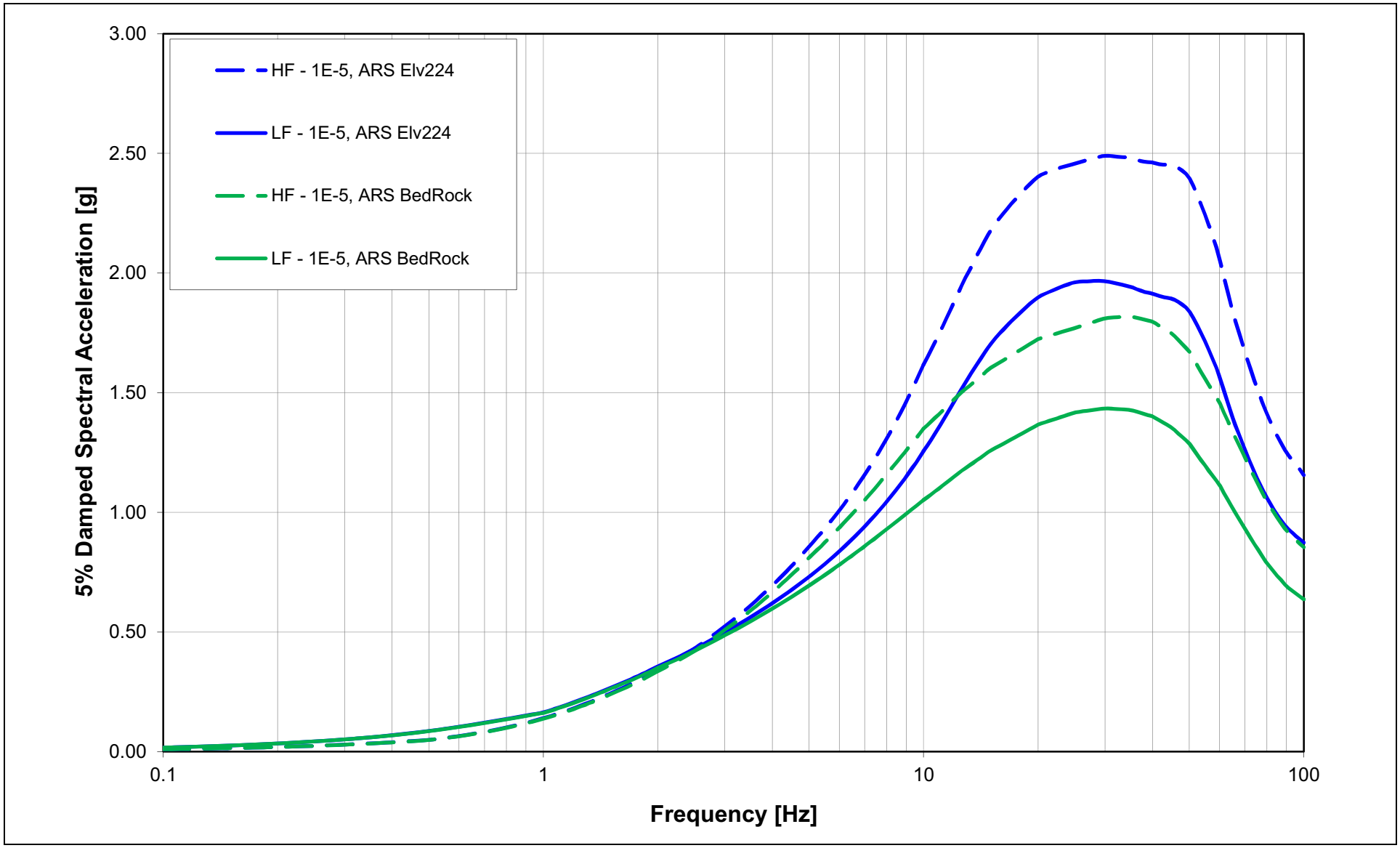

NAPS COL 2.0-27-A **Figure 2.5.2-290 Mean Full Column Outcrop ARS for CB Soil Column at 10^{-4} Hazard Level Input Ground Motion**

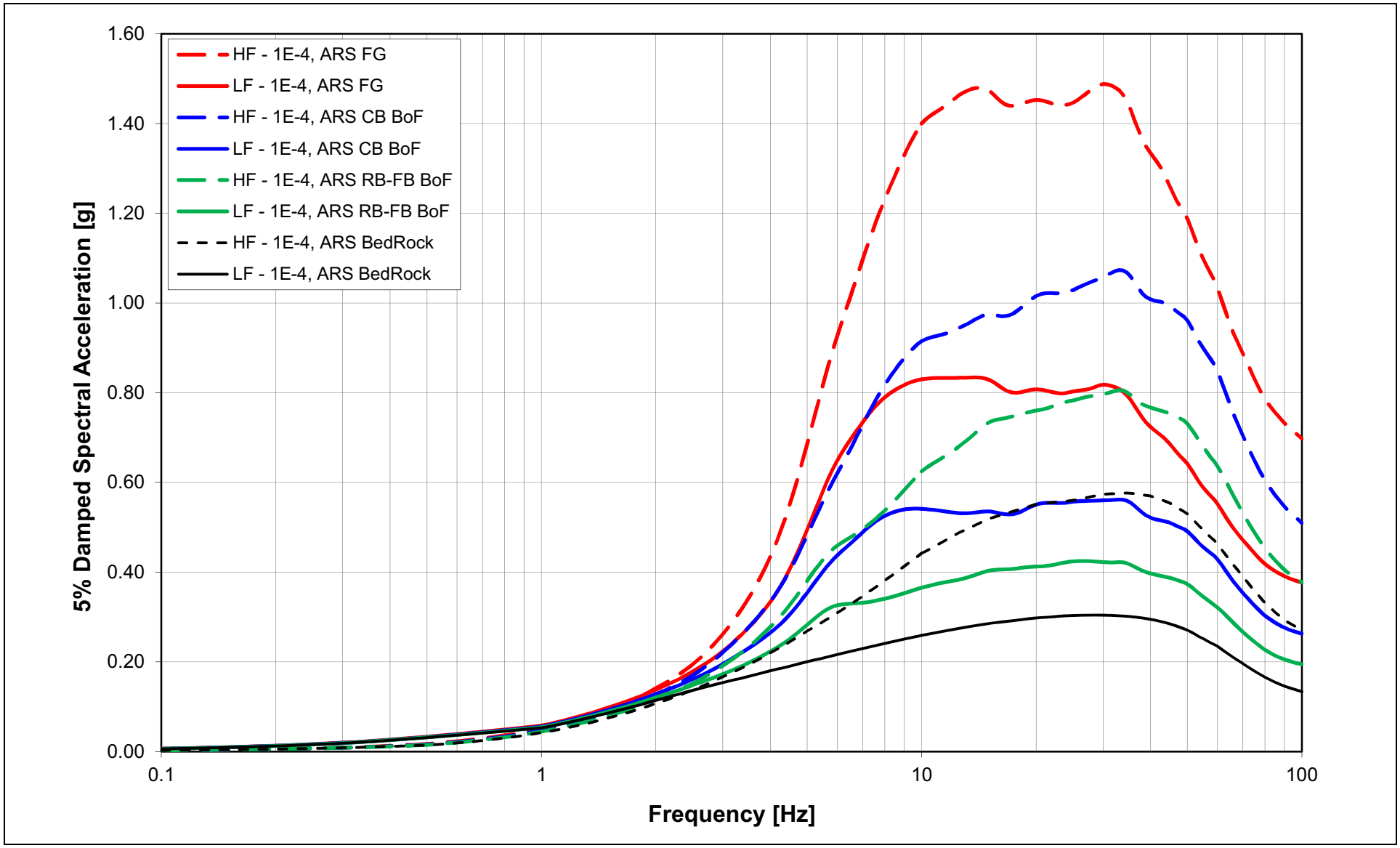

NAPS COL 2.0-27-A **Figure 2.5.2-291 Mean Full Column Outcrop ARS for CB Soil Column at 10^{-5} Hazard Level Input Ground Motion**

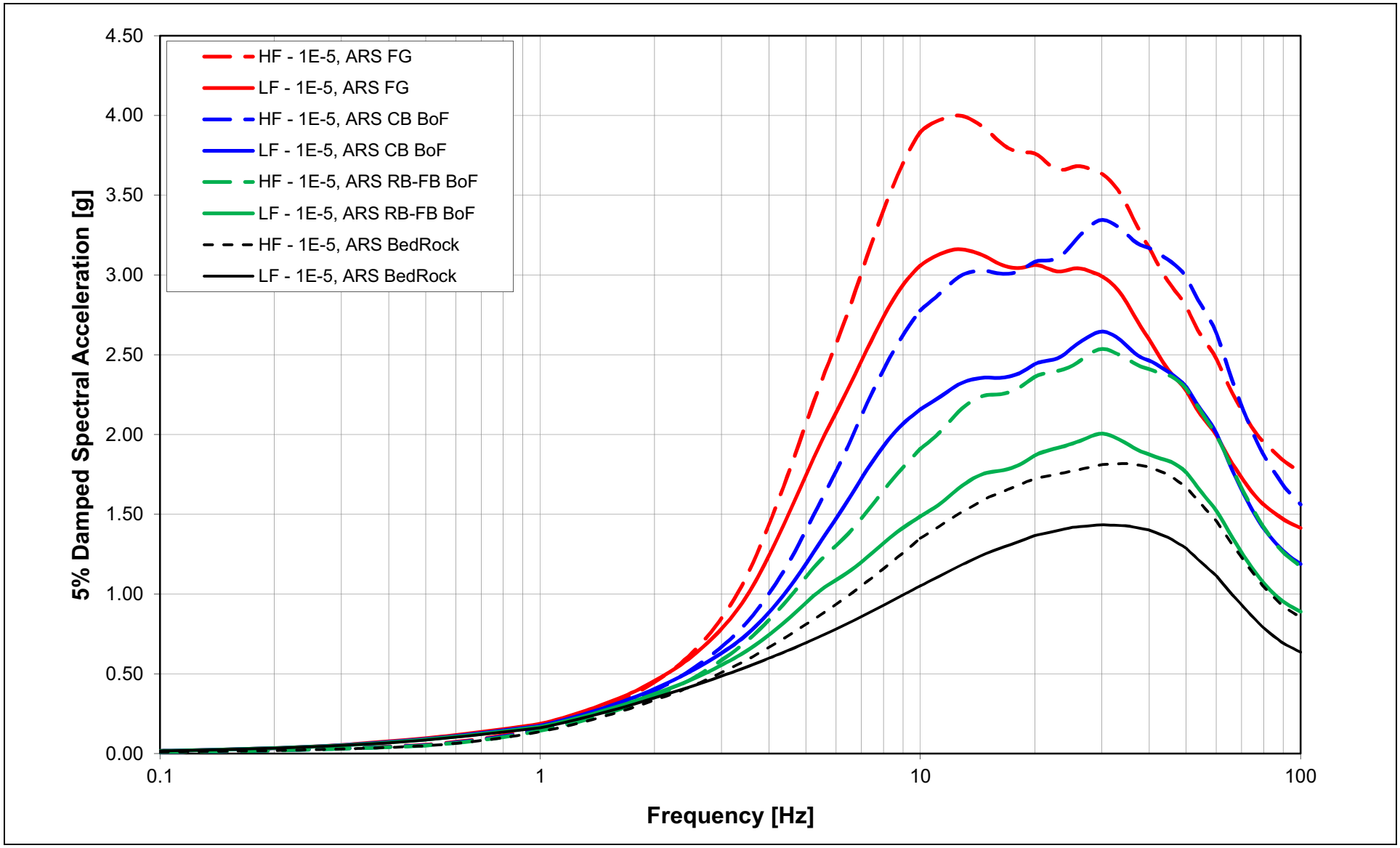

NAPS COL 2.0-27-A **Figure 2.5.2-292 Mean Full Column Outcrop ARS for FWSC Soil Column at 10^{-4} Hazard Level Input Ground Motion**

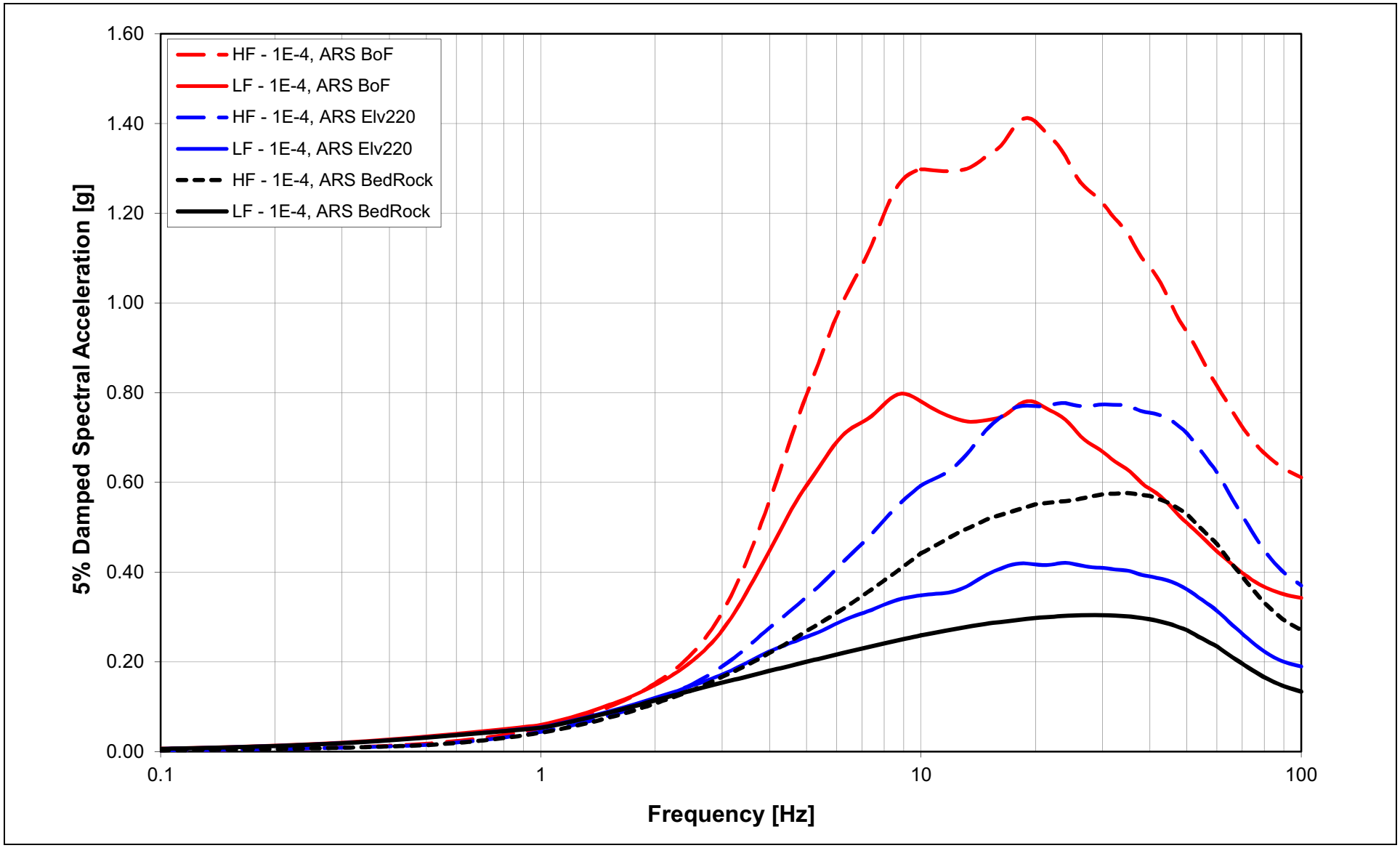

NAPS COL 2.0-27-A **Figure 2.5.2-293 Mean Full Column Outcrop ARS for FWSC Soil Column at 10^{-5} Hazard Level Input Ground Motion**

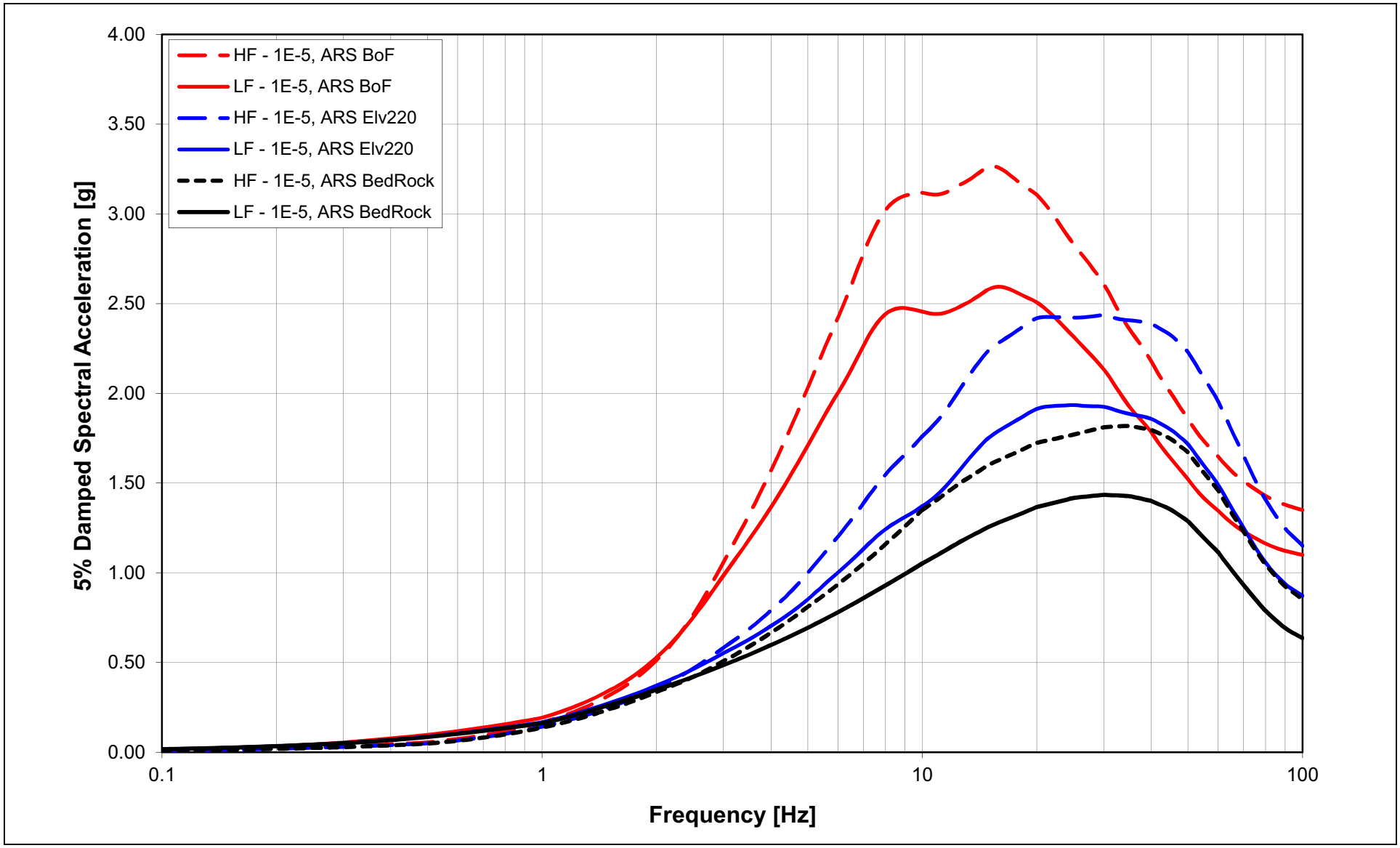

NAPS COL 2.0-27-A **Figure 2.5.2-294 Mean Horizontal Full Column Outcrop UHRS at 10^{-4} and 10^{-5} Hazard Levels and Full Column Outcrop DRS for RB/FB Soil Column at Elevation 224 ft (BoF for RB/FB)**

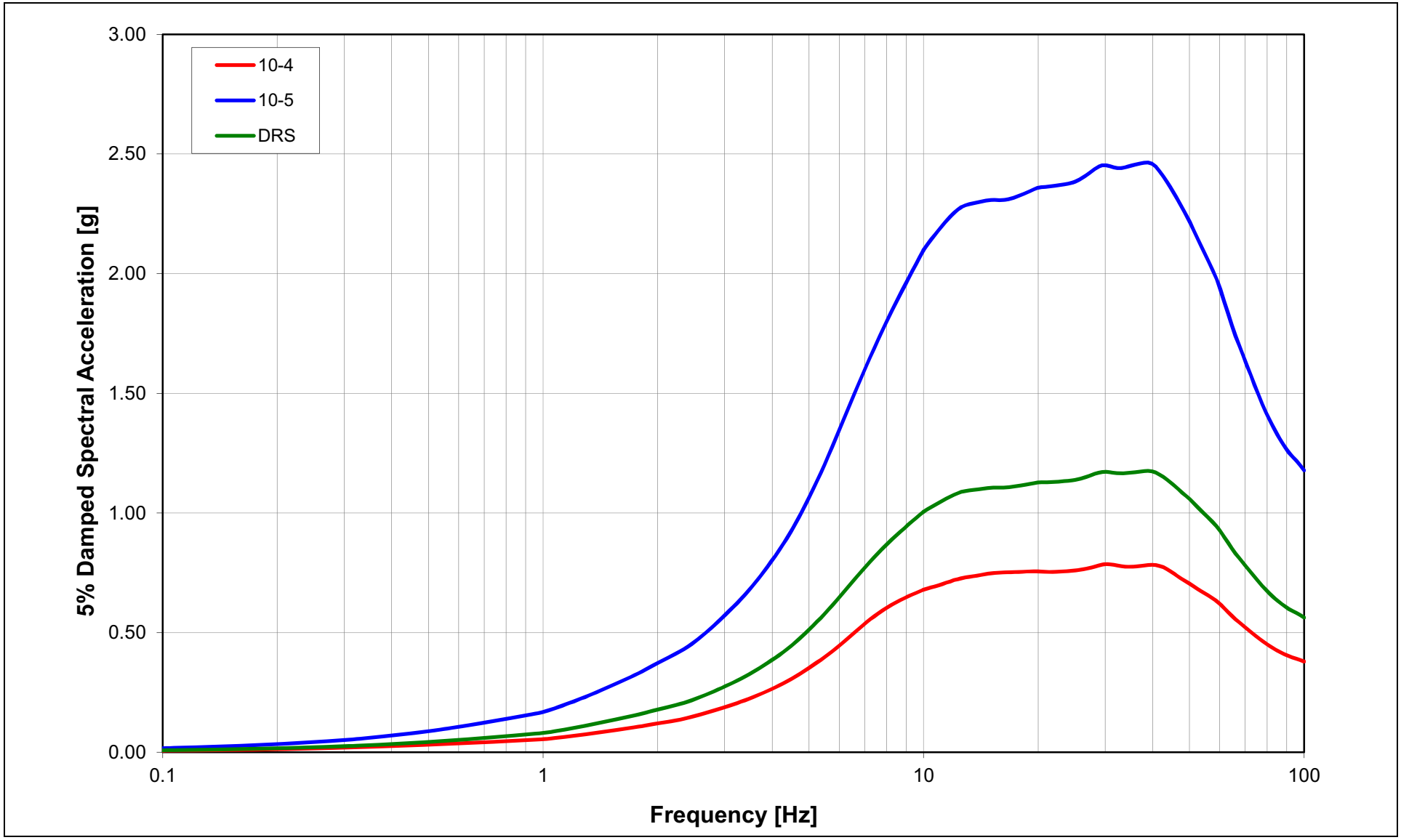

NAPS COL 2.0-27-A **Figure 2.5.2-295 Mean Horizontal Full Column Outcrop UHRS at 10^{-4} and 10^{-5} Hazard Levels and Full Column Outcrop DRS for RB/FB Soil Column at Elevation 241 ft (BoF for CB)**

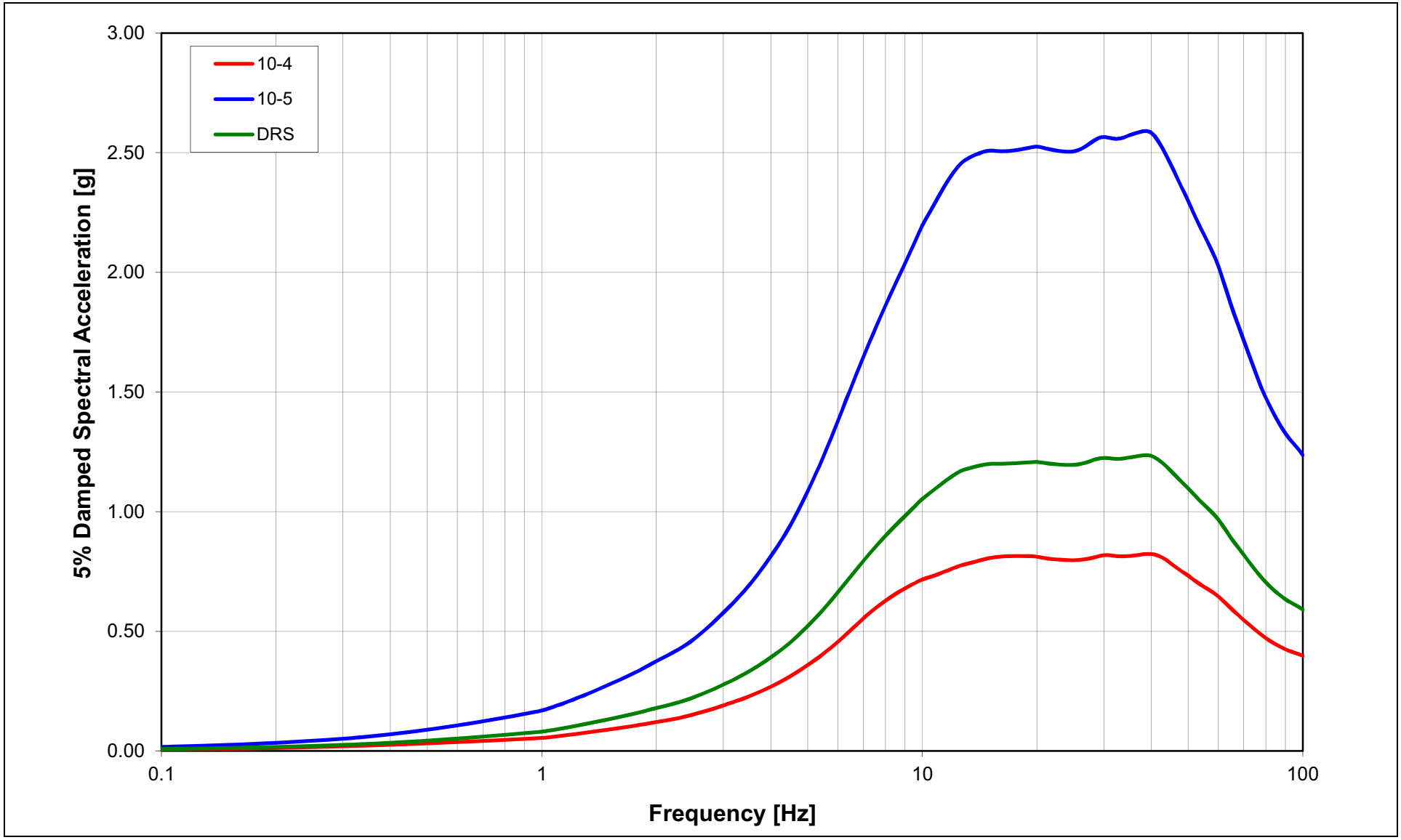

NAPS COL 2.0-27-A **Figure 2.5.2-296 Mean Horizontal Full Column Outcrop UHRS at 10^{-4} and 10^{-5} Hazard Levels and Full Column Outcrop DRS for RB/FB Soil Column at Elevation 290 ft (Finished Grade)**

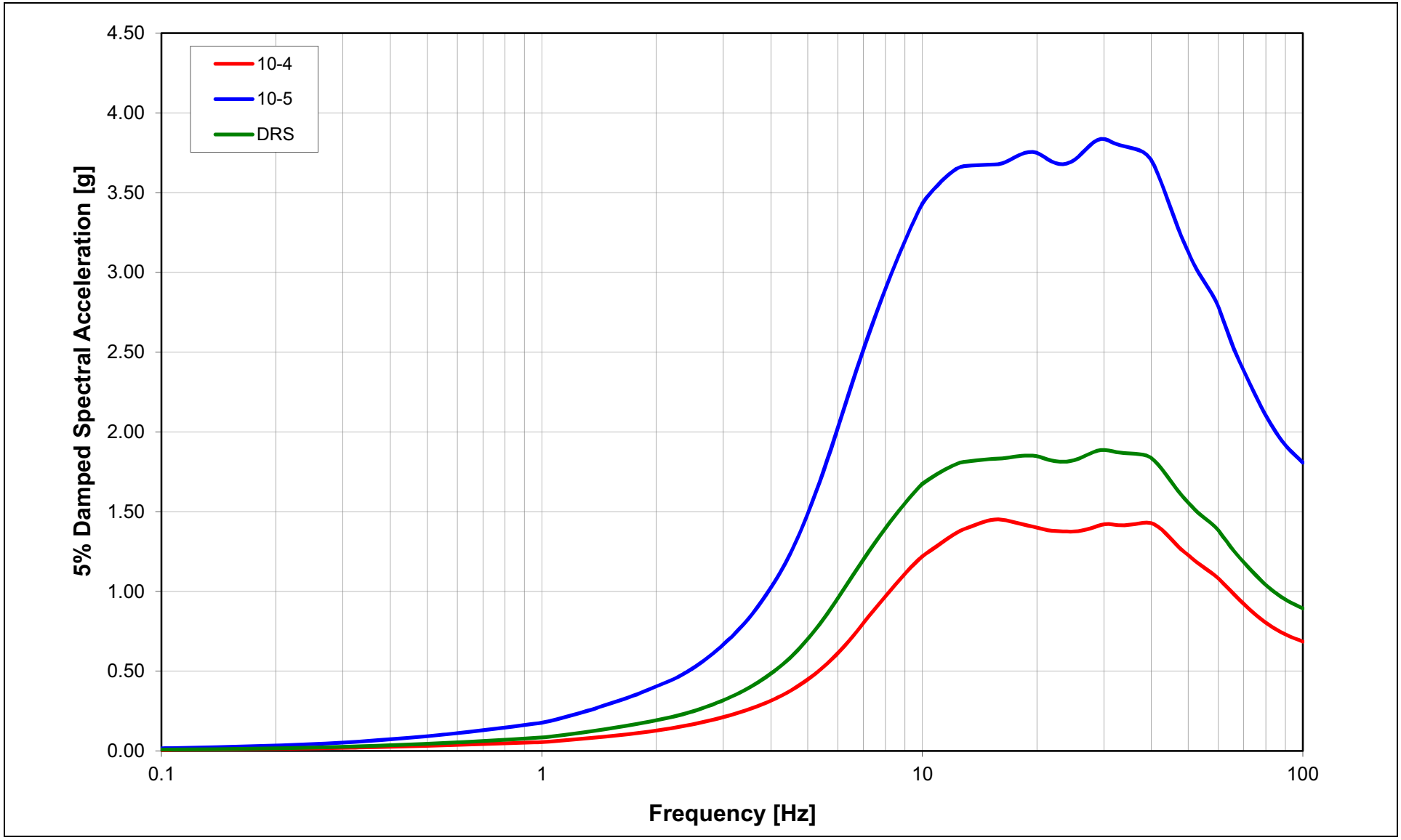

NAPS COL 2.0-27-A **Figure 2.5.2-297 Mean Horizontal Partial Column Outcrop UHRS at 10^{-4} and 10^{-5} Hazard Levels and Partial Column Outcrop DRS for RB/FB Soil Column at Elevation 224 ft (BoF for RB/FB)**

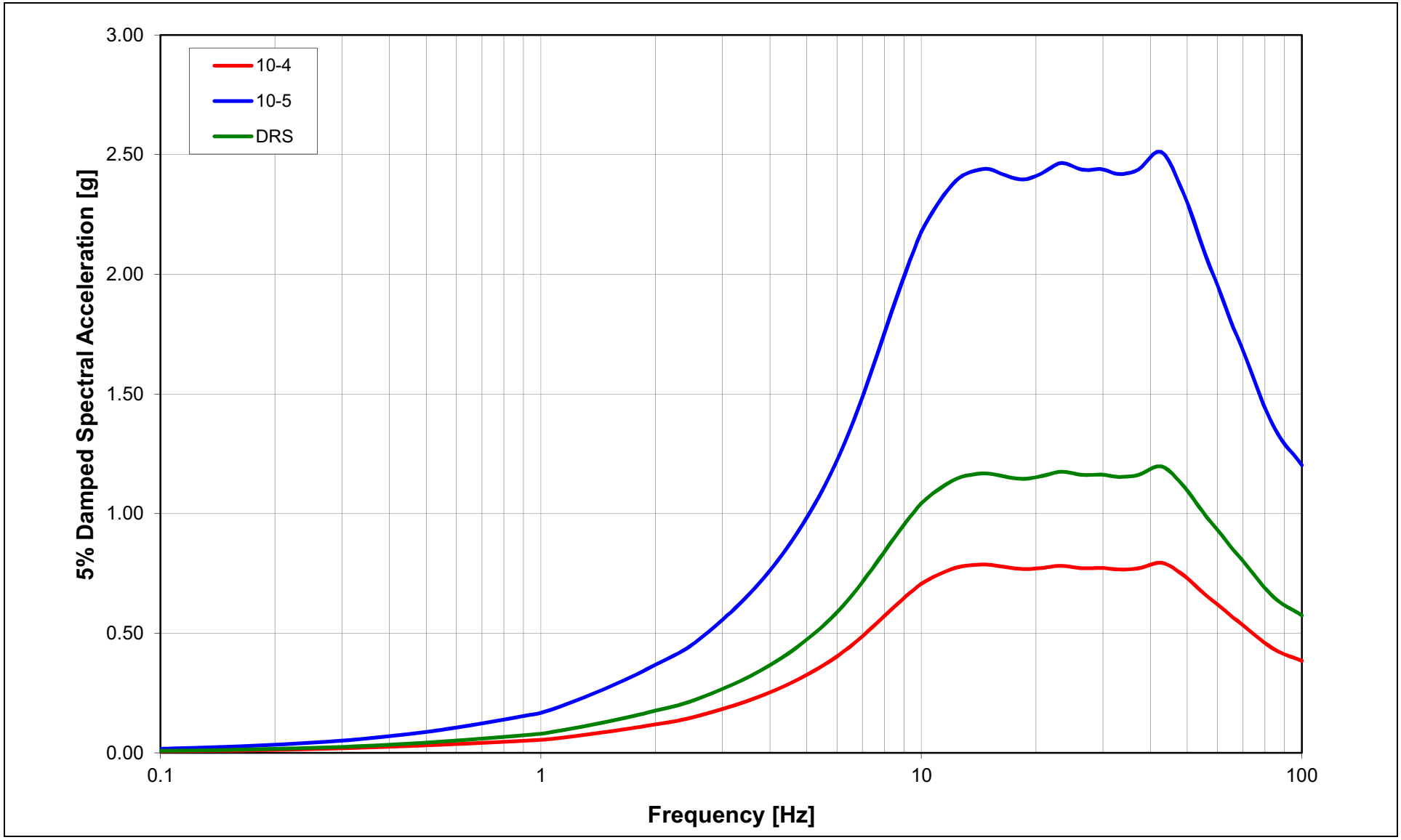

NAPS COL 2.0-27-A **Figure 2.5.2-298 Mean Horizontal Partial Column Outcrop UHRS at 10^{-4} and 10^{-5} Hazard Levels and Partial Column Outcrop DRS for RB/FB Soil Column at Elevation 241 ft (BoF for CB)**

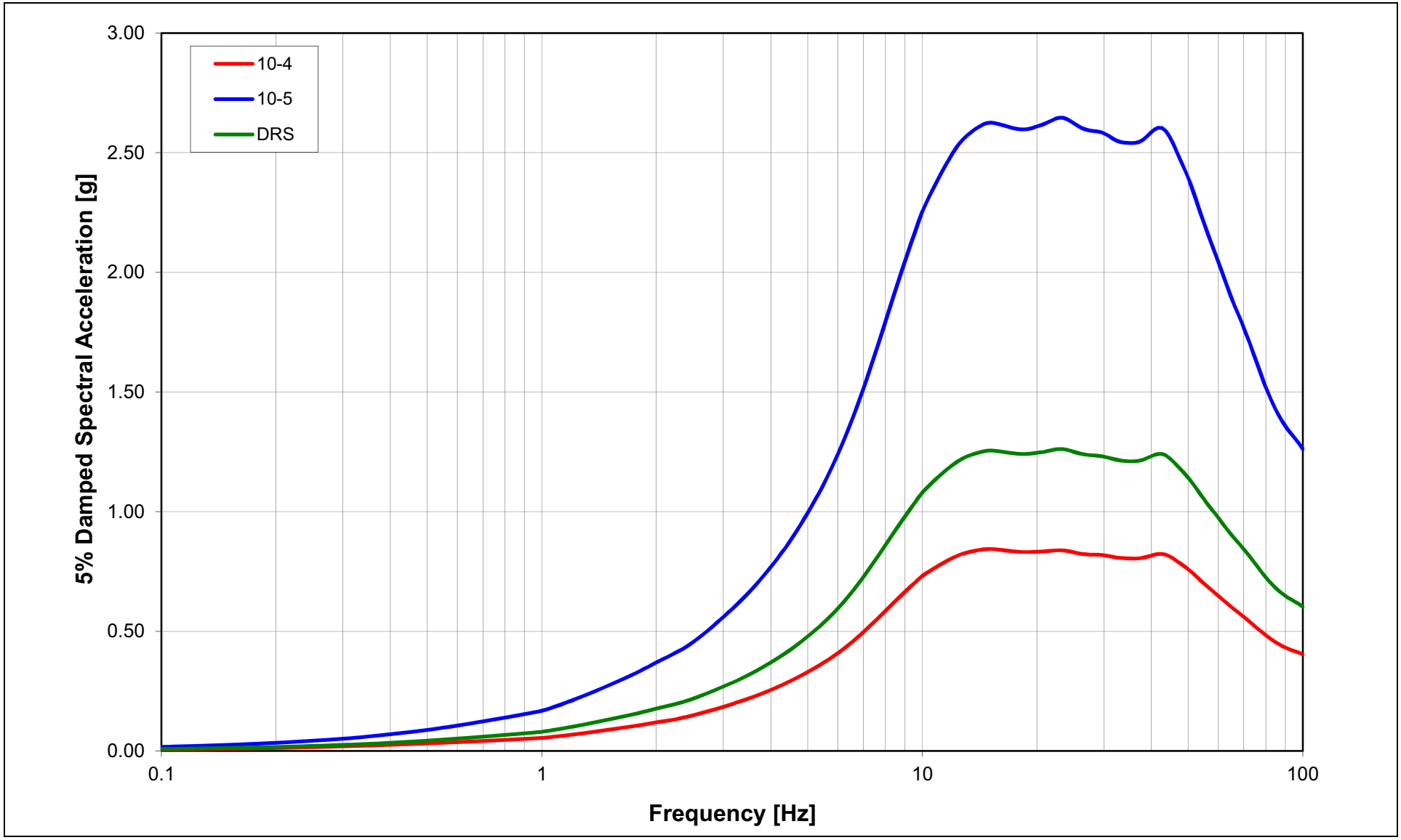

NAPS COL 2.0-27-A **Figure 2.5.2-299 Mean Horizontal Geologic Outcrop UHRS at 10^{-4} and 10^{-5} Hazard Levels and Geologic Outcrop DRS for RB/FB Soil Column at Elevation 224 ft (GMRS Horizon)**

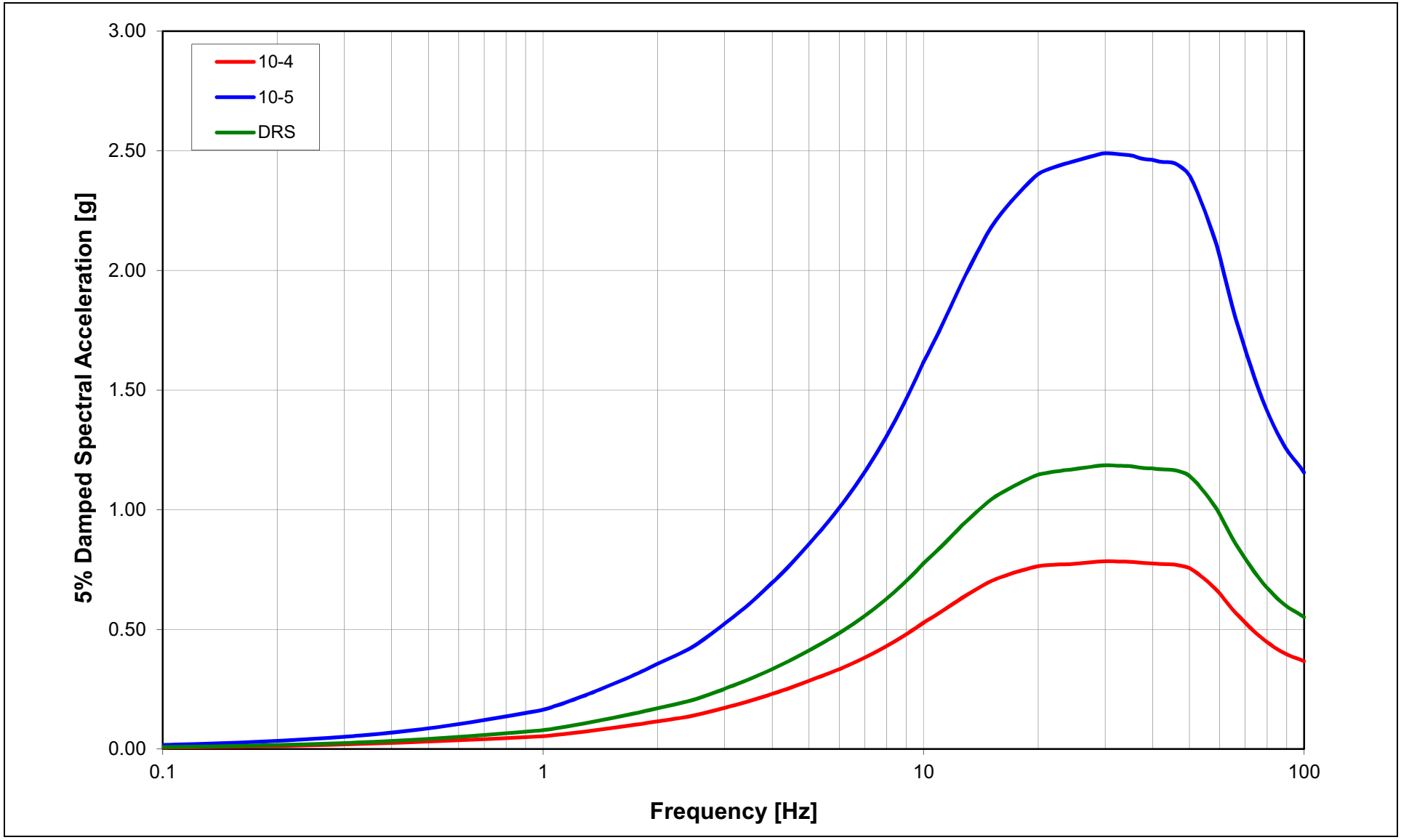

NAPS COL 2.0-27-A **Figure 2.5.2-300 Mean Horizontal Full Column Outcrop UHRS at 10^{-4} and 10^{-5} Hazard Levels and Full Column Outcrop DRS for CB Soil Column at Elevation 224 ft (BoF for RB/FB)**

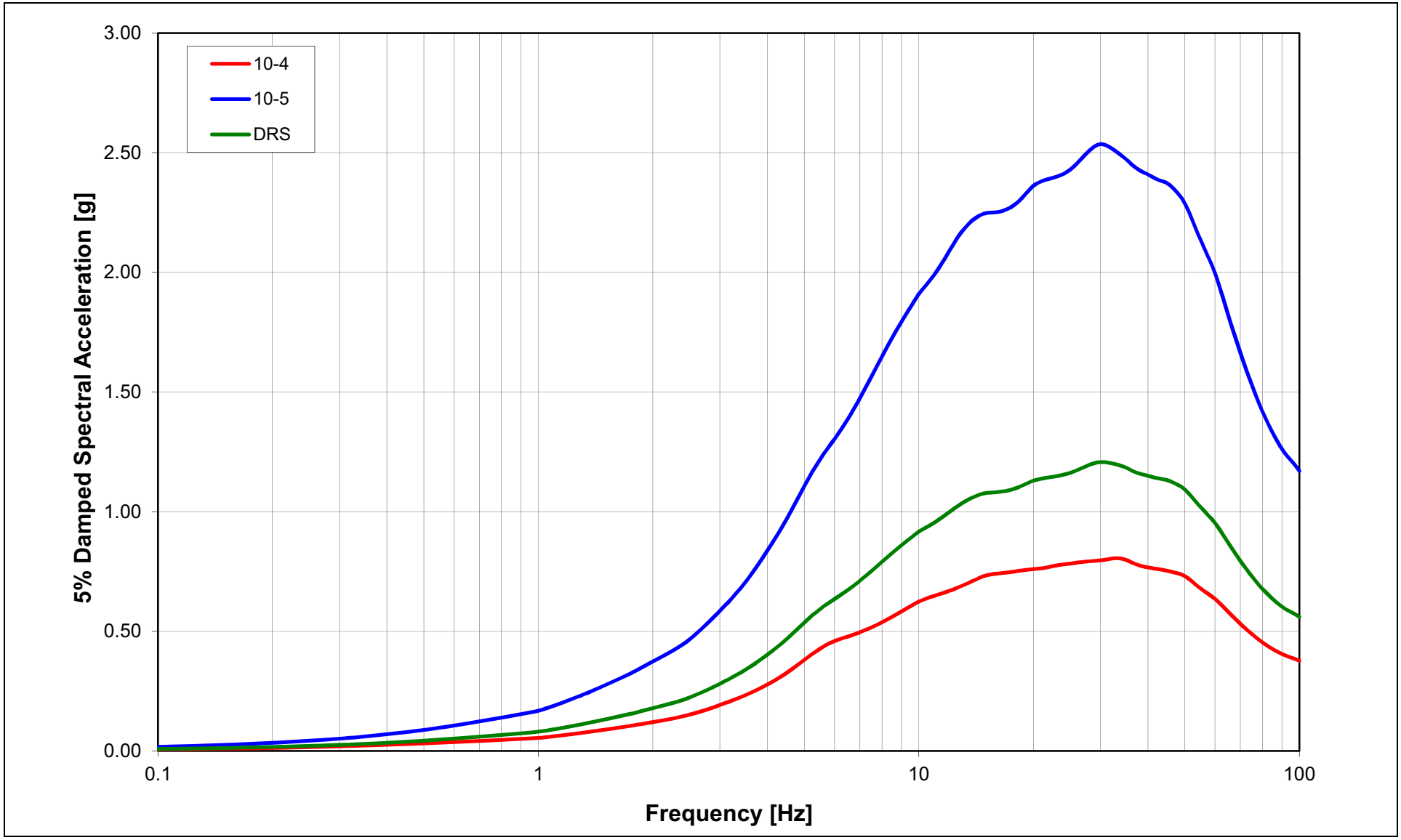

NAPS COL 2.0-27-A **Figure 2.5.2-301 Mean Horizontal Full Column Outcrop UHRS at 10^{-4} and 10^{-5} Hazard Levels and Full Column Outcrop DRS for CB Soil Column at Elevation 241 ft (BoF for CB)**

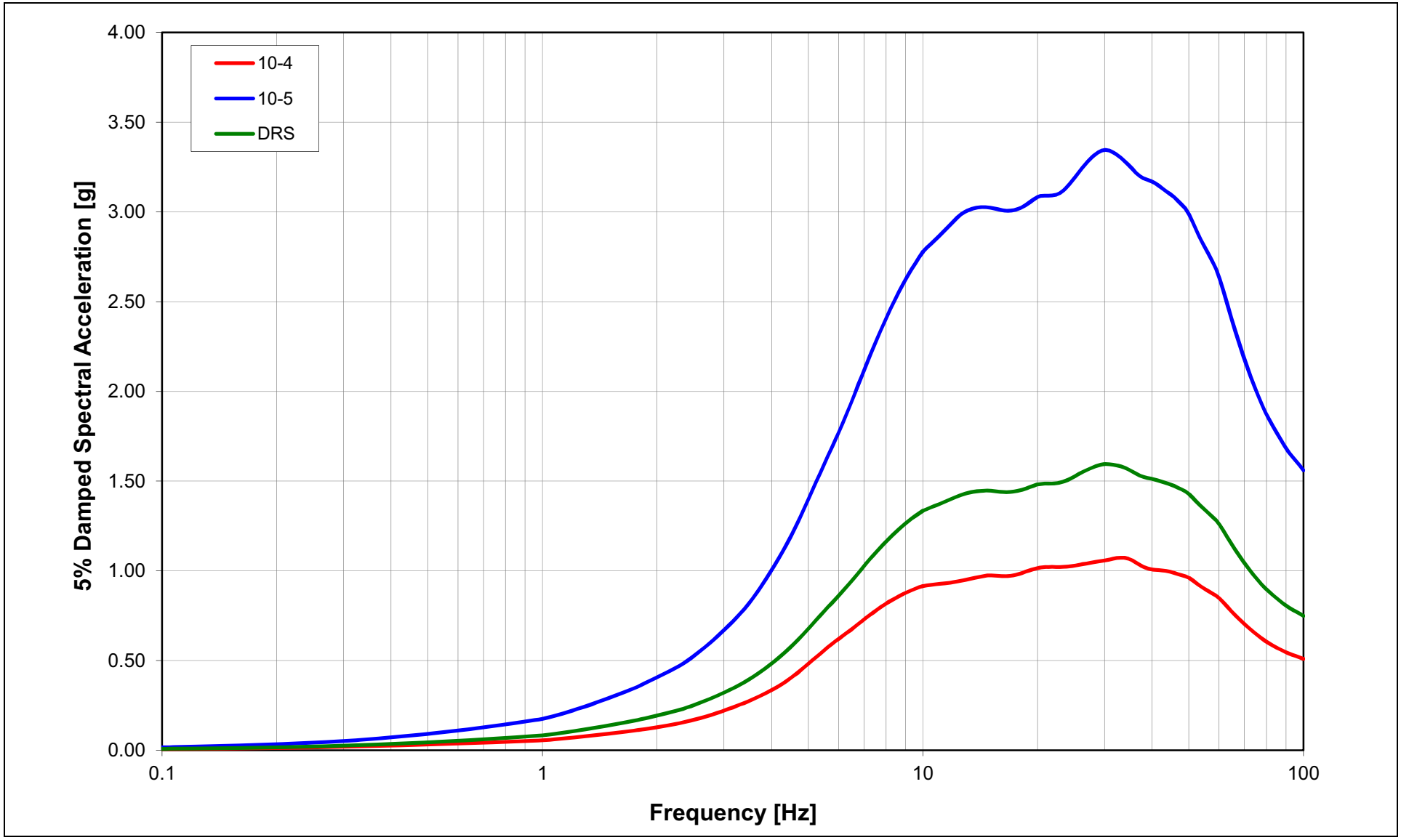

NAPS COL 2.0-27-A **Figure 2.5.2-302 Mean Horizontal Full Column Outcrop UHRS at 10^{-4} and 10^{-5} Hazard Levels and Full Column Outcrop DRS for CB Soil Column at Elevation 290 ft (Finished Grade)**

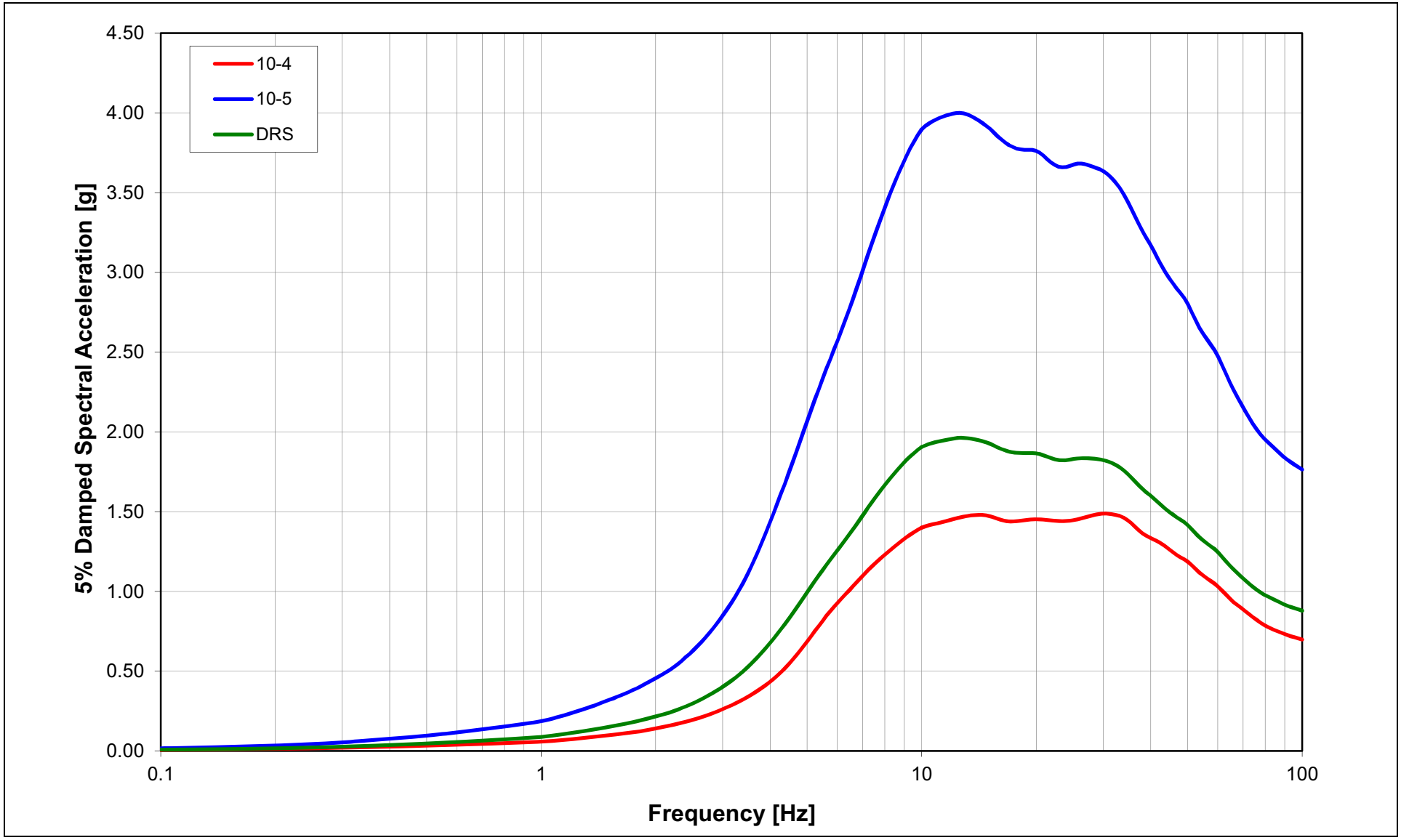

NAPS COL 2.0-27-A **Figure 2.5.2-303 Mean Horizontal Partial Column Outcrop UHRS at 10^{-4} and 10^{-5} Hazard Levels and Partial Column Outcrop DRS for CB Soil Column at Elevation 224 ft (BoF for RB/FB)**

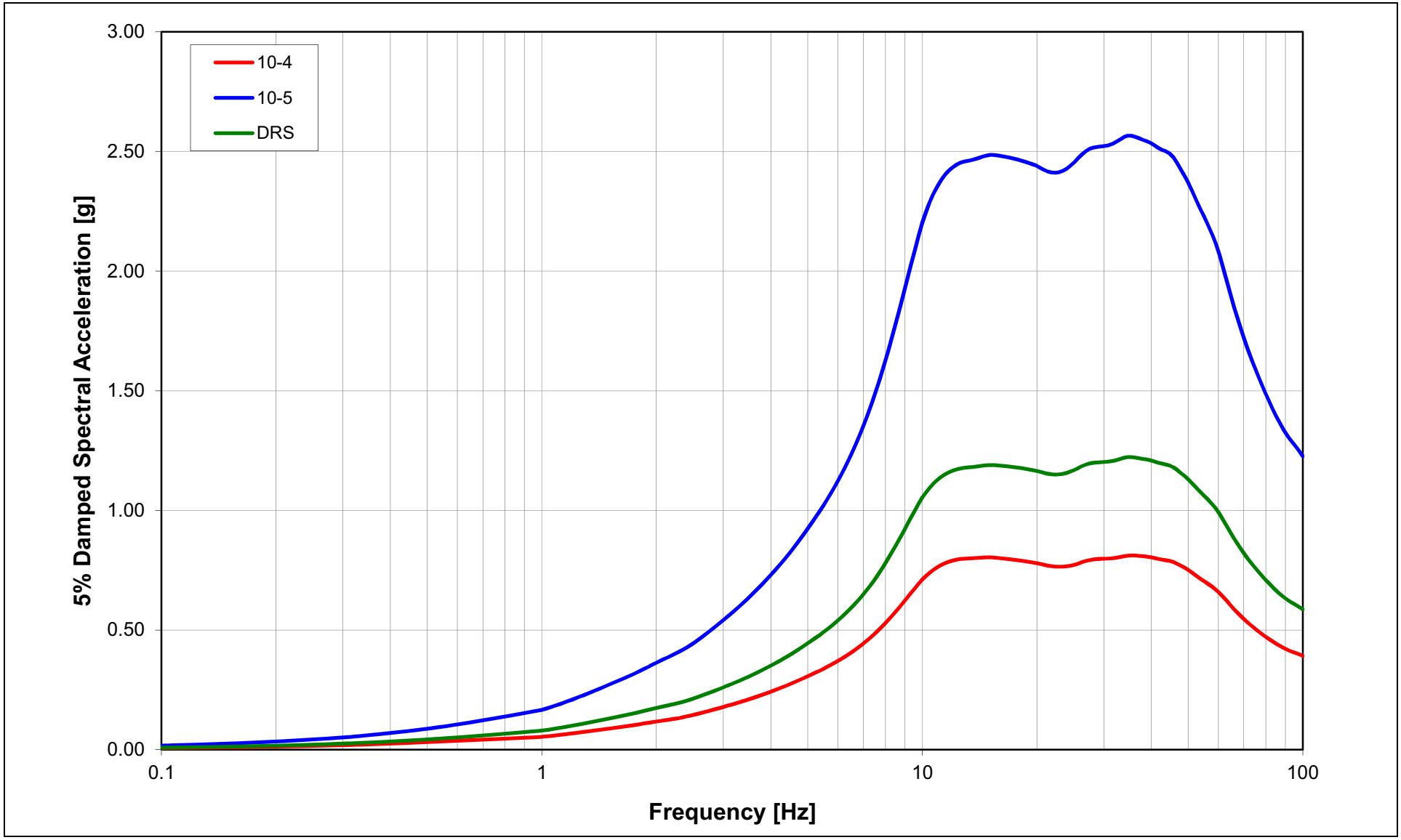

NAPS COL 2.0-27-A **Figure 2.5.2-304 Mean Horizontal Partial Column Outcrop UHRS at 10^{-4} and 10^{-5} Hazard Levels and Partial Column Outcrop DRS for CB Soil Column at Elevation 241 ft (BoF for CB)**

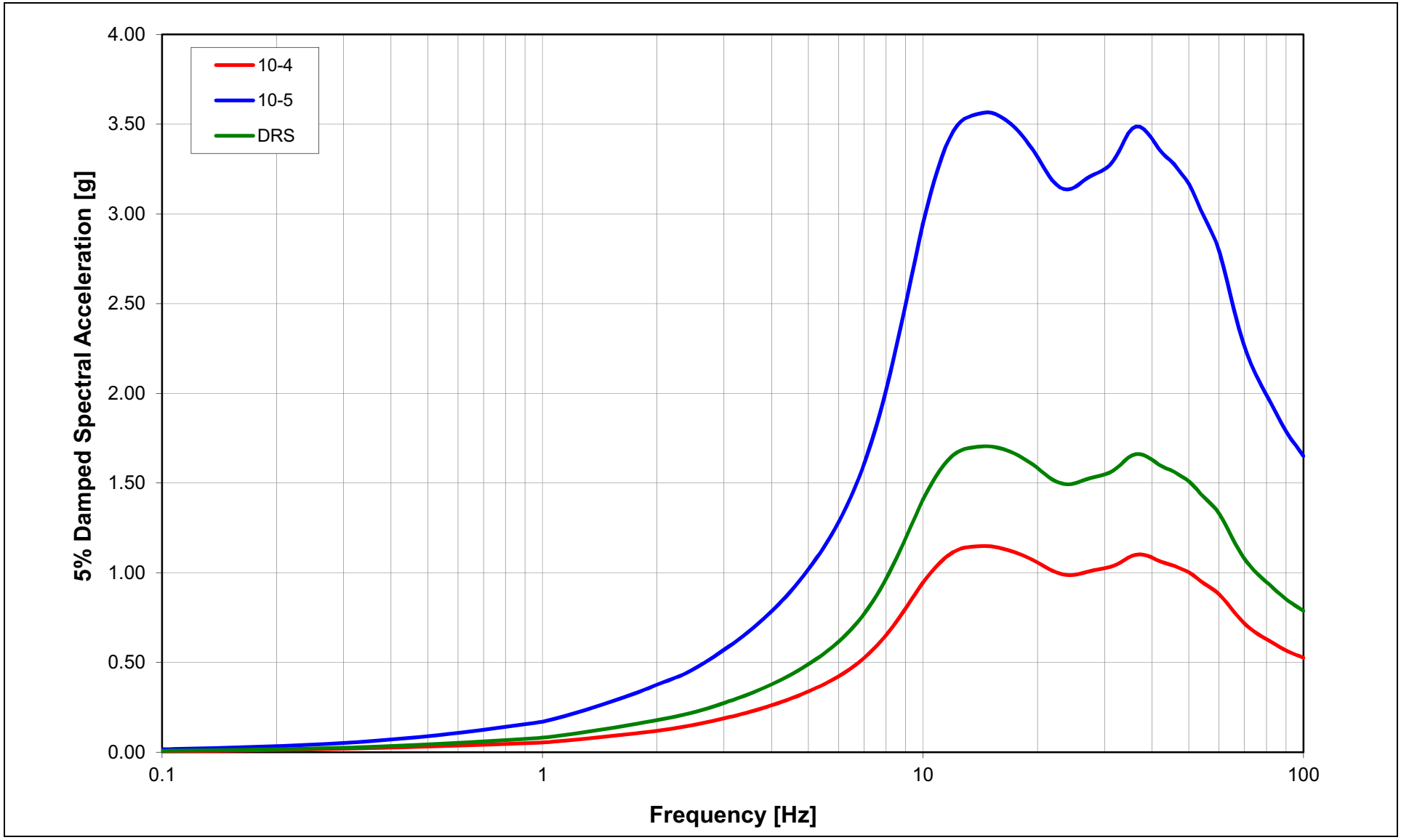

NAPS COL 2.0-27-A **Figure 2.5.2-305 Mean Horizontal Geologic Outcrop UHRS at 10^{-4} and 10^{-5} Hazard Levels and Geologic Outcrop DRS for CB Soil Column at Elevation 224 ft (GMRS Horizon)**

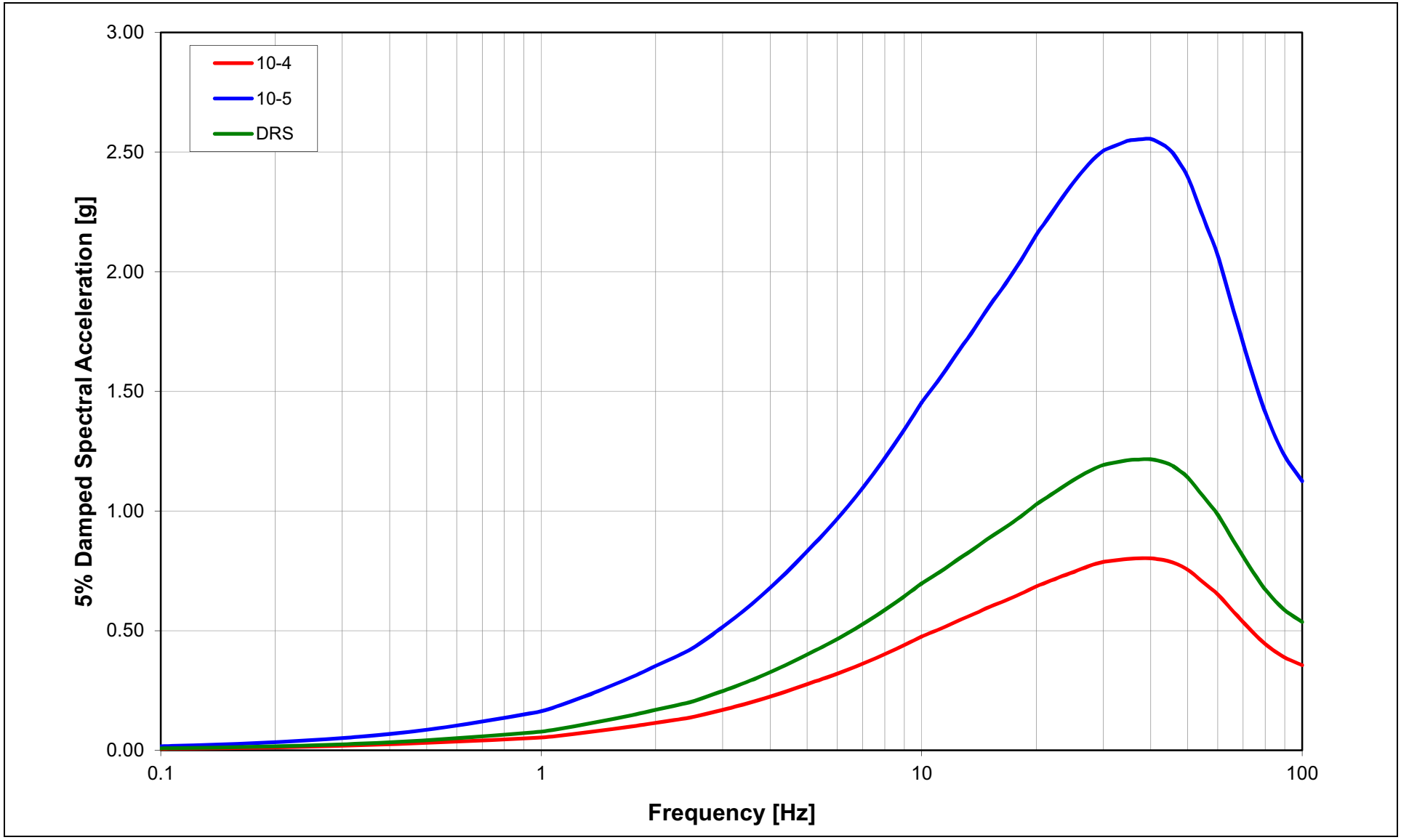

NAPS COL 2.0-27-A **Figure 2.5.2-306 Mean Horizontal Geologic Outcrop UHRS at 10^{-4} and 10^{-5} Hazard Levels and Geologic Outcrop DRS for FWSC Soil Column at Elevation 282 ft (BoF for FWSC)**

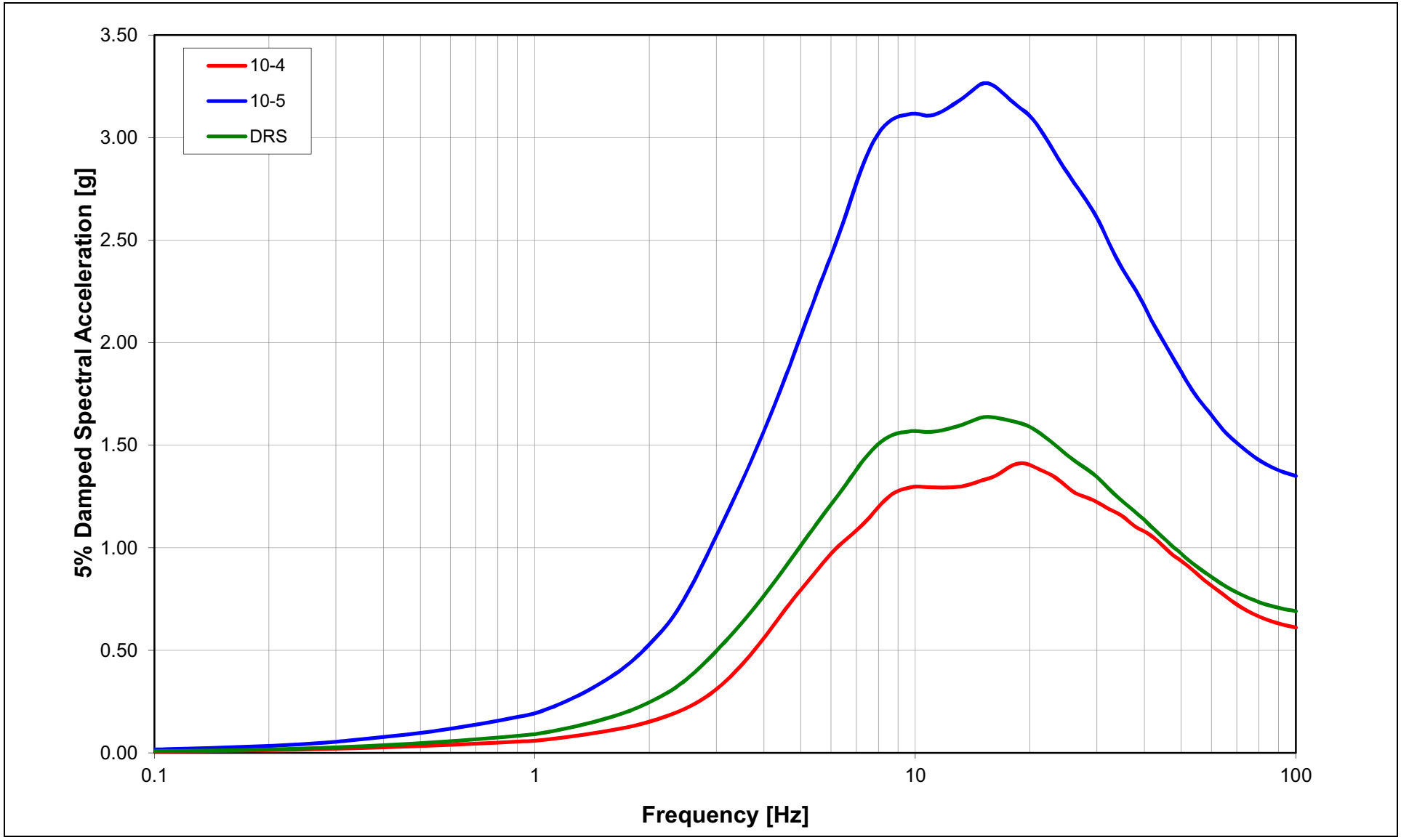

NAPS COL 2.0-27-A
NAPS DEP 3.7-1

Figure 2.5.2-307 Horizontal and Vertical RB/FB Full Column Outcrop FIRS

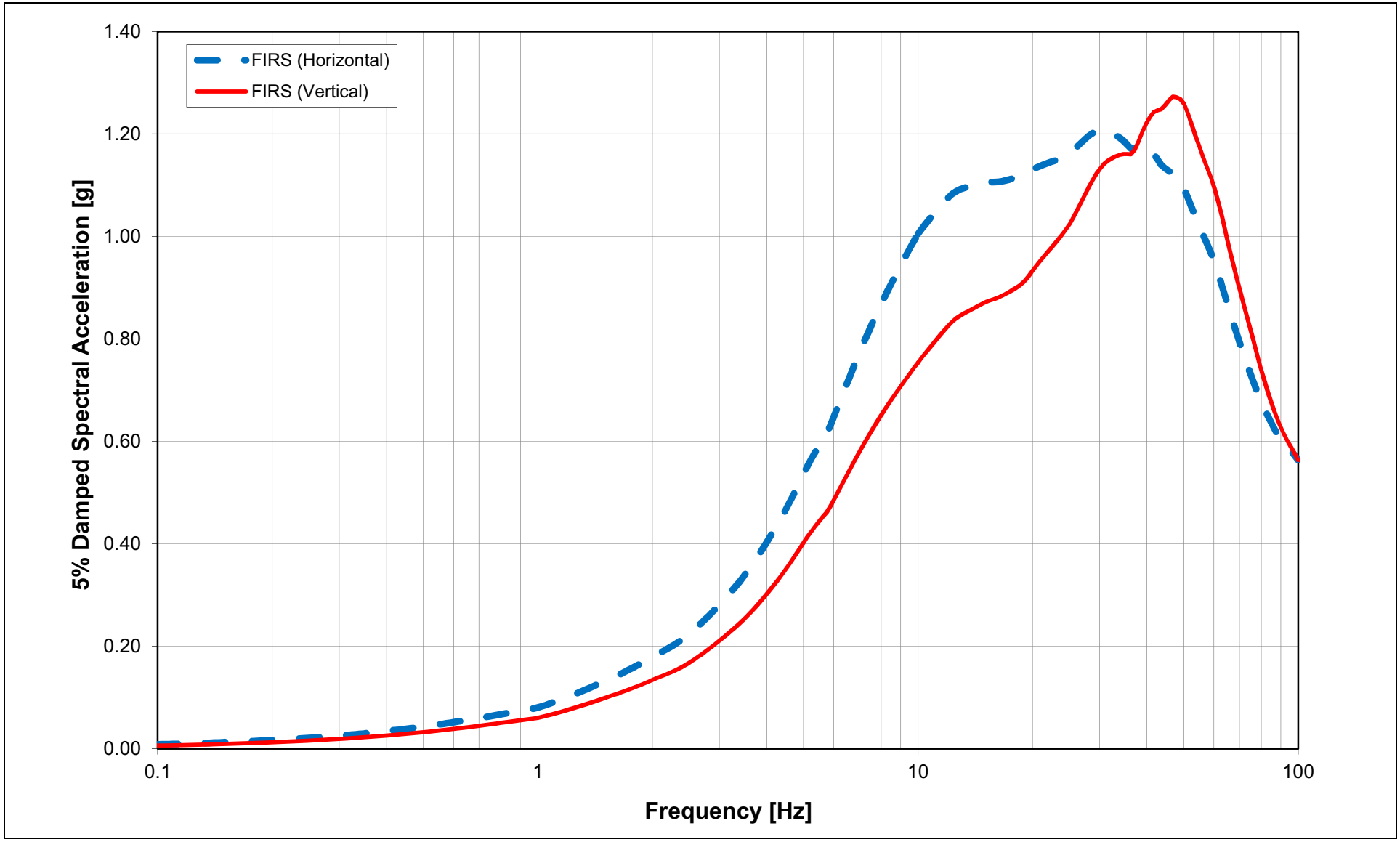

NAPS COL 2.0-27-A
NAPS DEP 3.7-1

Figure 2.5.2-308 Horizontal and Vertical CB Full Column Outcrop FIRS

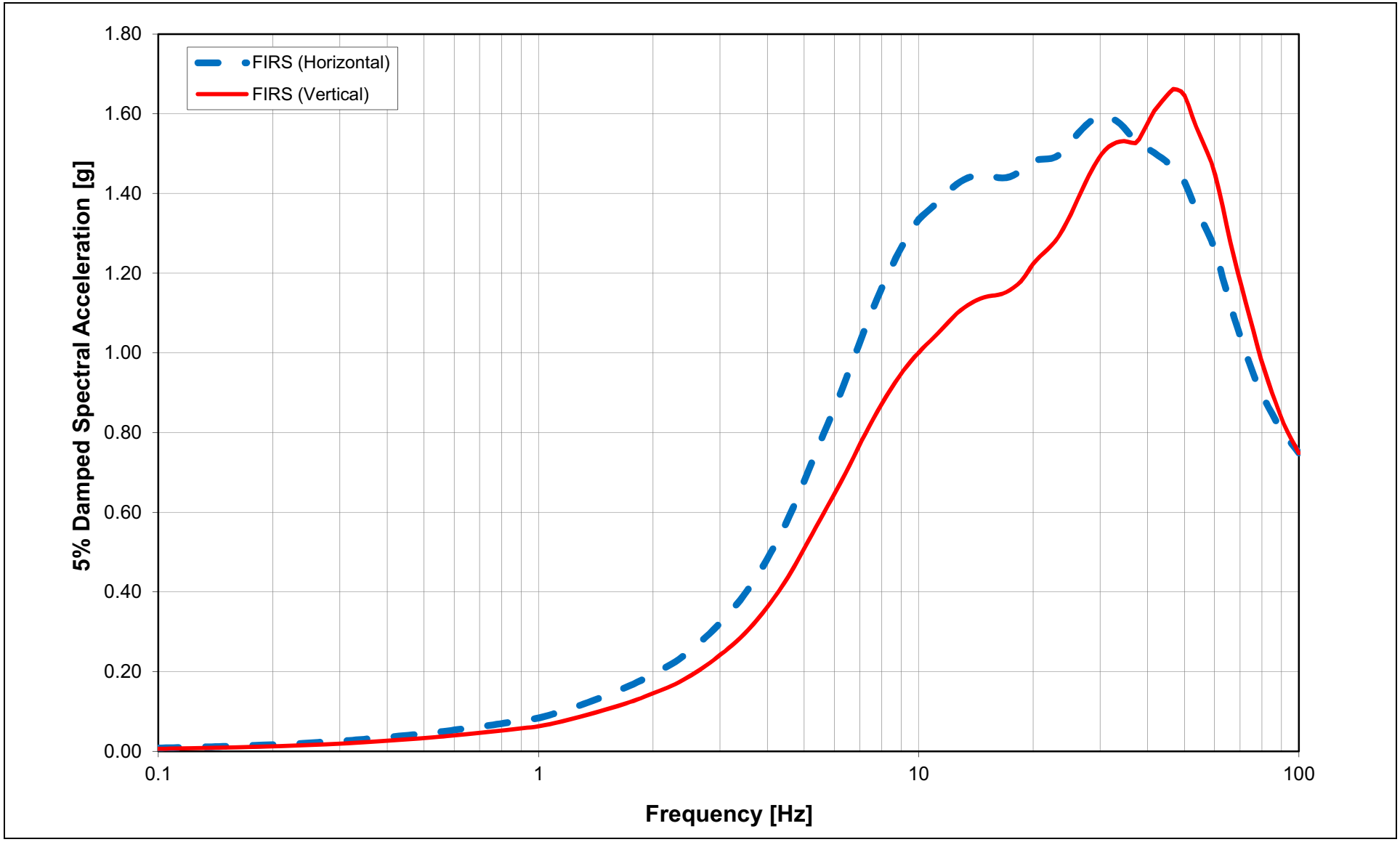

NAPS COL 2.0-27-A
NAPS DEP 3.7-1

Figure 2.5.2-309 Horizontal and Vertical RB/FB Partial Column Outcrop FIRS

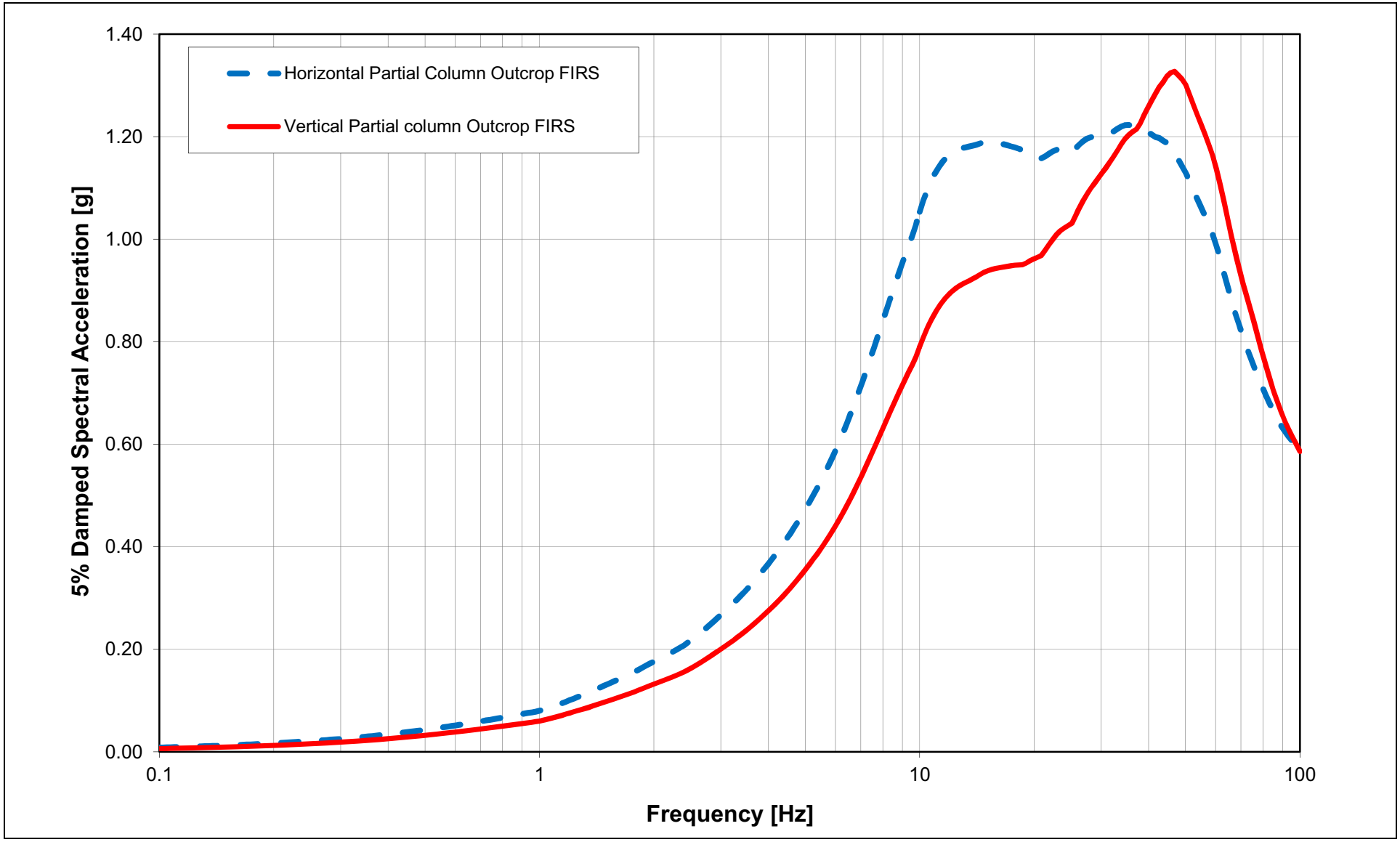

NAPS COL 2.0-27-A
NAPS DEP 3.7-1

Figure 2.5.2-310 Horizontal and Vertical CB Partial Column Outcrop FIRS

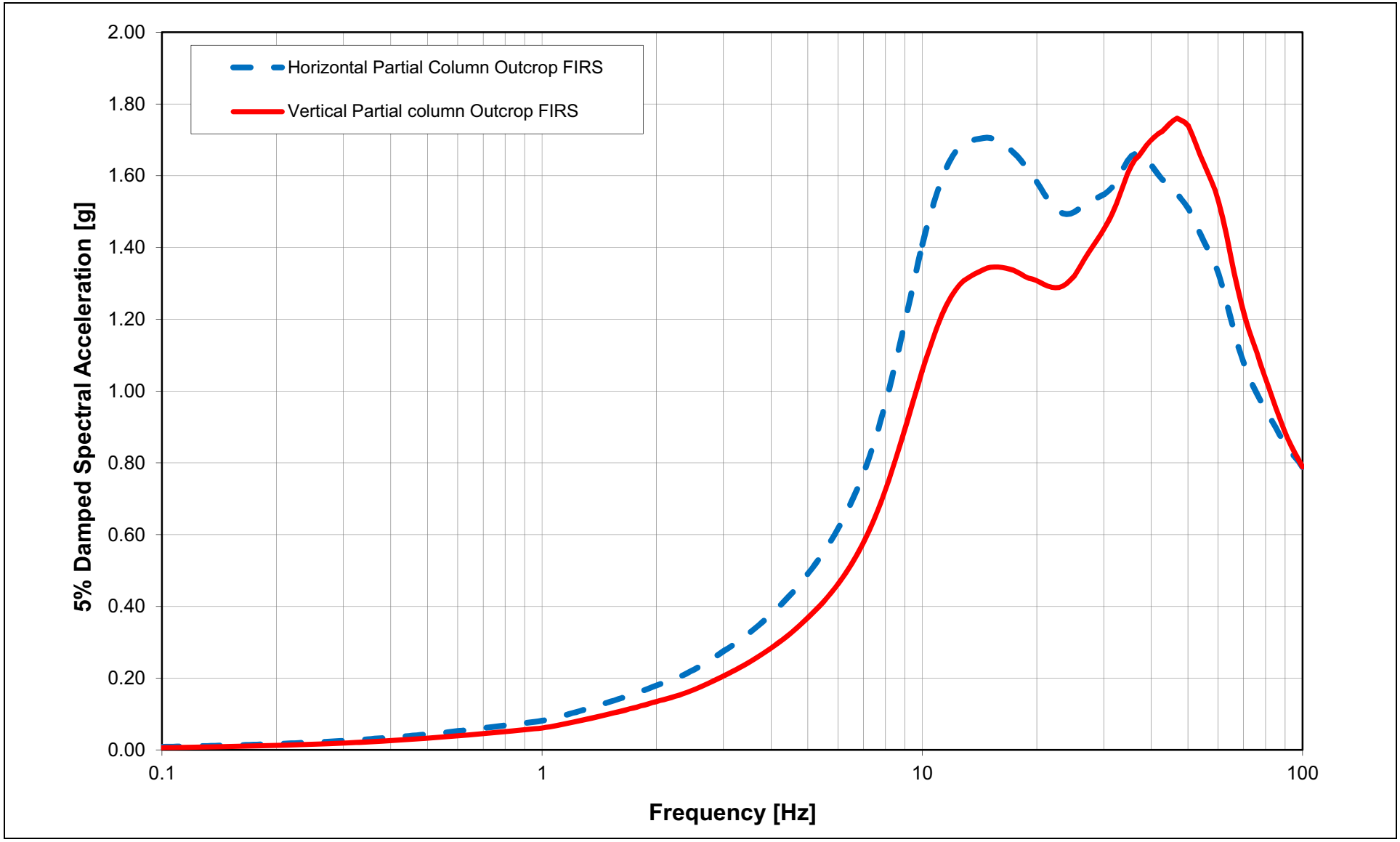

NAPS COL 2.0-27-A **Figure 2.5.2-311 Horizontal and Vertical PBSRS for RB/FB and CB**

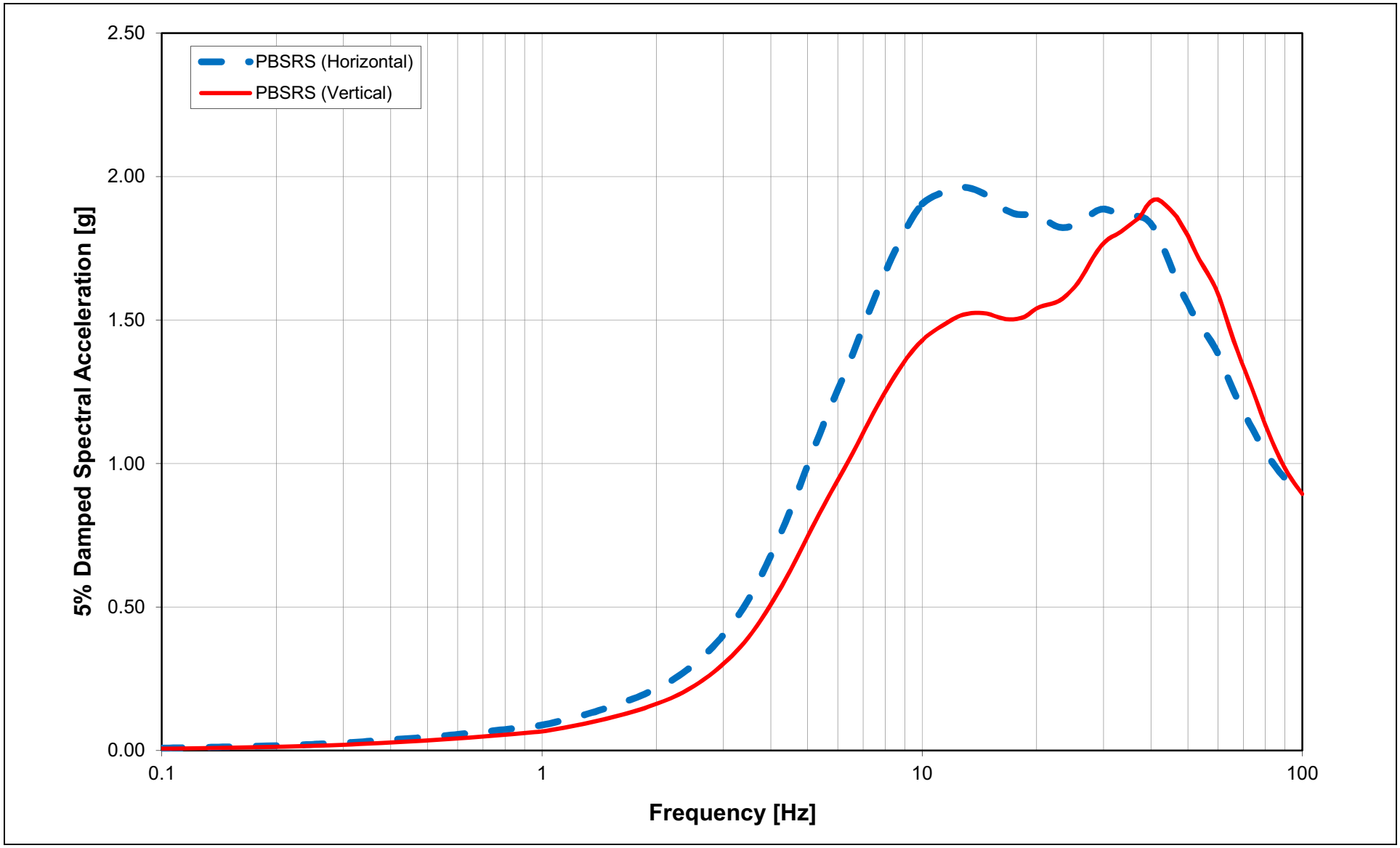

NAPS COL 2.0-27-A
NAPS DEP 3.7-1

Figure 2.5.2-312 Horizontal and Vertical FWSC Geologic Outcrop FIRS

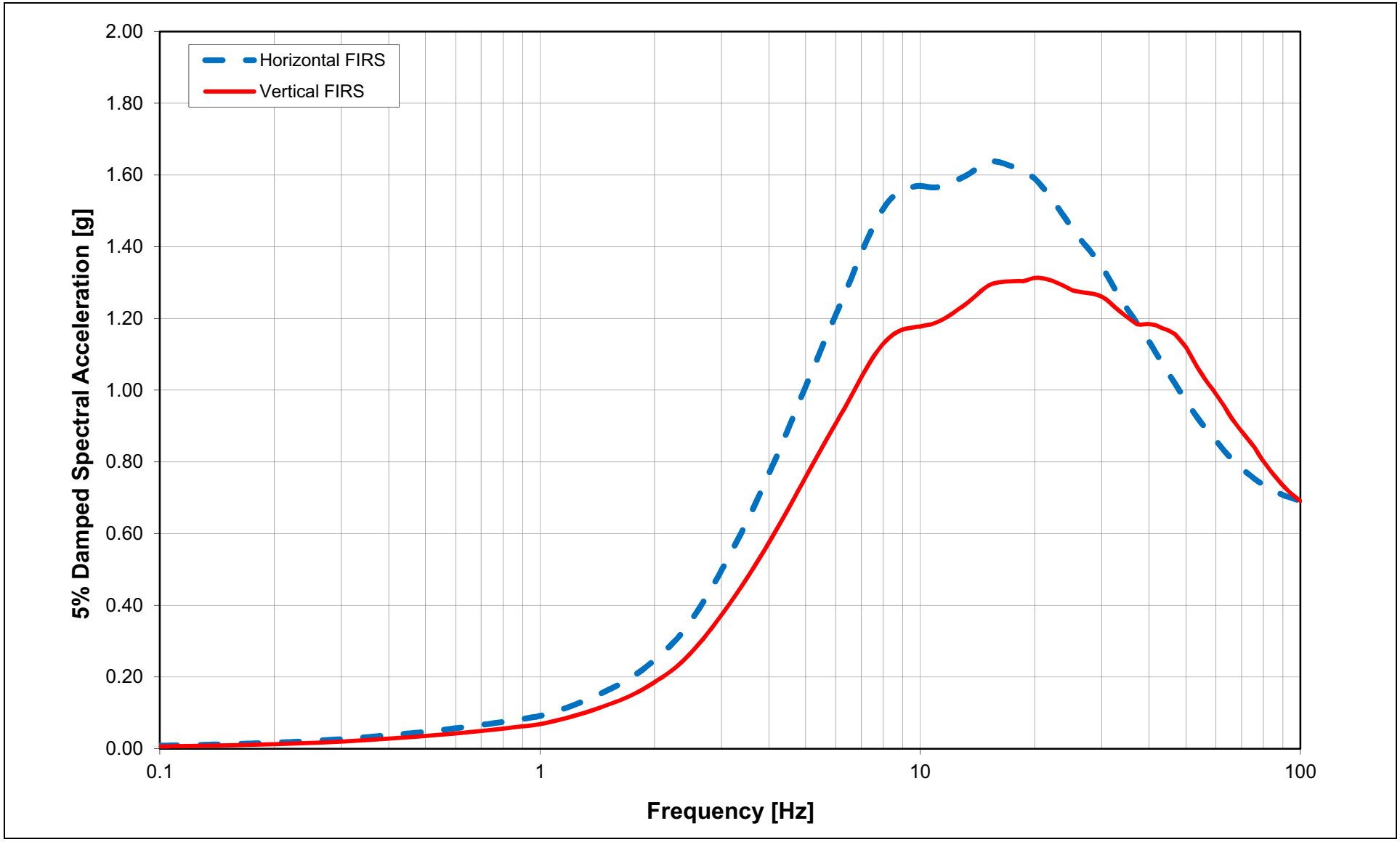

NAPS COL 2.0-27-A
NAPS ESP VAR 2.0-4

Figure 2.5.2-313 Horizontal and Vertical GMRS

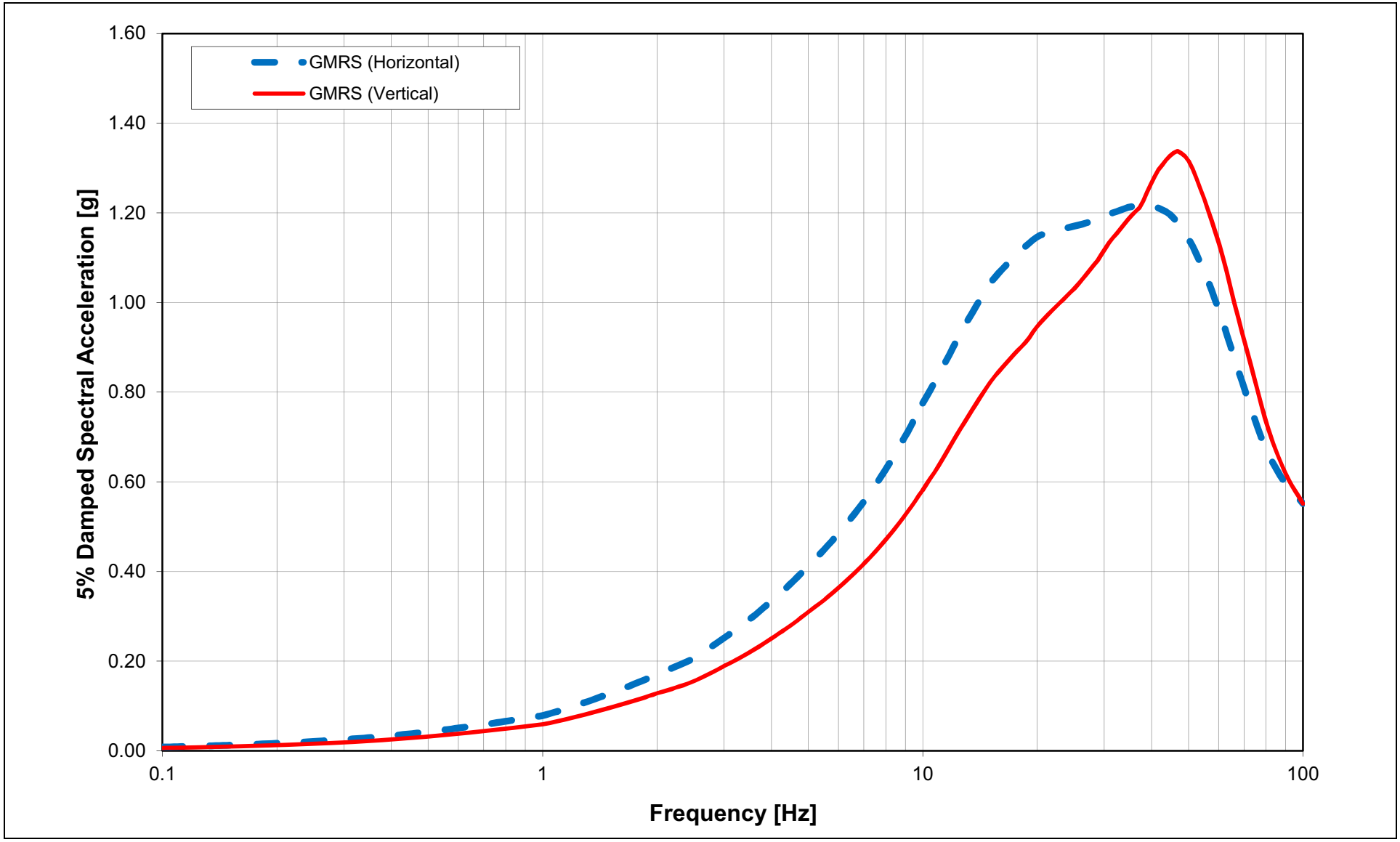

NAPS COL 2.0-27-A
NAPS ESP VAR 2.0-4

Figure 2.5.2-314 Rock V/H Ratios Recommended in NUREG/CR-6728 (Reference 2.5-385)

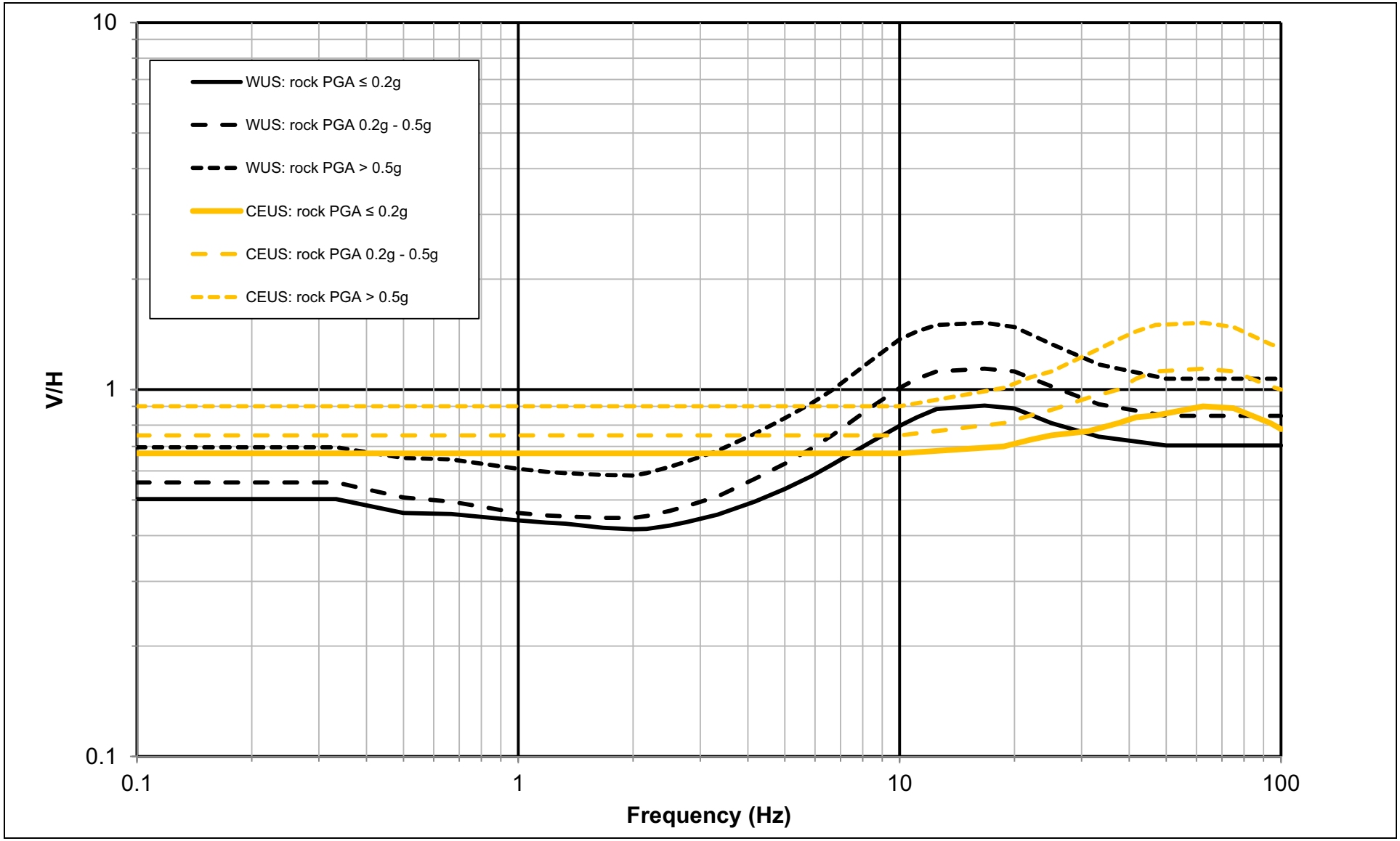

NAPS COL 2.0-27-A
NAPS ESP VAR 2.0-4

Figure 2.5.2-315 **$V/H_{WUS,soil}$ / $V/H_{WUS,rock}$ (*f* (Rock-to-Soil)) from GA11 V/H Model for the Suite of Controlling Magnitudes and Distances for Soil V_{S30} of 2,439 ft/s (743 m/s) and Rock V_{S30} of ~5,000 ft/s (1,500 m/s)**

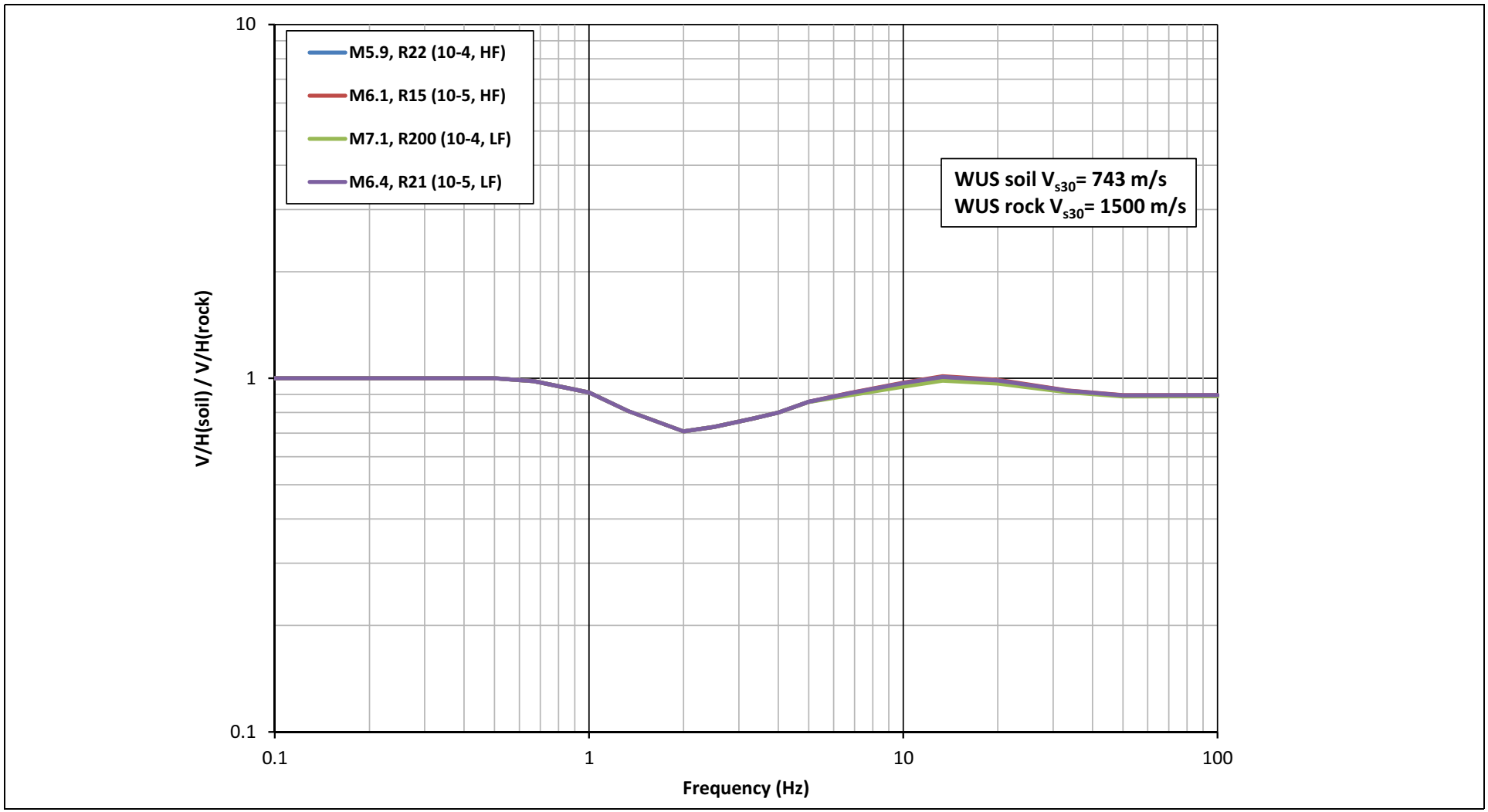

NOTE: ~~The LF distances have been capped to the maximum applicable distance (200 km) of the GA11 V/H model (Reference 2.5-388)~~
The rupture distance of 10^{-4} LF case of **M**7.1 has been capped to the maximum applicable distance (200 km) of the GA11 V/H model.

NAPS COL 2.0-27-A
NAPS ESP VAR 2.0-4

Figure 2.5.2-316 Frequency-Shifted Versions of $V/H_{WUS,soil}$ /$V/H_{WUS,rock}$ (*f* (Rock-to-Soil) × *f* (WUS-to-CEUS)) from Figure 2.5.2-315

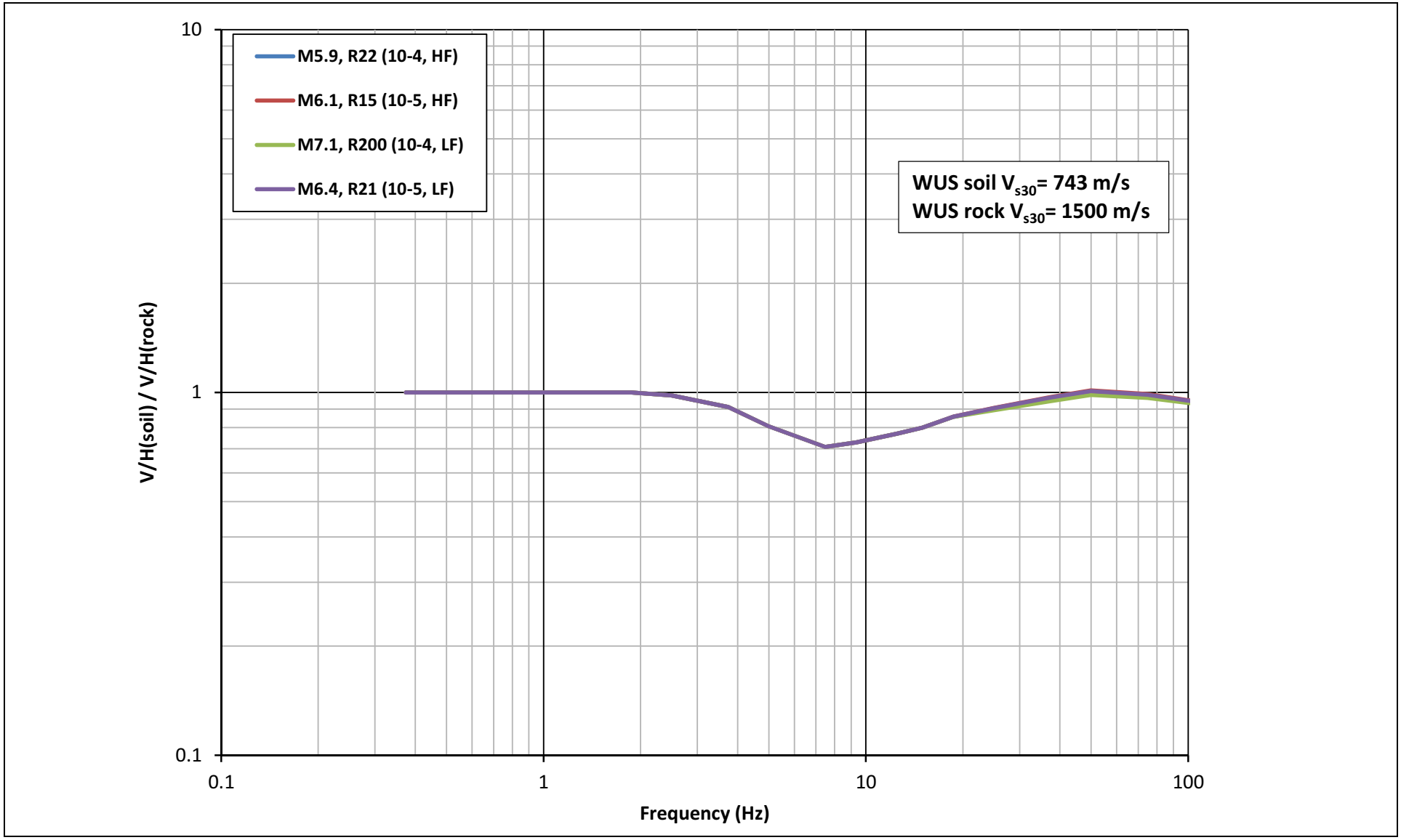

NAPS COL 2.0-27-A
NAPS ESP VAR 2.0-4

Figure 2.5.2-317 Initial $V/H_{CEUS,soil}$ for a Suite of Controlling Magnitudes and Distances and V_{S30} of 2,439 ft/s (743 m/s)

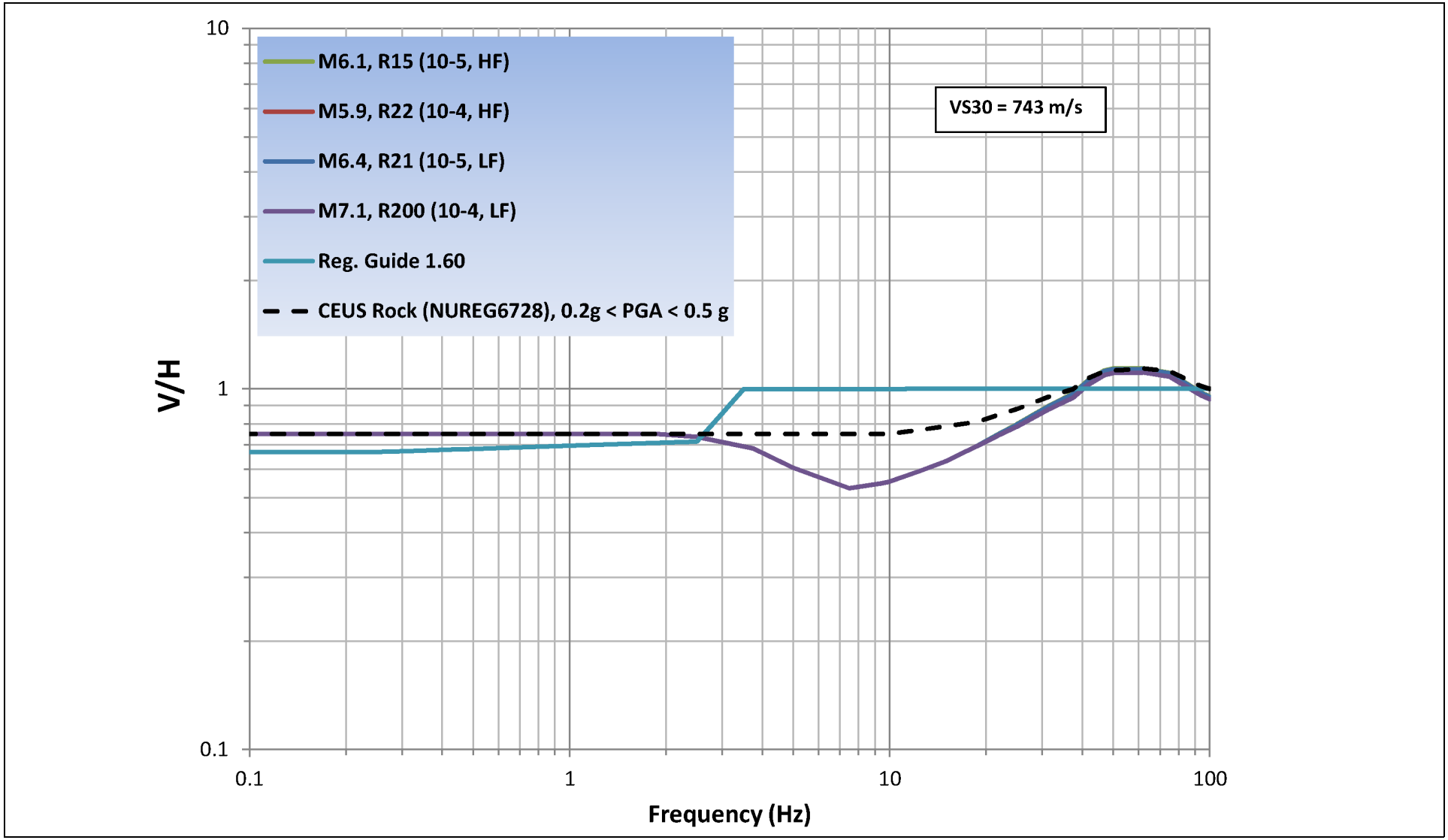

NOTE: Applicable $V/H_{CEUS,rock}$ and the V/H from RG 1.60 are shown for comparison.

NAPS COL 2.0-27-A
NAPS ESP VAR 2.0-4

Figure 2.5.2-318 Initial $V/H_{CEUS,soil}$ for a Suite of Controlling Magnitudes and Distances and V_{S30} of 3,423 ft/s (1,043 m/s)

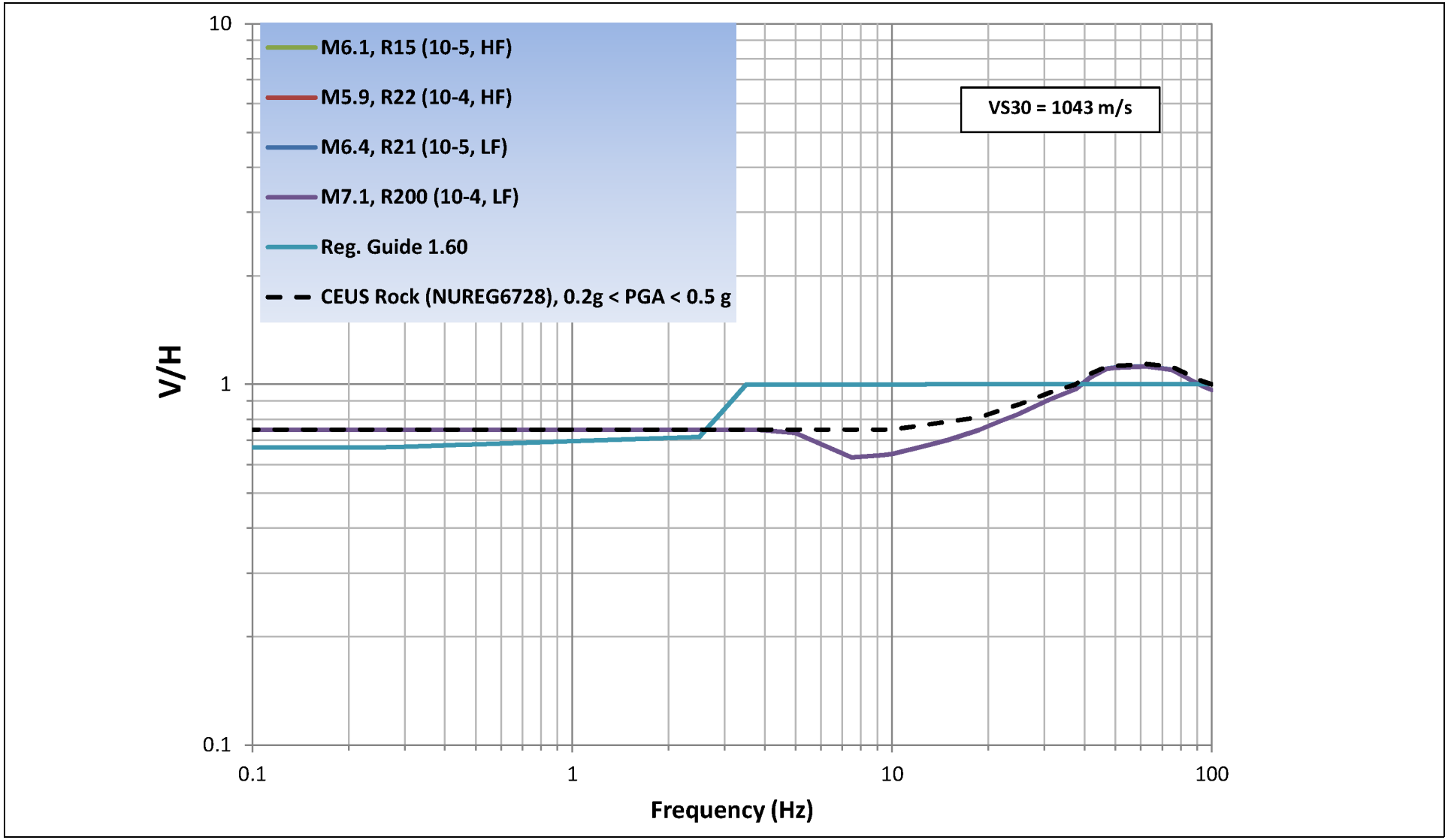

NOTE: Applicable $V/H_{CEUS,rock}$ and the V/H from RG 1.60 are shown for comparison.

NAPS COL 2.0-27-A
NAPS ESP VAR 2.0-4

Figure 2.5.2-319 Initial PBSRS $V/H_{CEUS,soil}$ Is the Envelope of 8 V/H curves (Figures 2.5.2-317 and 2.5.2-318)

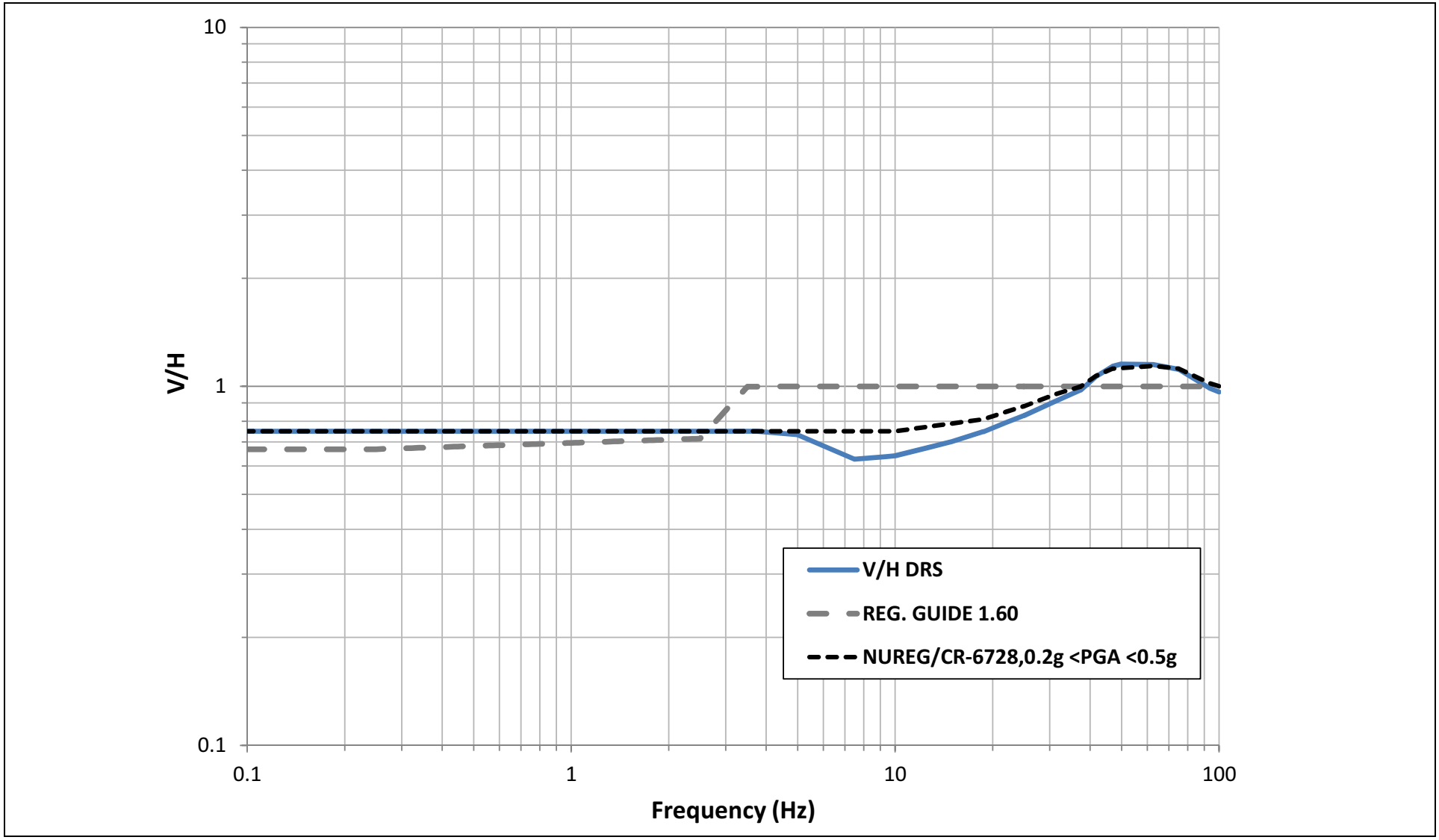

NOTE: Applicable $V/H_{CEUS,rock}$ and the V/H from RG 1.60 are shown for comparison.

NAPS COL 2.0-27-A
NAPS ESP VAR 2.0-4

Figure 2.5.2-320 Final PBSRS $V/H_{CEUS,soil}$ Where Mid-Frequency Dip Has Been Removed

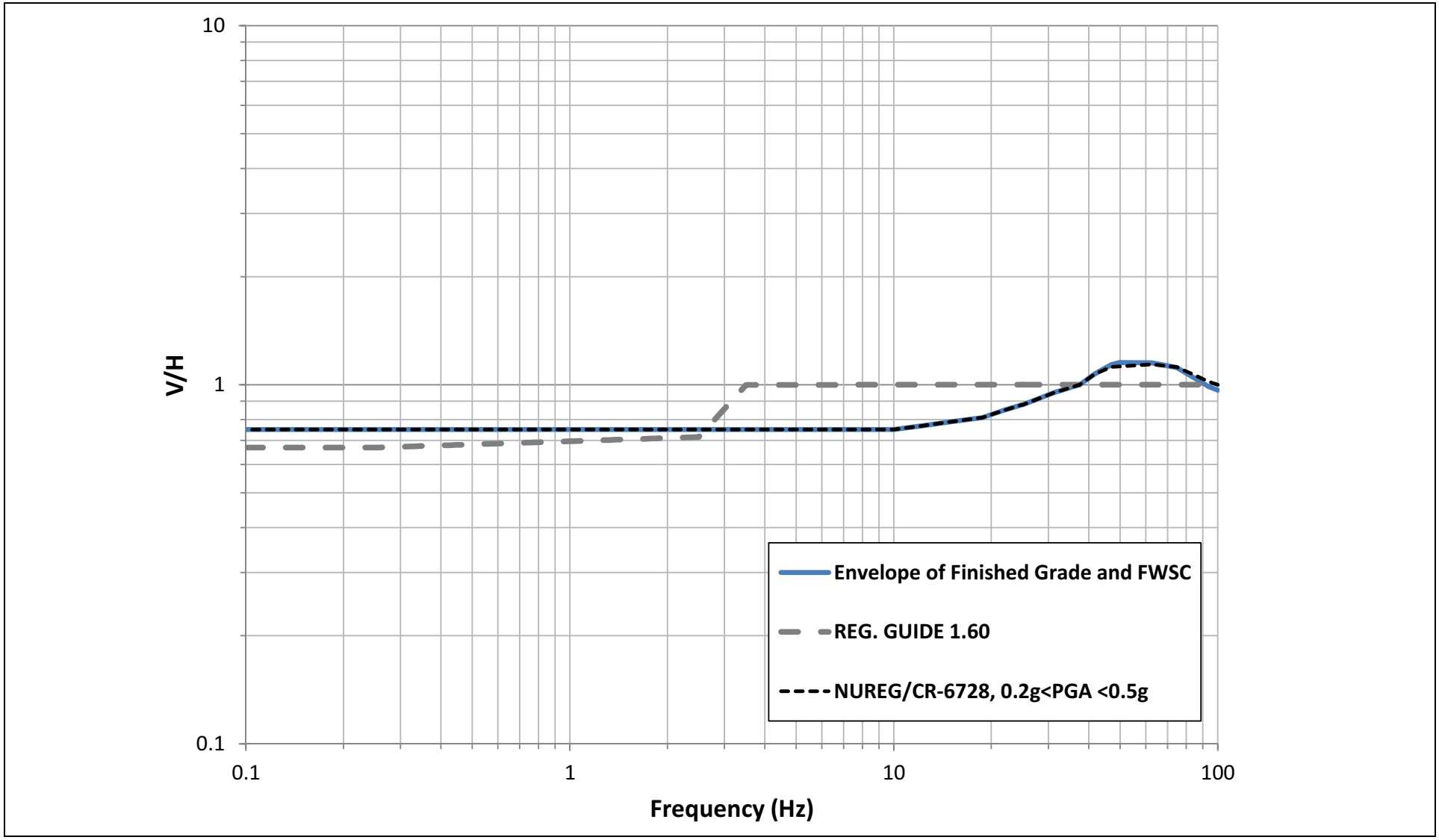

NOTE: Applicable $V/H_{CEUS,rock}$ and the V/H from RG 1.60 are shown for comparison.

demonstrate, along with the RQD profile in Figure 2.5.4-220, that above about Elevation 184 ft, weathered/fractured zones can be encountered; however, there is no pattern to where these zones occur, indicating the randomized process of weathering.

2.5.4.5 Excavation and Backfill

NAPS ESP COL 2.5-3

This section describes the following topics:

- The extent (horizontally and vertically) of Seismic Category I excavations, fills and slopes
- Excavation methods and stability
- Backfill sources, quantities, compaction specifications and quality control (QC)

2.5.4.5.1 Extent of Excavations, Fills and Slopes

Figure 2.5.4-206, the excavation plan, shows the extent of excavations, fills and slopes for Unit 3. These are shown in cross-section in Figures 2.5.4-225 through 2.5.4-234. To obtain the finish ground level grade of Elevation 289.5 ft, considerable quantities of soil will be excavated. The location of original ground surface is shown in the cross-sections. There are some lower areas to the northeast that will be backfilled. The total estimated cut within the power block area is about 625,380 cubic yards, while the amount of backfilling with compacted structural fill is about 241,750 cubic yards and concrete fill is about 109,620 cubic yards. Benched 3-horizontal to 1-vertical (3H:1V) slopes extend up from finish ground level grade around the southern and eastern perimeter of the area.

To the northeast of the Turbine Building, going towards the existing Units 1 and 2, ground surface elevation reduces at an approximately 5 percent slope down to Elevation 280 ft at the Service Water Building. Stormwater management pond #1 is between these structures and the boundary of Units 1 and 2 with yard grade at Elevation 270 ft. As existing grade falls off from the power block area northeast towards Units 1 and 2 some backfilling will be required to achieve final grade. As much as 30 ft of backfill will be needed to bring grade up to the planned ground surface area of the originally planned Units 3 and 4, where ground level is presently at around Elevation 250 ft.

Figures 2.5.4-206 and 2.5.4-217 show the outline of the power block foundations. As shown in Figures 2.5.4-225 through 2.5.4-234,

temporary excavation for Unit 3 construction will be supported by a wall system. This wall will be supported by tie-backs or other means.

The excavation will be backfilled first with concrete fill up to the surface of Zone III rock and after that with structural fill up to the finished grade. The south and the west supports of the excavation will be located at least 10.27 ft away from the RB/FB foundation. The lateral distance between the CB foundation and the north support of the excavation will be at least 12.24 ft. The east support of the excavation will be located at least 19.65 ft from the FWSC foundation.

2.5.4.5.2 Excavation Methods and Stability

a. **Excavation in Soil**

Excavation in the soils (Zones IIA and IIB) and any existing fills is achieved with conventional excavating equipment. Excavation of less than 20 ft in height will adhere to OSHA regulations (SSAR Reference 162). As noted in the previous section, a temporary vertical wall system will be used to support the power block excavation. The slopes around the perimeter of the power block area are no steeper than 3H to 1V, with a bench at approximately 25 ft height. Since the saprolitic soils can be highly erosive, even temporary slopes cut into the saprolite are sealed and protected.

b. **Excavation in Rock**

Excavation in the Zone III moderately to severely weathered rock is achieved using conventional earthmoving equipment. A temporary vertical wall system will be used to support the excavation, where necessary.

Excavation made for the originally planned Units 3 and 4 in the slightly to moderately weathered rock (Zone III-IV) and fresh to slightly weathered rock (Zone IV) is documented in SSAR Reference 163. Techniques employed were similar to those used for Units 1 and 2 (SSAR Reference 164) but with “lessons learned” applied. The methods of rock excavation outlined below for Unit 3 are based, in part, on the methods that worked successfully for Units 1 and 2 and the originally planned Units 3 and 4. Unit 3 is approximately 1500 ft from the center of the Unit 2 R/B, whereas the originally planned Unit 3 R/B was only about 300 ft from the Unit 2 R/B. Thus, the following techniques to reduce

2.5.4.7.4 Rock and Soil Column Amplification/Attenuation Analysis

NAPS ESP COL 2.5-5

The ARS derived from the P-SHAKE analyses for the Seismic Category I structures described in Section 2.5.4.7.1 are presented in Section 3.7.1.

The P-SHAKE program is used to obtain peak ground accelerations in the free-field for use in slope stability (Section 2.5.5) and liquefaction analysis (Section 2.5.4.8) using the V_S profile described in Section 2.5.4.7.1.d. Figure 2.5.4-250 shows the maximum acceleration versus depth profiles obtained from P-SHAKE for the high and low frequency earthquakes. The peak ground acceleration occur at about 42 ft depth and are about 0.56g for the high frequency earthquake and about 0.31g for the low frequency earthquake.

The accelerations shown in Figure 2.5.4-250 were obtained using input rock motions consistent with the EPRI (2004, 2006) (References 2.5-224, 2.5-225) ground motion model (GMM). These input rock motions were subsequently updated based on the EPRI (2013) (Reference 2.5-407) GMM for use in developing the GMRS and FIRS for all Seismic Category I buildings, as discussed in Sections 2.5.2.5 and 2.5.2.6. The updated input rock motions were not used to update the liquefaction, seismic lateral earth pressure, or pseudo-static slope stability analyses presented in Sections 2.5.4.8, 2.5.4.10, and 2.5.5.2.3.b, respectively. These updated rock motions are lower than those from the EPRI (2004, 2006) GMM and result in lower site ground motion response spectra, and correspondingly lower peak ground accelerations for low frequency and high frequency input motions. Therefore, Figure 2.5.4-250 is not updated because the accelerations shown on the figure are conservative.

NAPS COL 2.0-29-A

2.5.4.8 Liquefaction Potential

The Zone IIB saprolitic soils are extremely dense and the Zone III weathered rock has over 50 percent core stone and has typically been sampled by rock coring. Neither of these materials has liquefaction potential. The primary source of structural fill is bedrock excavated for the Unit 3 power block. This consists of crushed angular or sub-angular sand and gravel-sized particles compacted in thin lifts with a heavy vibratory steel-drummed roller. This fill is not liquefiable. The only material analyzed here for liquefaction is the Zone IIA saprolitic soil.

NAPS ESP PC 3.E(7)

All of the Seismic Category I structures are founded on rock or on concrete fill on rock at the Unit 3 site. Thus, even if the Zone IIA saprolite

is liquefiable, such liquefaction does not impact the stability of any Seismic Category I structure. As described in Section 2.5.4.10, the Zone IIA saprolite has relatively high resistance to bearing failure but can produce excessive settlements under certain conditions. Thus, the Zone IIA saprolite is not used to support Seismic Category I structures, whether it is potentially liquefiable or not.

The peak ground accelerations obtained from the Unit 3 P-SHAKE analyses through the natural soil profile are less than those reported in the SSAR, due to some slightly different rock and soil profiles, and the randomization process applied to these profiles. The previous liquefaction analyses are in Section 2.5.4.8.1. Section 2.5.4.8.2 presents the results of summarized liquefaction analyses performed on Zone IIA saprolites on slopes outside the power block area, based on borings and CPTs performed for Unit 3 in these areas, i.e., analyses of soils that will generally not be excavated.

Any failure of slopes due to liquefaction could impact adjacent safety-related structures. Locations having this potential are identified, and a liquefaction analysis of the slope soils is performed.

2.5.4.8.1 Previous Liquefaction Analyses Performed

The SSAR describes liquefaction analyses performed previously for the North Anna site. The primary analysis was performed for a seismic margin assessment. This included, for the main Units 1 and 2 plant area, an analysis using a version of the simplified procedure and a threshold strain analysis. For the Units 1 and 2 Service Water Reservoir, an analysis was performed based on the results of 15 stress-controlled cyclic triaxial tests. An updated seismic margin assessment was performed for the SSAR maintaining the same assumptions as used in the original study but substituting the ESP design accelerations and moment magnitudes. As noted previously, these accelerations were higher than those being used for the present analysis (Section 2.5.4.8.2). The SSAR also describes liquefaction analysis performed using subsurface data gathered for the ESP investigation.

2.5.4.8.2 Liquefaction Analyses Performed for Unit 3

This section was developed in accordance with, and conforms to guidance in RG 1.198 (Reference 2.5-214).

As noted earlier, at the locations of the majority of the borings and CPTs in the power block area that contains the Seismic Category I structures,

the Zone IIA saprolite will be excavated. Thus, analyzing the liquefaction potential of these soils prior to excavation is of little relevance.

The liquefaction analysis focuses on slopes whose failure could impact safety-related structures. The excavation plan (Figure 2.5.4-206) shows the cut slopes to the east and south of the power block are in the 30 to 35-ft high range. The bottom of the slope to the east of the FWSC is approximately 120 ft from the structures. This is the nearest point of the bottom of any slope to a Seismic Category I structure. The Seismic Category II Ancillary Diesel Building is slightly farther from the south slope. The liquefaction potential of the east and south slope soils was computed, as described below. Note that even if these slopes failed due to liquefaction (or other mechanisms) it is extremely unlikely the failed 35-ft high slopes would have any impact on structures 120 ft or more from the slope.

Six SPT sample borings were conducted on the east and south slopes (B-930, B-947, M-6, M-9, M-10 and M-11) along with two CPTs (C-909 and C-916). V_S measurements were taken in M-10 and C-916. The results from these explorations were analyzed to determine the liquefaction potential of the slope soils.

The analysis conservatively ignored mineralogy/fabric effects of the saprolite. The saprolite is estimated to be between 0.8 and 1.6 million years old, according to SSAR Reference 176. A conservative age factor of 1.4 was used in the analysis. Cohesive samples and/or samples above the groundwater table were considered non-susceptible to liquefaction.

The analysis followed the methods proposed by Youd, et al. (SSAR Reference 178). This state-of-the-art liquefaction methodology is based on the evolution of the Seed and Idriss “Simplified Procedure” since the early 1980s. Magnitude scaling factors of 1.05 and 1.93 were used in the analysis for the moment magnitude 7.4 (low frequency) and 6.0 (high frequency) earthquakes, respectively. The K_σ factor for high overburden pressures was incorporated into the analysis, using a relative density of 60 percent.

The analysis of the SPT results from the six borings gave factor of safety values against liquefaction greater than 1.1 for the approximately 80 Zone IIA saprolite samples that were potentially liquefiable, except for eight samples. For the two CPTs, the liquefaction analysis showed no measurement where the factor of safety against liquefaction was less

than 1.1. For the two sets of V_S measurements, one measurement in C-916 indicated a factor of safety of less than 1.1 against liquefaction. In M-10, seven measurements indicated a factor of safety of less than 1.1 against liquefaction. Youd et al. (SSAR Reference 178) express concerns about the applicability of V_S measurements to liquefaction potential evaluation because V_S is a small strain measurement whereas pore-water pressure buildup and the onset of liquefaction are medium- to high-strain phenomena.

The liquefaction analyses described above for Unit 3 used accelerations obtained from input rock motions consistent with the EPRI (2004, 2006) GMM. As noted in Section 2.5.4.7.4, these input motions were subsequently updated based on the EPRI (2013) GMM for use in developing the GMRS and FIRS for Seismic Category I buildings. These updated rock motions are lower than those from the EPRI (2004, 2006) GMM and result in lower site ground motion response spectra, and correspondingly lower peak ground accelerations for low frequency and high frequency input motions. Furthermore, the controlling earthquake magnitudes for low frequency and high frequency input motions are either reduced or remain unchanged in the EPRI (2013) GMM rock motions. Thus, the results of the liquefaction analyses described here, which are based on the EPRI (2004, 2006) GMM, can be conservatively used in place of the EPRI (2013) GMM, and are therefore not updated.

Using the method outlined in Tokimatsu and Seed (SSAR Reference 179), the maximum estimated dynamic settlement of the Zone IIA saprolite due to earthquake shaking was less than the 5 in. estimated based on soil encountered in one of the CPTs performed for the ESP investigation using the same computation method. This value of 5 in. is conservatively adopted as the maximum dynamic settlement that could occur in the saprolite due to the design seismic event.

2.5.4.8.3 Conclusions about Liquefaction

Only the Zone IIA saprolites fall into the gradation and relative density categories where liquefaction would be considered possible.

Any liquefaction of the Zone IIA saprolite will not impact the stability of any Seismic Category I structure.

The conclusions from the foregoing sections on the analysis of liquefaction potential of Zone IIA saprolite are as follows. These conclusions apply to measurements taken on or close to the slopes to the

Settlement estimates were made using the preceding relationships and the soil and rock properties given in Table 2.5.4-208. These estimates were made for each Seismic Category I and II structure, and the Radwaste Building, and are presented in Table 2.5.4-212. The applied pressures from the foundations are also shown on Table 2.5.4-212.

As would be anticipated, the settlement of the structures founded on Zone III-IV or Zone IV bedrock is negligible. Similarly, settlements of structures sitting on the dense to very dense structural fill or Zone IIB saprolite overlying rock are modest in light of the large applied pressures.

The total and differential settlements under the RB/FB, CB and FWSC are well within the limits stated in Table 2.0-201. Based on the computed settlement values in Table 2.5.4-212, the average settlement of these structures is 0.1 in. or less.

2.5.4.10.3 **Earth Pressures**

Static and seismic lateral earth pressures are addressed for plant below-ground walls. Both active and at-rest cases are included. Active earth pressure is used for temporary retaining wall installed to facilitate construction. For these, the earth pressure coefficients are Rankine values, assuming level backfill and a zero friction angle between the soil and the wall. Hydrostatic pressures are conservatively based on the groundwater table being at grade. An area wide surcharge pressure of 500 psf is used. Lateral pressures due to compaction are not included; these pressures are controlled by compacting backfill with light equipment near structures. The soil properties used in the calculation of lateral earth pressures are from Table 2.5.4-208.

For the active lateral earth pressure case, earthquake-induced horizontal ground accelerations are addressed by the application of $k_h \cdot g$ applying the Mononobe-Okabe method. Vertical ground accelerations ($k_v \cdot g$) are considered negligible and were ignored (Reference 2.5-217). The peak low frequency acceleration of 0.31g was used for developing the seismic active earth pressure diagram. Use of the peak high frequency acceleration was considered overly conservative given the low magnitude (energy) of this earthquake.

The method described in ASCE 4-98 Section 3.5.3.2 (Reference 2.5-218) can be used to estimate the dynamic component of seismic at-rest lateral earth pressure for the below-grade walls of the power block structures. Reference 2.5-218 provides an elastic solution

that is demonstrated by a nomograph. In the nomograph, a dimensionless normalized in-situ lateral stress at 1.0g horizontal earthquake acceleration is developed for a normalized depth at a given Poisson's ratio. The appropriate site-specific at-rest pressure is calculated from the nomograph at various depth intervals using the site-specific acceleration and Poisson's ratio.

Figures 2.5.4-225 through 2.5.4-234 show structural fill between some below-ground structures, e.g., between the FWSC and CB in Figure 2.5.4-228 (Section D-D), and between structures and the temporary retaining wall installed to facilitate construction. Figure 2.5.4-225 (Section A-A) shows approximately 50 ft of excavation is required from the existing ground surface to the bottom of excavation for the Turbine Building. This wall will hold back the natural in-situ soil (Zone IIA and IIB saprolites) which will be in an active condition. This case is used as an example of active earth pressure for the lateral earth pressure diagram in Figure 2.5.4-253. This figure includes active earth pressure along with the groundwater, surcharge and seismic components of lateral pressure against the temporary wall.

The same section shows approximately 60 ft depth of structural fill against the Turbine Building wall. This case is used as an example of at-rest earth pressure against an unyielding wall for the lateral earth pressure diagram in Figure 2.5.4-254. This figure includes at-rest earth pressure along with the groundwater, surcharge and seismic components of lateral pressure against the permanent wall.

The 0.31g peak low frequency acceleration used as input to the active and at-rest seismic (dynamic) lateral earth pressure computations was obtained using input rock motions consistent with the EPRI (2004, 2006) GMM. As noted in Section 2.5.4.7.4, these input motions were subsequently updated based on the EPRI (2013) GMM for use in developing the GMRS and FIRS for Seismic Category I buildings. These updated rock motions are lower than those from the EPRI (2004, 2006) GMM and result in lower site ground motion response spectra, and correspondingly lower peak ground acceleration for the low frequency input motions. Thus, the seismic lateral earth pressures shown in Figures 2.5.4-253 and 2.5.4-254, which are based on the EPRI (2004, 2006) GMM, can be conservatively used in place of the EPRI (2013) GMM, and are therefore not updated.

NAPS ESP COL 2.5-5 **Figure 2.5.4-250 Maximum Acceleration versus Depth for Free-Field Slope**

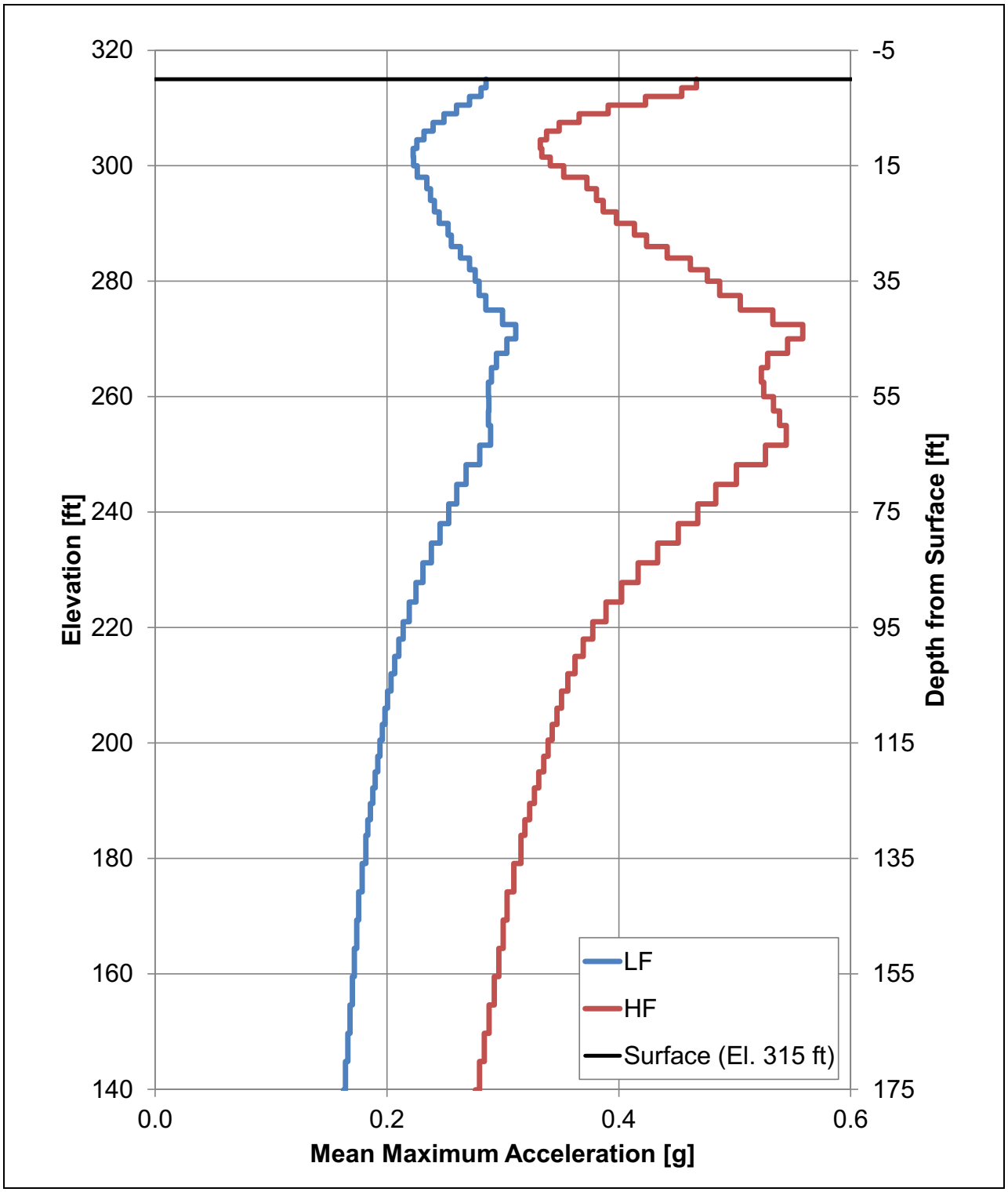

Note: The accelerations shown in this figure are obtained using input rock motions consistent with the EPRI (2004, 2006) GMM.

2.5.5.1.4 Slope Phreatic Surface

The phreatic surfaces shown in Figure 2.5.5-202 (existing slope ES) and Figure 2.5.5-203 (new slope DD) have been developed from the water table levels measured in OW-947 and derived in Section 2.4.12. The depth of this phreatic surface precludes any potential for liquefaction of the near-surface soils in the slope.

2.5.5.2 Design Criteria and Analyses

2.5.5.2.1 Required Factor of Safety

Minimum required factors of safety for stability of slopes under long-term static (non-seismic) loading and for dynamic (seismic) loading are 1.5 and 1.1, respectively.

2.5.5.2.2 Stability of Existing Slope

The photograph in SSAR Figure 2.5-67 of the existing 2.4h:1v slope to the north of the SWR was taken over 20 years ago. The condition of the slope is essentially the same today. It was thoroughly inspected during the ESP site investigation. The slope shows no signs of distress.

2.5.5.2.3 Analysis of Existing Slope

The static and dynamic stability of the existing slope to the north of the SWR was analyzed using the computer program SLOPE/W (Reference 2.5-219).

a. **Long-Term Static Analysis**

The SLOPE/W Program used the Bishop method of slices (SSAR Reference 185) for analysis of the long-term static condition. As noted in Section 2.5.5.1.3, the analysis assumed the saprolite was predominantly coarse grained. The effective strength parameters given in Table 2.5.4-208 are an angle of internal friction ϕ' = 33 degrees and effective cohesion c' = 0.125 ksf for the Zone IIA saprolite and ϕ' = 40 degrees and effective cohesion c' = 0 ksf for the Zone IIB saprolite. The underlying weathered rock used c = 70 ksf, approximately half of the value for unconfined compressive strength given in Table 2.5.4-208.

The input to the analysis and the results are shown in Figure 2.5.5-204. The computed factor of safety is 2.29. This value is above the minimum 1.5 factor of safety required.

b. **Seismic Slope Stability Analysis**

NAPS ESP COL 2.5-10

The pseudo-static approach is used as a first approximation for the seismic analysis of slopes. In this approach, the horizontal and vertical seismic forces are assumed to act on the slope in a static manner, that is, as a constant static force. This is an obviously conservative approach, since the actual seismic event occurs for only a short period of time, and during that time, the forces alternate their direction at a relatively high frequency. Also, the pseudo-static analysis tends to be run using the peak seismic acceleration; the mean acceleration during the design seismic event can be significantly less than the peak value. A pseudo-static analysis using peak acceleration values can be a useful tool in a limit analysis where the peak acceleration is relatively low. In such analyses, the computed factor of safety may well exceed the minimum of 1.1, thus requiring no further analysis. However, where the peak seismic acceleration values are high, the pseudo-static analysis produces unreasonably low safety factor values.

The pseudo-static analysis was run on the existing 45 ft high slope (Slope ES) using SLOPE/W with the Bishop method of slices. For the low frequency earthquake, the peak horizontal acceleration used was about 0.26g. This is the average peak acceleration in the top 45 ft of soil shown in Table 2.5.5-201. (The maximum horizontal acceleration is 0.31g at about 42 ft depth.) The vertical acceleration used was about 0.13g. The computed factor of safety was 1.30, more than the minimum 1.1 required. For the high frequency earthquake, the equivalent peak horizontal acceleration used was 0.42g with a vertical acceleration of 0.21g. (The maximum horizontal acceleration is 0.56g at about 42 ft depth.) The computed factor of safety was about 1.04, less than the minimum 1.1 required. The input to the analysis, and the results, are shown in Figure 2.5.5-205 for the low frequency earthquake and Figure 2.5.5-206 for the high frequency earthquake.

The low frequency and high frequency acceleration values noted in the previous paragraph were obtained using input rock motions consistent with the EPRI (2004, 2006) (References 2.5-224, 2.5-225) GMM. As noted in Section 2.5.4.7.4, these input motions were subsequently updated based on the EPRI (2013) (Reference 2.5-407) GMM for use in developing the GMRS and FIRS for Seismic Category I buildings. These updated rock motions are lower than those from the EPRI (2004, 2006) GMM and result in lower site ground motion response spectra, and

correspondingly lower ground accelerations for the low frequency and high frequency input motions. Thus, the factors of safety against slope failure shown in Figures 2.5.5-205 and 2.5.5-206, and in Figures 2.5.5-209 and 2.5.5-210 for Kramer's approach (below), which are based on the EPRI (2004, 2006) GMM, can be conservatively used in place of the EPRI (2013) GMM. These figures are therefore not updated.]

Seed (SSAR Reference 186), in the 19th Rankine Lecture, addressed the over-conservatism intrinsic in the pseudo-static analysis. He looked at the more rational approach proposed by Newmark (SSAR Reference 187), where the effective acceleration time-history is integrated to determine velocities and displacements of the slope. He also examined dams in California that had been subjected to seismic forces, including several dams that survived the 1906 San Francisco earthquake. Based on his studies, he concluded that for embankments that consist of materials that do not tend to build up large pore pressures or lose significant percentages of their shear strength during seismic shaking, seismic coefficients of only 0.15g are adequate to ensure acceptable embankment performance for earthquakes up to Magnitude M = 8.25 with PGAs of 0.75g. For earthquakes in the range of M = 6.5, Seed recommends a horizontal seismic coefficient of only 0.1g with a vertical seismic coefficient of zero. Note that it is the magnitude of the earthquake that determines the acceleration to be used here; magnitude is not part of the input to the pseudo-static analysis.

The liquefaction analysis of the Zone IIA saprolite indicated that only a limited amount of the material has a potential for liquefaction. Also, because of its age, fabric and interlocking angular grain structure, this material does not lose a significant proportion of its shear strength during shaking. Thus, for the low frequency earthquake, with a design Magnitude M = 7.2, the pseudo-static analysis should be limited to a horizontal acceleration of 0.15g. A pseudo-static design using an inertia force of 0.1g is adequate for the high frequency earthquake.

The pseudo-static analysis was run again using SLOPE/W. This time the horizontal accelerations used were 0.1g and 0.15g, with zero vertical acceleration. The computed factors of safety were 1.76 and 1.57, respectively, greater than the minimum 1.1 required. The input to the analysis, and the results, for the 0.1g and 0.15g cases are shown in Figures 2.5.5-207 and 2.5.5-208, respectively.

Other researchers have also recommended substantially reducing the peak acceleration when applying the pseudo-static analysis. Kramer (SSAR Reference 188) recommends using an acceleration of 50 percent of the peak acceleration. For the low frequency earthquake, where the average peak acceleration in the top 45 ft is about 0.26g, the horizontal input using Kramer's recommendations was about 0.13g and the vertical input was about 0.065g. This results in a factor of safety of 1.65. Using the average peak acceleration for the high frequency earthquake in the top 45 ft of 0.42g, the horizontal input using Kramer's recommendation was 0.21g and the vertical input was 0.105g. This level of input provides a factor of safety against slope failure of 1.41. Thus the low and high frequency inputs give factors of safety above the minimum 1.1 required. The input to the analysis, and the results, for the low frequency and high frequency cases are shown in Figures 2.5.5-209 and 2.5.5-210, respectively.

In the preceding analyses (both long-term static, and seismic), the only case that gave a factor of safety lower than the required minimum was the pseudo-static analysis using the high frequency peak acceleration. As noted above, the pseudo-static analysis does not take into account the frequency of the motion nor the magnitude of the earthquake. For high frequency, low magnitude earthquakes, (as is the case at North Anna) the pseudo-static analysis is particularly conservative. Thus, it is concluded that the existing 2.4h:1v slope to the north of the SWR remains stable under long-term static and design seismic conditions.

NAPS COL 2.0-30-A

2.5.5.2.4 Analysis of New Slope

The static and dynamic stability of the new 39-ft high 3h:1v slope (Slope DD) to the east of the FWSC was analyzed using the computer program SLOPE/W (Reference 2.5-219).

a. **Long-Term Static Analysis**

The SLOPE/W Program used the Bishop method of slices (SSAR Reference 185) for analysis of the long-term static condition. As noted in Section 2.5.5.1.3, the properties assumed for the Zone IIA and Zone IIB saprolite were the same as those for the existing slope that was analyzed.

The input to the analysis and the results are shown in Figure 2.5.5-211. The computed factor of safety is 2.27. This value is above the minimum 1.5 factor of safety required.

b. **Seismic Slope Stability Analysis**

NAPS ESP COL 2.5-10

The pseudo-static analysis was run on the new 39 ft high slope using SLOPE/W with the Bishop method of slices. For the low frequency earthquake, the average peak horizontal acceleration in the top 39 ft used was about 0.25g with a vertical acceleration of about 0.125g. (The maximum horizontal acceleration is 0.31g at about 42 ft depth.) The computed factor of safety was 1.24, greater than the minimum 1.1 required. For the high frequency earthquake, the peak horizontal acceleration used was about 0.41g. This is the average peak acceleration in the top 39 ft of soil shown in Table 2.5.5-201. (The maximum horizontal acceleration is 0.56g at ~~the ground surface~~ about 42 ft depth.) The vertical acceleration used was about 0.205g. The computed factor of safety was 1.00, less than the minimum 1.1 required. The input to the analysis, and the results, for the low frequency and high frequency cases are shown in Figures 2.5.5-212 and 2.5.5-213, respectively.

As noted for the existing slope in 2.5.5.2.3.b, the factors of safety against slope failure for the new slope shown in Figures 2.5.5-212 and 2.5.5-213, and in Figures 2.5.5-216 and 2.5.5-217 for Kramer's approach (below) that are based on the EPRI (2004, 2006) GMM can be conservatively used for the EPRI (2013) GMM. These figures are therefore not updated.

The pseudo-static analysis was run again using SLOPE/W and Seed's (SSAR Reference 186) approach described in Section 2.5.5.2.3. Again the horizontal accelerations used were 0.1g and 0.15g for the high and low frequency cases, respectively, with zero vertical acceleration. The computed factors of safety were 1.64 and 1.43, respectively, greater than the minimum 1.1. The input to the analysis, and the results, for the 0.1g and 0.15g cases are shown in Figures 2.5.5-214 and 2.5.5-215, respectively.

The pseudo-static analysis was then run using SLOPE/W and Kramer's (SSAR Reference 188) recommendations described in Section 2.5.5.2.3. For the low frequency earthquake, where the average peak acceleration in the top 39 ft is about 0.25g, the horizontal input using Kramer's recommendations was about 0.125g and the vertical input was about 0.063g. Using the average peak acceleration for the high frequency earthquake in the top 39 ft of about 0.41g, the horizontal input using Kramer's recommendation was 0.205g and the vertical input was 0.103g. These levels of input provide a factor of safety against slope failure of

2.5-388 Gülerce, Z, and N. Abrahamson (2011) [GA11], “Site-Specific Design Spectra for Vertical Ground Motion,” Earthquake Spectra, Volume 27, No. 4, pages 1023–1047.

2.5-389 Reinbold, D.J., and Johnston, A.C., 1987, Historical Seismicity in the Southern Appalachian Seismic Zone: U.S. Geological Survey Open-File Report 87-433, 40 pp.

2.5-390 Hurd, O., and M. D. Zoback, 2012, Intraplate Earthquakes, Regional Stress and Fault Mechanics in the Central and Eastern U.S. and Southeastern Canada, Tectonophysics, Volume 581, pages 182-192.

2.5-391 Mazzotti, S., and J. Townend, 2010, State of Stress in Central and Eastern North American Seismic Zones, lithosphere, Volume 2, pages 76-83.

2.5-392 McNamara, D. E., H. M. Benz, R. B. Herrmann, E. A. Bergman, P. Earle, A. Meltzner, M. Withers, and M. Chapman, 2014, The Mw 5.8 Mineral, Virginia, Earthquake of August 2011 and Aftershock Sequence: Constraints on Earthquake Source Parameters and Fault Geometry, Bulletin of the Seismological Society of America, Volume 104, No. 1, pages 40-54.

2.5-393 Horton, W. J., Geologic, Seismologic, and Engineering lessons learned from the 2011 Mineral Virginia Earthquake, Geological Society of America (GSA) Southeastern Section Meeting, April 10, 2014, Session No. 3, Abstract.

2.5-394 Berti, C., F. J. Pazzaglia, A. S. Meltzer, and R. W. Harrison, 2012, Geomorphic Evidence for Persistent Faulting Consistent with the 23 August, 2011 Louisa County, VA Earthquake, Geological Society of America (GSA) Annual Meeting in Charlotte, November 4-7, 2012, Paper No. 154-15, Abstract.

2.5-395 Burbank, D.W., and R. S. Anderson, 2007, Tectonic Geomorphology, Blackwell Science, Malden, MA, 274 pages.

2.5-396 Burton, W.C., D. B. Spears, R. W. Harrison, N. H.Evans, S. Schindler, and R. Counts, 2014, Geology and Neotectonism in the Epicentral Area of the 2011 M5.8 Mineral, Virginia, Earthquake, in C. M. Bailey and L. V. Coiner, eds., Elevating Geoscience in the Southeastern United States: New Ideas

About Old Terranes: Field Guides for the GSA Southeastern Section Meeting, Blacksburg, Virginia, 2014, Geological Society of America Field Guide 35, pages 103–127.

2.5-397 Chapman, M.C., 2013, On the Rupture Process of the 23 August 2011 Virginia Earthquake, Bulletin of the Seismological Society of America, Volume 103, No. 2A, pages 613-628.

2.5-398 Green, R. A., S. Lasley, M. W. Carter, J. W. Munsey, B. W. Maurer, and M. P. Tuttle, 2014 (in press), Geotechnical Aspects in the Epicentral Region of the 2011, Mw 5.8 Mineral, Virginia Earthquake, The 2011 Mineral, Virginia, Earthquake and Its Significance for Seismic Hazards in Eastern North America, Geological Society of America (GSA) Special Paper.

2.5-399 Hack, T. J., 1957, Studies of Longitudinal Stream Profiles in Virginia and Maryland, U.S. Geological Survey Professional Paper 294-B, 59 pages.

2.5-400 Harrison, R. W., 2012, A Preliminary Assessment of Neotectonic Features in the Central Virginia Seismic Zone, Geological Society of America (GSA) Southeastern Section Meeting, April 1-2, 2012, Paper No. 5-6, Abstract.

2.5-401 Harrison, R. W., J. W. Horton, Jr., M. W. Carter, and J. S. Schindler, 2011, Geology of the Central Virginia Seismic Zone in the Vicinity of the August, 2011 Earthquakes: What We Know and Don’t Know, And Suggested Approaches, Seismological Society of America (SSA) Eastern Section Meeting, October 16-18, 2011, Abstract.

2.5-402 Earthquake Engineering Research Institute (EERI), 2011, Special Earthquake Report – December 2011, The Mw 5.8 Virginia Earthquake of August 23, 2011, 13 pages.

2.5-403 Harrison, R.W., W. C. Burton, D. S. Powars, M. J. Pavich, and J. S. Schindler, 2014, Quaternary Faulting in the Central Virginia Seismic Zone and Possible Influence of Nearby Anomalous Crust, Geological Society of America (GSA) Southeastern Section Meeting, April 10, 2014, Session No. 3 Lessons Learned from the 2011 Virginia Earthquake, Abstract.

2.5-404 Dominion Nuclear North Anna, LLC (Dominion), 2004, North Anna Early Site Permit Application, Response to Request for Additional Information No. 3, Nuclear Regulatory Commission Accession No. ML042800292, July 8, 2004.

2.5-405 ASTM C1260-07, Standard Test Method for Potential Alkali Reactivity of Aggregates (Mortar-Bar Method)

2.5-406 ASTM C1293-08b, Standard Test Method for Determination of Length Change of Concrete Due to Alkali-Silica Reaction

2.5-407 Electric Power Research Institute (EPRI), 2013, EPRI (2004, 2006) Ground-Motion Model (GMM) Review Project: EPRI, Palo Alto, CA, 2013 Technical Report, 3002000717, Nuclear Regulatory Commission Accession No. ML13155A553.

2.5-408 Nuclear Regulatory Commission (NRC) (August 28, 2013). Letter to Ms. Kimberly A. Keithline of the Nuclear Energy Institute (NEI), Subject: Approval of Electric Power Research Institute Ground Motion Model Review Project Final Report for Use by Central and Eastern United States Nuclear Power Plants, Nuclear Regulatory Commission Accession No. ML13233A102.

2.5-409 Nuclear Energy Institute (NEI) (July 30, 2013). Letter to Mr. David L. Skeen of the Nuclear Regulatory Commission (NRC), Subject: Responses to NRC Questions on EPRI (2004, 2006) Ground Motion Model Review Final Report, Nuclear Regulatory Commission Accession No. ML13218A052.

ESBWR Standard Plant. The site-specific SSI analyses indicate that additional ground motion response spectra apply, as described in Section 3.7.2.

The information below relates to the CSDRS used for seismic design of the ESBWR Standard Plant. These design ground motion response spectra are used in conjunction with the site-specific ground motion response spectra, as described in Section 3.7.1.1.4.2.

NAPS SUP 3.7-1

3.7.1.1.4 Site-Specific Design Ground Motion Response Spectra

3.7.1.1.4.1 SSI Strain-Compatible Soil Profiles

Best estimate (BE), lower bound (LB), and upper bound (UB) soil properties are calculated consistent with the FIRS for each Seismic Category I structure from their corresponding probabilistic full column site response analysis results and are presented in the following sections. The details of the site response analysis are described in Section 2.5.2.5.

3.7.1.1.4.1.1 SSI Strain-Compatible Soil Profiles for the RB/FB

From the probabilistic full column site response analyses of the RB/FB soil column set (presented in Section 2.5.2.5), a set of 60 strain-compatible soil properties is obtained for each of the 4 input rock cases (10^{-4} and 10^{-5} annual-frequency-of-exceedance (1E-4 and 1E-5 hazard level) low frequency (LF) and high frequency (HF) as described in Section 2.5.2.4). The log-mean (μ_{ln}) and log-standard deviation (log-SD, σ_{ln}) for each of the 4 sets of shear wave velocity (V_s) and damping ratios are calculated. These values are used to establish the log-mean and log-SD of the strain compatible properties that are consistent to FIRS motions using A_R and *DF* factors (described in Section 2.5.2.6), calculated for the acceleration response spectra (ARS) at the ground surface.

The simulated (randomized) profiles described in Section 2.5.2.5 include a variation in the thickness of different strata (a stratum is defined as a thickness of rock or soil having the same initial dynamic and static properties). For deterministic SSI analysis, the strain-compatible soil profiles are obtained from the strain-compatible soil properties of the simulated profiles using the data for each soil layer type within the profile. The stratum log-mean and log-standard deviation strain compatible properties are used with the BE thicknesses for each stratum to obtain the LB, BE, and UB SSI input strain-compatible soil profiles.

The log-mean values of the FIRS-consistent strain-compatible damping ratios are used to determine the BE damping ratio profile. The LB and UB values for the strain compatible damping ratios are calculated as plus/minus one log-standard deviation from the log-mean values by applying Equations 3.7.1.1-1 and 3.7.1.1-2.

Lower bound and upper bound V_s corresponding to FIRS are calculated by applying Equations 3.7.1.1-1 and 3.7.1.1-2 in conjunction with the FIRS-consistent log-mean and log-standard deviation as described above. In these equations, *M* refers to damping or shear wave velocity, μ_{ln} refers to the log-mean of FIRS-consistent shear wave velocity or damping ratio and σ_{ln} refers to the corresponding log-standard deviations. However, lower bound shear wave velocity profiles are calculated as the minimum resulting from Equation 3.7.1.1-1 and $(V_S)_{FIRS}/(\sqrt{1.5})$, and upper bound shear wave velocity profiles are calculated as the maximum resulting from Equation 3.7.1.1-2 and $(V_S)_{FIRS} \times \sqrt{1.5}$ to satisfy the minimum variation requirements of ASCE 4-98, where $(V_S)_{FIRS}$ is the best estimate strain compatible shear wave velocity corresponding to the FIRS level of motion.

$$M_{LB} = \exp(\ln(\mu_{ln}) - \sigma_{ln}) \quad (3.7.1.1\text{-}1)$$

$$M_{UB} = \exp(\ln(\mu_{ln}) + \sigma_{ln}) \quad (3.7.1.1\text{-}2)$$

Primary (P- or compression) wave velocity V_P is calculated using Equation 3.7.1.1-3 (Reference 3.7-201), where Poisson's ratio ν values, at different depths, are provided in Section 2.5.4.

$$V_P = V_S\sqrt{\frac{2-2\nu}{1-2\nu}} \quad (3.7.1.1\text{-}3)$$

For soil layers below water table, a minimum P-wave velocity of 4800 ft/sec is maintained and, as needed, the Poisson's ratio is adjusted to obtain the minimum P-wave velocity. The maximum value of Poisson's ratio used is 0.48 to avoid numerical instability.

Figure 3.7.1-201 presents the SSI shear wave velocity profiles for the RB/FB. SSI damping and P-wave velocity profiles for this structure are presented in Figures 3.7.1-202 and 3.7.1-203, respectively. The depth of 0 ft in Figures 3.7.1-201, 3.7.1-202, and 3.7.1-203 corresponds to the top of the soil column at Elevation 290 ft. The lower shear wave and P-wave velocities are used in conjunction with the higher damping values to form the LB profile, and vice versa for the UB profile. Table 3.7.1-201 presents the digital values for the RB/FB SSI input strain-compatible soil profiles.

The provided soil profiles correspond to the fully embedded SSI analysis of the RB/FB. The top 17 ft of this profile (the top 7 layers in Table 3.7.1-201) correspond to saprolite and are removed in the partially embedded SSI analysis of the RB/FB.

As described in Section 2.5.4, adjacent to the structure, the in-situ saprolite is replaced by structural fill and Zone III rock is replaced by concrete fill. The strain-compatible properties for the structural fill for the RB/FB are obtained following the steps described above for the in-situ profile and applied to a companion fill profile for the RB/FB. The companion RB/FB profile is identical to the in-situ profile except that randomized saprolite and Zone III rock properties are replaced with randomized structural fill and concrete fill properties, respectively.

Although not used in the SSI analyses, the lower bound and upper bound shear wave velocities, P-wave velocities, and damping ratios for the structural fill compatible with FIRS are calculated following the methodology described above and presented in Table 3.7.1-202. The same table provides the LB, BE, and UB values for the concrete fill to be used in the SSI analysis model. The concrete fill is considered as linear material for the purpose of site response and SSI analyses.

3.7.1.1.4.1.2 SSI Strain-Compatible Soil Profiles for the CB

The SSI strain-compatible soil profiles for the CB are calculated from the probabilistic full column site response analyses of the CB soil column set (presented in Section 2.5.2.5) following the same approach as described above for the RB/FB structure.

Figure 3.7.1-204 presents the SSI shear wave velocity profiles for the CB. SSI damping and P-wave velocity profiles for this structure are presented in Figures 3.7.1-205 and 3.7.1-206, respectively. The depth of 0 ft in Figures 3.7.1-204, 3.7.1-205, and 3.7.1-206 corresponds to the top of the soil column at Elevation 290 ft.] The lower shear wave and P-wave velocities are used in conjunction with the higher damping values to form the LB profile, and vice versa for the UB profile. Table 3.7.1-203 presents the digital values for the CB SSI input strain-compatible soil profiles. The provided soil profiles correspond to the fully embedded SSI analysis of the CB. The top 25 ft of this profile (the top 10 layers in Table 3.7.1-203) correspond to saprolite and are removed in the partially embedded SSI analysis of the CB.

As described in Section 2.5.4, adjacent to the structure, the in-situ saprolite is replaced by structural fill and Zone III rock is replaced by concrete fill. Table 3.7.1-204 provides the LB, BE, and UB values for the concrete fill to be used in the SSI analysis model. The concrete fill is considered as linear material for the purpose of site response and SSI analyses. Although not used in the SSI analyses, the strain compatible properties for the structural fill for the CB are similarly obtained as those for the RB/FB and presented in Table 3.7.1-204.

3.7.1.1.4.1.3 SSI Strain-Compatible Soil Profiles for the FWSC

The SSI strain-compatible soil profiles for the FWSC are calculated from the probabilistic full column site response analyses of the FWSC soil column set (presented in Section 2.5.2.5) following the same approach as described above for the RB/FB structure.

Figure 3.7.1-207 presents the SSI shear wave velocity profiles for the FWSC. SSI damping and P-wave velocity profiles for this structure are presented in Figures 3.7.1-208 and 3.7.1-209, respectively. The lower shear wave and P-wave velocities are used in conjunction with the higher damping values to form the LB profile, and vice versa for the UB profile. Table 3.7.1-205 presents the digital values for the FWSC SSI input strain-compatible soil profiles.

As described in Section 2.5.4, for the FWSC, the foundation of the structure is supported by concrete fill situated on Zone III-IV rock. Adjacent to the structure, the in-situ saprolite is replaced by structural fill and Zone III rock is replaced by concrete fill. Table 3.7.1-206 provides the LB, BE, and UB values for the concrete fill to be used in the SSI analysis model. The concrete fill is considered as linear material for the purpose of site response and SSI analyses. Although not used in the SSI analyses, the strain compatible properties for the structural fill for the FWSC are similarly obtained as those for the RB/FB and presented in Table 3.7.1-206.

3.7.1.1.4.2 Site-Specific SSI Input Response Spectra

The FIRS for all Seismic Category I structures are presented in Section 2.5.2.6. For each Seismic Category I structure, the site-specific SSI input response spectra are obtained from its corresponding FIRS by ensuring that the requirements of ISG-17 (Reference 3.7-202) with regards to the adequacy of the input motion for embedded SSI analyses are met. This verification is referred to as the NEI check in reference to

the Nuclear Energy Institute (NEI) white paper (Reference 3.7-203). Once the NEI check is done for a given FIRS and any necessary adjustments are made, the resulting spectra is termed the "SSI input response spectra."

In addition, the site-specific SSI input response spectra are augmented by the broadband horizontal and vertical response spectra defined in RG 1.60 anchored at 0.1g to satisfy the minimum design ground motion requirements of 10 CFR 50, Appendix S. The resulting ARS are labeled as "Final SSI Input Response Spectra." The development of these spectra for all Seismic Category I structures is described in the following sections.

3.7.1.1.4.2.1 SSI Input Response Spectra for the RB/FB

The site-specific SSI input response spectra are calculated for SSI analysis of the RB/FB structure as partially embedded (only considering embedment in rock) and as fully embedded. The corresponding partial column outcrop FIRS and full column outcrop FIRS for this structure as well as the performance-based surface response spectra (PBSRS) are presented in Section 2.5.2.6.

The NEI check is conducted for the RB/FB by convolving the full column and partial column outcrop FIRS (from the foundation level, Elevation 224 ft NAVD88) through their corresponding LB, BE, and UB strain compatible soil profiles of the RB/FB (Section 3.7.1.1.4.1), and comparing the envelope of the resulting top-of-the-column ARS with the corresponding full column and partial column PBSRS. The partial column PBSRS are calculated consistent with the partially embedded SSI analyses, at the top of the partial columns (after removal of the saprolite layers) using the same methodology as described for the full column PBSRS in Section 2.5.2.6. The horizontal FIRS are convolved to the top of the soil column using vertically propagating shear waves and the vertical FIRS are convolved to the surface through vertically propagating P-waves. Shear wave damping is used for both horizontal and vertical analyses. The analyses are carried out linearly with no further degradation of the strain-compatible profiles. The horizontal and vertical 5 percent damped ARS at the top of the soil columns corresponding to each SSI input soil profile are determined and the horizontal and vertical envelope resulting from the LB, BE, and UB soil columns for the structure is compared to the horizontal and vertical PBSRS.

For each direction (horizontal or vertical) and each embedment configuration (fully or partially embedded FIRS), if the envelope of the LB, BE, and UB ARS (at the top of the SSI input soil column) does not envelope the corresponding PBSRS, the FIRS must be adjusted. The frequency dependent adjustment factor is either unity or the ratio of PBSRS to the envelope of LB, BE, and UB ARS, whichever is greater. In order to satisfy the NEI check, this adjustment factor is applied to the computed FIRS at the foundation level to yield the full column and partial column horizontal and vertical SSI input response spectra for the RB/FB.

Figures 3.7.1-210 and 3.7.1-211 present the envelope of the ground surface ARS for the horizontal and vertical full column FIRS, respectively. Figures 3.7.1-212 and 3.7.1-213 present the horizontal and vertical envelope ARS at surface as well as their corresponding FIRS and PBSRS. For the RB/FB full column FIRS, the adjustment occurs for the horizontal FIRS below ~~6.6~~ 6.9 Hz with the largest adjustment factor being 1.27. For the vertical FIRS, the adjustment is much more significant, especially between frequencies of 1 Hz and 20 Hz with the maximum adjustment factor being ~~1.73~~ 1.79. The adjusted full column FIRS for RB/FB are referred to as the SSI input response spectra for RB/FB and are also presented in Figures 3.7.1-212 and 3.7.1-213.

The NEI check for the partial column FIRS for RB/FB are carried out in a similar manner. The corresponding figures are provided in Figures 3.7.1-214 through 3.7.1-217. The surface ARS and PBSRS corresponding to the partial columns are calculated consistent with the partially embedded SSI analyses, at the top of the partial soil columns after removal of the saprolite layers. The necessary adjustment factors for RB/FB partial column FIRS are less than 1.01 for both horizontal and vertical directions. The adjusted partial column FIRS are referred to as the partial column SSI input response spectra for RB/FB and are presented in Figures 3.7.1-216 and 3.7.1-217.

For the full column analyses (applicable to fully embedded SSI analyses), the final horizontal and vertical SSI input response spectra are calculated as the envelope of the full column SSI input response spectra and the minimum required response spectra which are adopted from the horizontal and vertical broadband spectra defined in RG 1.60 and anchored at 0.1g. Similarly, for the partial soil column analyses (applicable to SSI analyses of the structures as partially embedded), the final horizontal and vertical SSI input motions are calculated as the

envelope of the partial column SSI input response spectra and the minimum required response spectra. These final SSI input response spectra are presented in Figures 3.7.1-218 through 3.7.1-220 and tabulated in Table 3.7.1-207. These spectra are used as target ARS for development of SSI input time histories in subsequent analyses.

3.7.1.1.4.2.2 SSI Input Response Spectra for the CB

The site-specific SSI input response spectra are calculated for SSI analysis of the CB structure as partially embedded (only considering embedment in rock) and as fully embedded. The corresponding partial column outcrop FIRS and full column outcrop FIRS for this structure as well as the PBSRS are presented in Section 2.5.2.6.

The SSI input response spectra for the CB are obtained after adjusting the FIRS as necessary for the NEI check following the same approach as described for RB/FB. For the CB, Figures 3.7.1-221 and 3.7.1-222 present the envelope of the ground surface ARS for the horizontal and vertical full column FIRS, respectively. Figures 3.7.1-223 and 3.7.1-224 present the horizontal and vertical envelope ARS at surface as well as their corresponding FIRS and PBSRS. Where the PBSRS exceed the envelope of surface ARS, the FIRS is adjusted (upward adjustment only, i.e., adjustment factor is always larger than one) by the ratio of the PBSRS to the envelope of surface ARS at each frequency. For the CB full column FIRS, the adjustment occurs for the horizontal FIRS below ~~3.7~~ 0.4 Hz with the largest adjustment factor being ~~1.03~~ 1.05. For the vertical full column FIRS, the adjustment is much more significant, especially between frequencies of 2 Hz and ~~13~~ 15 Hz with the maximum adjustment factor being ~~1.37~~ 1.39. The adjusted full column FIRS for CB are referred to as the SSI input response spectra for CB and are presented in Figures 3.7.1-223 and 3.7.1-224.

The NEI check for the partial column FIRS for the CB is carried out in a similar manner. The corresponding figures are provided in Figures 3.7.1-225 through 3.7.1-228. The surface ARS and PBSRS corresponding to the partial columns are calculated consistent with the partially embedded SSI analyses, at the top of the partial soil columns after removal of the saprolite layers. The necessary adjustment factors for the CB partial column FIRS are less than ~~1.08~~ 1.07 for horizontal and less than 1.16 for vertical directions. The adjusted partial column FIRS are referred to as the partial column SSI input response spectra for CB and are presented in Figures 3.7.1-227 and 3.7.1-228.

For the full column analyses (applicable to fully embedded SSI analyses), the final horizontal and vertical SSI input response spectra are calculated as the envelope of the full column SSI input response spectra and the minimum required response spectra which are adopted from the horizontal and vertical broadband spectra defined in RG 1.60 and anchored at 0.1g. Similarly, for the partial soil column analyses (applicable to SSI analyses of the structures as partially embedded), the final horizontal and vertical SSI input motions are calculated as the envelope of the partial column SSI input response spectra and the minimum required response spectra. These final SSI input response spectra are presented in Figures 3.7.1-229 through 3.7.1-231 and tabulated in Table 3.7.1-208. These spectra are used as target ARS for development of SSI input time histories in subsequent analyses.

3.7.1.1.4.2.3 **SSI Input Response Spectra for the FWSC**

Two sets of site-specific SSI input response spectra with control motion, defined at the bottom of the FWSC foundation (Elevation 282 ft NAVD88) and at the average elevation of the bottom of the concrete fill (Elevation 220 ft NAVD88), are calculated for SSI analysis of the FWSC. The geologic outcrop FIRS for this structure is calculated at Elevation 282 ft corresponding to the bottom of the foundation and top of the considered FWSC soil column, as presented in Section 2.5.2.6. The FWSC geologic outcrop FIRS also represent the PBSRS for the FWSC soil column. Additional NEI check for the FWSC SSI input response spectra is not warranted because the SSI results from the application of the SSI input motions at the top of the soil column and Elevation 220 ft are enveloped by the design basis for this structure as described in Section 3.7.2.4.1.

The final horizontal and vertical SSI input response spectra at Elevation 282 ft for FWSC are calculated as the envelope of the geologic outcrop FIRS and the minimum required response spectra which are adopted from the horizontal and vertical broadband spectra defined in RG 1.60 and anchored at 0.1g. The final SSI input response spectra at Elevation 282 ft are presented in Figures 3.7.1-232 through 3.7.1-234 and tabulated in Table 3.7.1-209. Similarly, the final horizontal and vertical SSI input response spectra at Elevation 220 ft are calculated as the envelope of the design response spectra (DRS) at Elevation 220 ft and the minimum required response spectra. The DRS at Elevation 220 ft are calculated consistent with the FIRS for FWSC using

the same methodology as described in Sections 2.5.2.5 and 2.5.2.6. The final SSI input response spectra at Elevation 220 ft are presented in Figures 3.7.1-283 through 3.7.1-285. These spectra are used as target ARS for development of SSI input time histories in subsequent analyses.

NAPS SUP 3.7-2

3.7.1.1.5 Site-Specific Design Ground Motion Time History

3.7.1.1.5.1 SSI Input Acceleration Time Histories

Corresponding to each set of horizontal and vertical final SSI input response spectra, described in Section 3.7.1.1.4.2, a three component set (two horizontal and one vertical) of spectrum compatible acceleration time histories is developed for use as input time histories for SSI analysis. The starting seed time histories are selected from the database of acceleration time histories in NUREG/CR-6728 (Reference 3.7-204). The candidate time histories were considered from the CEUS rock database bin with magnitudes between moment magnitude (**M**) 6 and **M** 7 and distances between 10 km and 50 km. This magnitude-distance bin was selected based on the high frequency deaggregation of the PSHA having mean magnitude and distance values of **M** 5.9 and ~~21~~ 22 km for the 10^{-4} hazard level, and **M** ~~6.2~~ 6.1 and 15 km for the 10^{-5} hazard level (Section 2.5.2.4). For the low frequency hazard deaggregation, the results are a magnitude of **M** ~~7.4~~ 7.1 and a distance of ~~540~~ 340 km for the 10^{-4} and **M** ~~7.5~~ 6.4 and a distance of ~~480~~ 21 km for the 10^{-5} hazard levels (Section 2.5.2.4). Based on the large distance associated with the low frequency 10^{-4} controlling event, the selected seed input acceleration time history for the spectral matching procedure was governed by the high frequency controlling events.

In selecting a candidate acceleration time history set from the applicable magnitude-distance bin from NUREG/CR-6728, the following aspects of a given time history set were considered:

- Similarity between the spectral shape of the candidate acceleration time history and the target spectrum
- Total time history duration of at least 20 seconds
- Zero-lag cross correlation coefficient between any two components of acceleration time histories should be less than 0.16
- Appropriate magnitude and distance values relative to the controlling event values
- Non-stationary phasing consistent with seismological principals.

NAPS SUP 3.7-1

Table 3.7.1-201 Strain-Compatible SSI Input Properties for RB/FB (In-situ Material)

Layer #	Thickness (ft)	Top-Depth (ft)	Unit Weight (kcf)	BE-RB/FB			LB-RB/FB			UB-RB/FB		
				Vs (ft/sec)	Vp (ft/sec)	Damping (%)	Vs (ft/sec)	Vp (ft/sec)	Damping (%)	Vs (ft/sec)	Vp (ft/sec)	Damping (%)
1	2.00	0	0.125	908	2224	2.07	616	1508	3.50	1339	3279	1.22
2	2.50	2	0.125	875	2498	3.38	534	1523	7.02	1435	4095	1.63
3	2.50	4.5	0.125	875	2498	3.38	534	1523	7.02	1435	4095	1.63
4	2.50	7	0.13	1302	5471	2.89	814	4152	5.52	2081	8745	1.52
5	2.50	9.5	0.13	1302	5471	2.89	814	4152	5.52	2081	8745	1.52
6	2.50	12	0.13	1887	5082	2.50	1259	4800	4.40	2829	7616	1.42
7	2.50	14.5	0.13	1887	5082	2.50	1259	4800	4.40	2829	7616	1.42
8	3.00	17	0.145	4324	10593	0.58	3212	7869	1.02	5821	14259	0.33
9	3.00	20	0.145	4324	10593	0.58	3212	7869	1.02	5821	14259	0.33
10	3.00	23	0.145	4324	10593	0.58	3212	7869	1.02	5821	14259	0.33
11	3.00	26	0.145	4324	10593	0.58	3212	7869	1.02	5821	14259	0.33
12	3.00	29	0.145	4324	10593	0.58	3212	7869	1.02	5821	14259	0.33
13	3.00	32	0.145	4324	10593	0.58	3212	7869	1.02	5821	14259	0.33
14	3.00	35	0.145	4324	10593	0.58	3212	7869	1.02	5821	14259	0.33
15	2.00	38	0.145	4324	10593	0.58	3212	7869	1.02	5821	14259	0.33
16	3.00	40	0.145	4324	10593	0.58	3212	7869	1.02	5821	14259	0.33
17	3.00	43	0.145	4324	10593	0.58	3212	7869	1.02	5821	14259	0.33
18	3.00	46	0.145	4324	10593	0.58	3212	7869	1.02	5821	14259	0.33
19	4.00	49	0.145	4324	10593	0.58	3212	7869	1.02	5821	14259	0.33
20	3.00	53	0.145	4324	10593	0.58	3212	7869	1.02	5821	14259	0.33

NAPS SUP 3.7-1

Table 3.7.1-201 Strain-Compatible SSI Input Properties for RB/FB (In-situ Material)

Layer #	Thickness (ft)	Top-Depth (ft)	Unit Weight (kcf)	BE-RB/FB			LB-RB/FB			UB-RB/FB		
				Vs (ft/sec)	Vp (ft/sec)	Damping (%)	Vs (ft/sec)	Vp (ft/sec)	Damping (%)	Vs (ft/sec)	Vp (ft/sec)	Damping (%)
21	3.00	56	0.145	4324	10593	0.58	3212	7869	1.02	5821	14259	0.33
22	3.00	59	0.145	4324	10593	0.58	3212	7869	1.02	5821	14259	0.33
23	4.00	62	0.145	4324	10593	0.58	3212	7869	1.02	5821	14259	0.33
24	3.00	66	0.163	5449	13347	1.00	4037	9888	1.82	7355	18017	0.55
25	4.00	69	0.163	5449	13347	1.00	4037	9888	1.82	7355	18017	0.55
26	4.00	73	0.163	5449	13347	1.00	4037	9888	1.82	7355	18017	0.55
27	4.00	77	0.163	5449	13347	1.00	4037	9888	1.82	7355	18017	0.55
28	4.00	81	0.163	5449	13347	1.00	4037	9888	1.82	7355	18017	0.55
29	4.00	85	0.163	5178	12682	1.00	3471	8501	1.82	7724	18920	0.55
30	4.00	89	0.163	5178	12682	1.00	3471	8501	1.82	7724	18920	0.55
31	4.00	93	0.163	5178	12682	1.00	3471	8501	1.82	7724	18920	0.55
32	4.00	97	0.163	5178	12682	1.00	3471	8501	1.82	7724	18920	0.55
33	5.00	101	0.163	5178	12682	1.00	3471	8501	1.82	7724	18920	0.55
34	4.00	106	0.164	8800	15678	1.00	7185	12801	1.82	10778	19201	0.55
35	5.00	110	0.164	8800	15678	1.00	7185	12801	1.82	10778	19201	0.55
36	5.00	115	0.164	8800	15678	1.00	7185	12801	1.82	10778	19201	0.55
37	5.00	120	0.164	8800	15678	1.00	7185	12801	1.82	10778	19201	0.55
38	5.00	125	0.164	8800	15678	1.00	7185	12801	1.82	10778	19201	0.55
39	5.00	130	0.164	8800	15678	1.00	7185	12801	1.82	10778	19201	0.55
40	5.00	135	0.164	8800	15678	1.00	7185	12801	1.82	10778	19201	0.55

NAPS SUP 3.7-1

Table 3.7.1-201 Strain-Compatible SSI Input Properties for RB/FB (In-situ Material)

Layer #	Thickness (ft)	Top-Depth (ft)	Unit Weight (kcf)	BE-RB/FB			LB-RB/FB			UB-RB/FB		
				Vs (ft/sec)	Vp (ft/sec)	Damping (%)	Vs (ft/sec)	Vp (ft/sec)	Damping (%)	Vs (ft/sec)	Vp (ft/sec)	Damping (%)
41	5.00	140	0.164	8800	15678	1.00	7185	12801	1.82	10778	19201	0.55
42	5.00	145	0.164	8800	15678	1.00	7185	12801	1.82	10778	19201	0.55
43	5.00	150	0.164	8800	15678	1.00	7185	12801	1.82	10778	19201	0.55
44		155	0.164	9200	16390	1.00	7512	13383	1.82	11268	20074	0.55

The top 7 layers correspond to saprolite and are removed in the partially embedded SSI analysis of the RB/FB.
Groundwater table is considered at the top of the fourth layer at Elevation 283 ft.

NAPS SUP 3.7-1

Table 3.7.1-202 Strain-Compatible SSI Input Properties for RB/FB (Structural Fill and Concrete Fill)

Layer #	Thickness (ft)	Top-Depth (ft)	Unit Weight (kcf)	BE-RB/FB			LB-RB/FB			UB-RB/FB		
				Vs (ft/sec)	Vp (ft/sec)	Damping (%)	Vs (ft/sec)	Vp (ft/sec)	Damping (%)	Vs (ft/sec)	Vp (ft/sec)	Damping (%)
1	2.00	0	0.130	734	1372	2.18	531	993	3.12	1014	1897	1.52
2	2.50	2	0.130	649	1213	4.24	418	781	7.00	1007	1884	2.57
3	2.50	4.5	0.130	649	1213	4.24	418	781	7.00	1007	1884	2.57
4	2.50	7	0.130	710	3619	5.13	444	2262	8.45	1135	4800	3.11
5	2.50	9.5	0.130	710	3619	5.13	444	2262	8.45	1135	4800	3.11
6	2.50	12	0.130	736	3752	5.80	469	2392	9.40	1154	4800	3.58
7	2.50	14.5	0.130	736	3752	5.80	469	2392	9.40	1154	4800	3.58
Concrete Fill		17	0.145	7000	10909	1.00	6000	9350	1.80	8000	12467	0.55

Groundwater table is considered at the top of the fourth layer at Elevation 283 ft.

NAPS SUP 3.7-1

Table 3.7.1-203 Strain-Compatible SSI Input Properties for CB (In-situ Material)

Layer #	Thickness (ft)	Top-Depth (ft)	Unit Weight (kcf)	BE-CB			LB-CB			UB-CB		
				Vs (ft/sec)	Vp (ft/sec)	Damping (%)	Vs (ft/sec)	Vp (ft/sec)	Damping (%)	Vs (ft/sec)	Vp (ft/sec)	Damping (%)
1	2.50	0	0.125	873	1773	2.78	590	1198	4.83	1292	2625	1.60
2	2.50	2.5	0.125	873	1773	2.78	590	1198	4.83	1292	2625	1.60
3	2.50	5	0.125	1007	4231	3.93	611	2567	7.42	1659	6975	2.08
4	2.50	7.5	0.125	1007	4800	3.93	611	3114	7.42	1659	6975	2.08
5	2.50	10	0.125	1007	4800	3.93	611	3114	7.42	1659	6975	2.08
6	2.50	12.5	0.125	1007	4800	3.93	611	3114	7.42	1659	6975	2.08
7	2.50	15	0.13	1419	5966	3.78	990	4800	6.53	2036	8557	2.19
8	2.50	17.5	0.13	1419	5966	3.78	990	4800	6.53	2036	8557	2.19
9	2.50	20	0.13	1419	5966	3.78	990	4800	6.53	2036	8557	2.19
10	2.50	22.5	0.13	1419	5966	3.78	990	4800	6.53	2036	8557	2.19
11	2.50	25	0.145	2024	6184	0.62	1545	4800	1.06	2651	8100	0.36
12	2.50	27.5	0.145	2024	6184	0.62	1545	4800	1.06	2651	8100	0.36
13	2.50	30	0.145	2024	6184	0.62	1545	4800	1.06	2651	8100	0.36
14	2.50	32.5	0.145	2024	6184	0.62	1545	4800	1.06	2651	8100	0.36
15	2.50	35	0.145	2475	7561	0.63	1841	5625	1.14	3327	10163	0.35
16	2.50	37.5	0.145	2475	7561	0.63	1841	5625	1.14	3327	10163	0.35
17	2.50	40	0.145	2475	7561	0.63	1841	5625	1.14	3327	10163	0.35
18	2.50	42.5	0.145	2475	7561	0.63	1841	5625	1.14	3327	10163	0.35
19	2.50	45	0.145	2475	7561	0.63	1841	5625	1.14	3327	10163	0.35
20	1.50	47.5	0.145	2475	7561	0.63	1841	5625	1.14	3327	10163	0.35

NAPS SUP 3.7-1

Table 3.7.1-203 Strain-Compatible SSI Input Properties for CB (In-situ Material)

Layer #	Thickness (ft)	Top-Depth (ft)	Unit Weight (kcf)	BE-CB			LB-CB			UB-CB		
				Vs (ft/sec)	Vp (ft/sec)	Damping (%)	Vs (ft/sec)	Vp (ft/sec)	Damping (%)	Vs (ft/sec)	Vp (ft/sec)	Damping (%)
21	3.50	49	0.145	2475	7561	0.63	1841	5625	1.14	3327	10163	0.35
22	2.50	52.5	0.145	2475	7561	0.63	1841	5625	1.14	3327	10163	0.35
23	2.50	55	0.145	2660	8127	0.53	2172	6635	0.96	3258	9953	0.29
24	2.50	57.5	0.145	2660	8127	0.53	2172	6635	0.96	3258	9953	0.29
25	2.50	60	0.145	2660	8127	0.53	2172	6635	0.96	3258	9953	0.29
26	2.50	62.5	0.145	2660	8127	0.53	2172	6635	0.96	3258	9953	0.29
27	1.00	65	0.163	6483	13861	1.00	5293	11318	1.82	7940	16976	0.55
28	3.00	66	0.163	6483	13861	1.00	5293	11318	1.82	7940	16976	0.55
29	3.00	69	0.163	6483	13861	1.00	5293	11318	1.82	7940	16976	0.55
30	3.00	72	0.163	6483	13861	1.00	5293	11318	1.82	7940	16976	0.55
31	3.00	75	0.163	6983	14018	1.00	5701	11445	1.82	8552	17168	0.55
32	2.00	78	0.163	6983	14018	1.00	5701	11445	1.82	8552	17168	0.55
33	5.00	80	0.163	6983	14018	1.00	5701	11445	1.82	8552	17168	0.55
34	5.00	85	0.163	6983	14018	1.00	5701	11445	1.82	8552	17168	0.55
35	5.00	90	0.163	6983	14018	1.00	5701	11445	1.82	8552	17168	0.55
36	5.00	95	0.163	7942	15135	1.00	6485	12358	1.82	9727	18536	0.55
37	5.00	100	0.163	7942	15135	1.00	6485	12358	1.82	9727	18536	0.55
38	5.00	105	0.164	8655	15657	1.00	7067	12784	1.82	10600	19176	0.55
39	5.00	110	0.164	8655	15657	1.00	7067	12784	1.82	10600	19176	0.55
40	5.00	115	0.164	8242	15707	1.00	6730	12824	1.82	10094	19236	0.55

NAPS SUP 3.7-1

Table 3.7.1-203 Strain-Compatible SSI Input Properties for CB (In-situ Material)

Layer #	Thickness (ft)	Top-Depth (ft)	Unit Weight (kcf)	BE-CB			LB-CB			UB-CB		
				Vs (ft/sec)	Vp (ft/sec)	Damping (%)	Vs (ft/sec)	Vp (ft/sec)	Damping (%)	Vs (ft/sec)	Vp (ft/sec)	Damping (%)
41	5.00	120	0.164	8242	15707	1.00	6730	12824	1.82	10094	19236	0.55
42	5.00	125	0.164	8658	16198	1.00	7069	13225	1.82	10604	19838	0.55
43	5.00	130	0.164	8658	16198	1.00	7069	13225	1.82	10604	19838	0.55
44	5.00	135	0.164	8822	15491	1.00	7203	12648	1.82	10805	18972	0.55
45	5.00	140	0.164	8822	15491	1.00	7203	12648	1.82	10805	18972	0.55
46	5.00	145	0.164	9340	16897	1.00	7626	13796	1.82	11439	20694	0.55
47	5.00	150	0.164	9340	16897	1.00	7626	13796	1.82	11439	20694	0.55
48	5.00	155	0.164	9198	17208	1.00	7510	14050	1.82	11265	21075	0.55
49	5.00	160	0.164	9198	17208	1.00	7510	14050	1.82	11265	21075	0.55
50		165	0.164	9200	15729	1.00	7512	12843	1.82	11268	19264	0.55

The top 10 layers correspond to saprolite and are removed in the partially embedded SSI analysis of the CB.
Groundwater table is considered at the top of the fourth layer at Elevation 282.5 ft.

NAPS SUP 3.7-1

Table 3.7.1-204 Strain-Compatible SSI Input Properties for CB (Structural Fill and Concrete Fill)

Layer #	Thickness (ft)	Top-Depth (ft)	Unit Weight (kcf)	BE-CB			LB-CB			UB-CB		
				Vs (ft/sec)	Vp (ft/sec)	Damping (%)	Vs (ft/sec)	Vp (ft/sec)	Damping (%)	Vs (ft/sec)	Vp (ft/sec)	Damping (%)
1	2.50	0	0.130	649	1214	3.14	440	823	4.98	958	1791	1.98
2	2.50	2.5	0.130	649	1214	3.14	440	823	4.98	958	1791	1.98
3	2.50	5	0.130	747	1397	4.41	486	909	7.17	1149	2149	2.72
4	2.50	7.5	0.130	747	3809	4.41	486	2477	7.17	1149	4800	2.72
5	2.50	10	0.130	751	3831	5.21	478	2436	8.38	1182	4800	3.24
6	2.50	12.5	0.130	751	3831	5.21	478	2436	8.38	1182	4800	3.24
7	2.50	15	0.130	759	3872	5.92	492	2507	9.11	1173	4800	3.84
8	2.50	17.5	0.130	759	3872	5.92	492	2507	9.11	1173	4800	3.84
9	2.50	20	0.130	813	4147	5.67	515	2626	8.93	1284	4800	3.60
10	2.50	22.5	0.130	813	4147	5.67	515	2626	8.93	1284	4800	3.60
Concrete Fill		25	0.145	7000	10909	1.00	6000	9350	1.80	8000	12467	0.55

Groundwater table is considered at the top of the fourth layer at Elevation 282.5 ft.

NAPS SUP 3.7-1

Table 3.7.1-205 Strain-Compatible SSI Input Properties for FWSC (In-situ Material)

Layer #	Thickness (ft)	Top-Depth (ft)	Unit Weight [kcf]	BE-FWSC			LB-FWSC			UB-FWSC		
				Vs (ft/sec)	Vp (ft/sec)	Damping (%)	Vs (ft/sec)	Vp (ft/sec)	Damping (%)	Vs (ft/sec)	Vp (ft/sec)	Damping (%)
1	3.00	0	0.125	742	3783	4.18	483	2460	6.63	1141	4800	2.64
2	3.00	3	0.125	742	3783	4.18	483	2460	6.63	1141	4800	2.64
3	3.00	6	0.125	742	3783	4.18	483	2460	6.63	1141	4800	2.64
4	3.00	9	0.125	742	3783	4.18	483	2460	6.63	1141	4800	2.64
5	3.00	12	0.125	979	4800	5.00	605	3083	8.25	1585	6661	3.03
6	3.00	15	0.125	979	4800	5.00	605	3083	8.25	1585	6661	3.03
7	3.00	18	0.125	979	4800	5.00	605	3083	8.25	1585	6661	3.03
8	4.00	21	0.125	979	4800	5.00	605	3083	8.25	1585	6661	3.03
9	4.00	25	0.125	979	4800	5.00	605	3083	8.25	1585	6661	3.03
10	4.00	29	0.13	1416	5952	3.97	1018	4800	6.08	1970	8280	2.60
11	3.00	33	0.13	1955	5974	2.89	1431	4800	4.37	2672	8164	1.92
12	2.00	36	0.13	1955	5974	2.89	1431	4800	4.37	2672	8164	1.92
13	4.00	38	0.145	2503	7647	0.64	1907	5825	1.14	3286	10040	0.36
14	4.00	42	0.145	2503	7647	0.64	1907	5825	1.14	3286	10040	0.36
15	4.00	46	0.145	2503	7647	0.64	1907	5825	1.14	3286	10040	0.36
16	4.00	50	0.145	2503	7647	0.64	1907	5825	1.14	3286	10040	0.36
17	4.00	54	0.145	2693	8228	0.53	2150	6568	0.94	3373	10306	0.30
18	4.00	58	0.145	2693	8228	0.53	2150	6568	0.94	3373	10306	0.30
19	3.00	62	0.163	6483	13861	1.00	4803	10269	1.82	8751	18711	0.55
20	3.00	65	0.163	6483	13861	1.00	4803	10269	1.82	8751	18711	0.55

NAPS SUP 3.7-1

Table 3.7.1-205 Strain-Compatible SSI Input Properties for FWSC (In-situ Material)

Layer #	Thickness (ft)	Top-Depth (ft)	Unit Weight [kcf]	BE-FWSC			LB-FWSC			UB-FWSC		
				Vs (ft/sec)	Vp (ft/sec)	Damping (%)	Vs (ft/sec)	Vp (ft/sec)	Damping (%)	Vs (ft/sec)	Vp (ft/sec)	Damping (%)
21	3.00	68	0.163	6983	14018	1.00	5701	11445	1.82	8552	17168	0.55
22	4.00	71	0.163	6983	14018	1.00	5701	11445	1.82	8552	17168	0.55
23	4.00	75	0.163	6983	14018	1.00	5701	11445	1.82	8552	17168	0.55
24	3.00	79	0.164	7942	15135	1.00	6485	12358	1.82	9727	18536	0.55
25	4.00	82	0.164	7942	15135	1.00	6485	12358	1.82	9727	18536	0.55
26	4.00	86	0.164	7942	15135	1.00	6485	12358	1.82	9727	18536	0.55
27	3.00	90	0.164	8655	15657	1.00	7067	12784	1.82	10600	19176	0.55
28	4.00	93	0.164	8655	15657	1.00	7067	12784	1.82	10600	19176	0.55
29	4.00	97	0.164	8655	15657	1.00	7067	12784	1.82	10600	19176	0.55
30	3.00	101	0.164	8242	15707	1.00	6730	12824	1.82	10094	19236	0.55
31	4.00	104	0.164	8242	15707	1.00	6730	12824	1.82	10094	19236	0.55
32	4.00	108	0.164	8242	15707	1.00	6730	12824	1.82	10094	19236	0.55
33	3.00	112	0.164	8658	16198	1.00	7069	13225	1.82	10604	19838	0.55
34	4.00	115	0.164	8658	16198	1.00	7069	13225	1.82	10604	19838	0.55
35	4.00	119	0.164	8658	16198	1.00	7069	13225	1.82	10604	19838	0.55
36	3.00	123	0.164	8822	15491	1.00	7203	12648	1.82	10805	18972	0.55
37	4.00	126	0.164	8822	15491	1.00	7203	12648	1.82	10805	18972	0.55
38	4.00	130	0.164	8822	15491	1.00	7203	12648	1.82	10805	18972	0.55
39	3.00	134	0.164	9340	16897	1.00	7626	13796	1.82	11439	20694	0.55
40	4.00	137	0.164	9340	16897	1.00	7626	13796	1.82	11439	20694	0.55

NAPS SUP 3.7-1

Table 3.7.1-205 Strain-Compatible SSI Input Properties for FWSC (In-situ Material)

Layer #	Thickness (ft)	Top-Depth (ft)	Unit Weight [kcf]	BE-FWSC			LB-FWSC			UB-FWSC		
				Vs (ft/sec)	Vp (ft/sec)	Damping (%)	Vs (ft/sec)	Vp (ft/sec)	Damping (%)	Vs (ft/sec)	Vp (ft/sec)	Damping (%)
41	4.00	141	0.164	9340	16897	1.00	7626	13796	1.82	11439	20694	0.55
42	3.00	145	0.164	9198	17208	1.00	7510	14050	1.82	11265	21075	0.55
43	4.00	148	0.164	9198	17208	1.00	7510	14050	1.82	11265	21075	0.55
44	4.00	152	0.164	9198	17208	1.00	7510	14050	1.82	11265	21075	0.55
45		156	0.164	9200	15729	1.00	7512	12843	1.82	11268	19264	0.55

Depth is measured with respect to the bottom of the foundation at Elevation 282 ft.
Groundwater table is considered at the top of the first layer at Elevation 282 ft.

NAPS SUP 3.7-1

Table 3.7.1-206 Strain-Compatible SSI Input Properties for FWSC (Structural Fill and Concrete Fill)

Layer #	Thickness (ft)	Top-Depth (ft)	Unit Weight [kcf]	BE-FWSC			LB-FWSC			UB-FWSC		
				Vs (ft/sec)	Vp (ft/sec)	Damping (%)	Vs (ft/sec)	Vp (ft/sec)	Damping (%)	Vs (ft/sec)	Vp (ft/sec)	Damping (%)
1	3.00	0	0.130	745	3799	4.74	479	2440	7.33	1160	4800	3.06
2	3.00	3	0.130	759	3872	4.83	491	2504	7.50	1174	4800	3.11
3	3.00	6	0.130	784	4000	4.97	503	2567	7.85	1223	4800	3.15
4	3.00	9	0.130	783	3991	5.33	507	2586	8.29	1208	4800	3.42
5	3.00	12	0.130	845	4311	5.17	526	2683	8.02	1358	4800	3.33
6	3.00	15	0.130	830	4234	5.47	509	2593	8.50	1356	4800	3.52
7	3.00	18	0.130	830	4235	5.65	518	2640	8.54	1332	4800	3.74
8	4.00	21	0.130	852	4347	5.67	520	2654	8.87	1396	4800	3.63
9	4.00	25	0.130	848	4325	5.96	514	2620	9.19	1400	4800	3.87
10	4.00	29	0.130	894	4558	5.75	551	2809	8.74	1451	4800	3.78
11	3.00	33	0.130	890	4538	5.95	531	2706	9.35	1492	4800	3.79
12	2.00	36	0.130	890	4538	5.95	531	2706	9.35	1492	4800	3.79
Concrete Fill		38	0.145	7000	10909	1.00	6000	9350	1.82	8000	12467	0.55

Depth is measured with respect to the bottom of the foundation at Elevation 282 ft.
Groundwater table is considered at the top of the first layer at Elevation 282 ft.

NAPS SUP 3.7-1

Table 3.7.1-207 5% Damped Final SSI Input Response Spectra for RB/FB

	Final Full Column SSI Input Response Spectra		Final Partial Column SSI Input Response Spectra	
Frequency (Hz)	Horizontal (g)	Vertical (g)	Horizontal (g)	Vertical (g)
100	0.563	0.563	0.586	0.586
90	0.605	0.627	0.632	0.656
80	0.677	0.739	0.708	0.772
70	0.795	0.899	0.821	0.929
60	0.953	1.10	0.992	1.14
50	1.09	1.26	1.13	1.30
45	1.13	1.26	1.19	1.32
40	1.17	1.22	1.21	1.26
35	1.18	1.16	1.22	1.20
30	1.21	1.13	1.20	1.13
25	1.16	1.02	1.17	1.03
20	1.13	0.98	1.16	0.962
15	1.11	1.15	1.19	0.938
12.5	1.09	1.22	1.17	0.905
10	1.00	1.22	1.05	0.790
9	0.943	1.18	0.953	0.715
8	0.868	1.11	0.841	0.631
7	0.776	1.00	0.713	0.535
6	0.754	0.866	0.587	0.440
5	0.674	0.695	0.474	0.355
4	0.508	0.481	0.367	0.292
3	0.327	0.288	0.305	0.261
2.5	0.312	0.224	0.312	0.224
2	0.261	0.185	0.261	0.185
1.5	0.206	0.145	0.206	0.145
1.25	0.177	0.124	0.177	0.124
1	0.147	0.103	0.147	0.103

NAPS SUP 3.7-1

Table 3.7.1-207 5% Damped Final SSI Input Response Spectra for RB/FB

	Final Full Column SSI Input Response Spectra		Final Partial Column SSI Input Response Spectra	
Frequency (Hz)	Horizontal (g)	Vertical (g)	Horizontal (g)	Vertical (g)
0.9	0.135	0.0938	0.135	0.0938
0.8	0.123	0.0848	0.123	0.0848
0.7	0.110	0.0757	0.110	0.0757
0.6	0.0969	0.0664	0.0969	0.0664
0.5	0.0834	0.0569	0.0834	0.0569
0.4	0.0694	0.0470	0.0694	0.0470
0.3	0.0548	0.0368	0.0548	0.0368
0.2	0.0302	0.0202	0.0302	0.0202
0.167	0.0210	0.0141	0.0210	0.0141
0.125	0.0118	0.00798	0.0118	0.00792
0.1	0.00852	0.00639	0.00842	0.00631

NAPS SUP 3.7-1

Table 3.7.1-208 5% Damped Final SSI Input Response Spectra for CB

	Final Full Column SSI Input Response Spectra		Final Partial Column SSI Input Response Spectra	
Frequency (Hz)	Horizontal (g)	Vertical (g)	Horizontal (g)	Vertical (g)
100	0.749	0.749	0.800	0.838
90	0.807	0.837	0.854	0.932
80	0.896	0.977	0.948	1.08
70	1.04	1.18	1.08	1.27
60	1.26	1.45	1.33	1.60
50	1.43	1.65	1.51	1.85
45	1.48	1.65	1.57	1.88
40	1.51	1.58	1.63	1.87
35	1.56	1.53	1.67	1.81
30	1.59	1.49	1.63	1.67
25	1.53	1.34	1.61	1.52
20	1.48	1.22	1.70	1.48
15	1.45	1.23	1.79	1.46
12.5	1.42	1.29	1.74	1.37
10	1.33	1.27	1.44	1.10
9	1.26	1.23	1.22	0.928
8	1.16	1.15	0.988	0.749
7	1.03	1.03	0.786	0.594
6	0.861	0.885	0.626	0.473
5	0.679	0.708	0.498	0.375
4	0.483	0.488	0.382	0.293
3	0.322	0.292	0.305	0.261
2.5	0.312	0.224	0.312	0.224
2	0.261	0.185	0.261	0.185
1.5	0.206	0.145	0.206	0.145
1.25	0.177	0.124	0.177	0.124
1	0.147	0.103	0.147	0.103

NAPS SUP 3.7-1

Table 3.7.1-208 5% Damped Final SSI Input Response Spectra for CB

	Final Full Column SSI Input Response Spectra		Final Partial Column SSI Input Response Spectra	
Frequency (Hz)	Horizontal (g)	Vertical (g)	Horizontal (g)	Vertical (g)
0.9	0.135	0.0938	0.135	0.0938
0.8	0.123	0.0848	0.123	0.0848
0.7	0.110	0.0757	0.110	0.0757
0.6	0.0969	0.0664	0.0969	0.0664
0.5	0.0834	0.0569	0.0834	0.0569
0.4	0.0694	0.0470	0.0694	0.0470
0.3	0.0548	0.0368	0.0548	0.0368
0.2	0.0302	0.0202	0.0302	0.0202
0.167	0.0210	0.0141	0.0210	0.0141
0.125	0.0118	0.00794	0.0118	0.00793
0.1	0.00845	0.00642	0.00844	0.00633

NAPS SUP 3.7-1

Table 3.7.1-209 5% Damped Final SSI Input Response Spectra at Elevation 282 ft for FWSC

	Final SSI Input Response Spectra	
Frequency (Hz)	Horizontal (g)	Vertical (g)
100	0.691	0.691
90	0.708	0.734
80	0.735	0.802
70	0.783	0.886
60	0.859	0.989
50	0.972	1.12
45	1.05	1.17
40	1.14	1.18
35	1.23	1.20
30	1.35	1.26
25	1.45	1.28
20	1.59	1.31
15	1.64	1.29
12.5	1.59	1.22
10	1.57	1.18
9	1.56	1.17
8	1.51	1.13
7	1.38	1.04
6	1.21	0.908
5	1.01	0.758
4	0.766	0.575
3	0.497	0.373
2.5	0.358	0.269
2	0.261	0.186
1.5	0.206	0.145
1.25	0.177	0.124
1	0.147	0.103

NAPS SUP 3.7-1

Table 3.7.1-209 5% Damped Final SSI Input Response Spectra at Elevation 282 ft for FWSC

	Final SSI Input Response Spectra	
Frequency (Hz)	Horizontal (g)	Vertical (g)
0.9	0.135	0.0938
0.8	0.123	0.0848
0.7	0.110	0.0757
0.6	0.0969	0.0664
0.5	0.0834	0.0569
0.4	0.0694	0.0470
0.3	0.0548	0.0368
0.2	0.0302	0.0202
0.167	0.0210	0.0141
0.125	0.0118	0.00799
0.1	0.00853	0.00640

NAPS SUP 3.7-2

Table 3.7.1-210 Zero-Lag Cross-Correlation Coefficients for the Final Scaled Spectrum Compatible Acceleration Time-Histories for the RB/FB

RB/FB Full Profile

Components	Zero-Lag Cross-Correlation Coefficient of Final Matched Time Histories
H1 – H2	0.018
H1 – UP	0.015
H2 – UP	-0.014

RB/FB Partial Profile

Components	Zero-Lag Cross-Correlation Coefficient of Final Matched Time Histories
H1 – H2	0.042
H1 – UP	0.033
H2 – UP	-0.016

NAPS SUP 3.7-2

Table 3.7.1-211 Peak Ground Motion Parameters, Associated Ratios, and Strong Motion Duration Values for the Final Scaled Spectrum Compatible Acceleration Time-Histories for the RB/FB

Parameter	H1	H2	UP
RB/FB Full Profile			
PGA (g)	0.572	0.565	0.568
PGV (cm/sec)	21.622	15.950	18.257
PGD (cm)	7.964	8.745	7.279
PGV/PGA (cm/sec/g)	37.769	28.243	32.142
PGA*PGD/PGV^2	9.562	19.033	12.162
5-75% Duration Time (sec)	7.495	10.215	6.420
5% Duration Time (sec)	1.085	1.245	0.960
75% Duration Time (sec)	8.580	11.460	7.380
0% Extrapolated Duration Time (sec)	0.550	0.515	0.501
100% Extrapolated Duration Time (sec)	11.257	15.108	9.673
0-100% Extrapolated Duration Time (sec)	10.707	14.593	9.171
RB/FB Partial Profile			
PGA (g)	0.586	0.587	0.591
PGV (cm/sec)	21.446	14.915	16.383
PGD (cm)	7.527	8.795	7.359
PGV/PGA (cm/sec/g)	36.586	25.408	27.706
PGA*PGD/PGV^2	9.405	22.755	15.897
5-75% Duration Time (sec)	7.590	10.465	7.380
5% Duration Time (sec)	1.070	1.210	0.985
75% Duration Time (sec)	8.660	11.675	8.365
0% Extrapolated Duration Time (sec)	0.528	0.463	0.458
100% Extrapolated Duration Time (sec)	11.371	15.413	11.001
0-100% Extrapolated Duration Time (sec)	10.843	14.950	10.543

NAPS SUP 3.7-2

Table 3.7.1-212 Zero-Lag Cross-Correlation Coefficients for the Final Scaled Spectrum Compatible Acceleration Time-Histories for the CB

CB Full Profile

Components	Zero-Lag Cross-Correlation Coefficient of Final Matched Time Histories
H1 – H2	0.041
H1 – UP	0.024
H2 – UP	-0.022

CB Partial Profile

Components	Zero-Lag Cross-Correlation Coefficient of Final Matched Time Histories
H1 – H2	0.040
H1 – UP	0.031
H2 – UP	-0.025

NAPS SUP 3.7-2

Table 3.7.1-213 Peak Ground Motion Parameters, Associated Ratios, and Strong Motion Duration Values for the Final Scaled Spectrum Compatible Acceleration Time-Histories for the CB

Parameter	H1	H2	UP
CB Full Profile			
PGA (g)	0.745	0.753	0.756
PGV (cm/sec)	20.604	18.030	17.793
PGD (cm)	6.862	7.384	6.355
PGV/PGA (cm/sec/g)	27.656	23.959	23.551
$PGA*PGD/PGV^2$	11.808	16.759	14.870
5-75% Duration Time (sec)	7.975	10.840	6.180
5% Duration Time (sec)	1.085	1.240	0.955
75% Duration Time (sec)	9.060	12.080	7.135
0% Extrapolated Duration Time (sec)	0.515	0.466	0.514
100% Extrapolated Duration Time (sec)	11.908	15.951	9.342
0-100% Extrapolated Duration Time (sec)	11.393	15.486	8.829
CB Partial Profile			
PGA (g)	0.798	0.807	0.838
PGV (cm/sec)	19.890	16.990	15.259
PGD (cm)	7.072	7.917	6.186
PGV/PGA (cm/sec/g)	24.922	21.045	18.203
$PGA*PGD/PGV^2$	13.988	21.711	21.836
5-75% Duration Time (sec)	7.910	10.725	6.320
5% Duration Time (sec)	1.055	1.195	1.000
75% Duration Time (sec)	8.965	11.920	7.320
0% Extrapolated Duration Time (sec)	0.490	0.429	0.549
100% Extrapolated Duration Time (sec)	11.790	15.750	9.577
0-100% Extrapolated Duration Time (sec)	11.300	15.321	9.029

NAPS SUP 3.7-2

Table 3.7.1-214 Zero-Lag Cross-Correlation Coefficients for the Final Scaled Spectrum Compatible Acceleration Time Histories for the FWSC at Elevation 282 ft

~~FWSC~~

Components	Zero-Lag Cross-Correlation Coefficient of Final Matched Time Histories
H1 – H2	0.016
H1 – UP	-0.012
H2 – UP	0.017

NAPS SUP 3.7-2

Table 3.7.1-215 Peak Ground Motion Parameters, Associated Ratios, and Strong Motion Duration Values for the Final Scaled Spectrum Compatible Acceleration Time Histories for the FWSC at Elevation 282 ft

~~FWSC~~

Parameter	H1	H2	UP
PGA (g)	0.697	0.686	0.668
PGV (cm/sec)	21.061	19.057	16.151
PGD (cm)	9.360	9.108	6.072
PGV/PGA (cm/sec/g)	30.212	27.793	24.190
$PGA*PGD/PGV^2$	14.424	16.860	15.238
5-75% Duration Time (sec)	7.120	10.185	6.505
5% Duration Time (sec)	1.085	1.340	0.955
75% Duration Time (sec)	8.205	11.525	7.460
0% Extrapolated Duration Time (sec)	0.576	0.613	0.490
100% Extrapolated Duration Time (sec)	10.748	15.163	9.783
0-100% Extrapolated Duration Time (sec)	10.171	14.550	9.293

NAPS SUP 3.7-2

Table 3.7.1-216 Site-Dependent SSE and OBE 5% Damping Acceleration Response Spectra at Grade

Frequency (Hz)	Horizontal SSE at Grade (g)	Vertical SSE at Grade (g)	Horizontal OBE at Grade (g)	Vertical OBE at Grade (g)
100	0.894	0.894	0.298	0.298
90	0.949	0.984	0.316	0.328
80	1.04	1.13	0.347	0.378
70	1.18	1.34	0.394	0.446
60	1.38	1.59	0.461	0.531
50	1.56	1.79	0.519	0.598
45	1.69	1.88	0.564	0.628
40	1.84	1.91	0.612	0.638
35	1.87	1.83	0.622	0.610
30	1.89	1.77	0.629	0.589
25	1.83	1.61	0.610	0.537
20	1.87	1.54	0.622	0.513
15	1.93	1.52	0.643	0.507
12.5	1.96	1.51	0.654	0.504
10	1.90	1.43	0.635	0.476
9	1.81	1.36	0.603	0.452
8	1.67	1.25	0.555	0.417
7	1.48	1.11	0.492	0.369
6	1.26	0.942	0.419	0.314
5	0.994	0.746	0.331	0.249
4	0.679	0.509	0.226	0.170
3	0.402	0.302	0.134	0.101
2.5	0.312	0.224	0.104	0.075
2	0.261	0.185	0.0869	0.0617
1.5	0.206	0.145	0.0686	0.0483
1.25	0.177	0.124	0.0590	0.0414
1	0.147	0.103	0.0491	0.0342

NAPS SUP 3.7-2

Table 3.7.1-216 Site-Dependent SSE and OBE 5% Damping Acceleration Response Spectra at Grade

Frequency (Hz)	Horizontal SSE at Grade (g)	Vertical SSE at Grade (g)	Horizontal OBE at Grade (g)	Vertical OBE at Grade (g)
0.9	0.135	0.0938	0.0451	0.0313
0.8	0.123	0.0848	0.0409	0.0283
0.7	0.110	0.0757	0.0367	0.0252
0.6	0.0969	0.0664	0.0323	0.0221
0.5	0.0834	0.0569	0.0278	0.0190
0.4	0.0694	0.0470	0.0231	0.0157
0.3	0.0548	0.0368	0.0183	0.0123
0.2	0.0302	0.0202	0.0101	0.00673
0.167	0.0210	0.0141	0.00701	0.00469
0.125	0.0118	0.00796	0.00393	0.00265
0.1	0.00850	0.00638	0.00283	0.00213

NAPS SUP 3.7-2

Table 3.7.1-217 Site-Dependent SSE and OBE 5% Damping Pseudo Velocity Response Spectra at Grade

Frequency (Hz)	Horizontal SSE at Grade (in/sec)	Vertical SSE at Grade (in/sec)	Horizontal OBE at Grade (in/sec)	Vertical OBE at Grade (in/sec)
100	0.549	0.549	0.183	0.183
90	0.648	0.673	0.216	0.224
80	0.800	0.872	0.267	0.291
70	1.04	1.17	0.346	0.392
60	1.42	1.63	0.472	0.544
50	1.92	2.21	0.638	0.736
45	2.31	2.57	0.771	0.858
40	2.82	2.94	0.940	0.980
35	3.28	3.21	1.09	1.07
30	3.87	3.62	1.29	1.21
25	4.50	3.96	1.50	1.32
20	5.74	4.74	1.91	1.58
15	7.91	6.23	2.64	2.08
12.5	9.65	7.44	3.22	2.48
10	11.7	8.78	3.90	2.93
9	12.4	9.27	4.12	3.09
8	12.8	9.61	4.27	3.20
7	13.0	9.73	4.32	3.24
6	12.9	9.66	4.29	3.22
5	12.2	9.17	4.08	3.06
4	10.4	7.83	3.48	2.61
3	8.25	6.19	2.75	2.06
2.5	7.67	5.51	2.56	1.84
2	8.01	5.69	2.67	1.90
1.5	8.43	5.94	2.81	1.98
1.25	8.71	6.10	2.90	2.03
1	9.06	6.31	3.02	2.10

NAPS SUP 3.7-2

Table 3.7.1-217 Site-Dependent SSE and OBE 5% Damping Pseudo Velocity Response Spectra at Grade

Frequency (Hz)	Horizontal SSE at Grade (in/sec)	Vertical SSE at Grade (in/sec)	Horizontal OBE at Grade (in/sec)	Vertical OBE at Grade (in/sec)
0.9	9.24	6.41	3.08	2.14
0.8	9.43	6.52	3.14	2.17
0.7	9.66	6.65	3.22	2.22
0.6	9.93	6.81	3.31	2.27
0.5	10.3	6.99	3.42	2.33
0.4	10.7	7.23	3.56	2.41
0.3	11.2	7.55	3.74	2.52
0.2	9.28	6.21	3.09	2.07
0.167	7.75	5.18	2.58	1.73
0.125	5.80	3.92	1.93	1.31
0.1	5.23	3.92	1.74	1.31

NAPS SUP 3.7-2

Table 3.7.1-218 Zero-Lag Cross Correlation Coefficients for the Final Scaled Spectrum Compatible Acceleration Time Histories for the FWSC at Elevation 220 ft

Components	Zero-Lag Cross Correlation Coefficient of Final Matched Time Histories
H1 – H2	0.019
H1 – UP	0.043
H2 – UP	-0.019

NAPS SUP 3.7-2

Table 3.7.1-219 Peak Ground Motion Parameters, Associated Ratios, and Strong Motion Duration Values for the Final Scaled Spectrum Compatible Acceleration Time Histories for the FWSC at Elevation 220 ft

~~FWSC at Elevation 220 ft~~

Parameter	H1 ~~(Comp 067)~~	H2 ~~(Comp 337)~~	UP ~~(Vertical)~~
PGA (g)	0.556	0.553	0.552
PGV (cm/sec)	18.131	15.590	14.323
PGD (cm)	6.523	9.159	4.814
PGV/PGA (cm/~~s~~ sec/g)	32.614	28.183	25.932
PGA*PGD/PGV^2	10.817	20.440	12.707
5-75% Duration Time (sec)	7.560	11.770	7.675
5% Duration Time (sec)	1.095	1.245	0.955
75% Duration Time (sec)	8.655	13.015	8.630
0% Extrapolated Duration Time (sec)	0.555	0.404	0.407
100% Extrapolated Duration Time (sec)	11.355	17.219	11.371
0-100% Extrapolated Duration Time (sec)	10.800	16.814	10.964

NAPS SUP 3.7-1 **Figure 3.7.1-201 SSI Input Strain Compatible Shear-Wave Velocity Profiles – RB/FB**

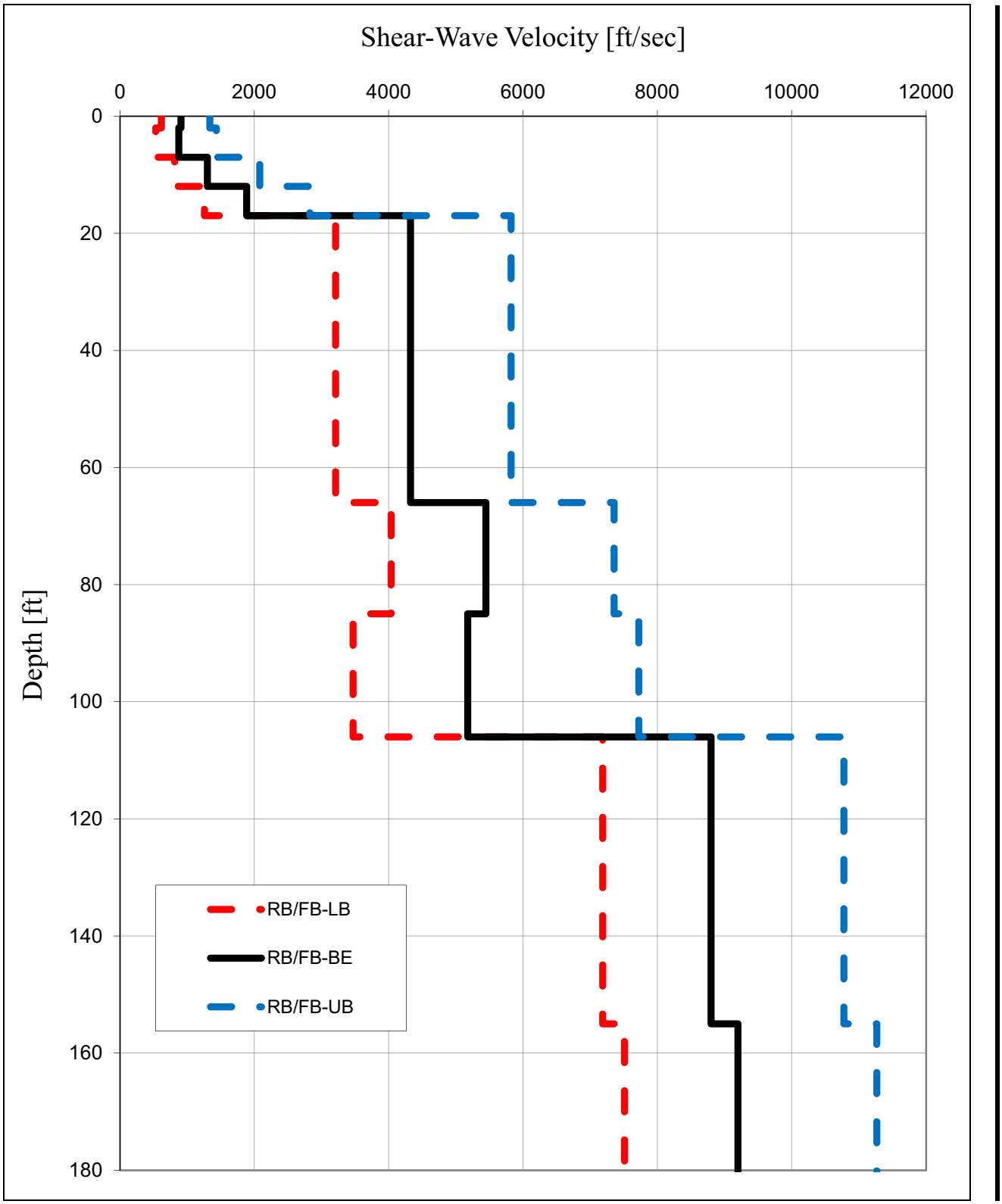

NAPS SUP 3.7-1 **Figure 3.7.1-202 SSI Input Strain Compatible ~~Shear Wave~~ Damping Profiles – RB/FB**

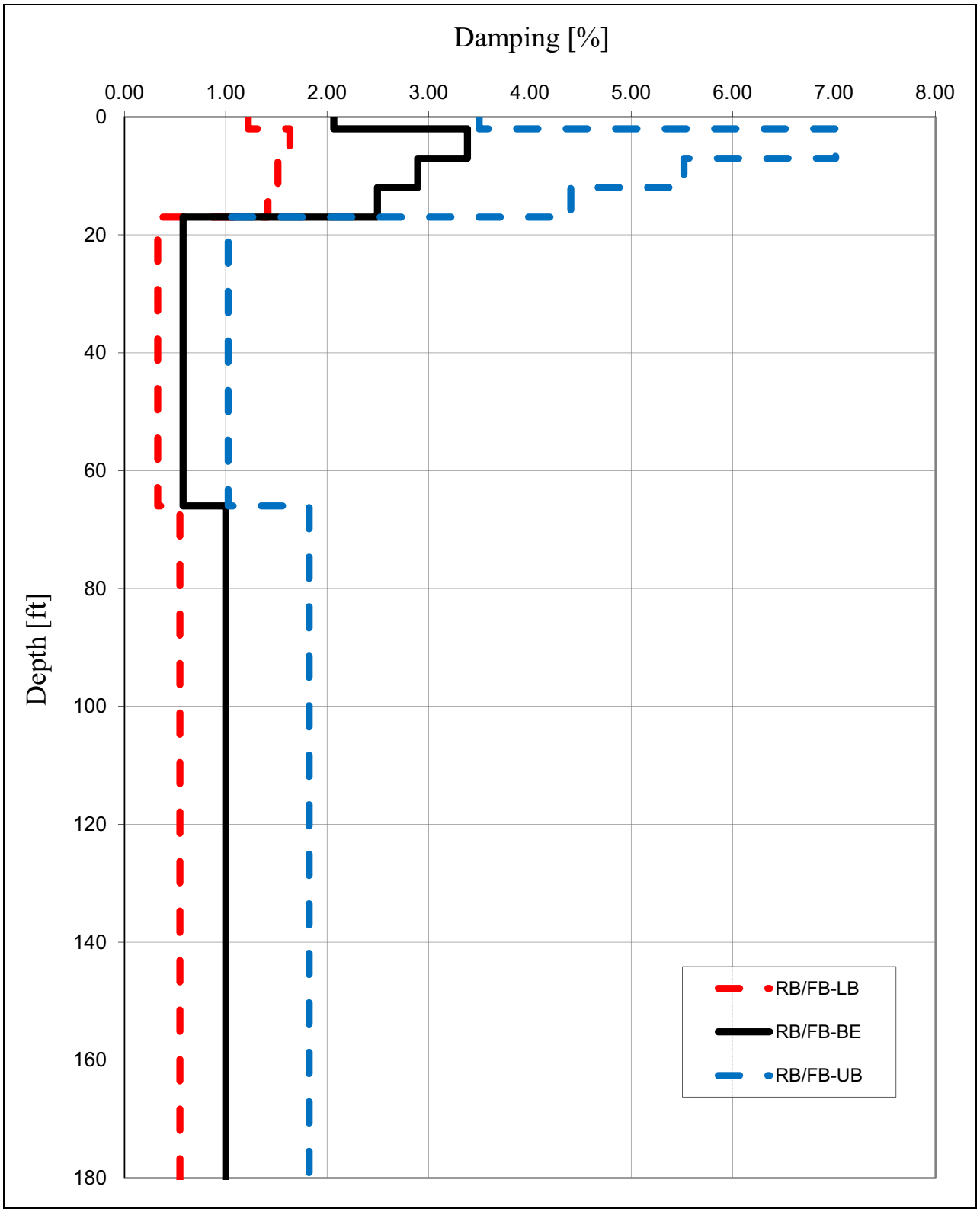

NAPS SUP 3.7-1

Figure 3.7.1-203 SSI Input Strain Compatible P-Wave Velocity Profiles – RB/FB

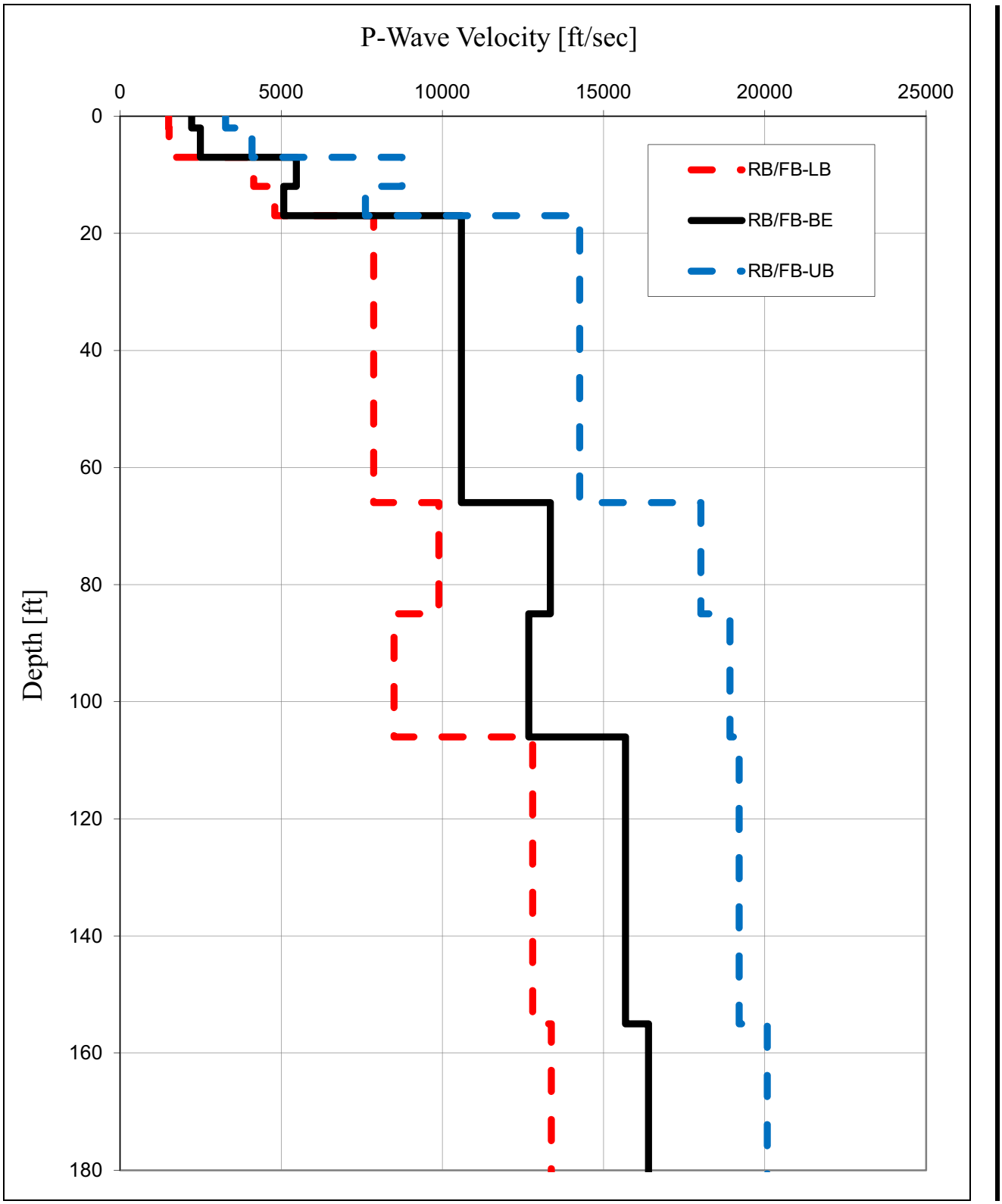

NAPS SUP 3.7-1

Figure 3.7.1-204 SSI Input Strain Compatible Shear-Wave Velocity Profiles – CB

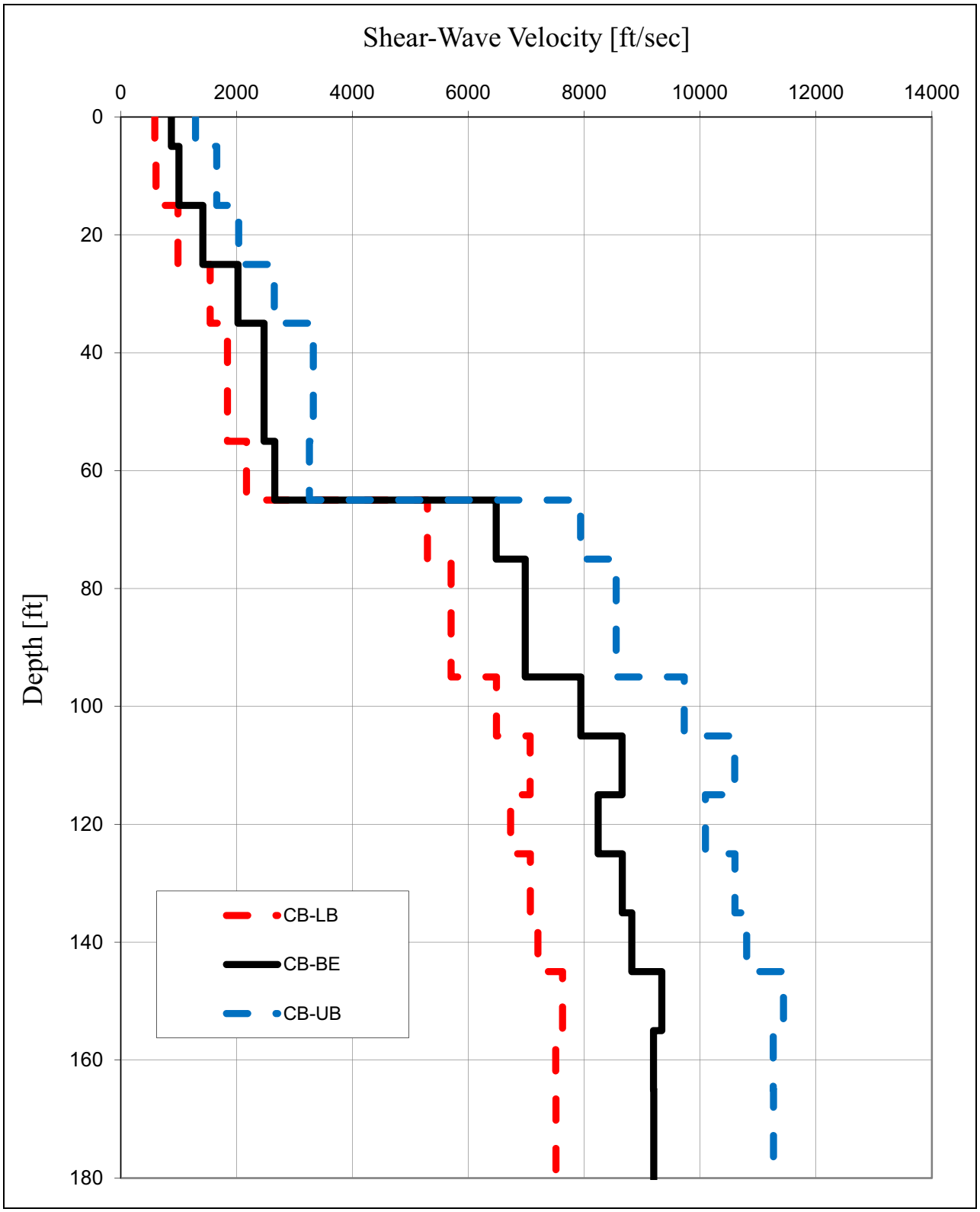

NAPS SUP 3.7-1

Figure 3.7.1-205 SSI Input Strain Compatible ~~Shear Wave~~ Damping Profiles – CB

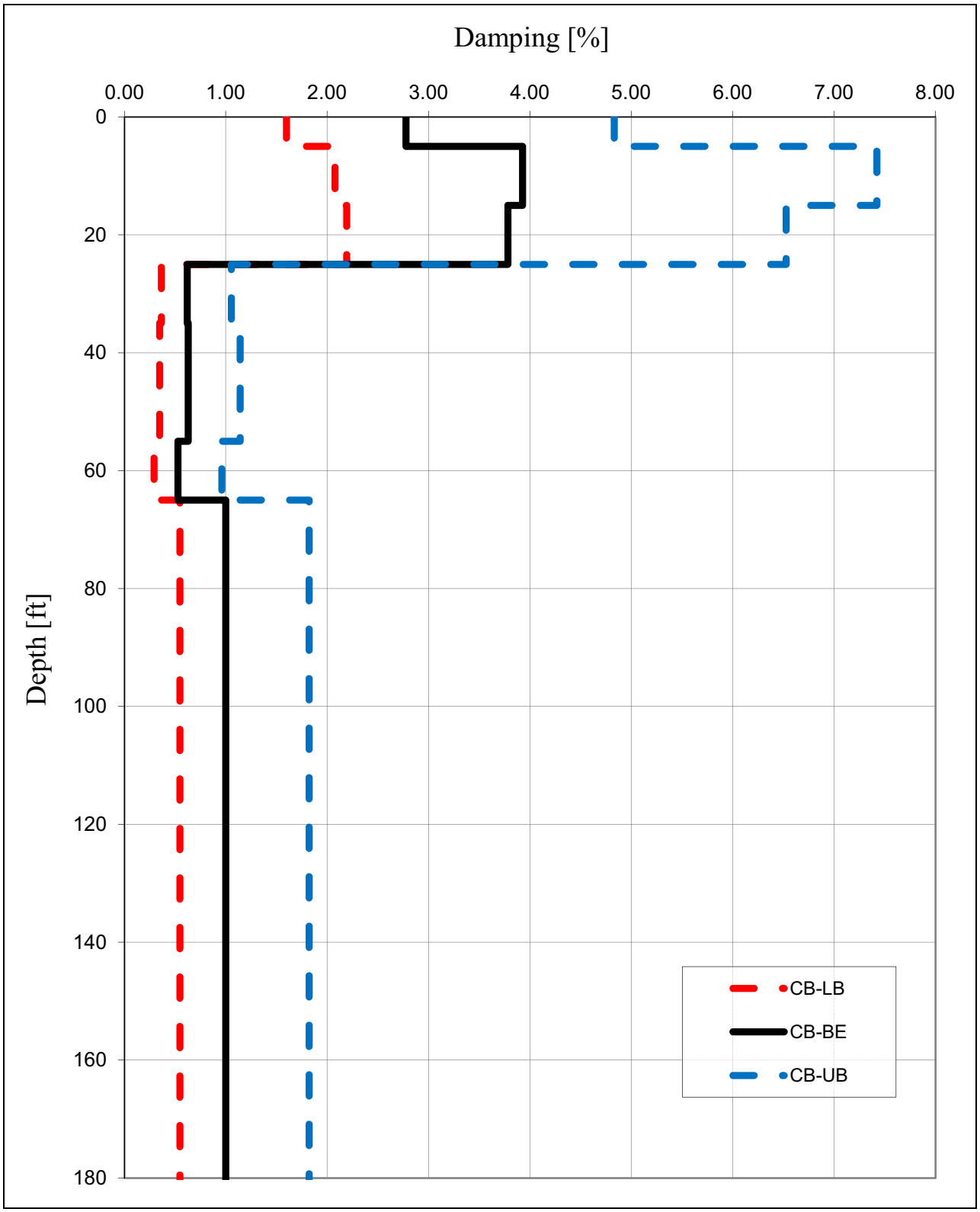

NAPS SUP 3.7-1 **Figure 3.7.1-206 SSI Input Strain Compatible P-Wave Velocity Profiles – CB**

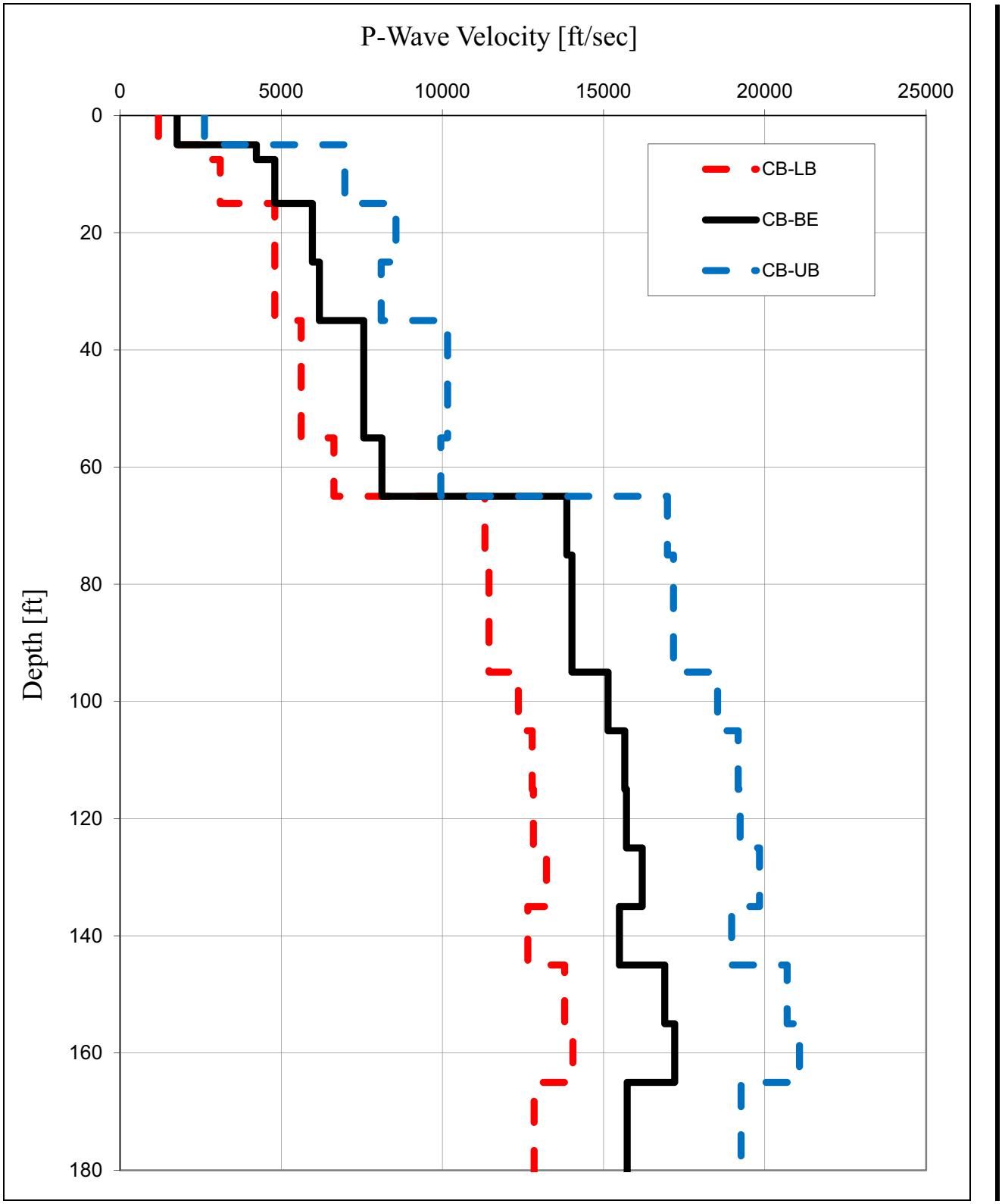

NAPS SUP 3.7-1

Figure 3.7.1-207 SSI Input Strain Compatible Shear-Wave Velocity Profiles – FWSC

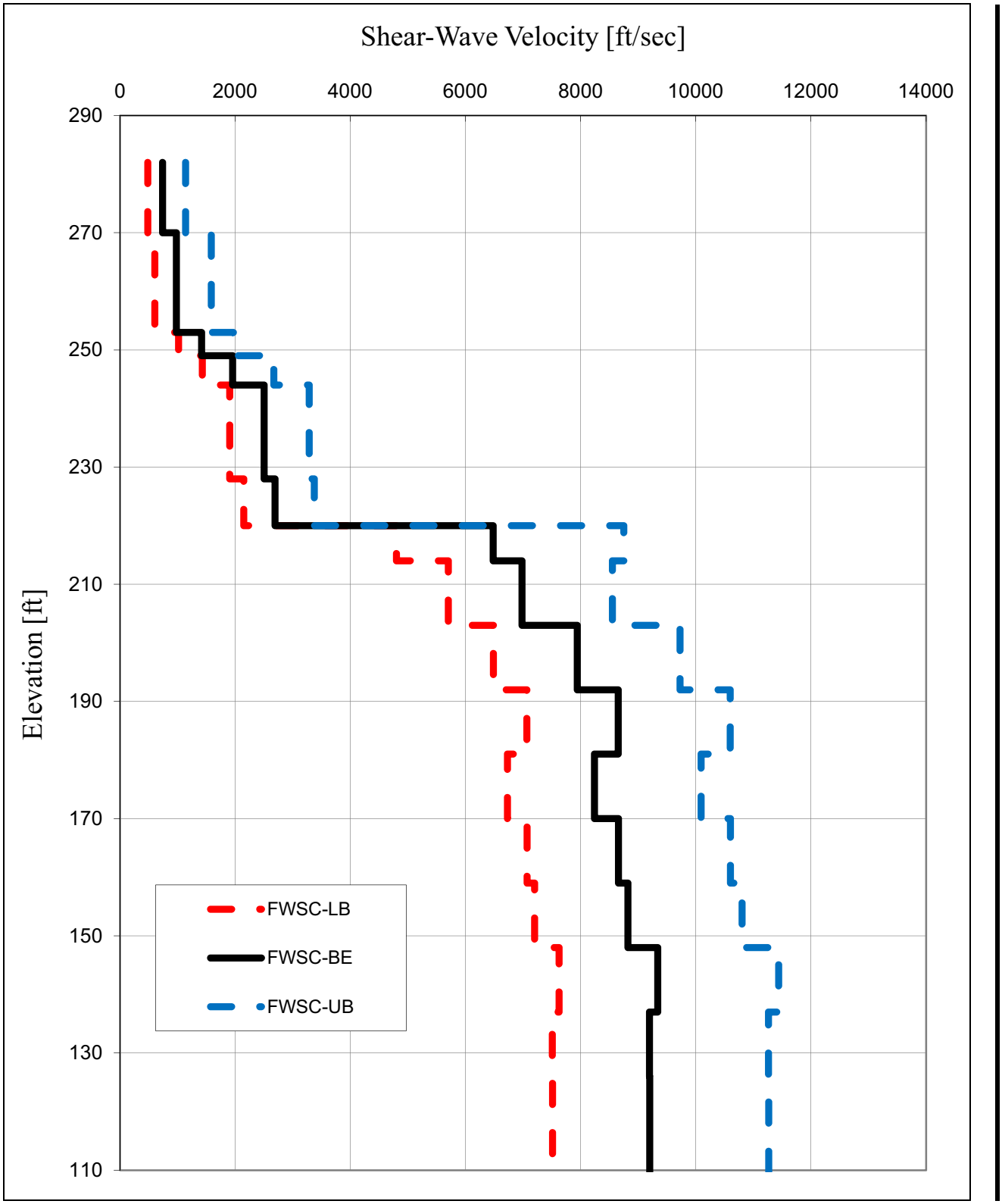

NAPS SUP 3.7-1 **Figure 3.7.1-208 SSI Input Strain Compatible ~~Shear Wave~~ Damping Profiles – FWSC**

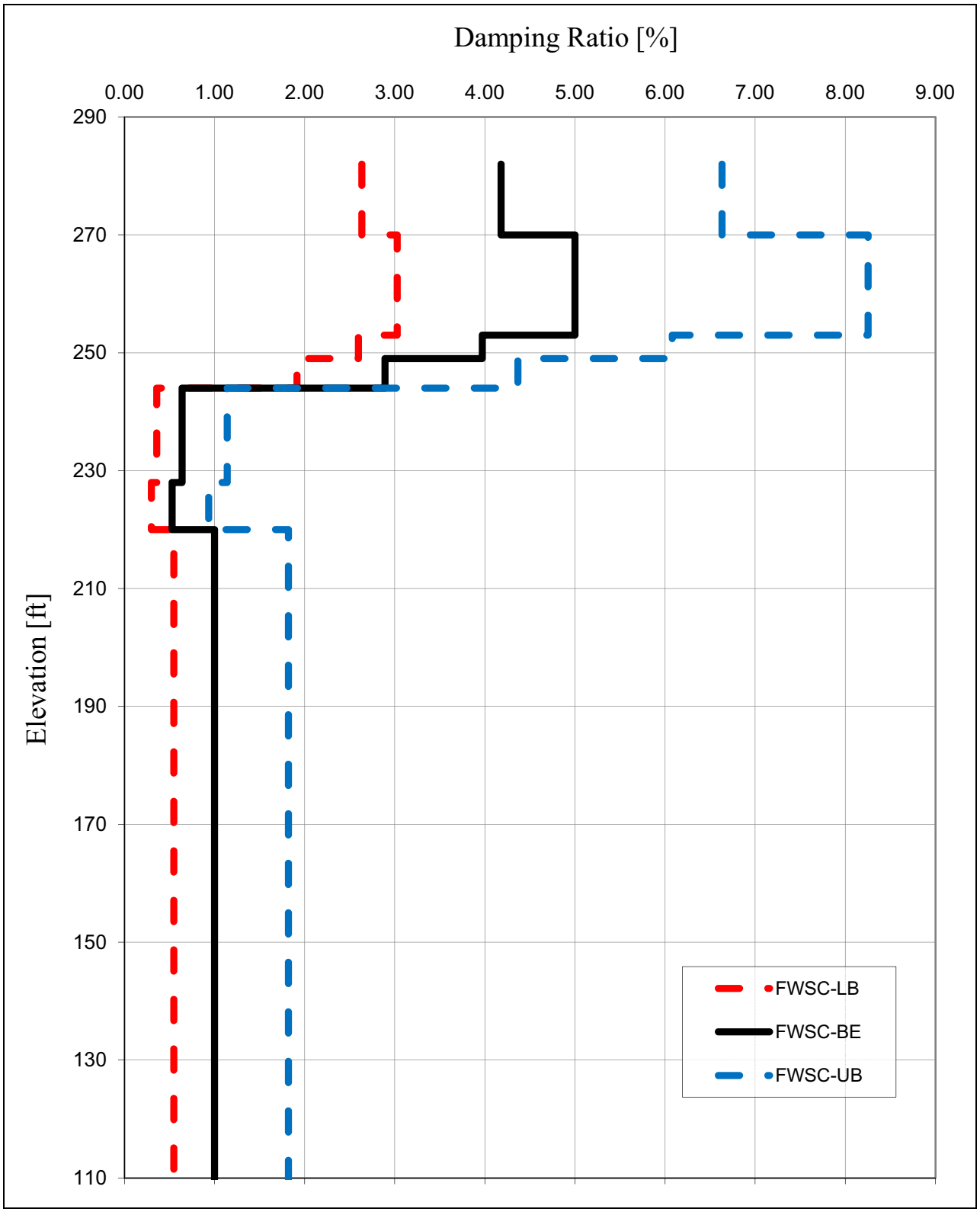

NAPS SUP 3.7-1 **Figure 3.7.1-209 SSI Input Strain Compatible P-Wave Velocity Profiles – FWSC**

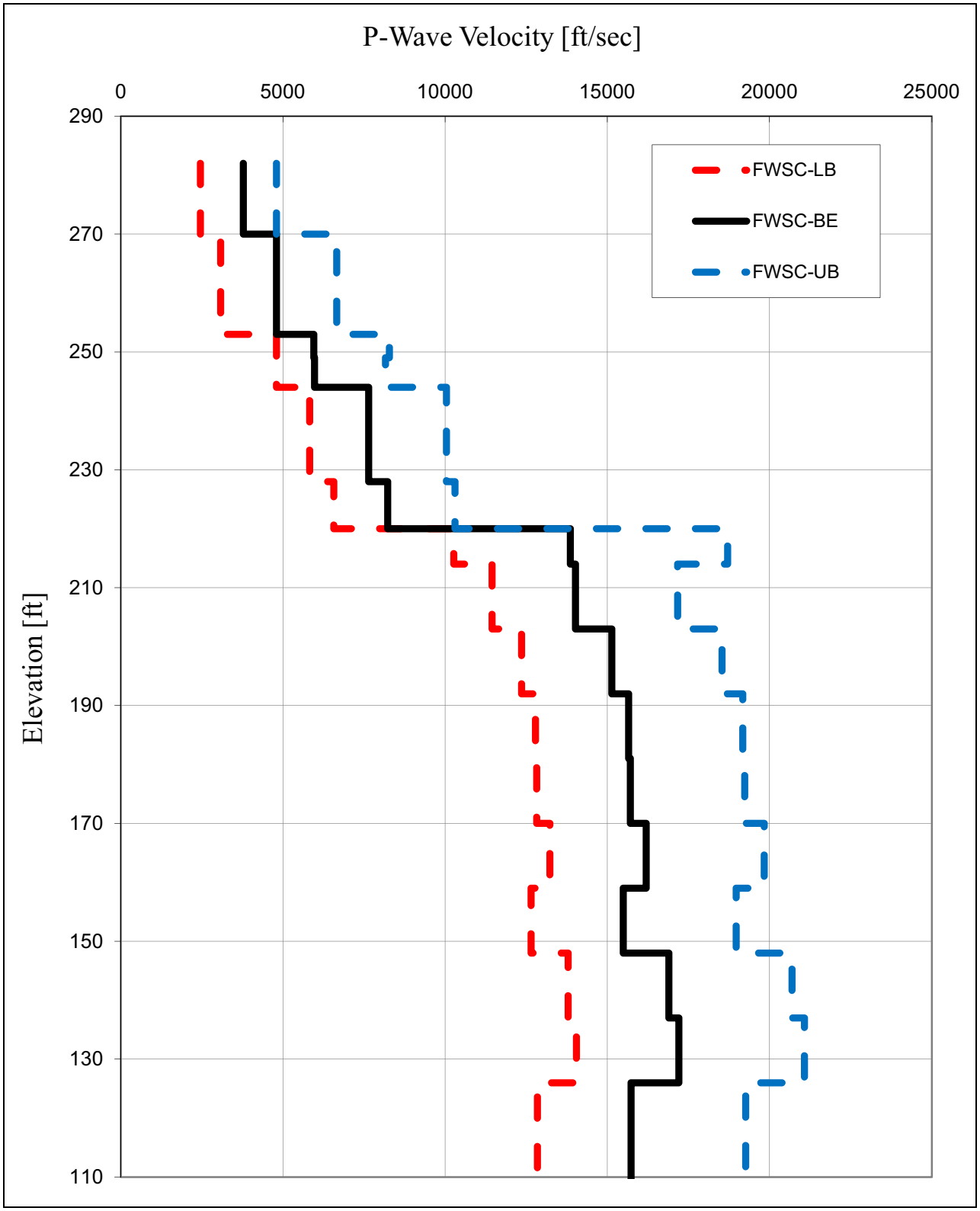

NAPS SUP 3.7-1 **Figure 3.7.1-210 Envelope of Horizontal FIRS Propagated to the Ground Surface through Full Column SSI Input Profiles – RB/FB**

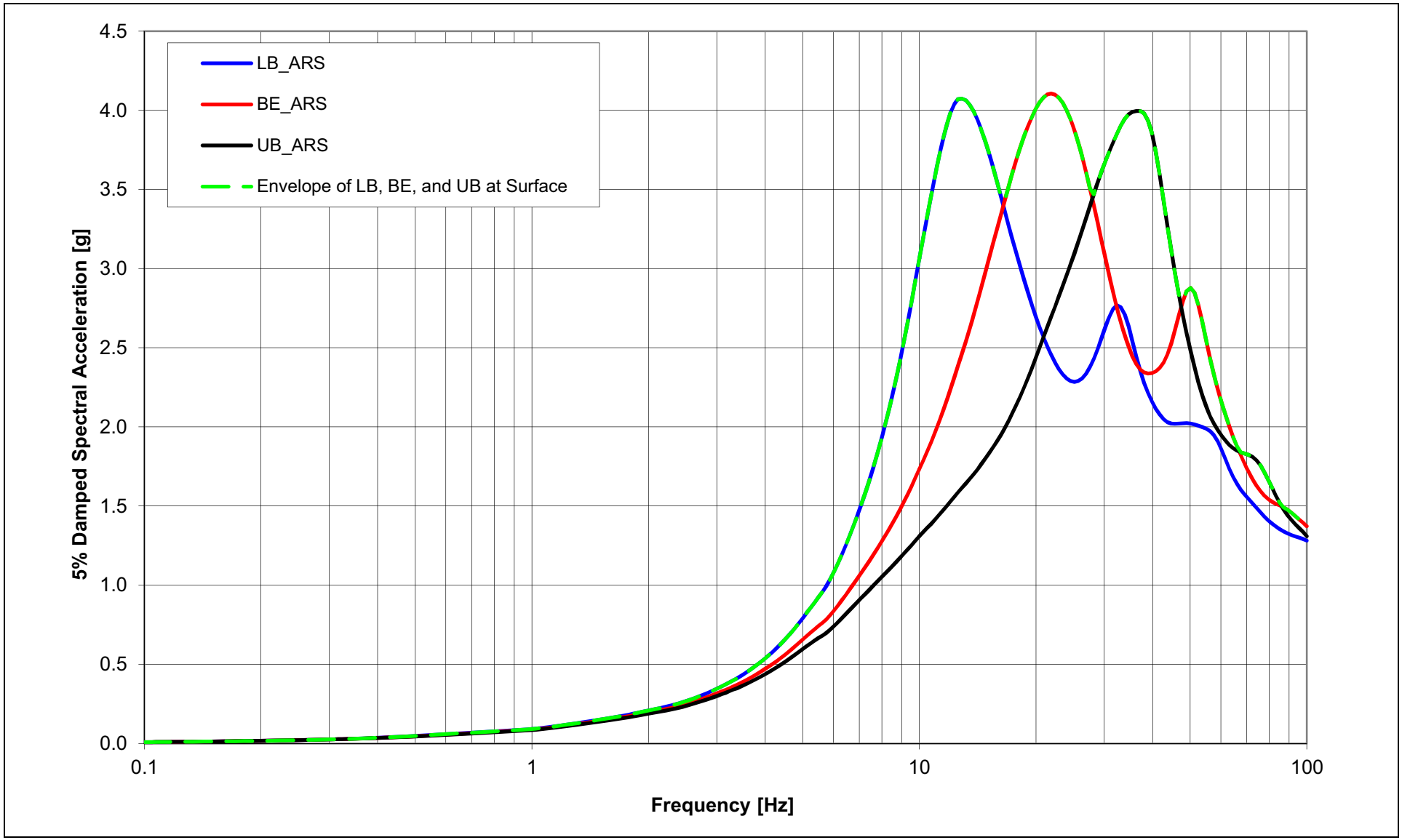

NAPS SUP 3.7-1 **Figure 3.7.1-211 Envelope of Vertical FIRS Propagated to the Ground Surface through Full Column SSI Input Profiles – RB/FB**

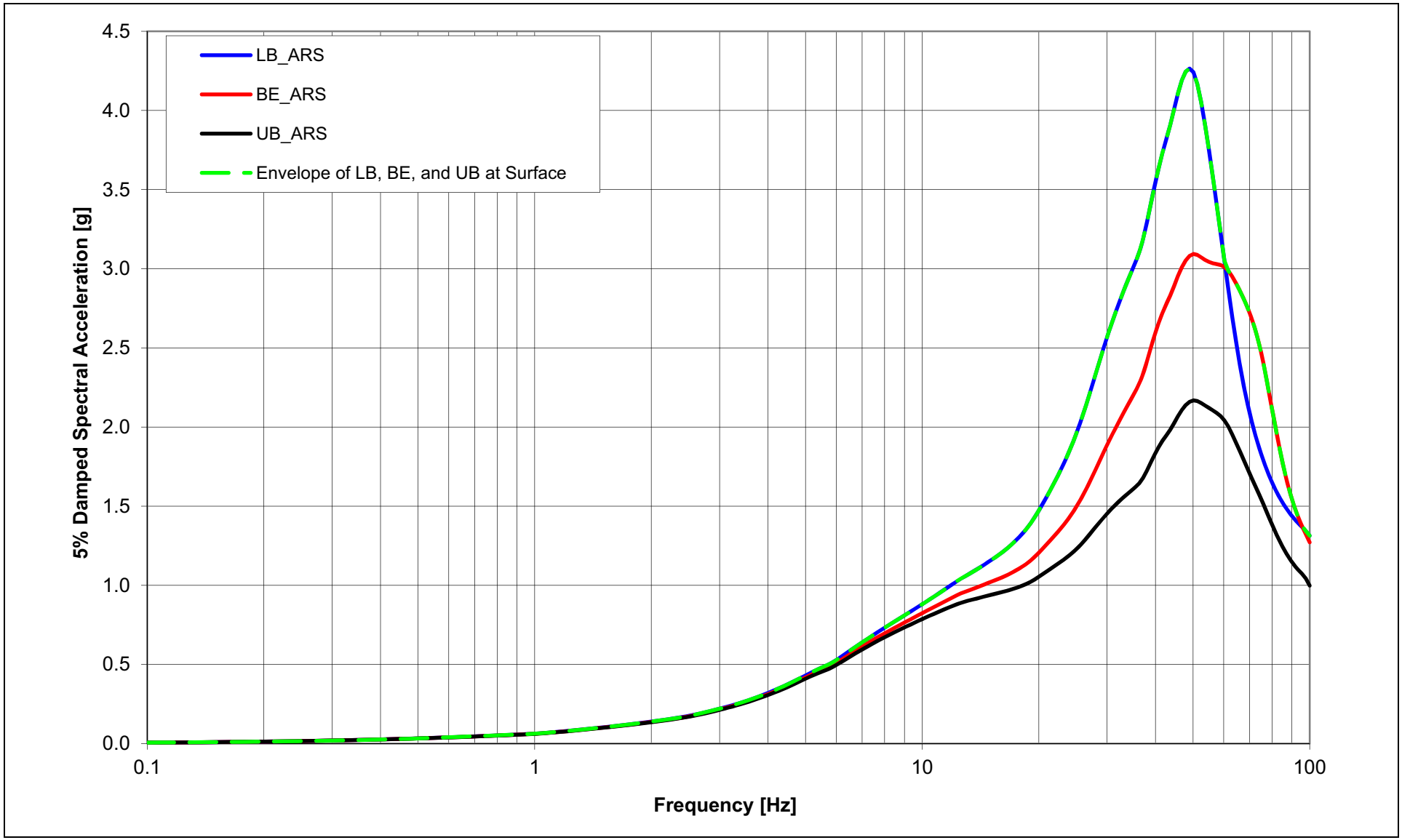

NAPS SUP 3.7-1 **Figure 3.7.1-212 NEI Check and SSI Input Response Spectra for Horizontal Full Column FIRS – RB/FB**

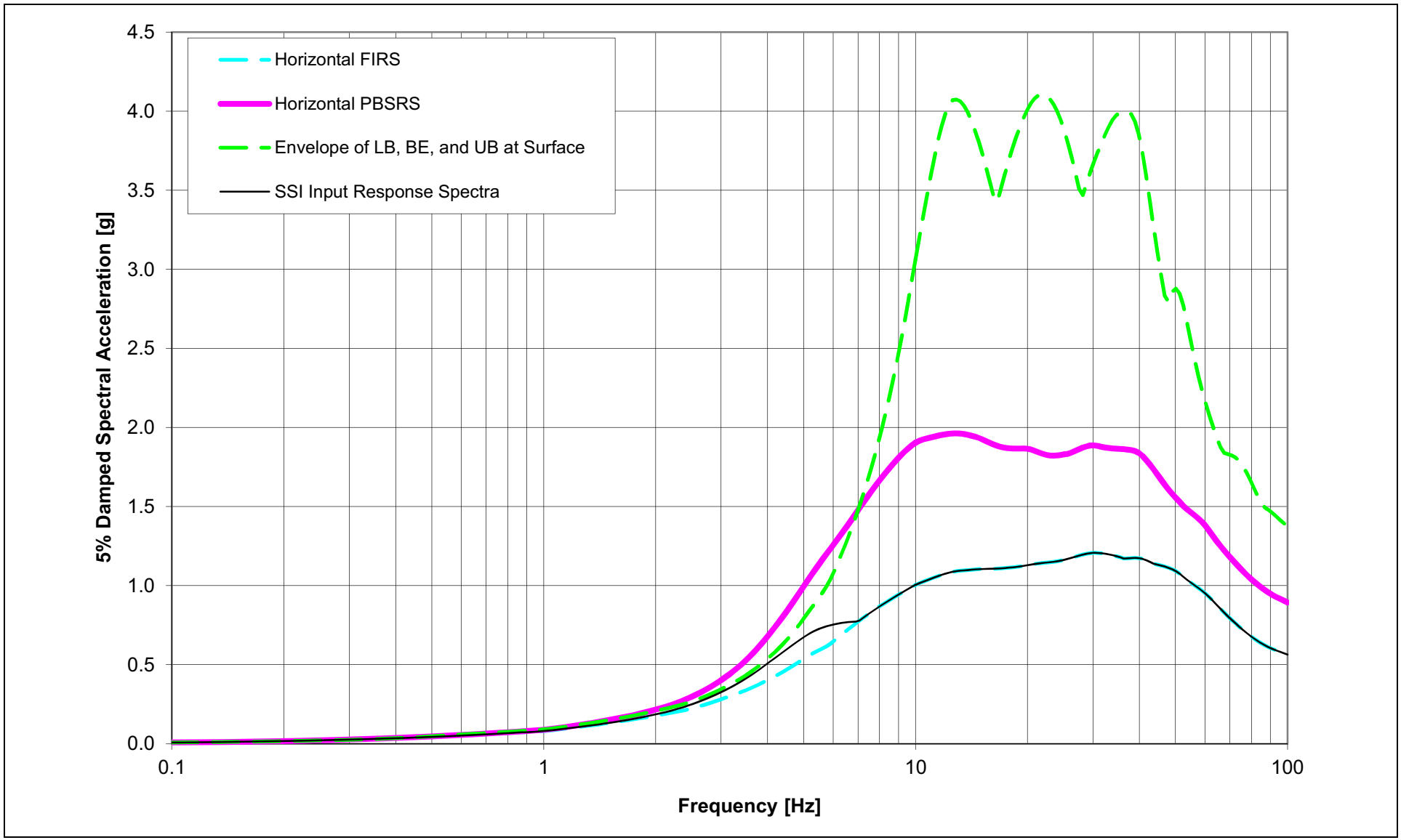

NAPS SUP 3.7-1 **Figure 3.7.1-213 NEI Check and SSI Input Response Spectra for Vertical Full Column FIRS – RB/FB**

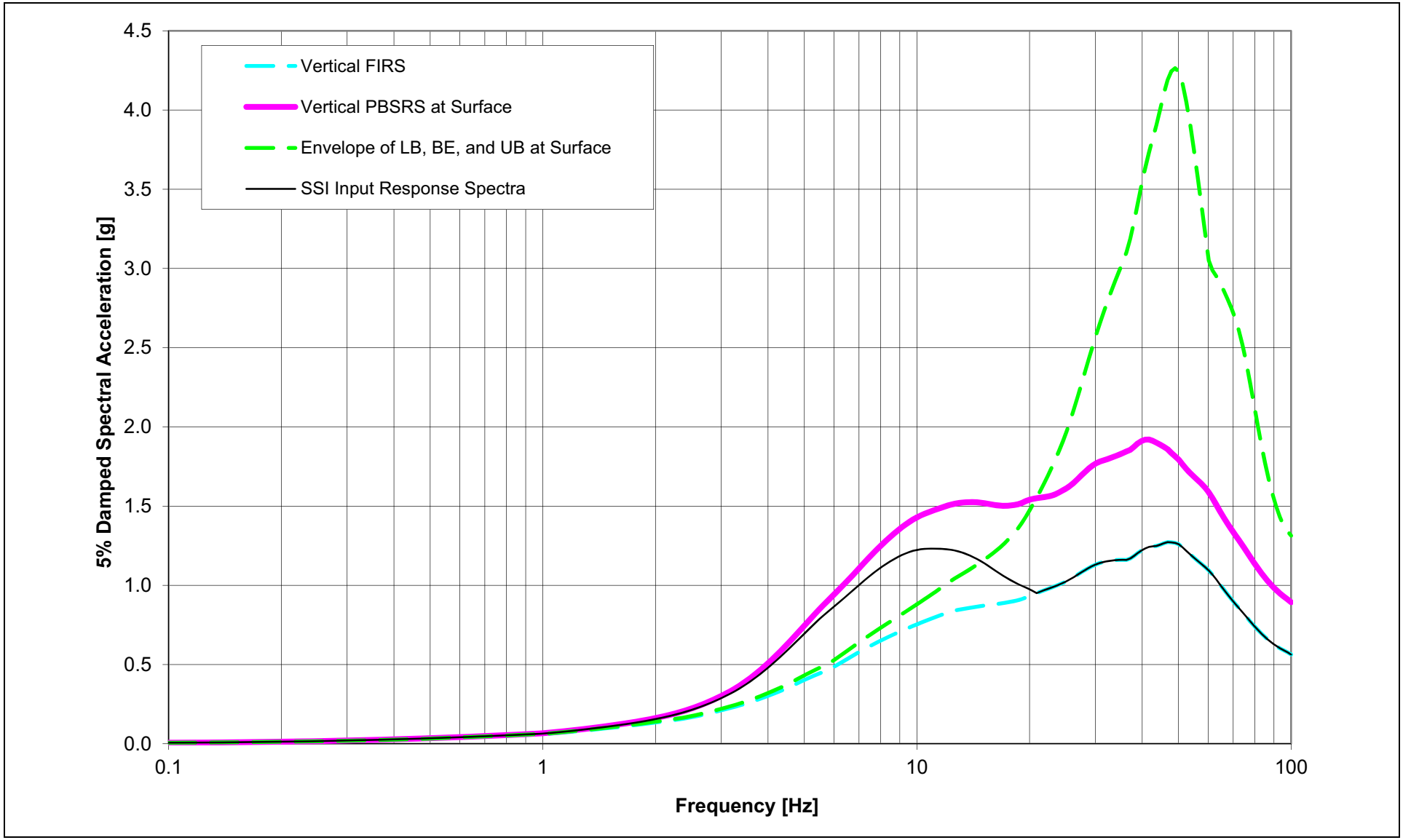

NAPS SUP 3.7-1 **Figure 3.7.1-214 Envelope of Horizontal FIRS Propagated to the Ground Surface through Partial Column SSI Input Profiles – RB/FB**

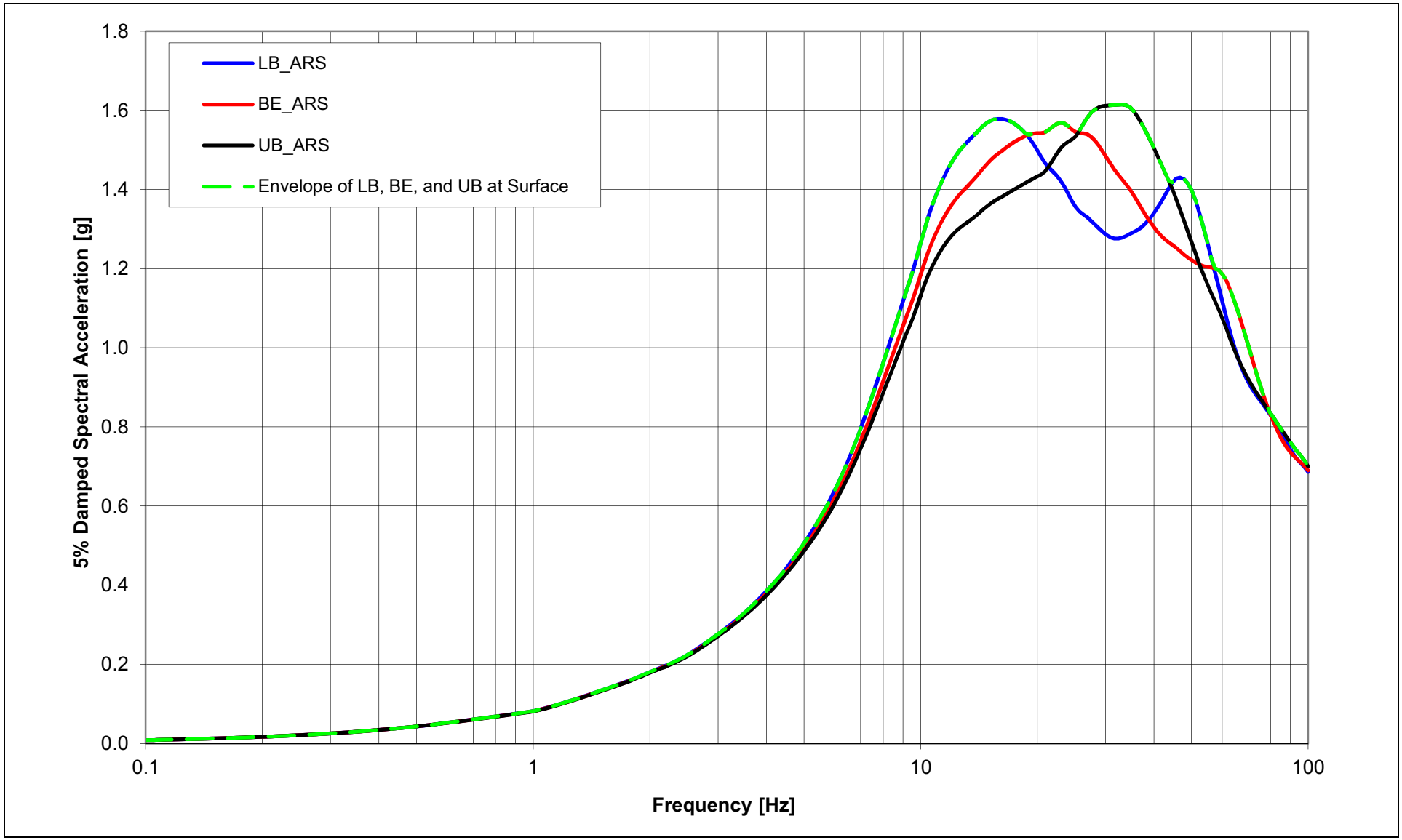

NAPS SUP 3.7-1 **Figure 3.7.1-215 Envelope of Vertical FIRS Propagated to the Ground Surface through Partial Column SSI Input Profiles – RB/FB**

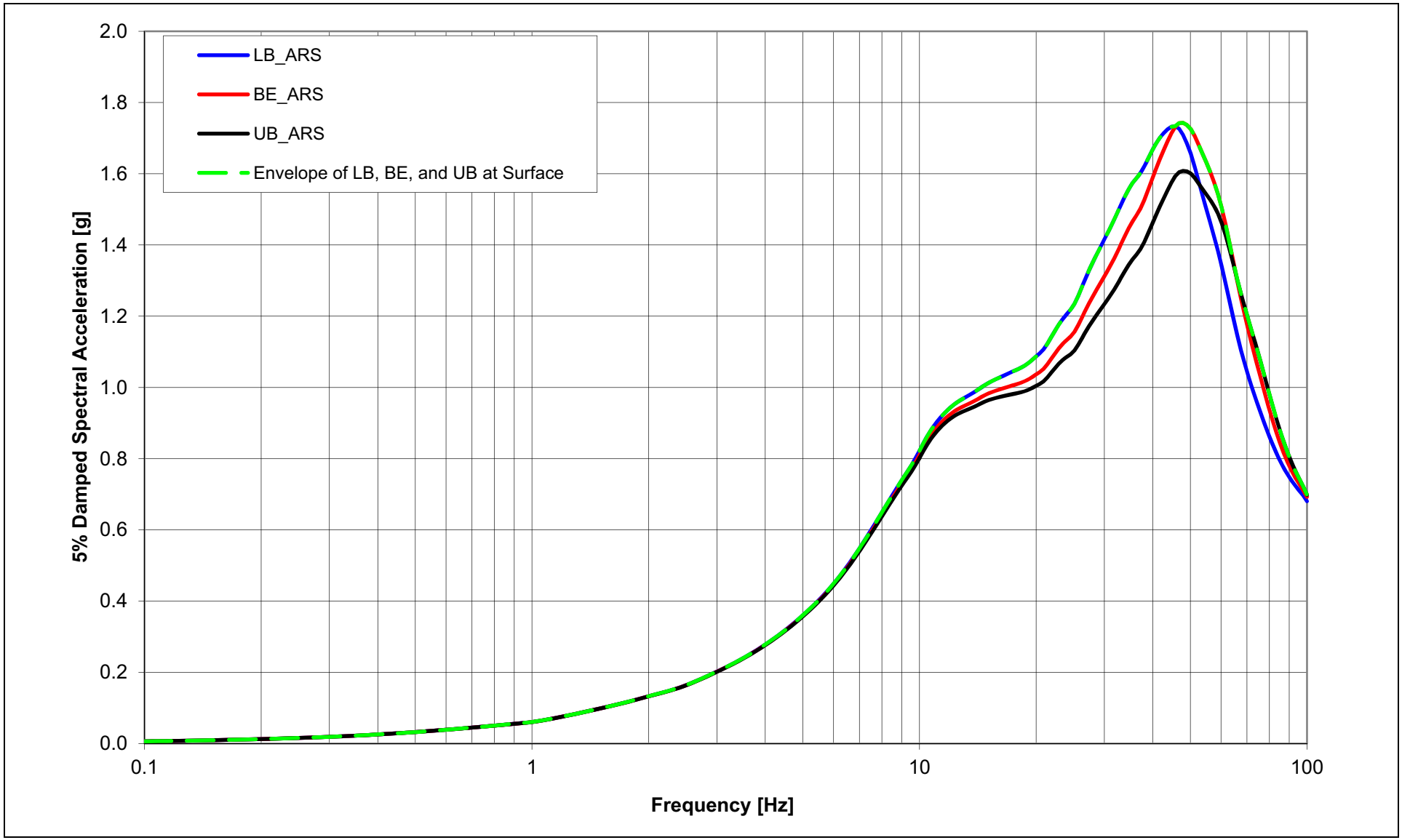

NAPS SUP 3.7-1 **Figure 3.7.1-216 NEI Check and SSI Input Response Spectra for Horizontal Partial Column FIRS – RB/FB**

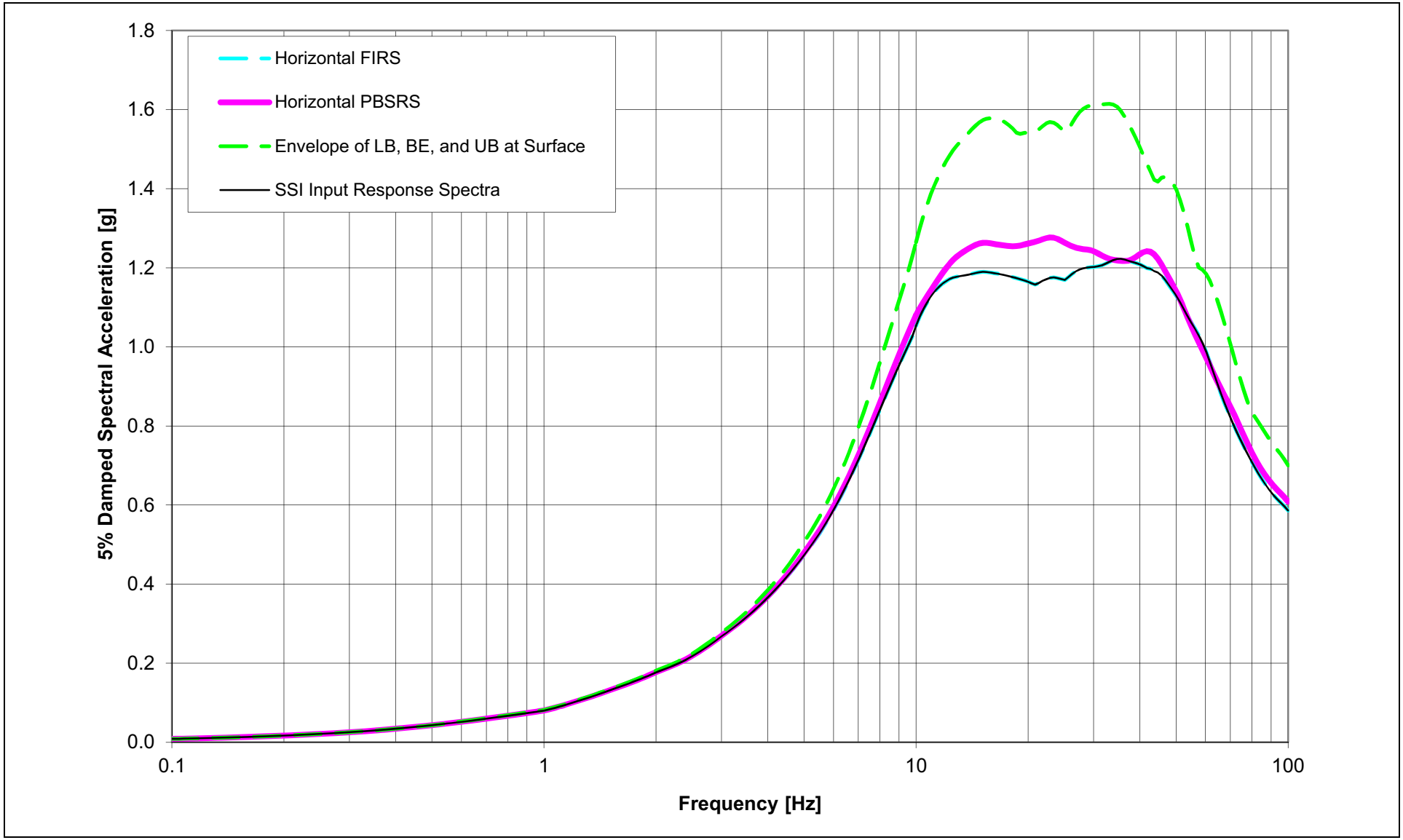

NAPS SUP 3.7-1 **Figure 3.7.1-217 NEI Check and SSI Input Response Spectra for Vertical Partial Column FIRS – RB/FB**

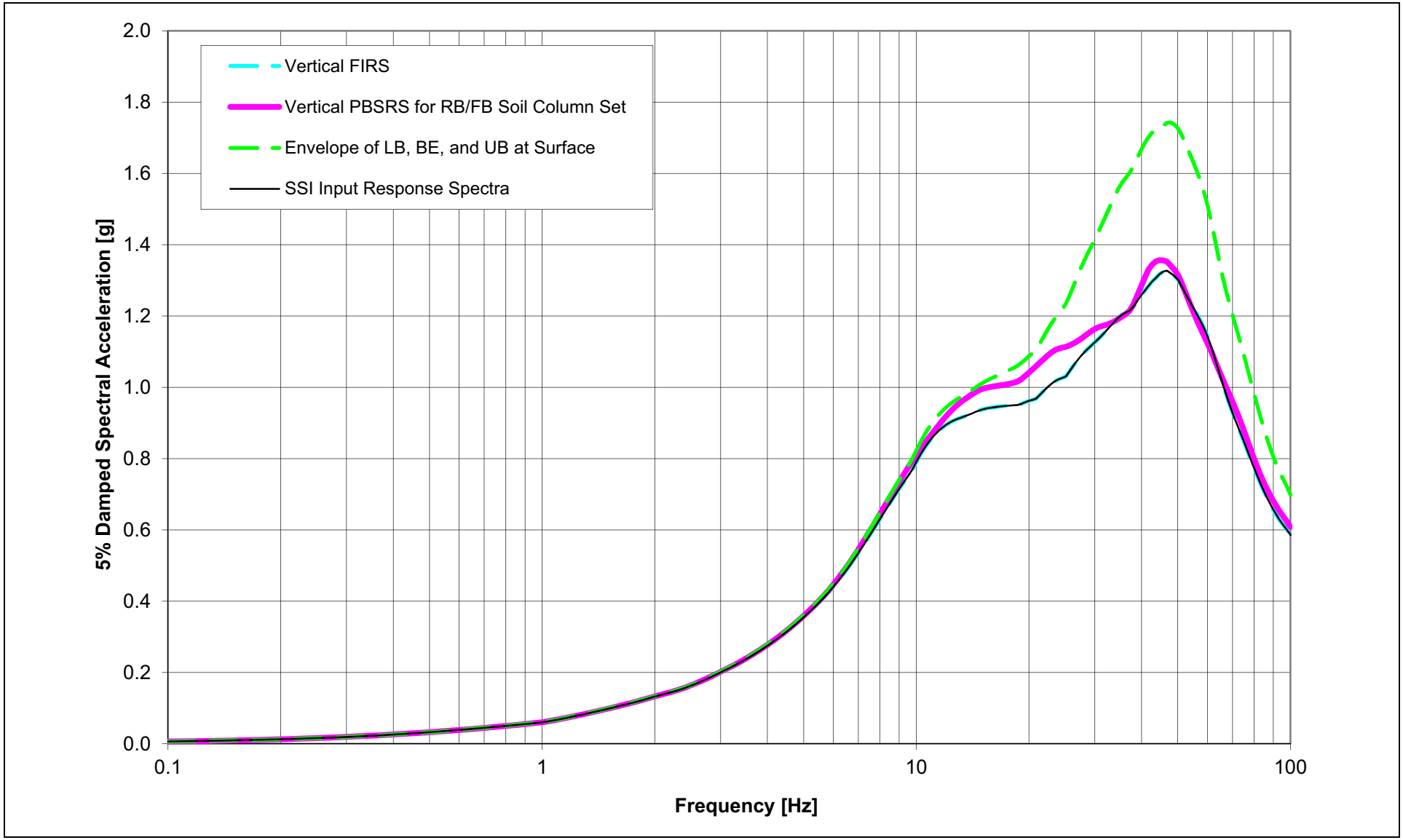

NAPS SUP 3.7-1 **Figure 3.7.1-218 Development of 5% Damped Final Horizontal SSI Input Response Spectra for RB/FB**

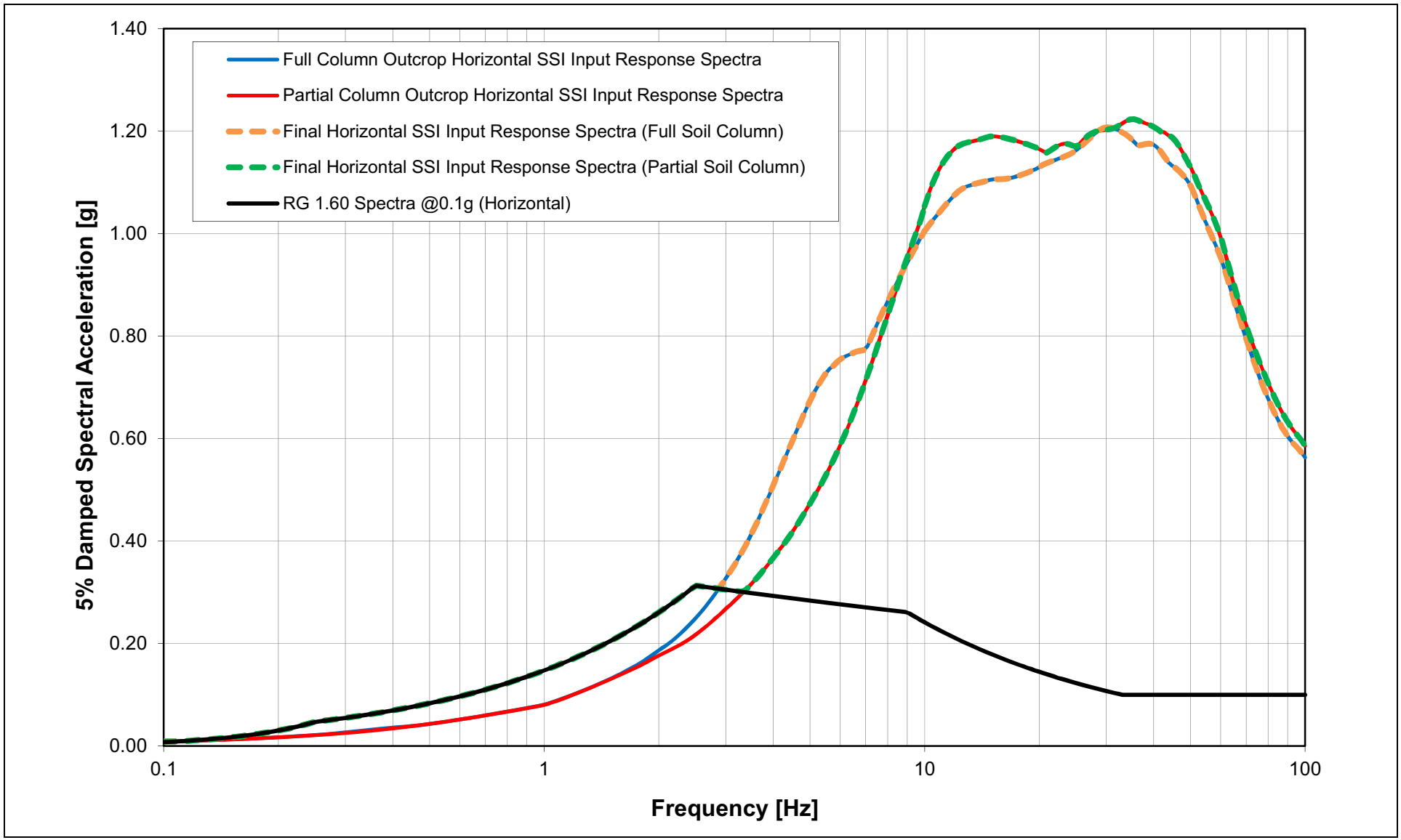

NAPS SUP 3.7-1 **Figure 3.7.1-219 Development of 5% Damped Final Vertical SSI Input Response Spectra for RB/FB**

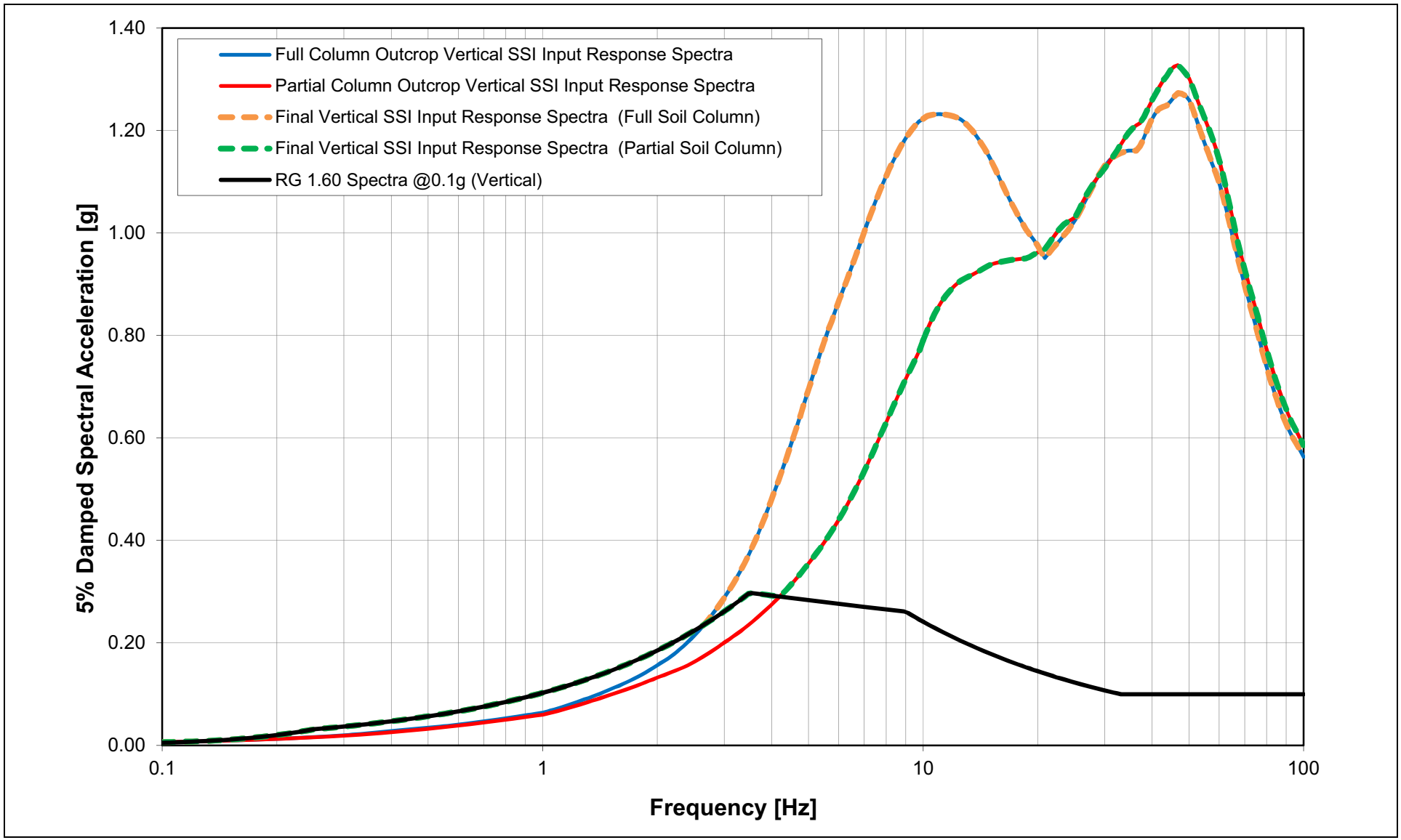

NAPS SUP 3.7-1 **Figure 3.7.1-220 5% Damped Final SSI Input Response Spectra for RB/FB**

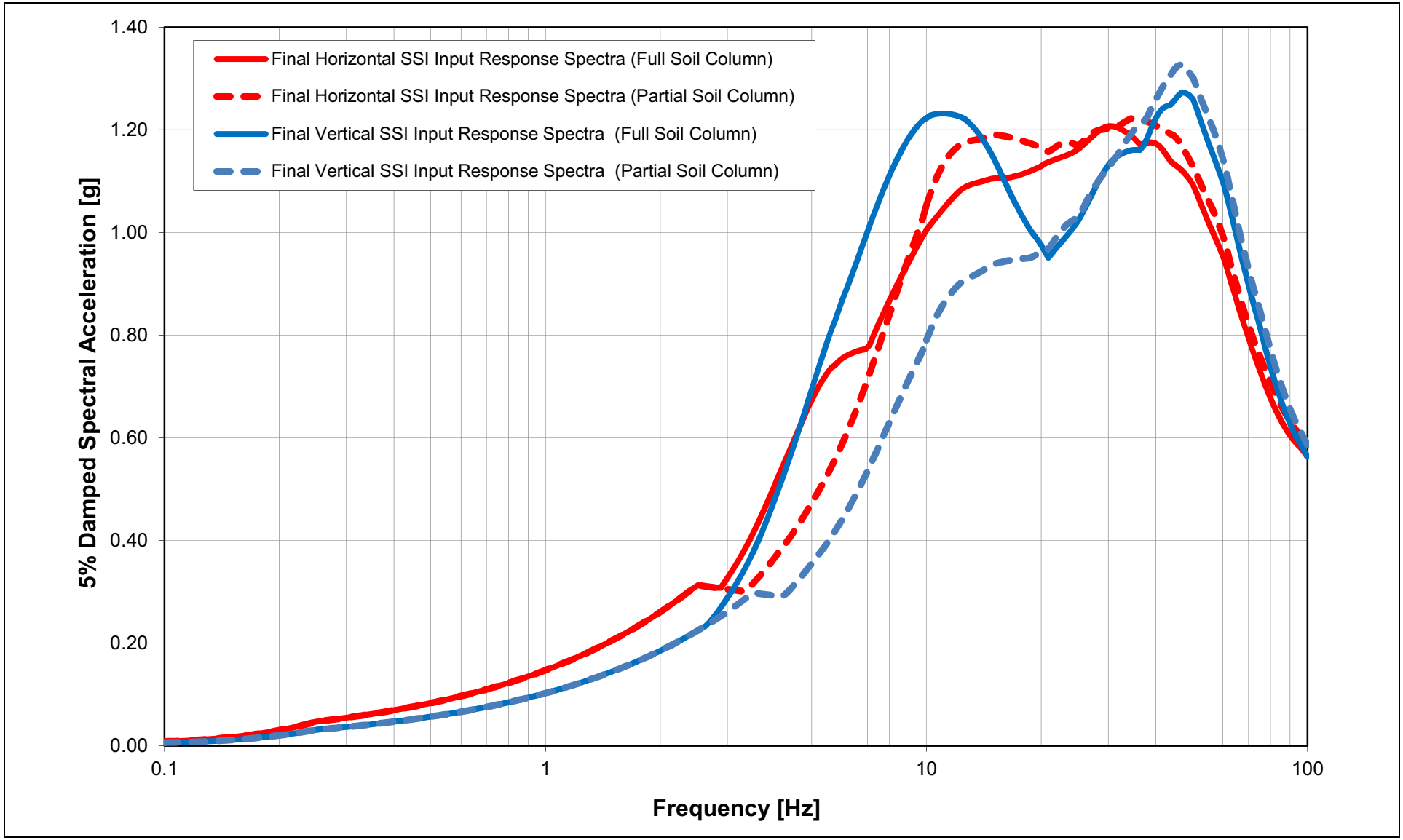

NAPS SUP 3.7-1 **Figure 3.7.1-221 Envelope of Horizontal FIRS Propagated to the Ground Surface through Full Column SSI Input Profiles – CB**

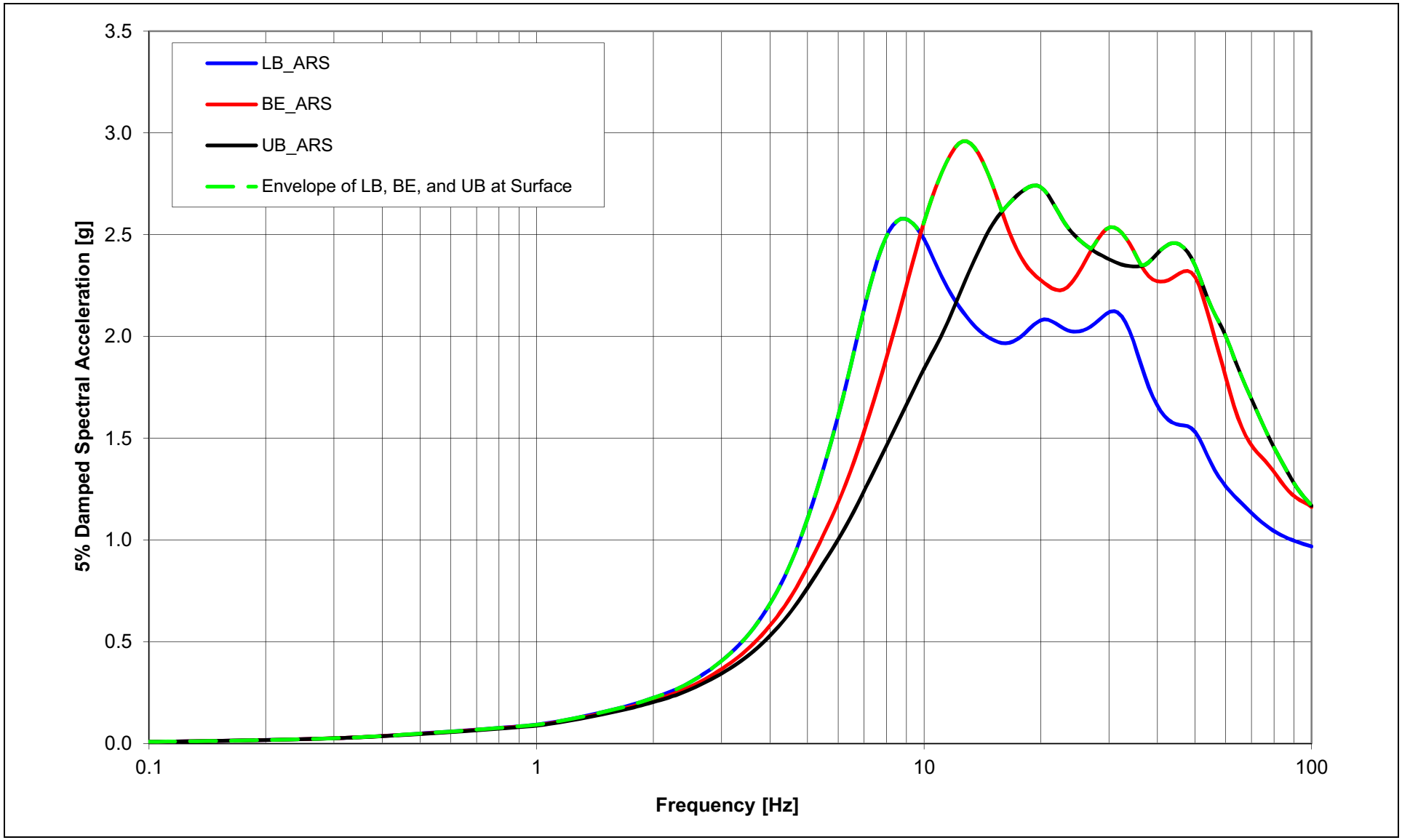

NAPS SUP 3.7-1 **Figure 3.7.1-222 Envelope of Vertical FIRS Propagated to the Ground Surface through Full Column SSI Input Profiles – CB**

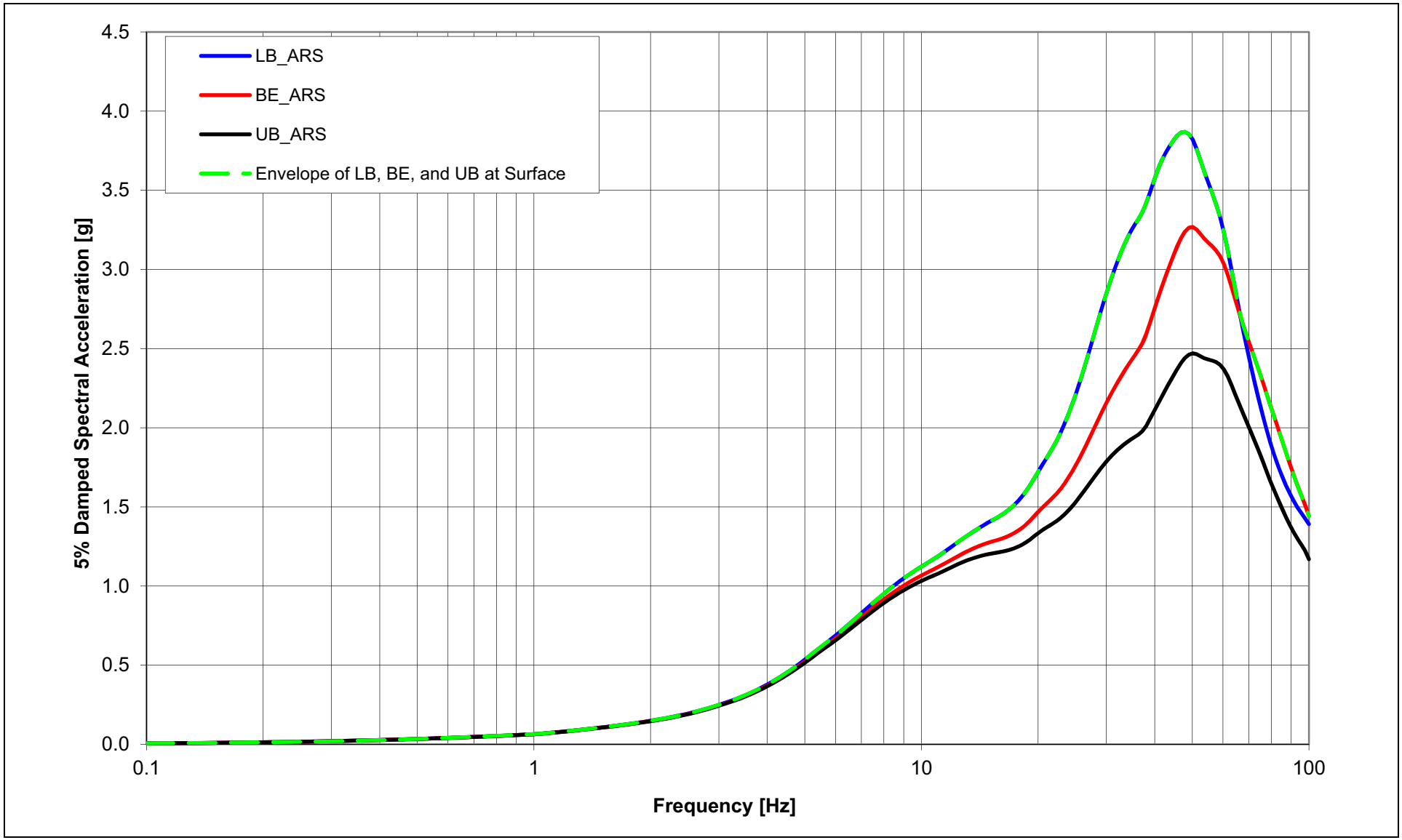

NAPS SUP 3.7-1 **Figure 3.7.1-223 NEI Check and SSI Input Response Spectra for Horizontal Full Column FIRS – CB**

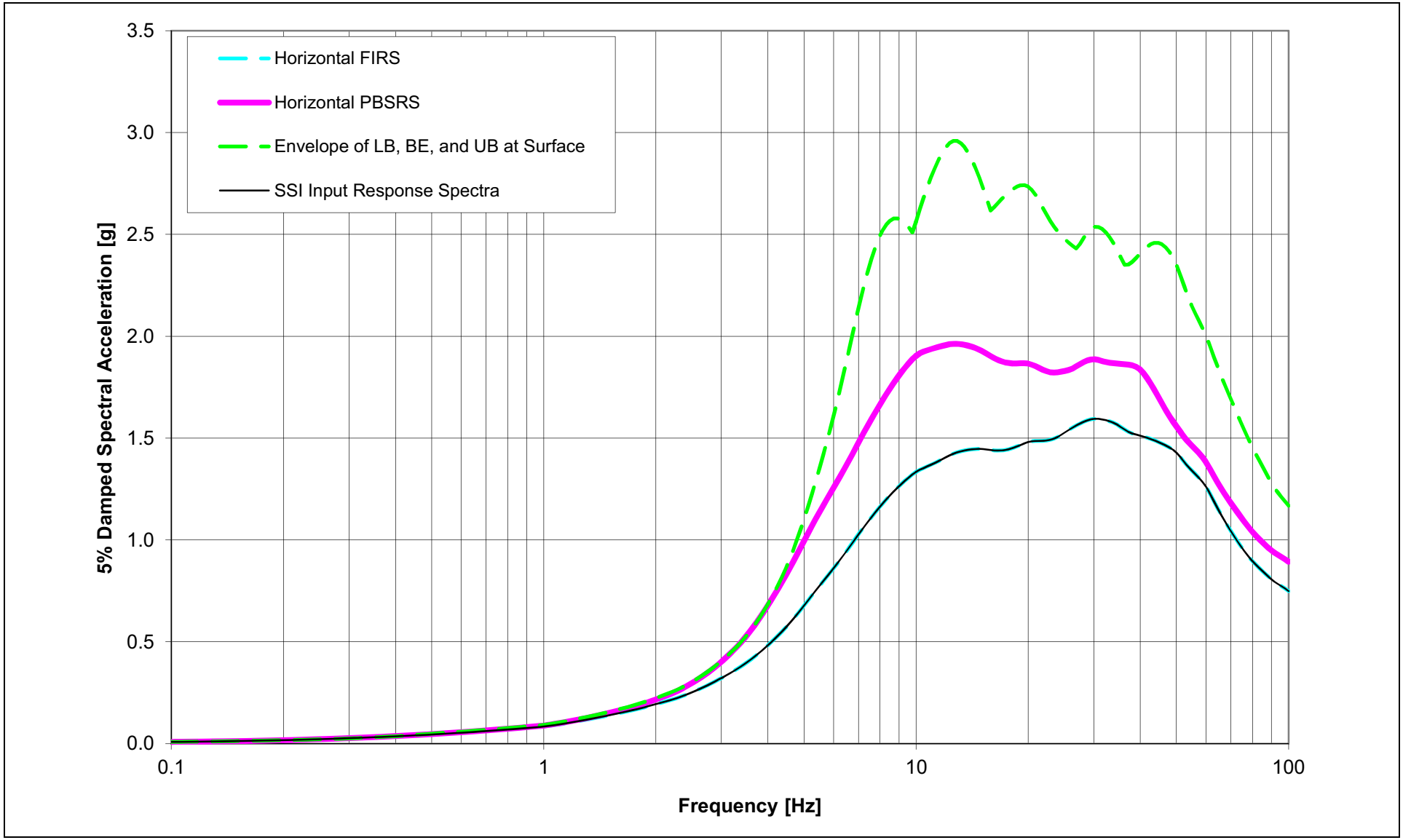

NAPS SUP 3.7-1 **Figure 3.7.1-224 NEI Check and SSI Input Response Spectra for Vertical Full Column FIRS – CB**

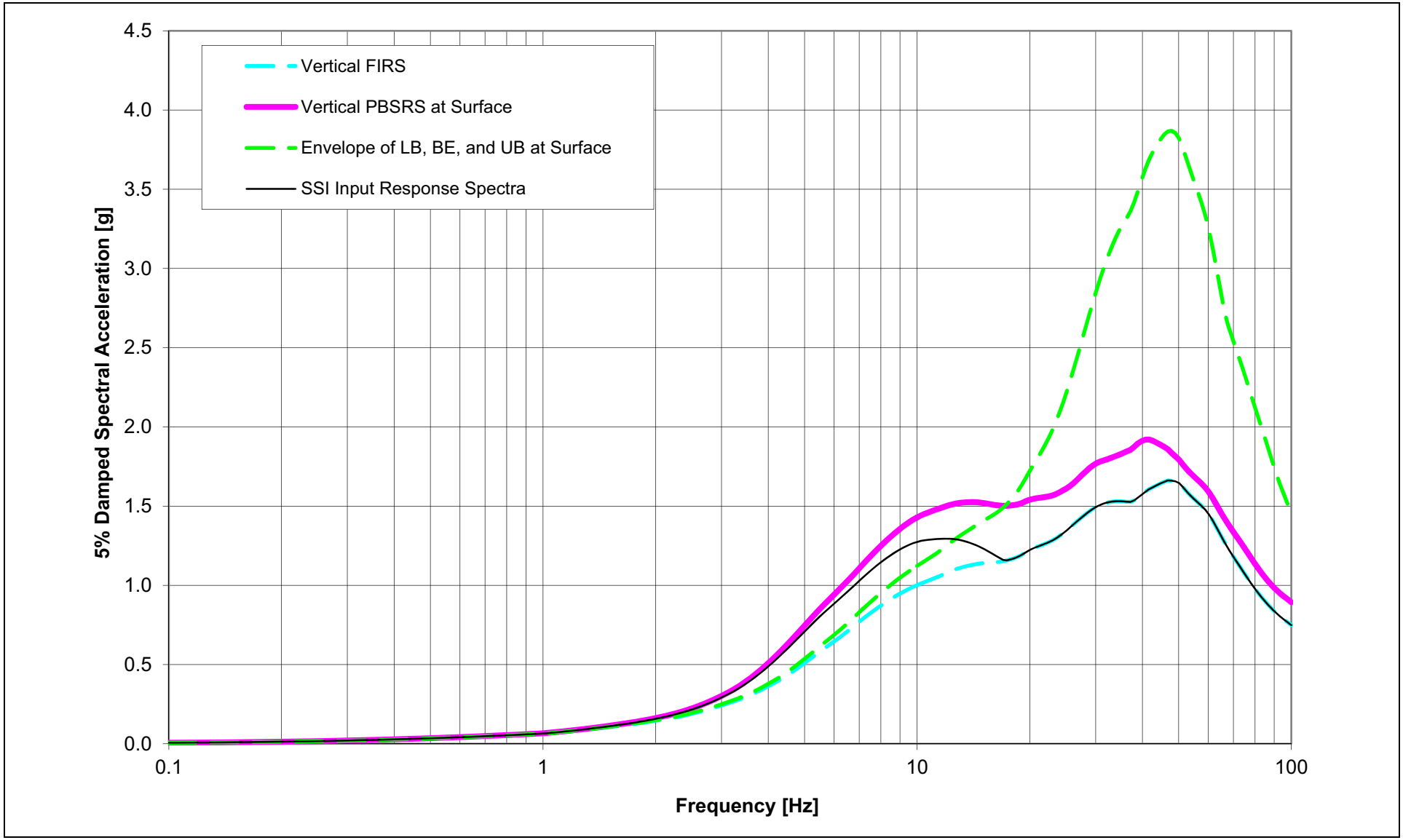

NAPS SUP 3.7-1 **Figure 3.7.1-225 Envelope of Horizontal FIRS Propagated to the Ground Surface through Partial Column SSI Input Profiles – CB**

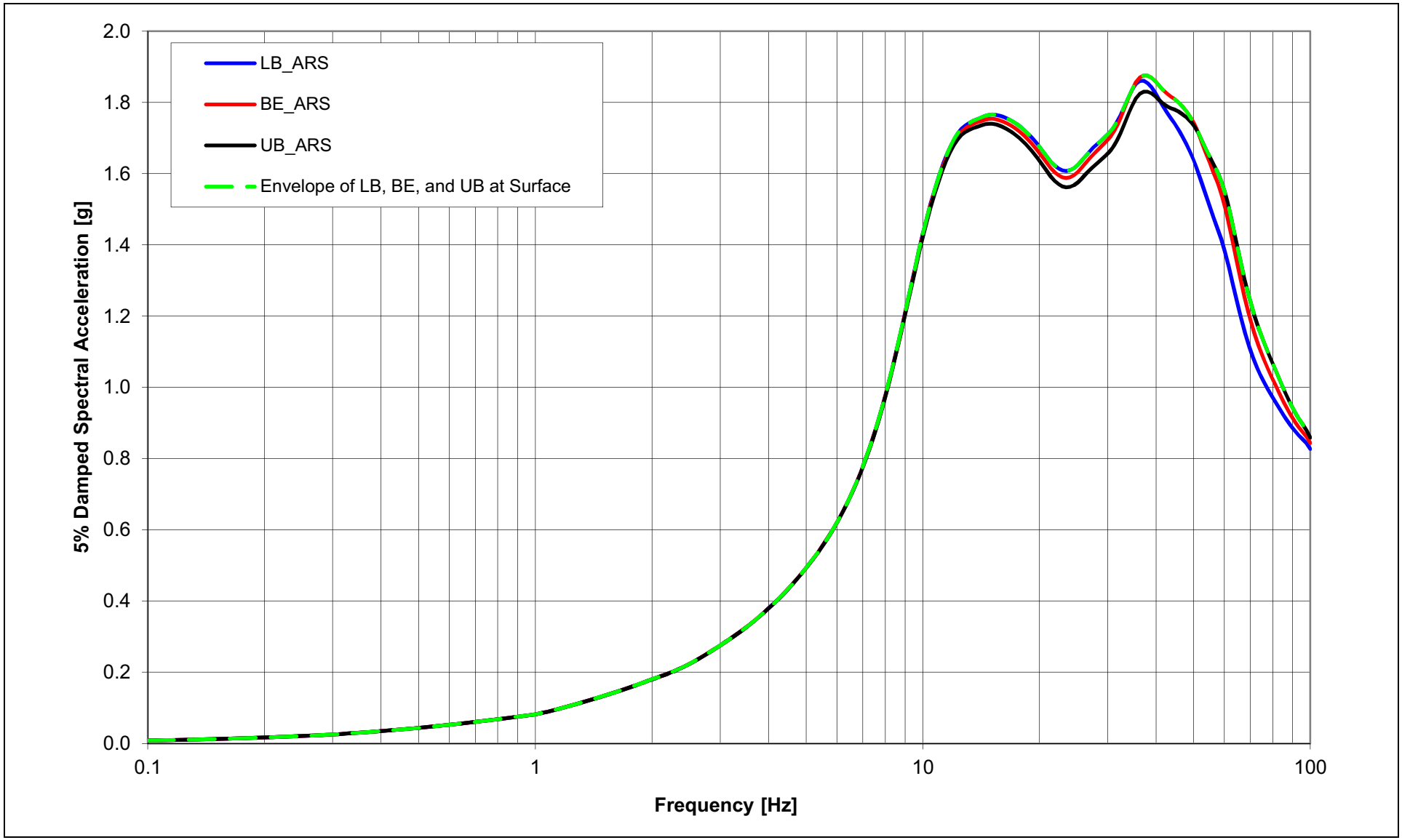

NAPS SUP 3.7-1 **Figure 3.7.1-226 Envelope of Vertical FIRS Propagated to the Ground Surface through Partial Column SSI Input Profiles – CB**

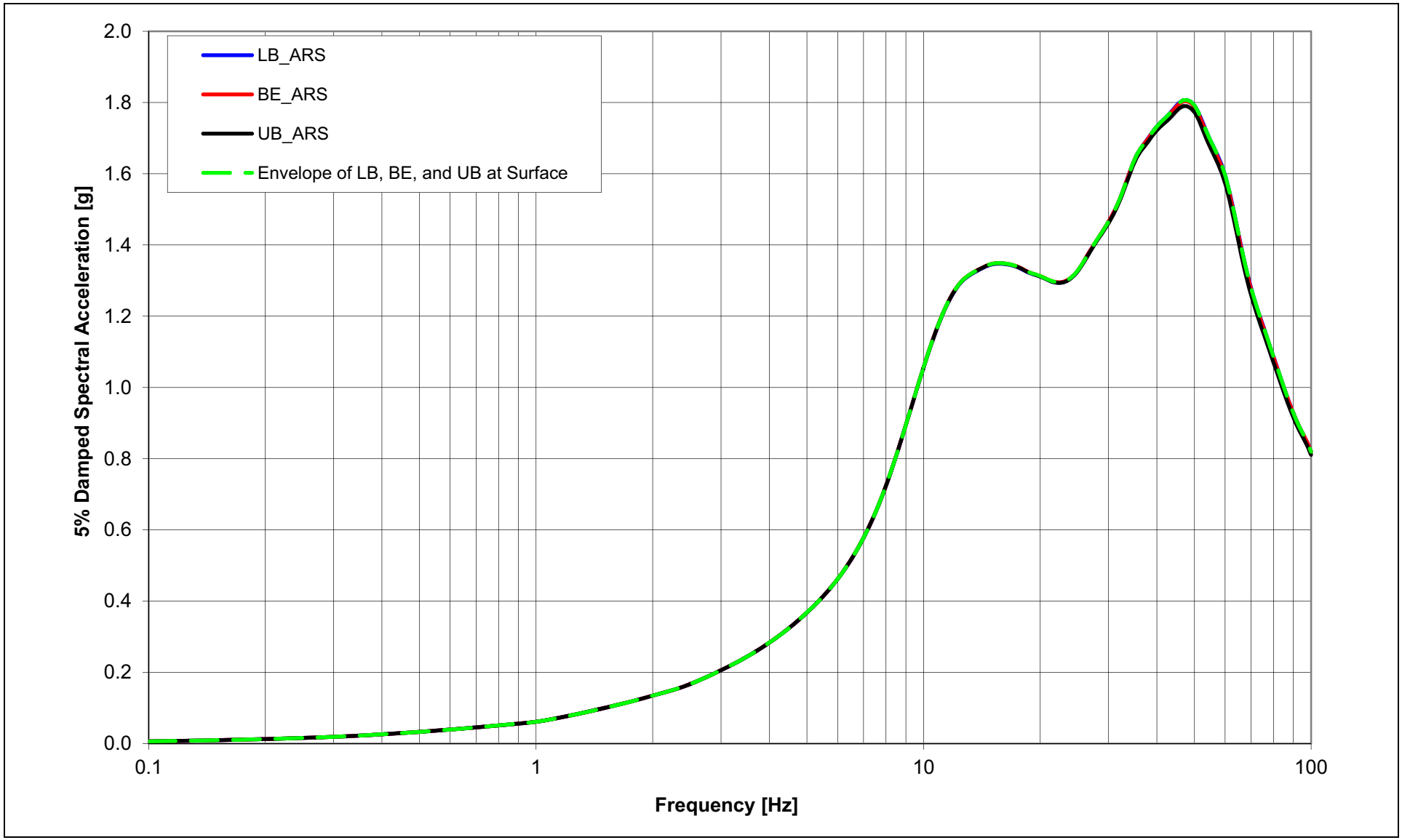

NAPS SUP 3.7-1 **Figure 3.7.1-227 NEI Check and SSI Input Response Spectra for Horizontal Partial Column FIRS – CB**

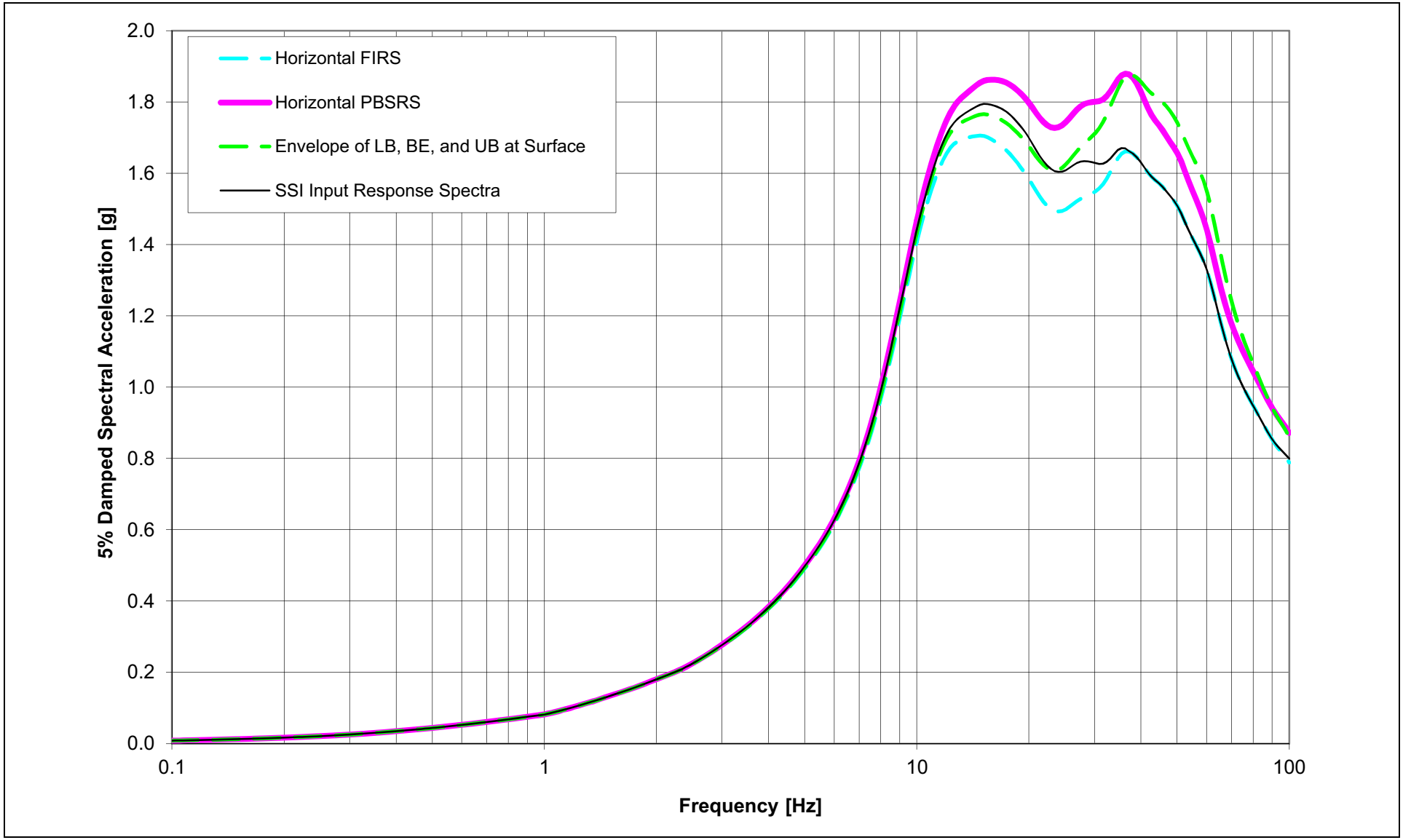

NAPS SUP 3.7-1 **Figure 3.7.1-228 NEI Check and SSI Input Response Spectra for Vertical Partial Column FIRS – CB**

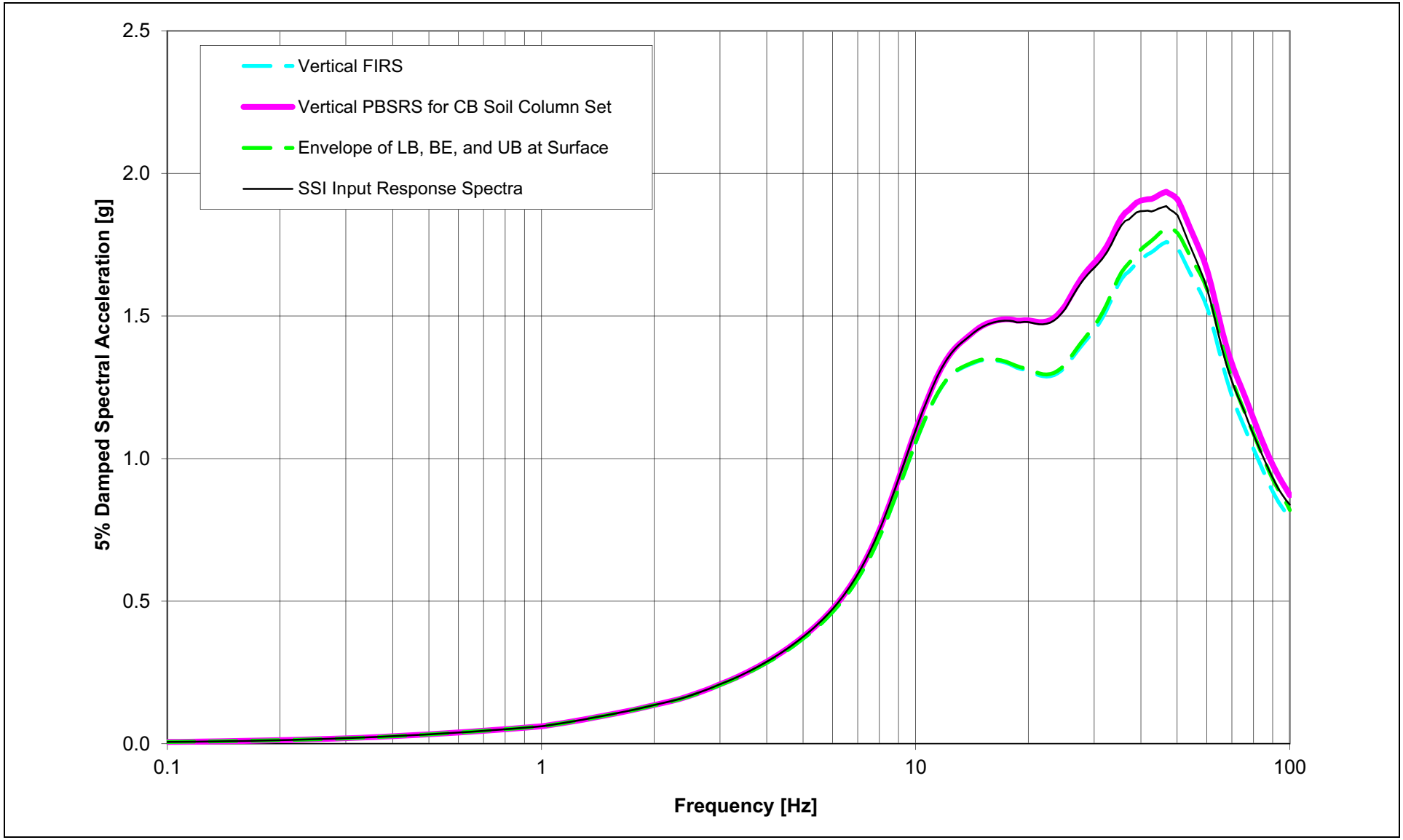

NAPS SUP 3.7-1 **Figure 3.7.1-229 Development of 5% Damped Final Horizontal SSI Input Response Spectra for CB**

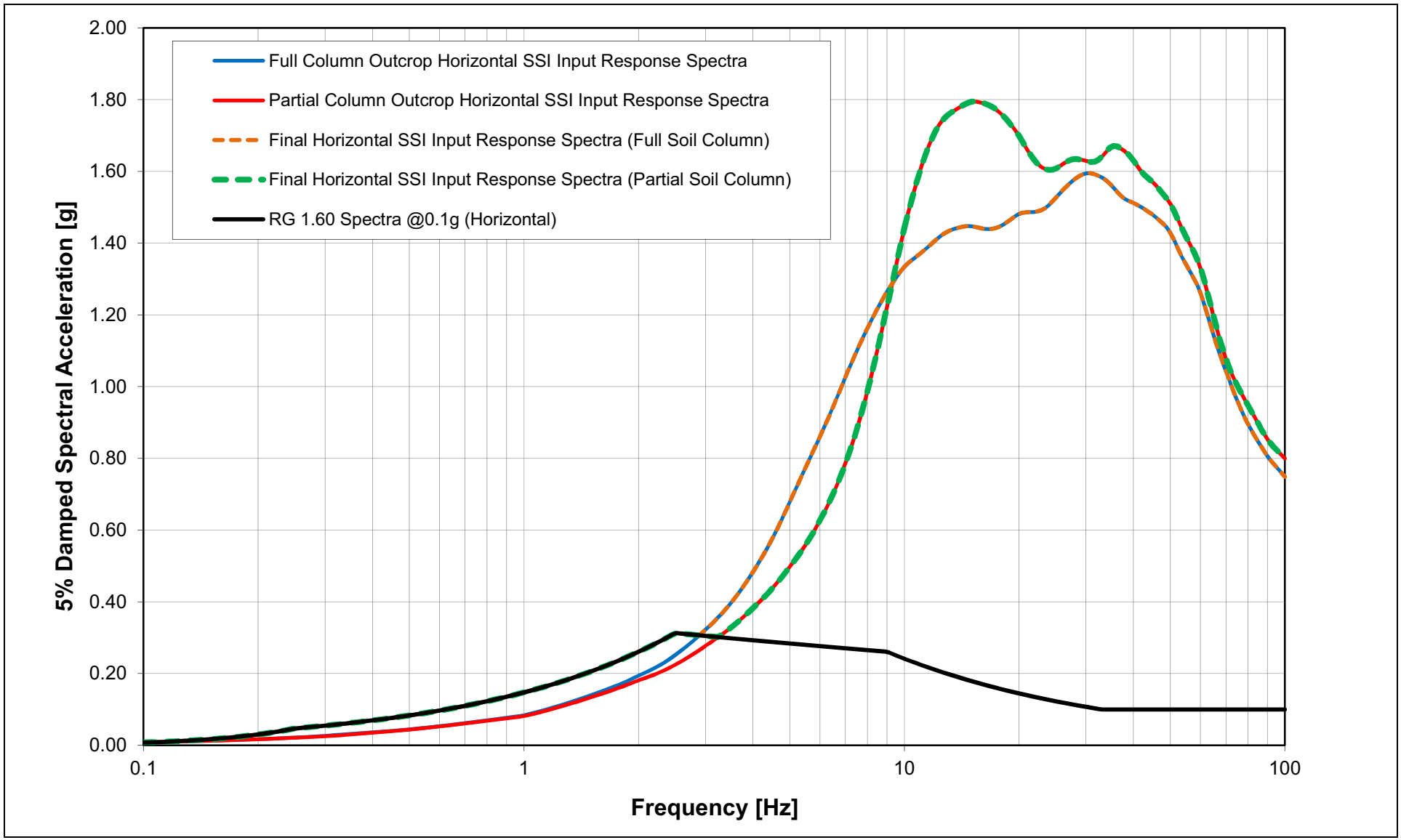

NAPS SUP 3.7-1 **Figure 3.7.1-230 Development of 5% Damped Final Vertical SSI Input Response Spectra for CB**

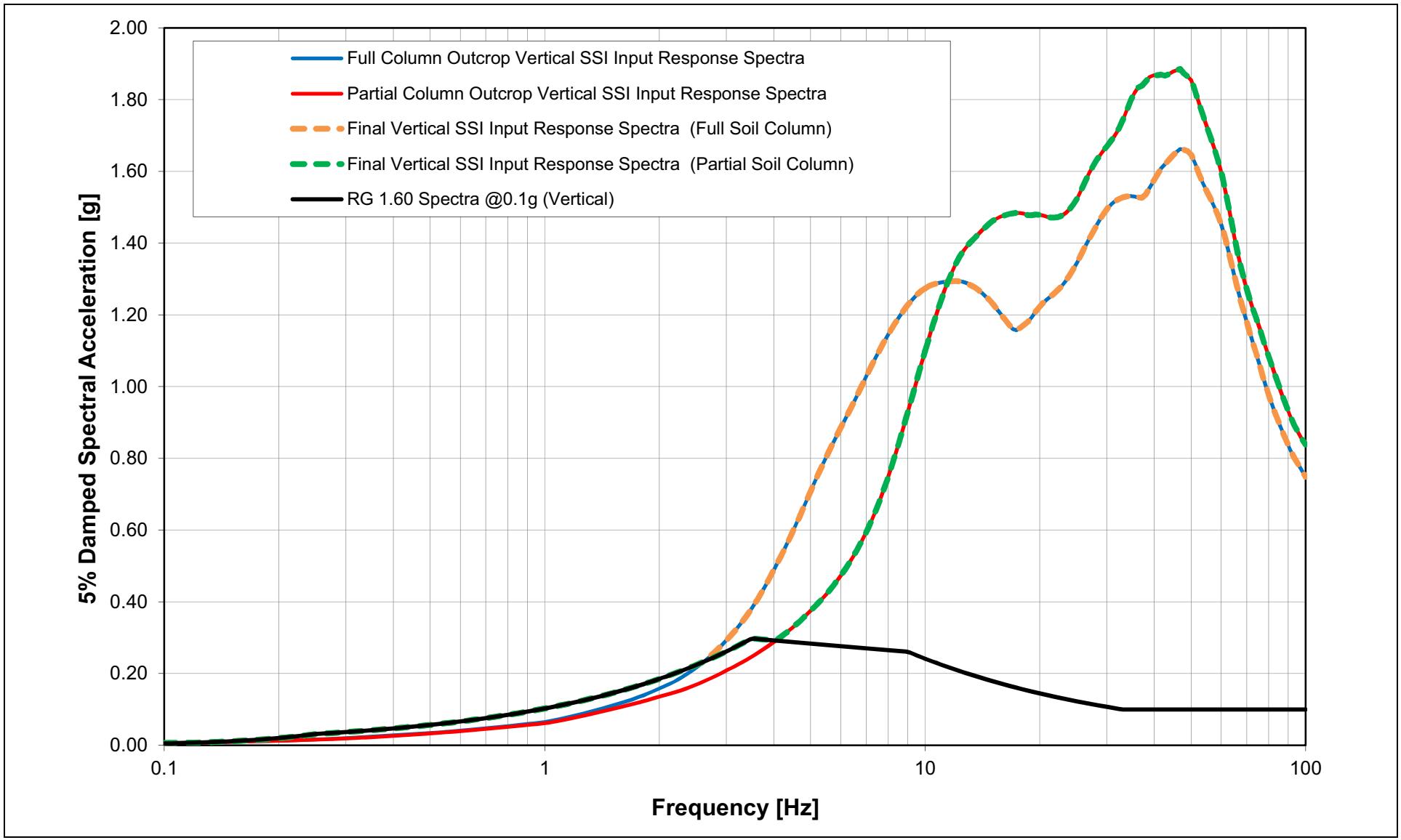

NAPS SUP 3.7-1 **Figure 3.7.1-231 5% Damped Final SSI Input Response Spectra for CB**

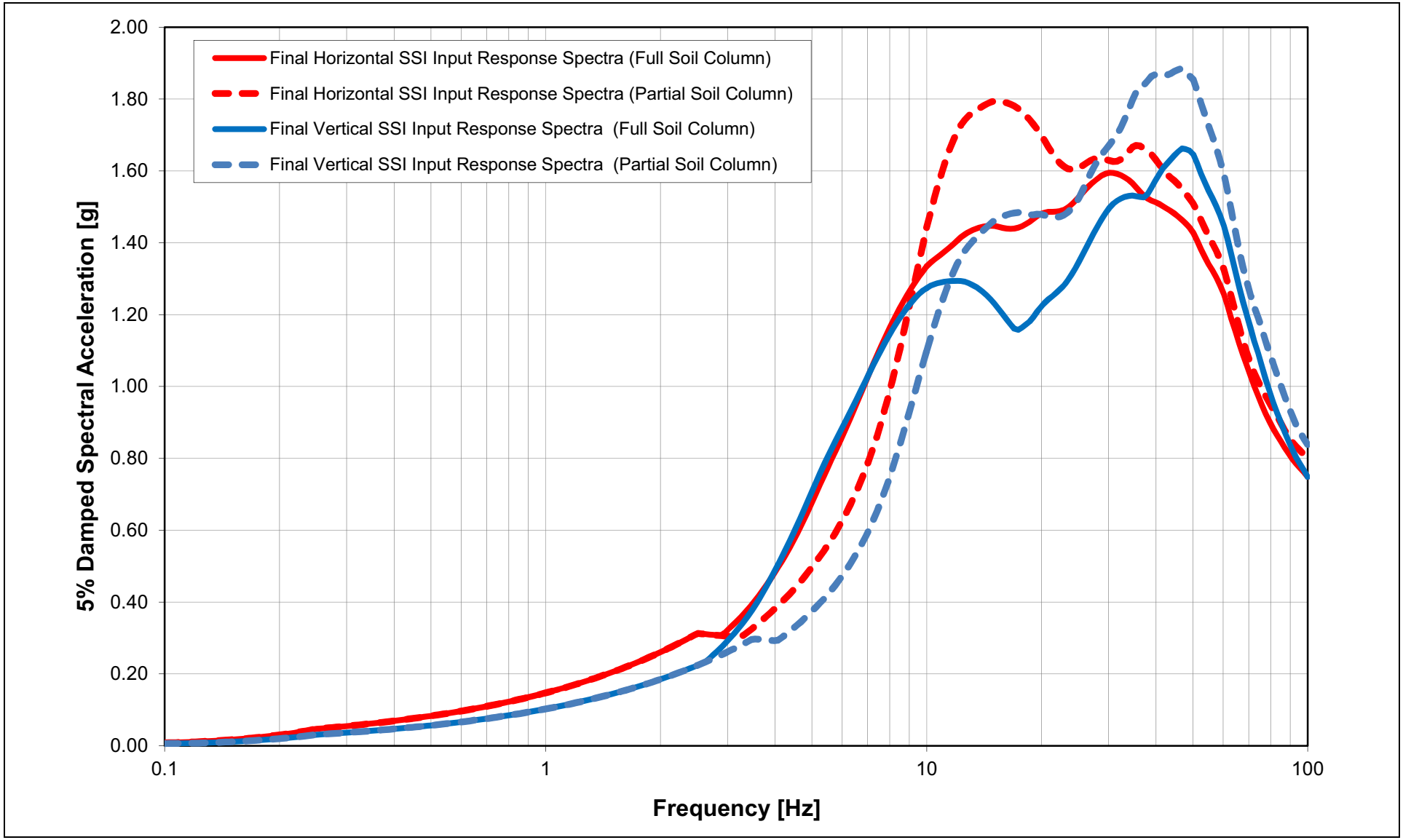

NAPS SUP 3.7-1 **Figure 3.7.1-232 Development of 5% Damped Final Horizontal SSI Input Response Spectrum at Elevation 282 ft for FWSC**

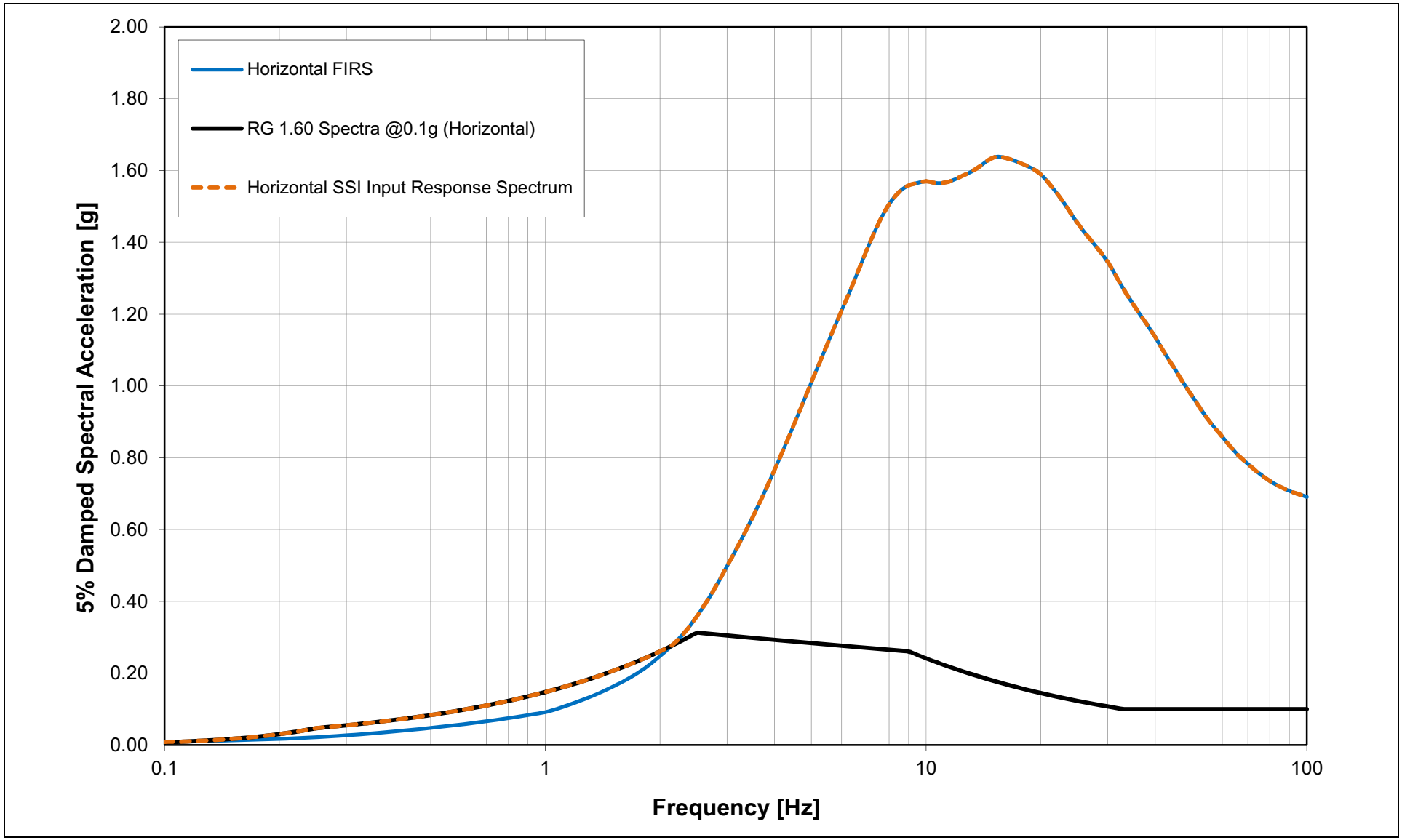

NAPS SUP 3.7-1

Figure 3.7.1-233 Development of 5% Damped Final Vertical SSI Input Response Spectrum at Elevation 282 ft for FWSC

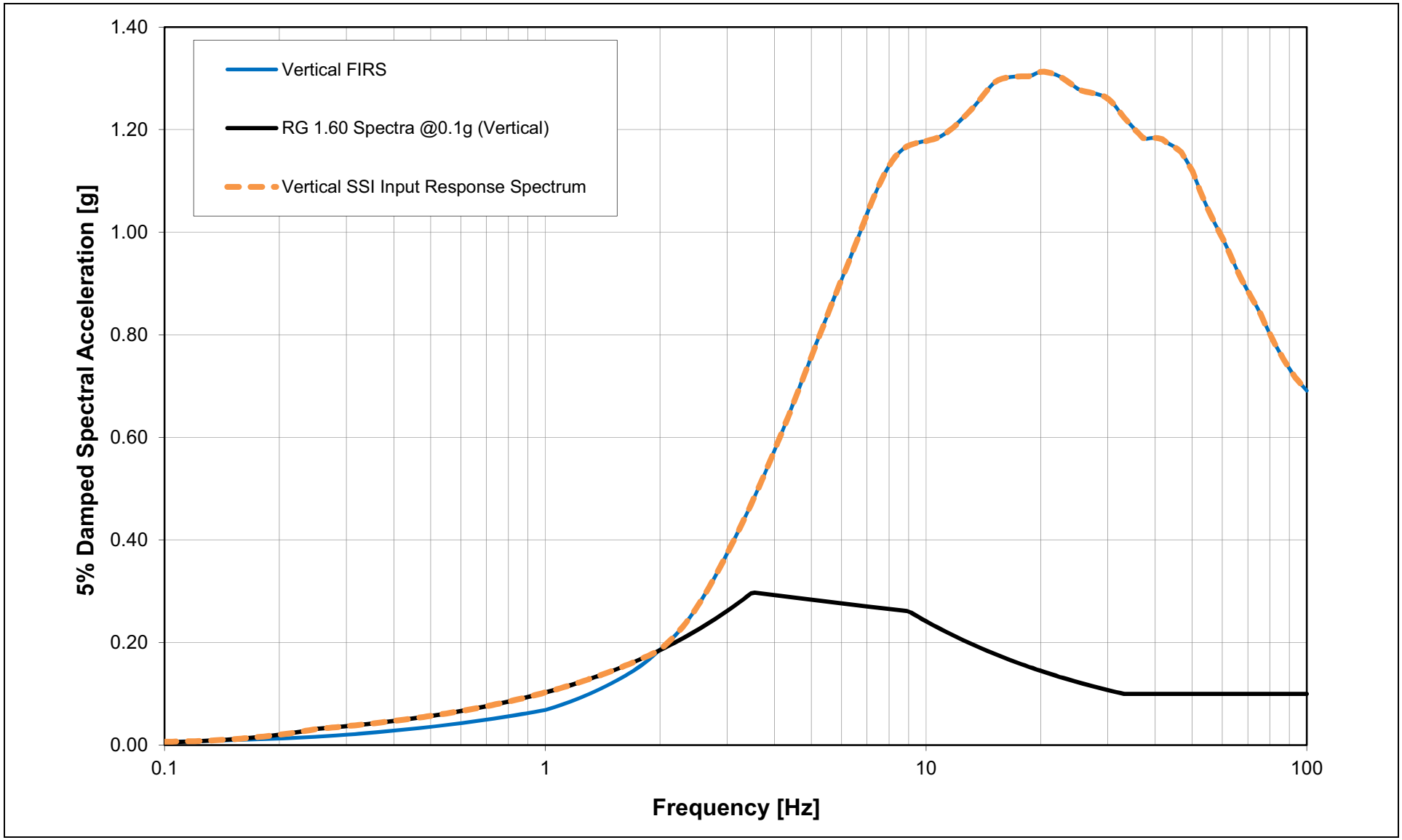

NAPS SUP 3.7-1

Figure 3.7.1-234 5% Damped Final SSI Input Response Spectra at Elevation 282 ft for FWSC

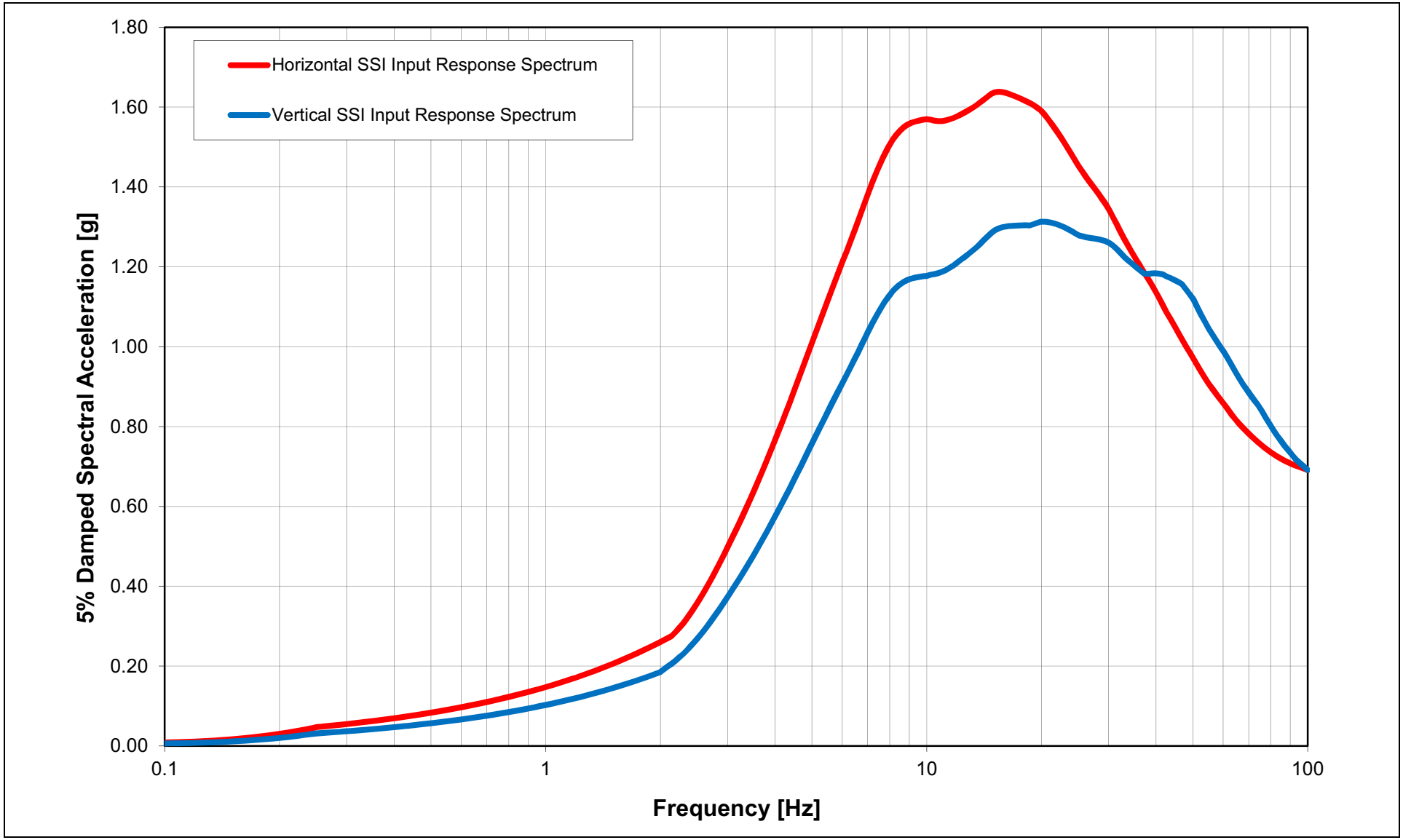

NAPS SUP 3.7-2 **Figure 3.7.1-235 Comparison between the Final Scaled Spectrum Compatible Response Spectrum, the Target Spectrum, and Upper and Lower Target Spectrum Bounds for the Partial Column RB/FB case, H1 Component**

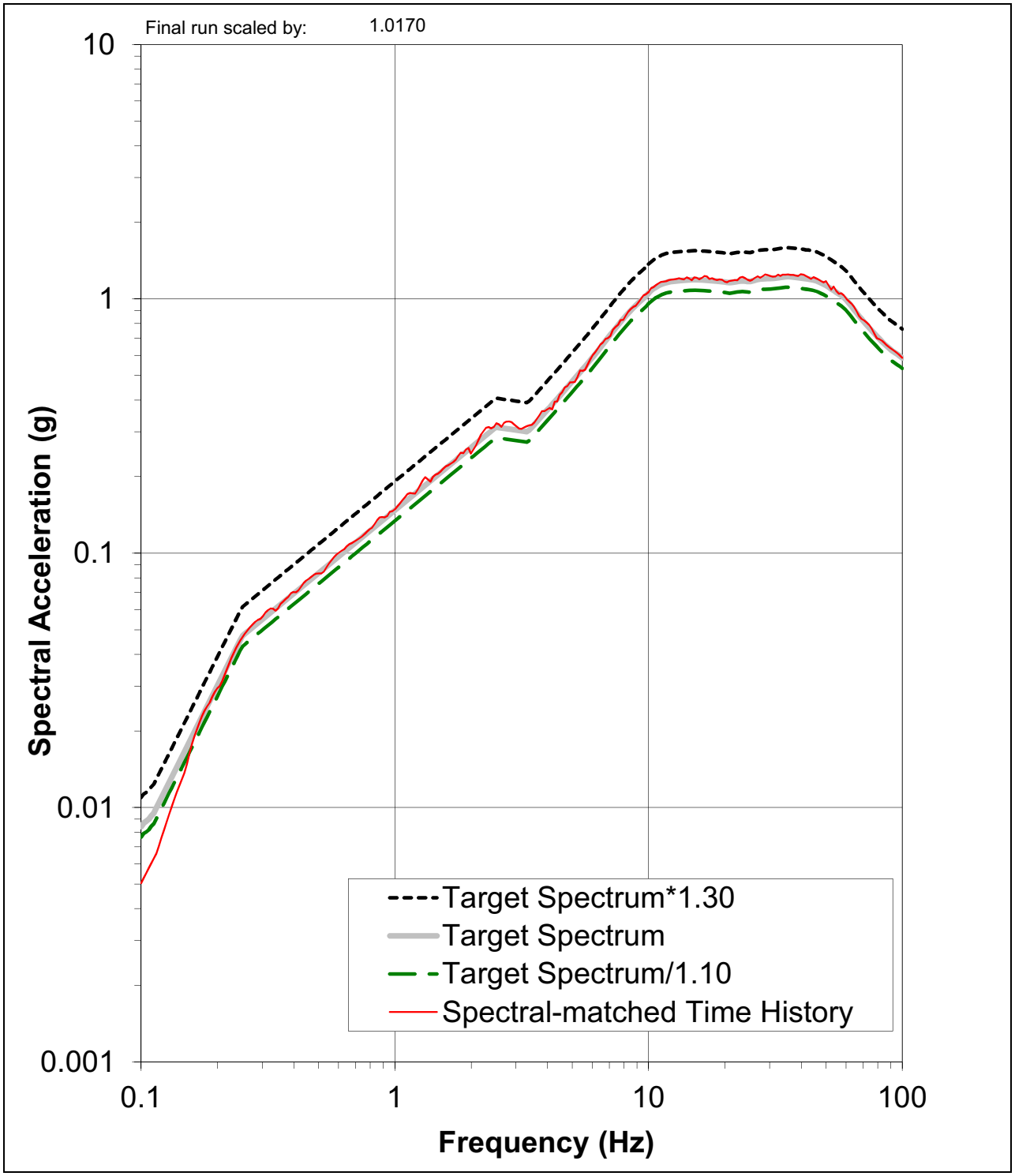

NAPS SUP 3.7-2

Figure 3.7.1-236 Comparison between the Final Scaled Spectrum Compatible Response Spectrum, the Target Spectrum, and Upper and Lower Target Spectrum Bounds for the Partial Column RB/FB case, H2 Component

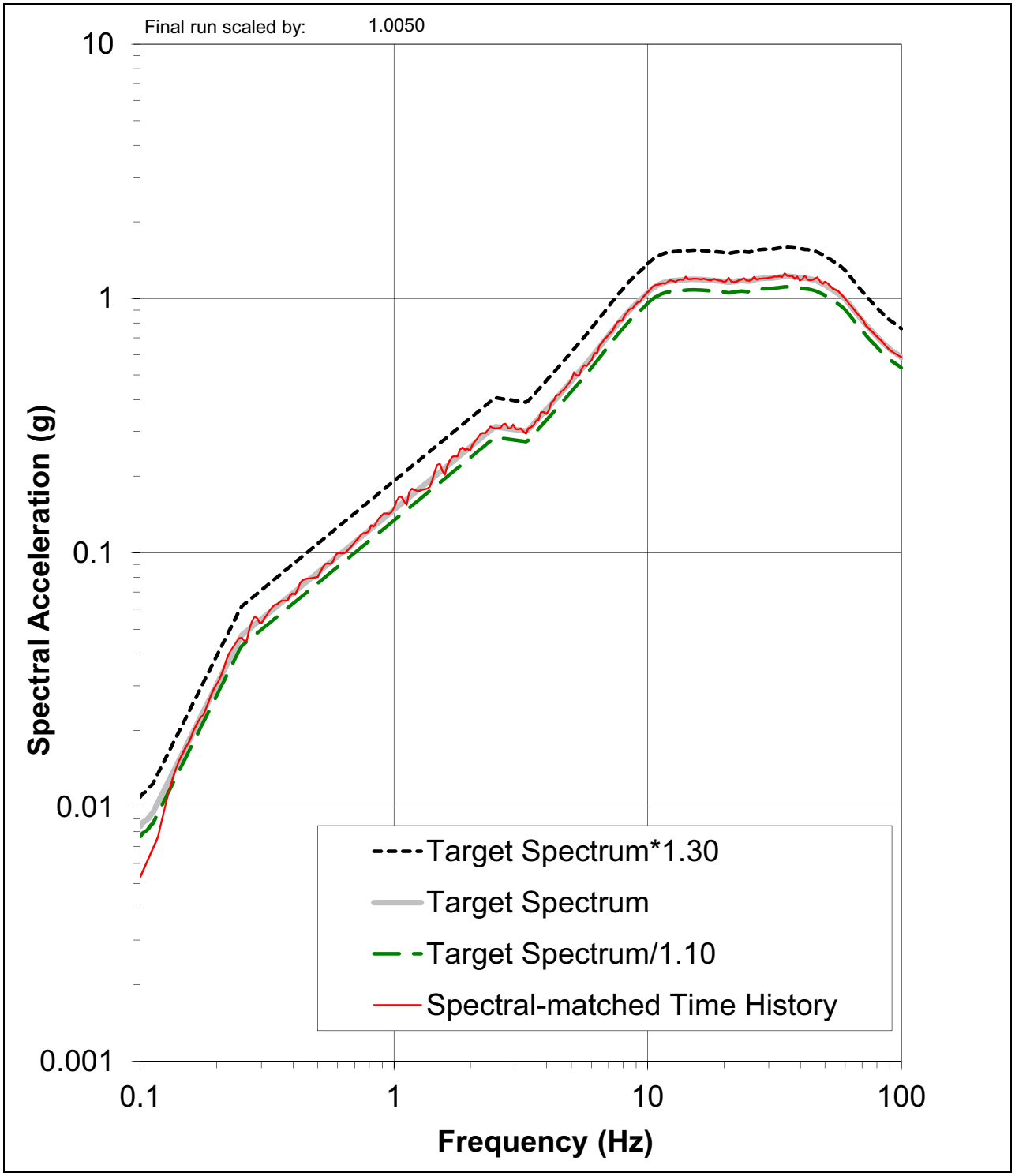

NAPS SUP 3.7-2 **Figure 3.7.1-237 Comparison between the Final Scaled Spectrum Compatible Response Spectrum, the Target Spectrum, and Upper and Lower Target Spectrum Bounds for the Partial Column RB/FB case, UP Component**

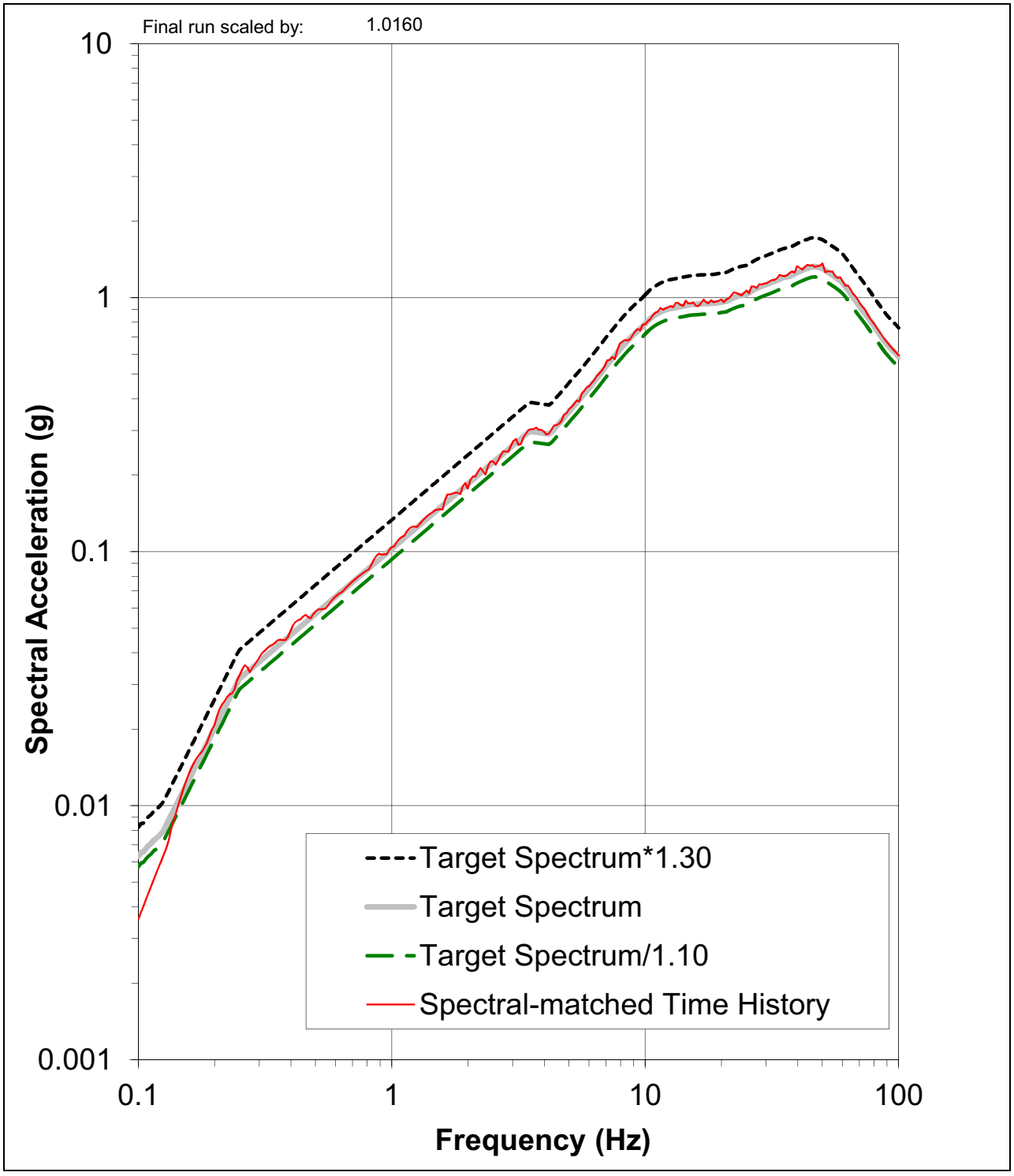

NAPS SUP 3.7-2 **Figure 3.7.1-238 Comparison between the Final Scaled Spectrum Compatible Response Spectrum, the Target Spectrum, and Upper and Lower Target Spectrum Bounds for the Full Column RB/FB case, H1 Component**

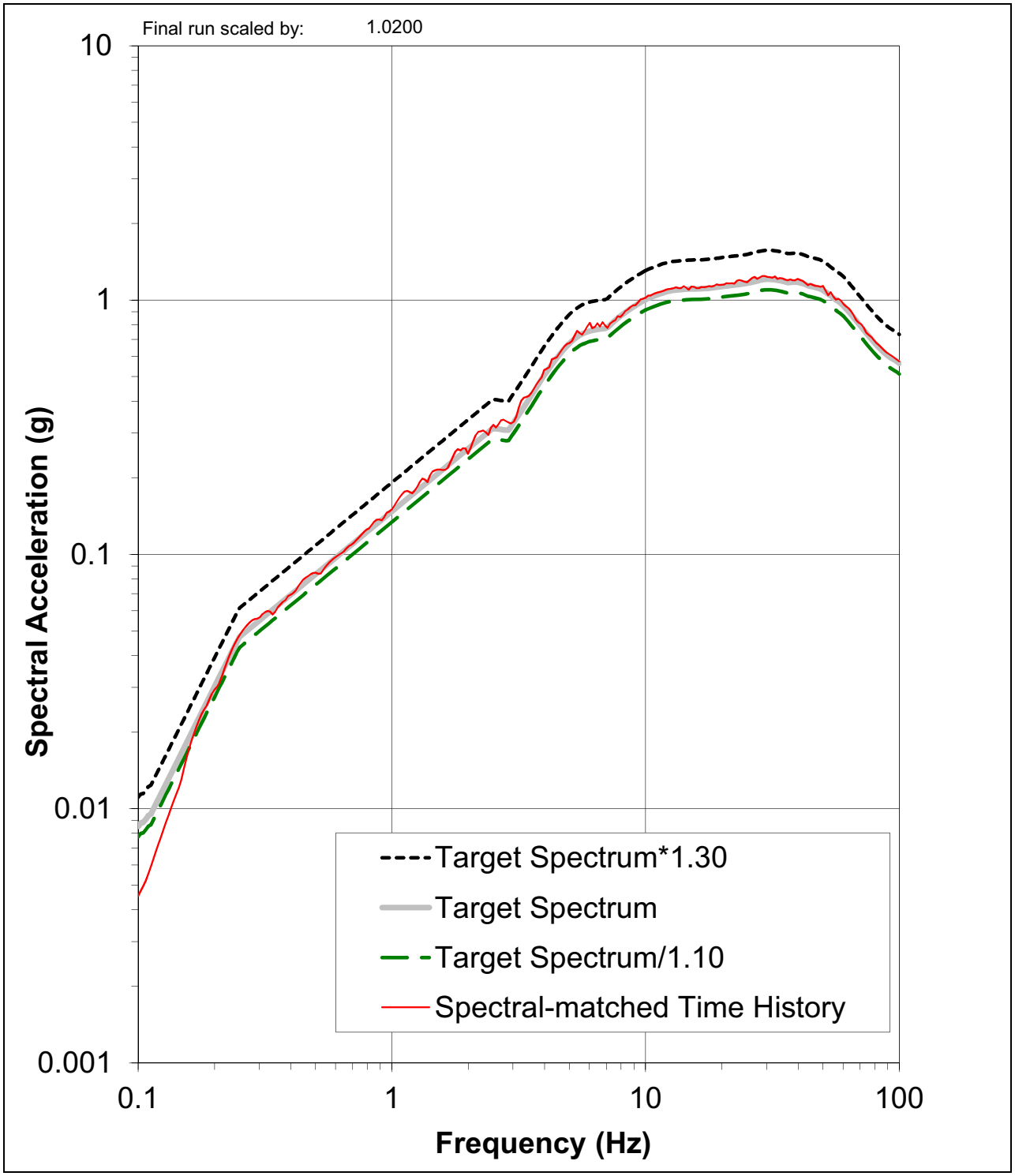

NAPS SUP 3.7-2 **Figure 3.7.1-239 Comparison between the Final Scaled Spectrum Compatible Response Spectrum, the Target Spectrum, and Upper and Lower Target Spectrum Bounds for the Full Column RB/FB case, H2 Component**

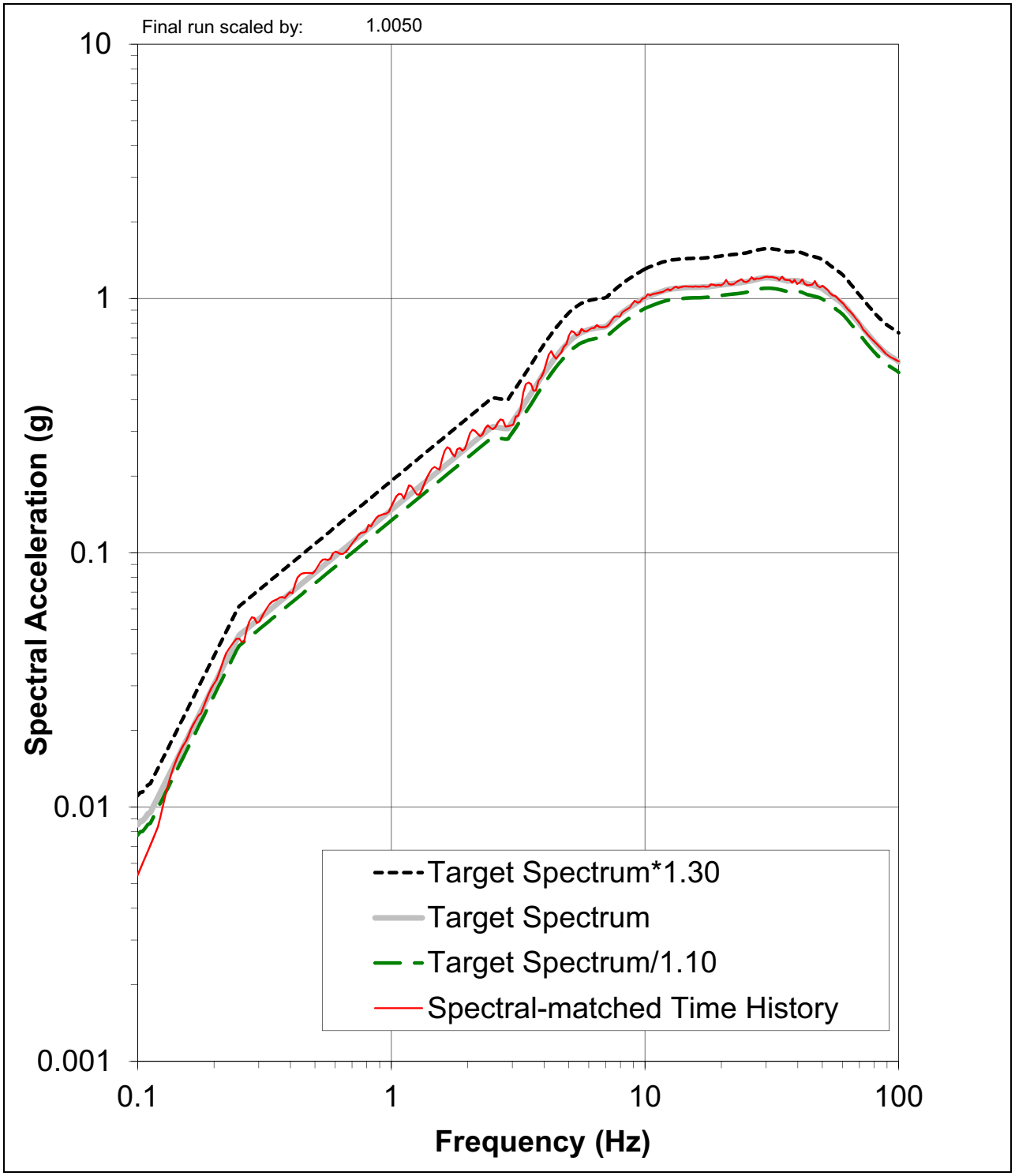

NAPS SUP 3.7-2

Figure 3.7.1-240 Comparison between the Final Scaled Spectrum Compatible Response Spectrum, the Target Spectrum, and Upper and Lower Target Spectrum Bounds for the Full Column RB/FB case, UP Component

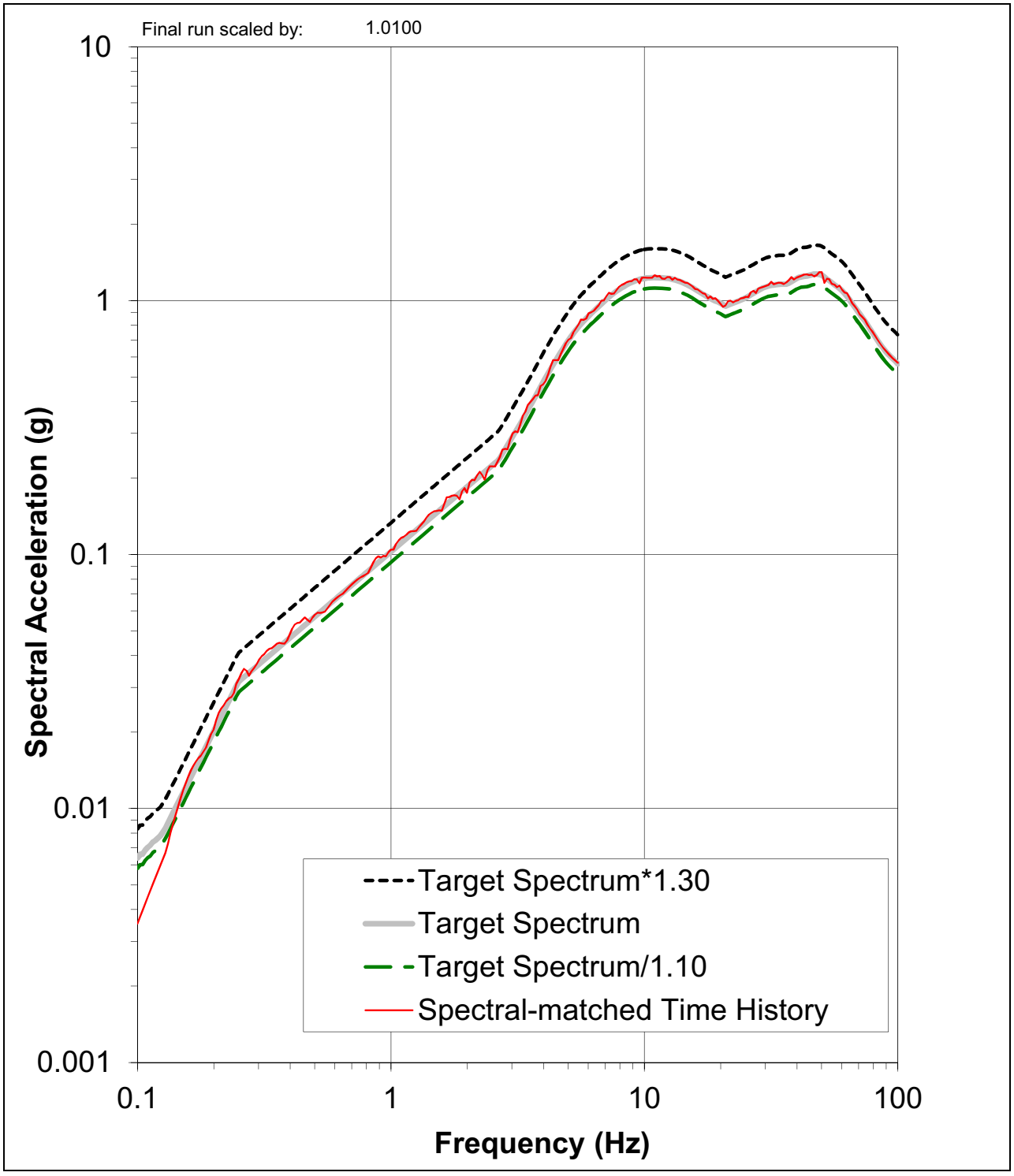

NAPS SUP 3.7-2 **Figure 3.7.1-241 Acceleration, Velocity, and Displacement Spectrally Matched Partial Column Outcrop Time-Histories for RB/FB, H1 Component**

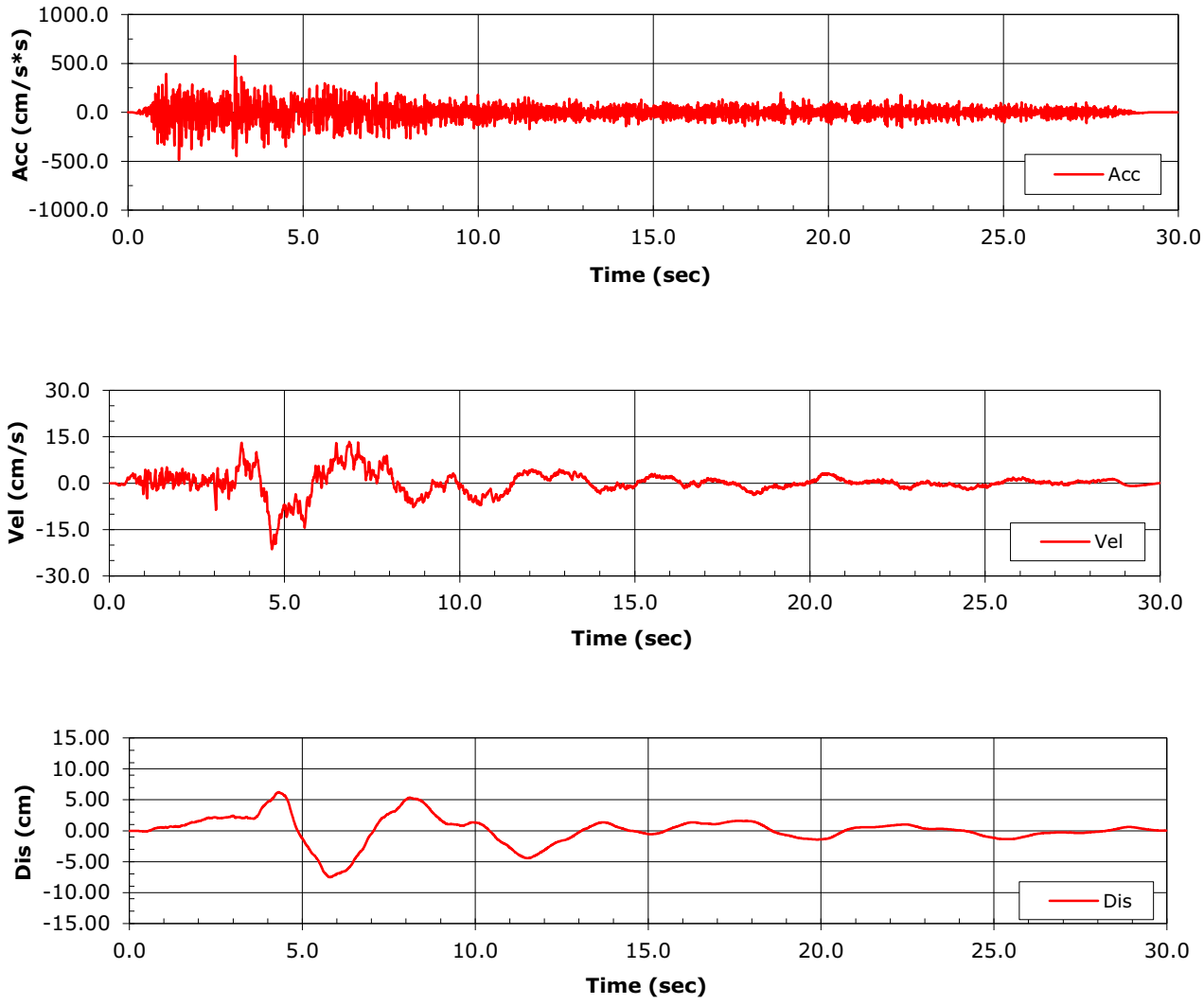

NAPS SUP 3.7-2 **Figure 3.7.1-242 Acceleration, Velocity, and Displacement Spectrally Matched Partial Column Outcrop Time-Histories for RB/FB, H2 Component**

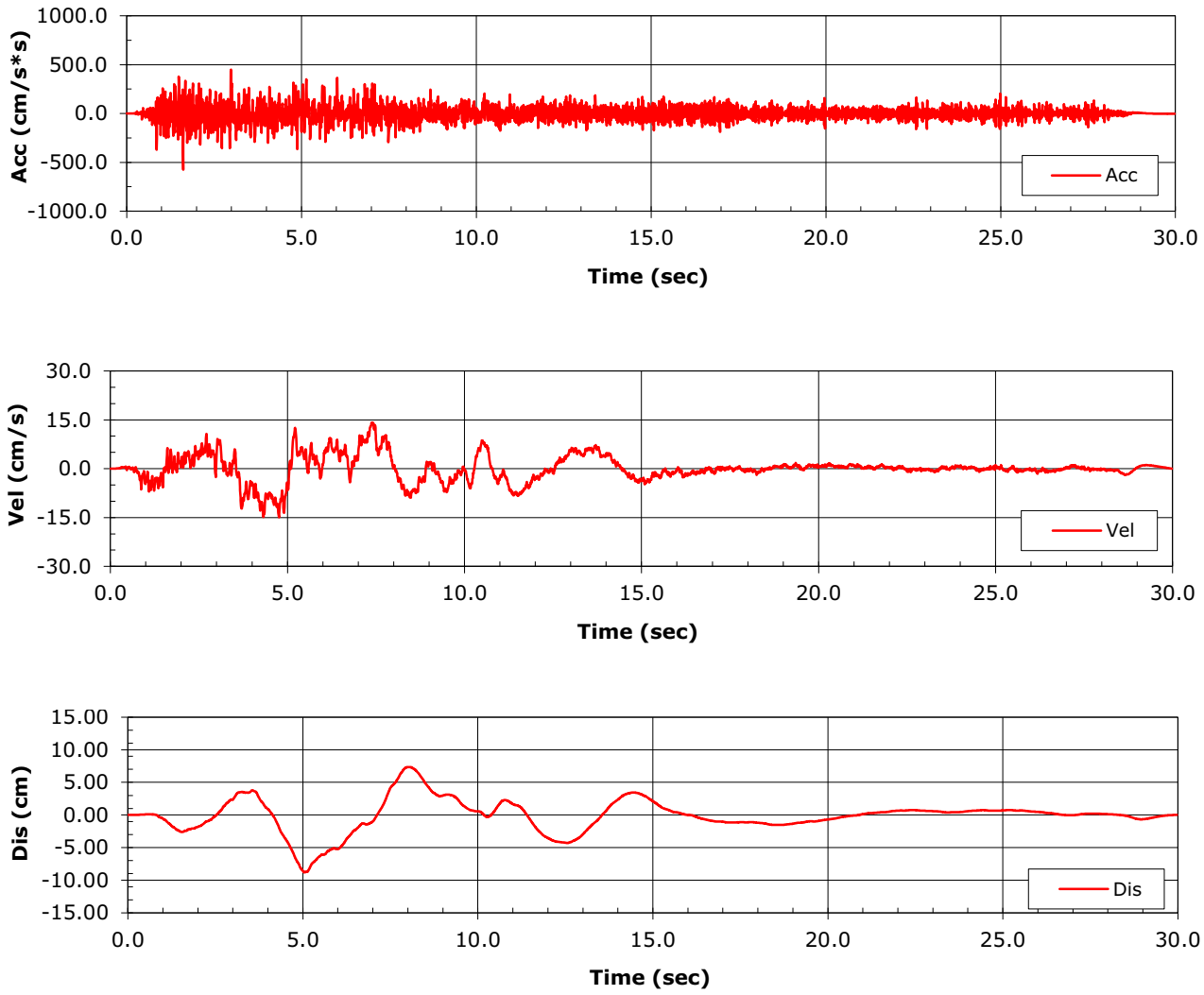

NAPS SUP 3.7-2 **Figure 3.7.1-243 Acceleration, Velocity, and Displacement Spectrally Matched Partial Column Outcrop Time-Histories for RB/FB, UP Component**

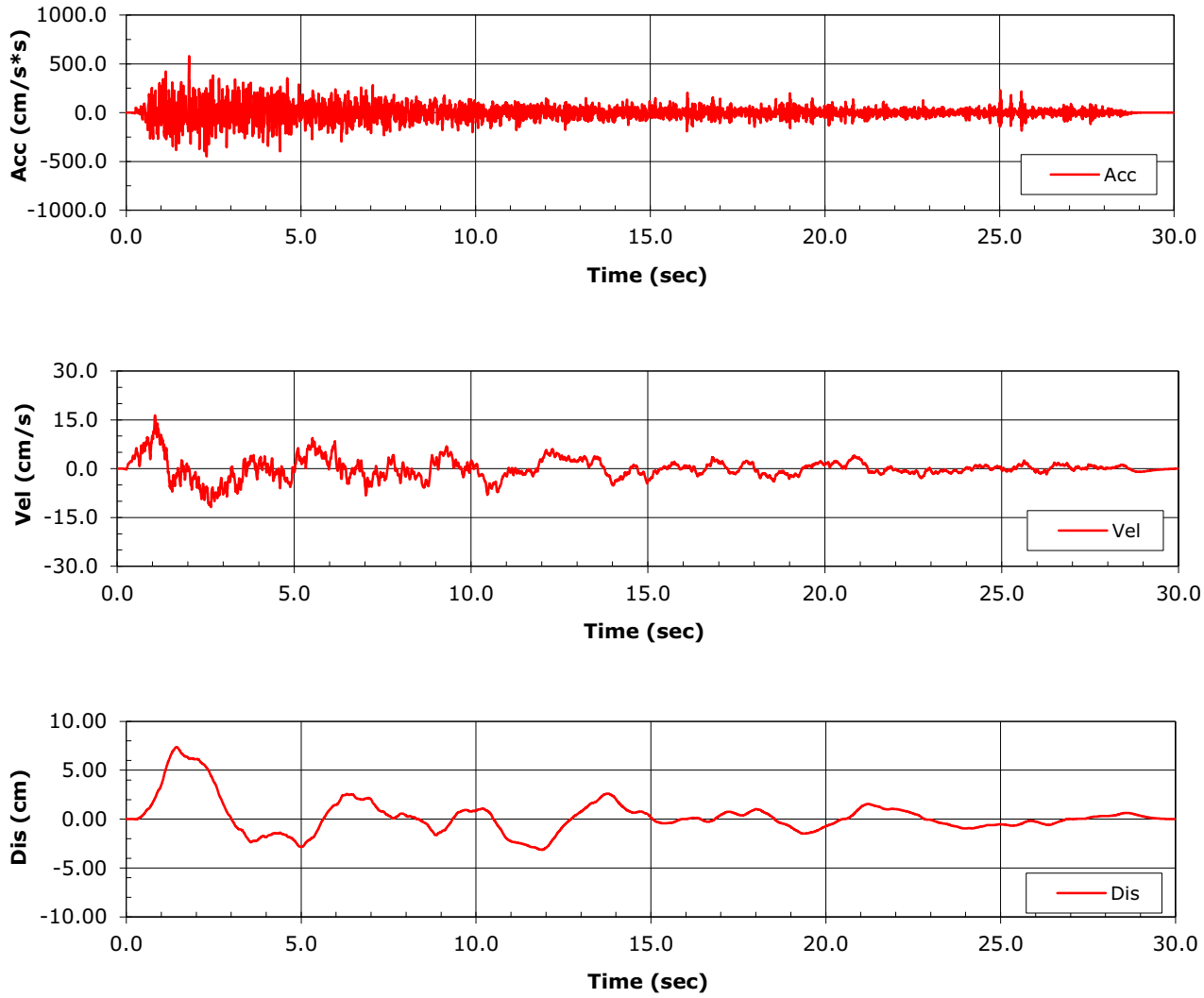

NAPS SUP 3.7-2 **Figure 3.7.1-244 Acceleration, Velocity, and Displacement Spectrally Matched Full Column Outcrop Time-Histories for RB/FB, H1 Component**

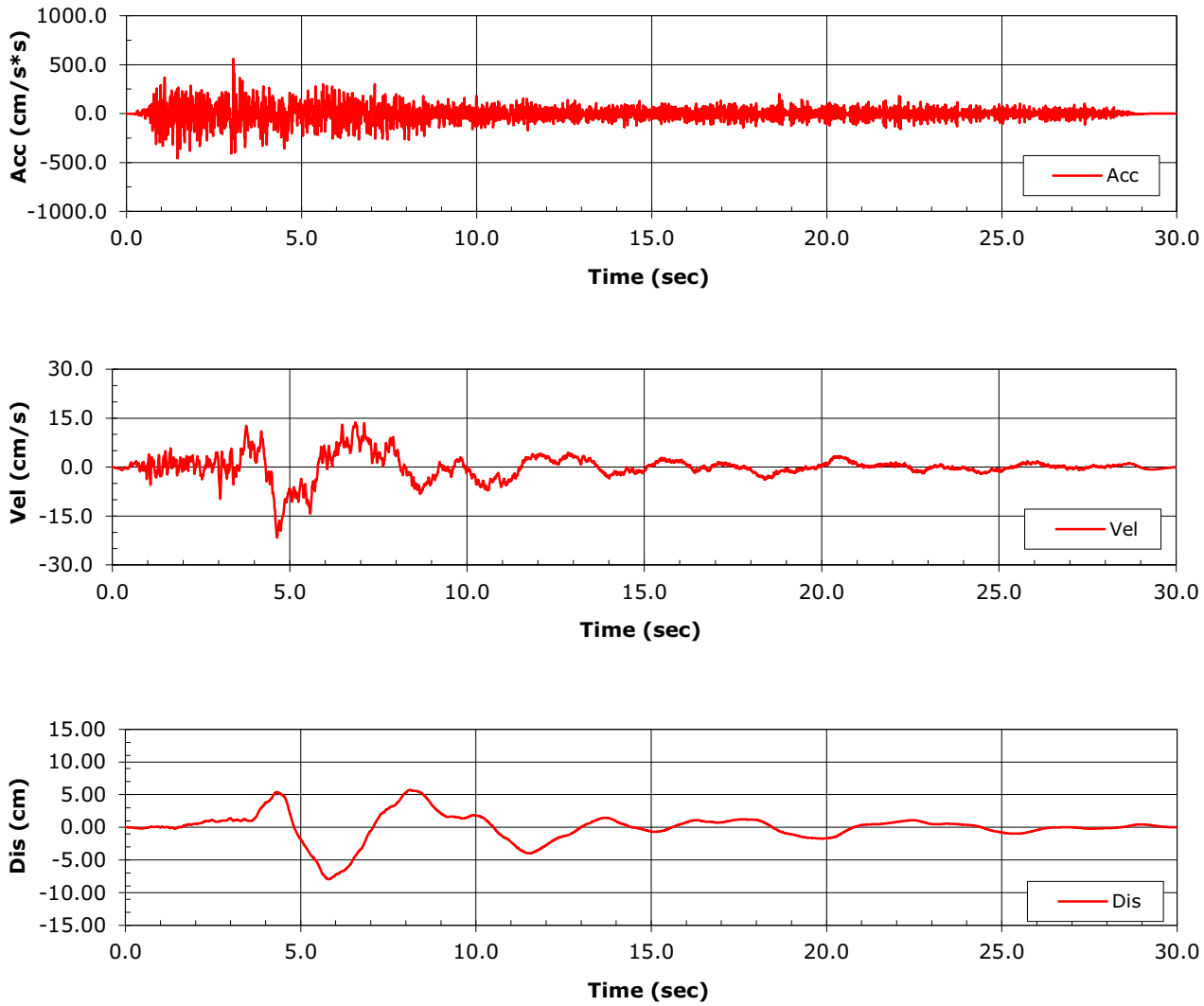

NAPS SUP 3.7-2 **Figure 3.7.1-245 Acceleration, Velocity, and Displacement Spectrally Matched Full Column Outcrop Time-Histories for RB/FB, H2 Component**

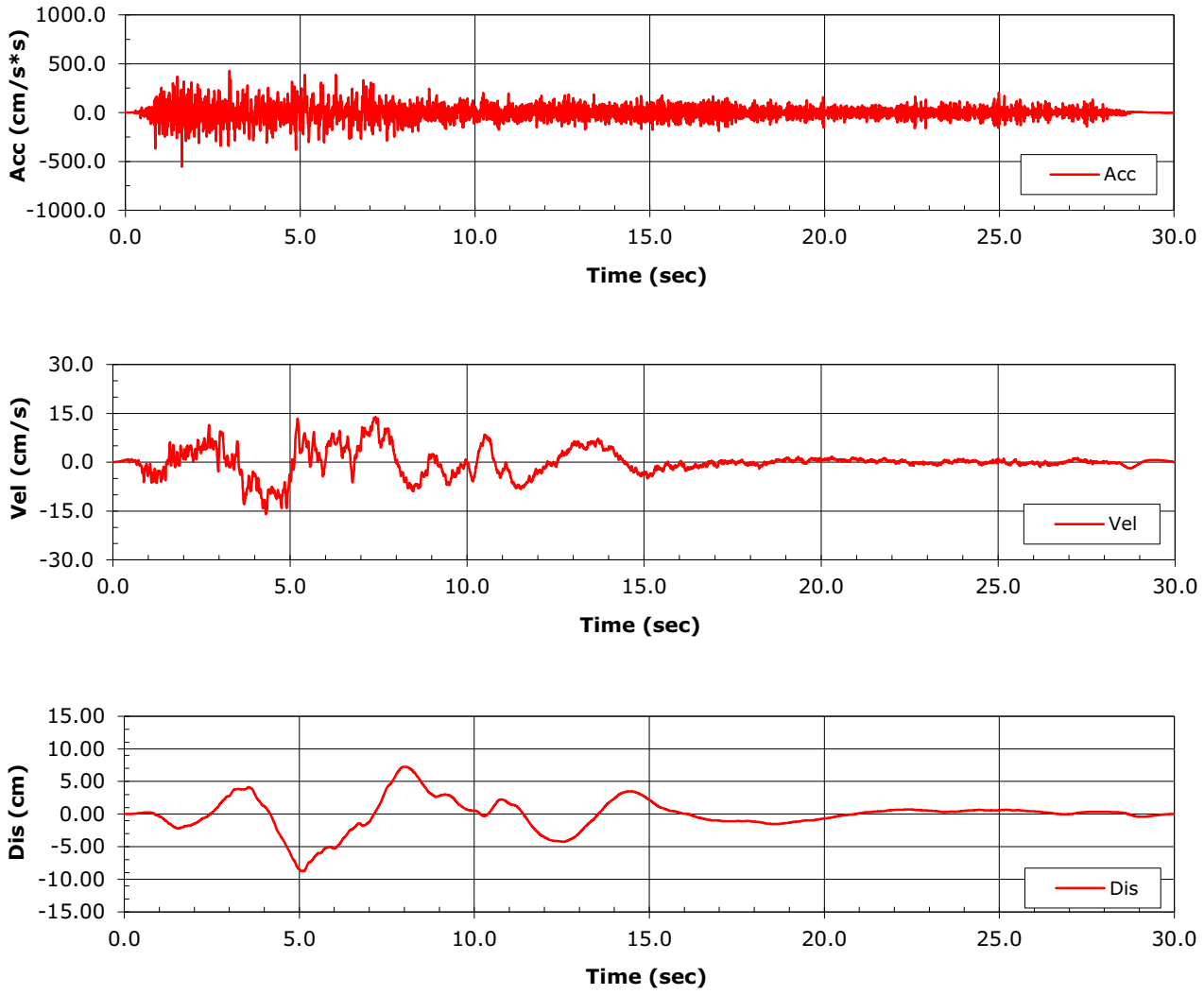

NAPS SUP 3.7-2 **Figure 3.7.1-246 Acceleration, Velocity, and Displacement Spectrally Matched Full Column Outcrop Time-Histories for RB/FB, UP Component**

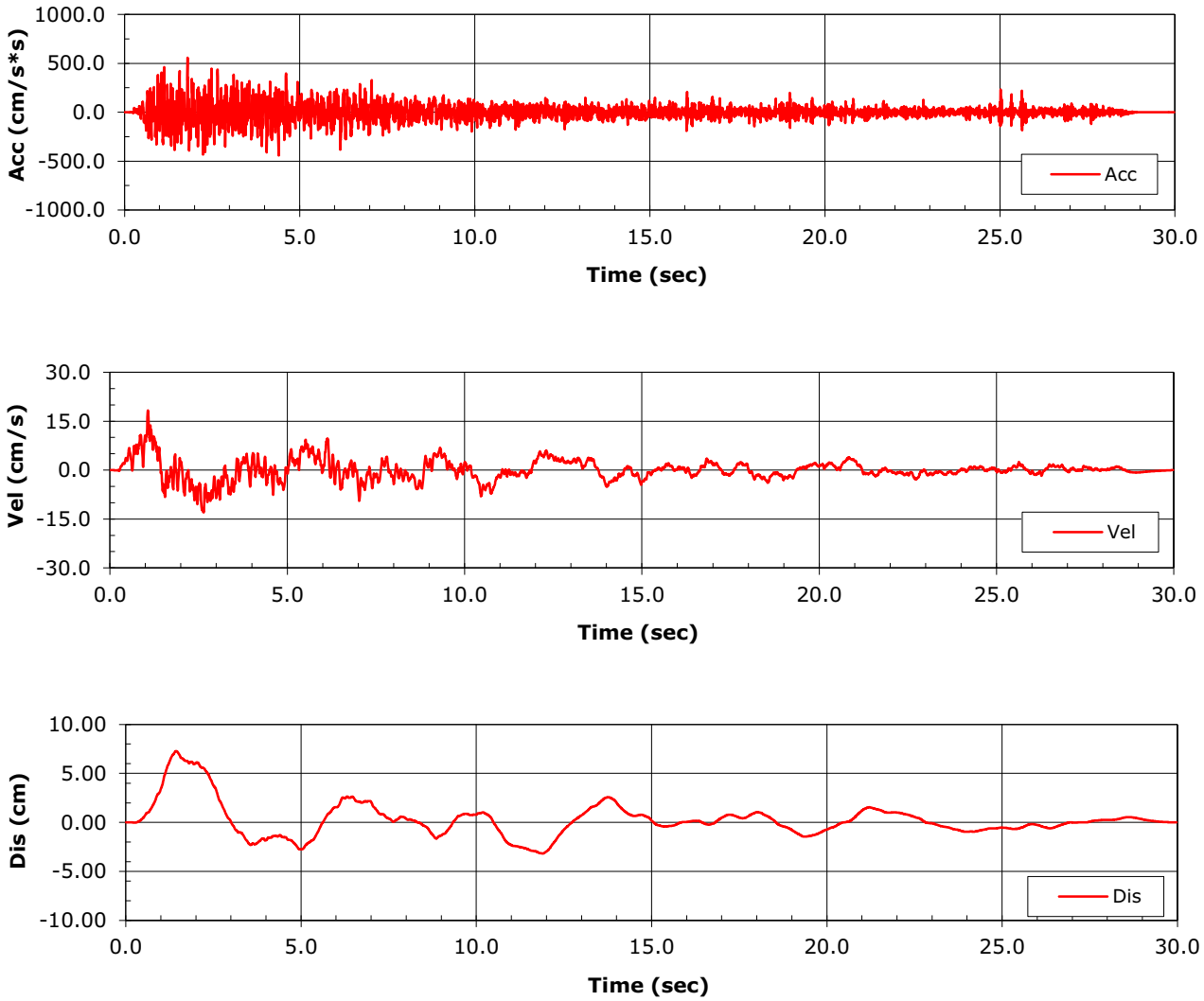

NAPS SUP 3.7-2 **Figure 3.7.1-247 Comparison between the Final Scaled Spectrum Compatible Response Spectrum, the Target Spectrum, and Upper and Lower Target Spectrum Bounds for the Partial Column CB case, H1 Component**

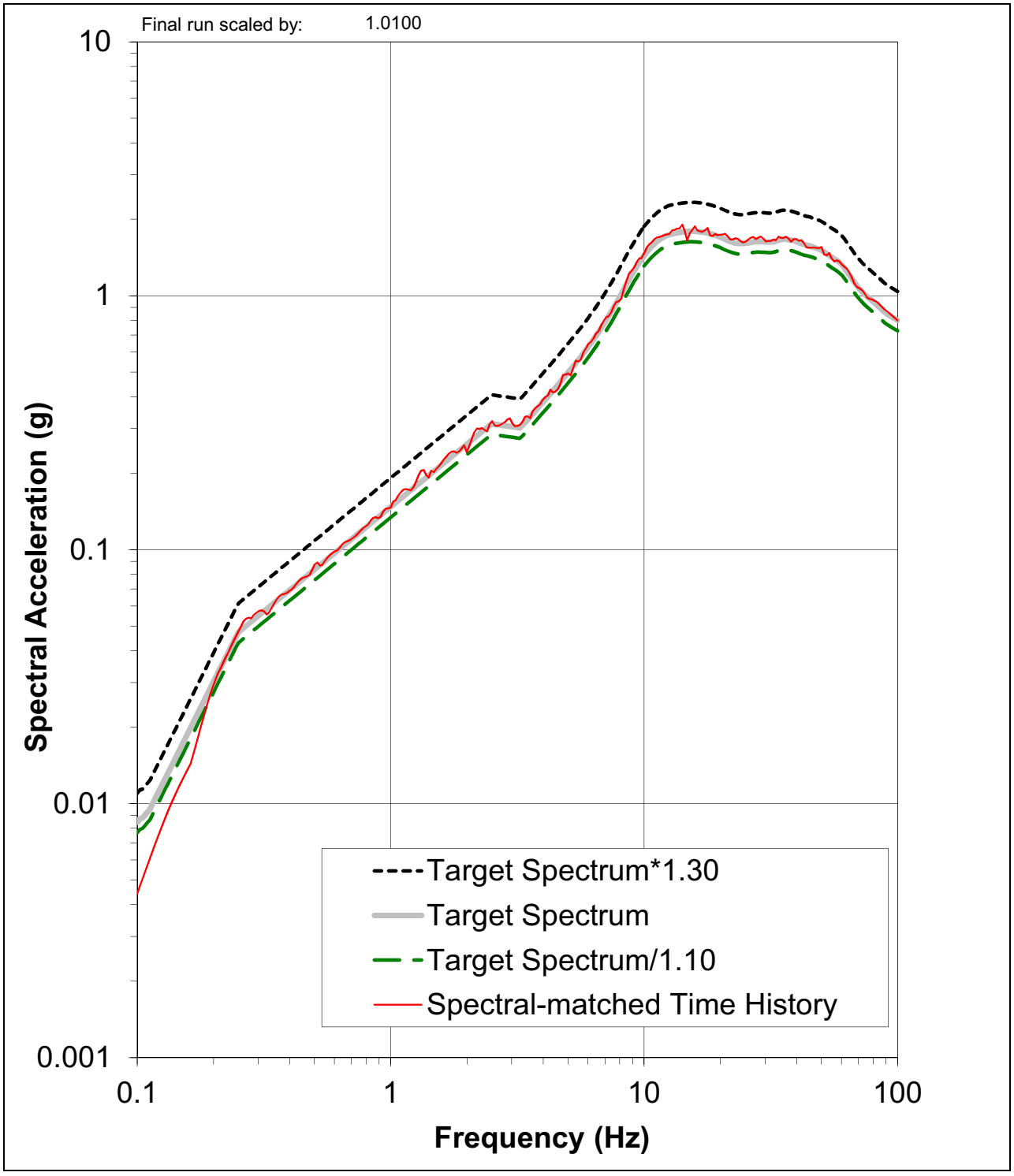

NAPS SUP 3.7-2 **Figure 3.7.1-248 Comparison between the Final Scaled Spectrum Compatible Response Spectrum, the Target Spectrum, and Upper and Lower Target Spectrum Bounds for the Partial Column CB case, H2 Component**

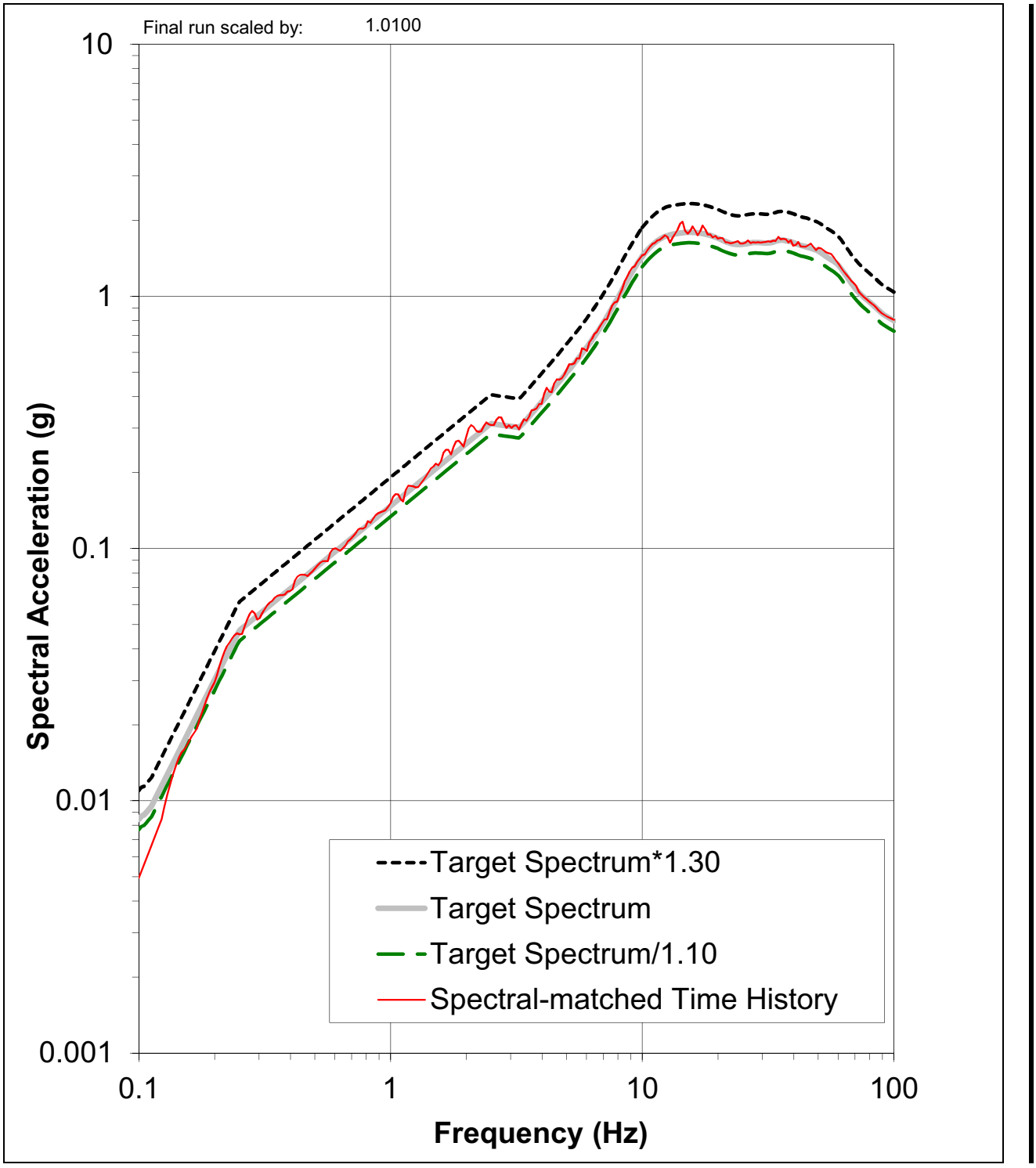

NAPS SUP 3.7-2 **Figure 3.7.1-249 Comparison between the Final Scaled Spectrum Compatible Response Spectrum, the Target Spectrum, and Upper and Lower Target Spectrum Bounds for the Partial Column CB case, UP Component**

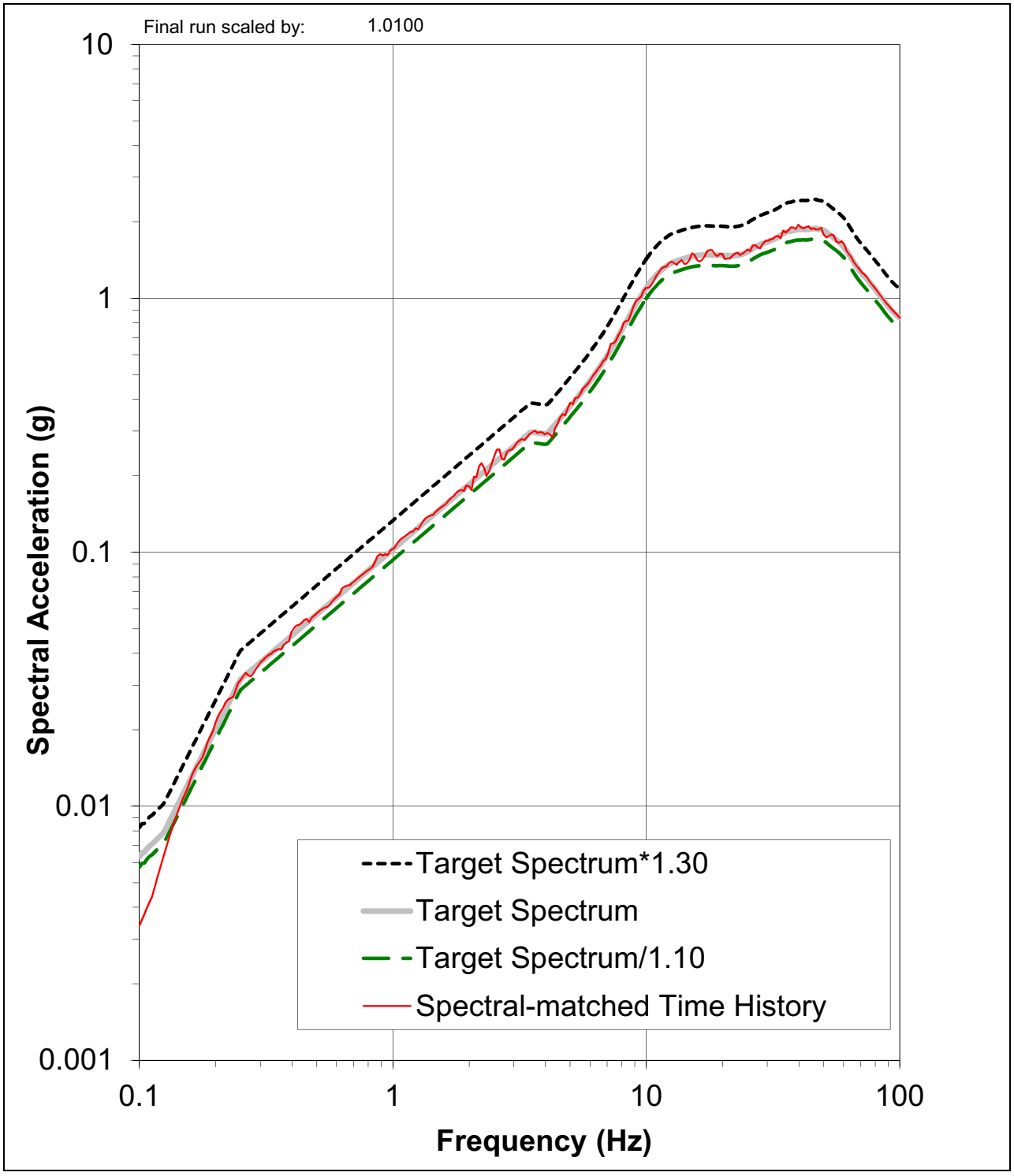

NAPS SUP 3.7-2 **Figure 3.7.1-250 Comparison between the Final Scaled Spectrum Compatible Response Spectrum, the Target Spectrum, and Upper and Lower Target Spectrum Bounds for the Full Column CB case, H1 Component**

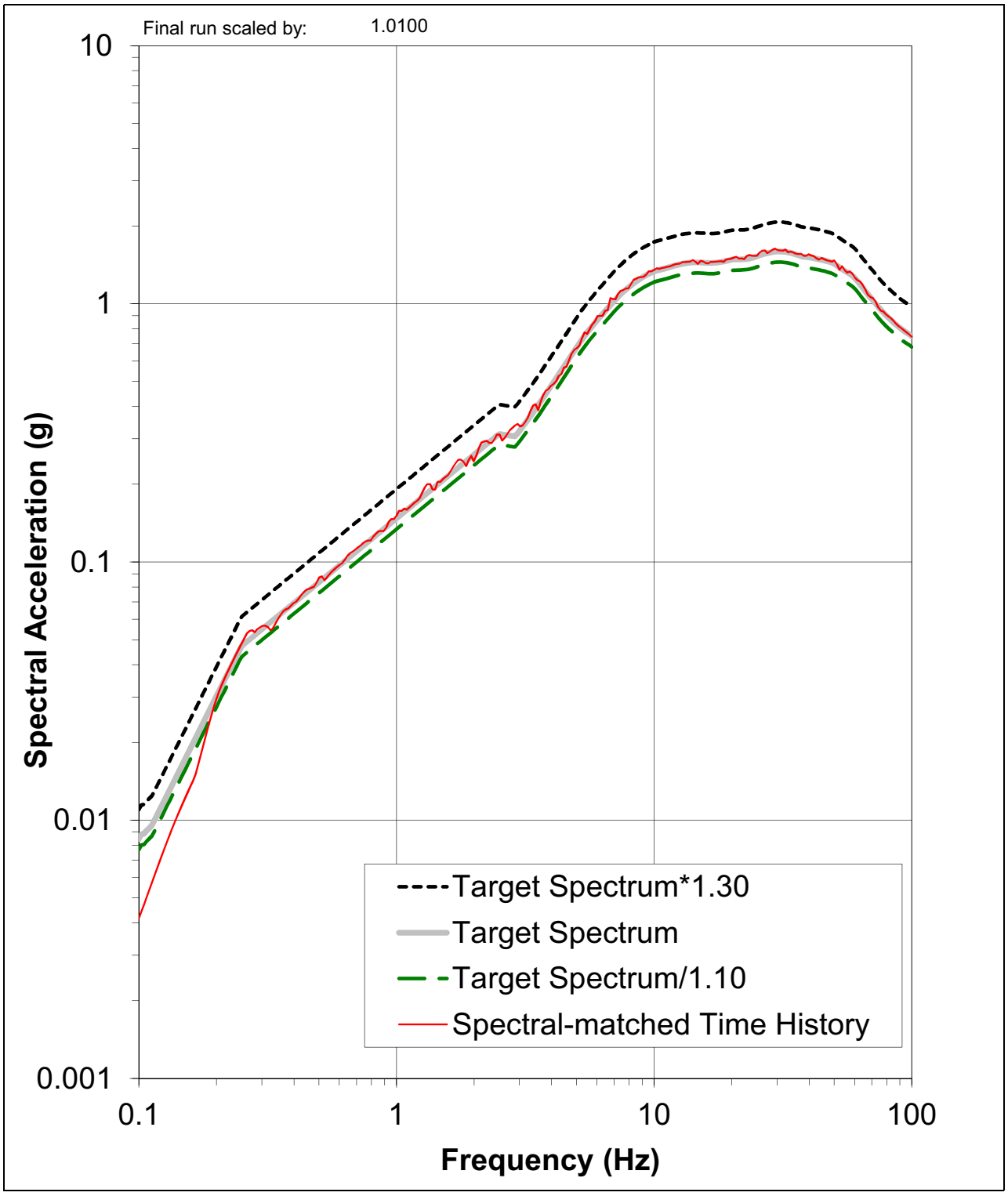

NAPS SUP 3.7-2 **Figure 3.7.1-251 Comparison between the Final Scaled Spectrum Compatible Response Spectrum, the Target Spectrum, and Upper and Lower Target Spectrum Bounds for the Full Column CB case, H2 Component**

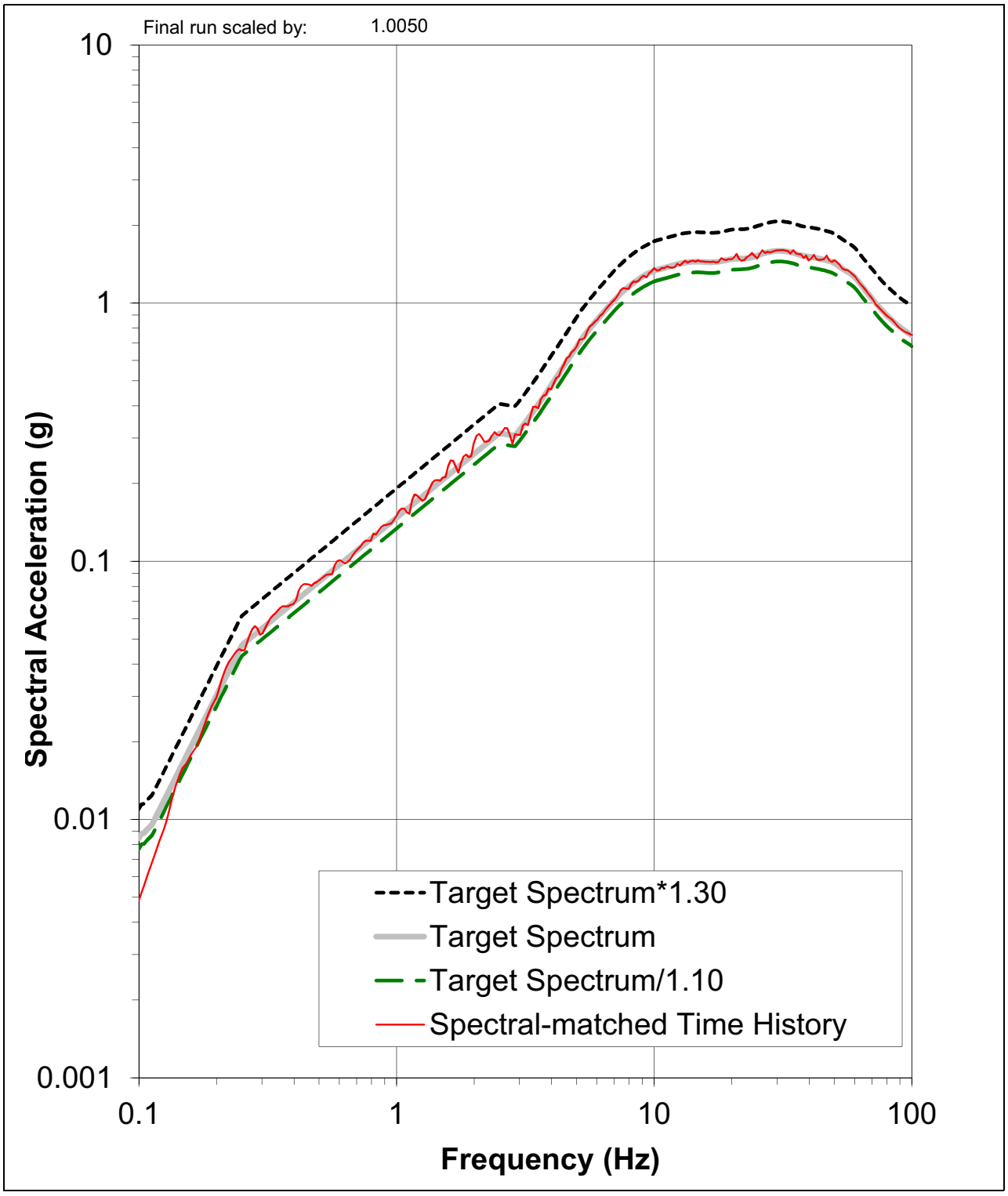

NAPS SUP 3.7-2

Figure 3.7.1-252 Comparison between the Final Scaled Spectrum Compatible Response Spectrum, the Target Spectrum, and Upper and Lower Target Spectrum Bounds for the Full Column CB case, UP Component

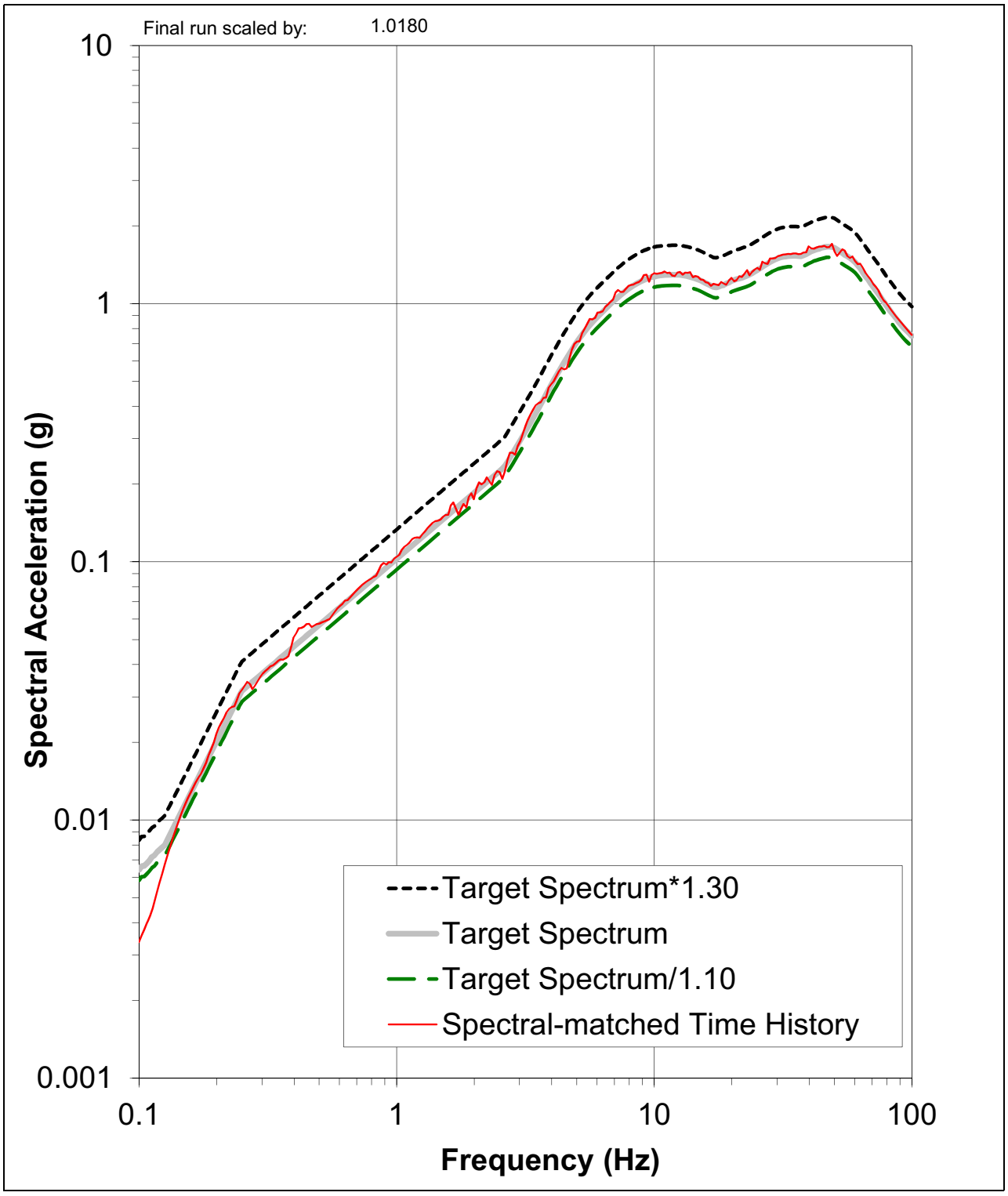

NAPS SUP 3.7-2 **Figure 3.7.1-253 Acceleration, Velocity, and Displacement Spectrally Matched Partial Column Outcrop Time-Histories for CB, H1 Component**

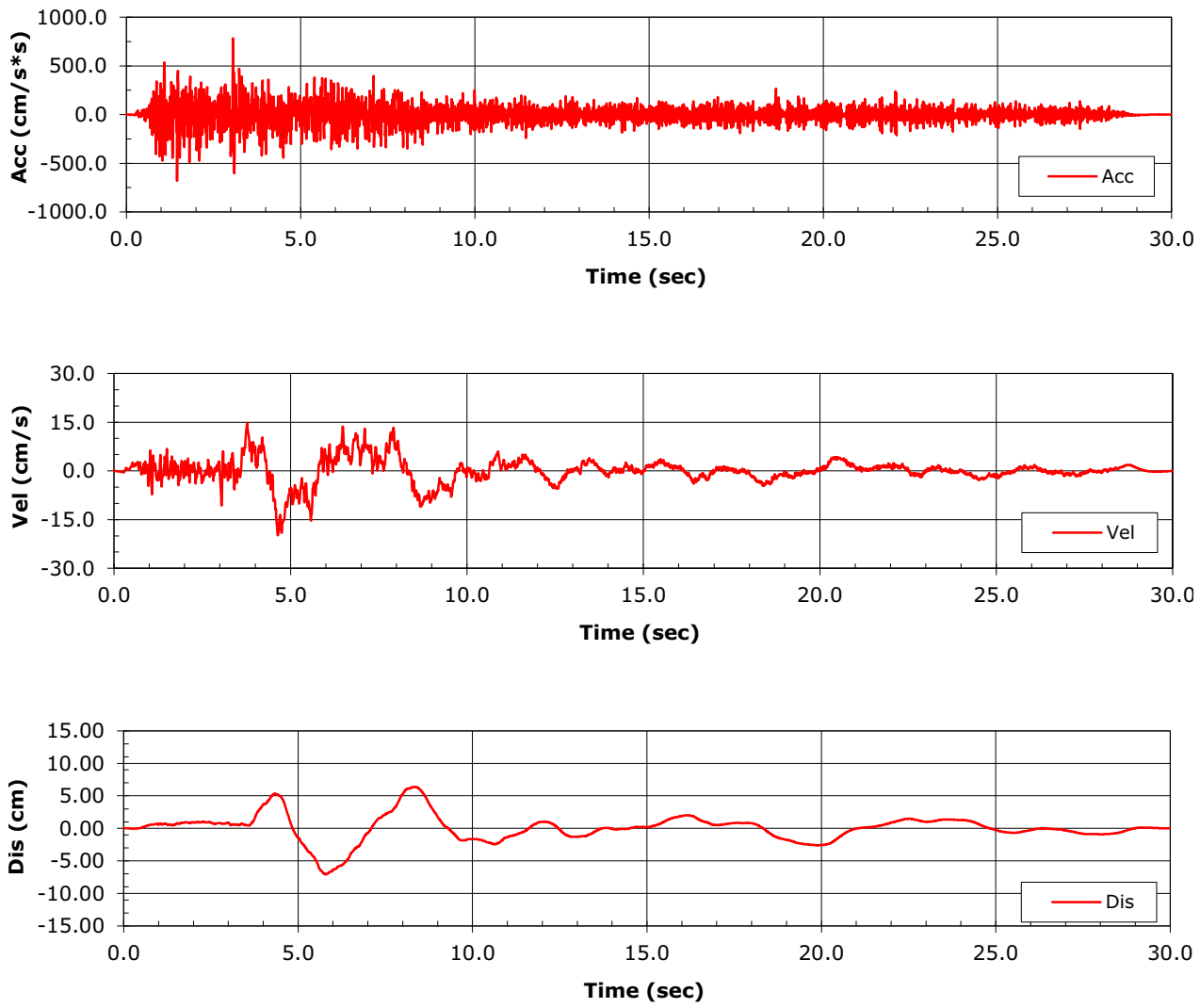

NAPS SUP 3.7-2 **Figure 3.7.1-254 Acceleration, Velocity, and Displacement Spectrally Matched Partial Column Outcrop Time-Histories for CB, H2 Component**

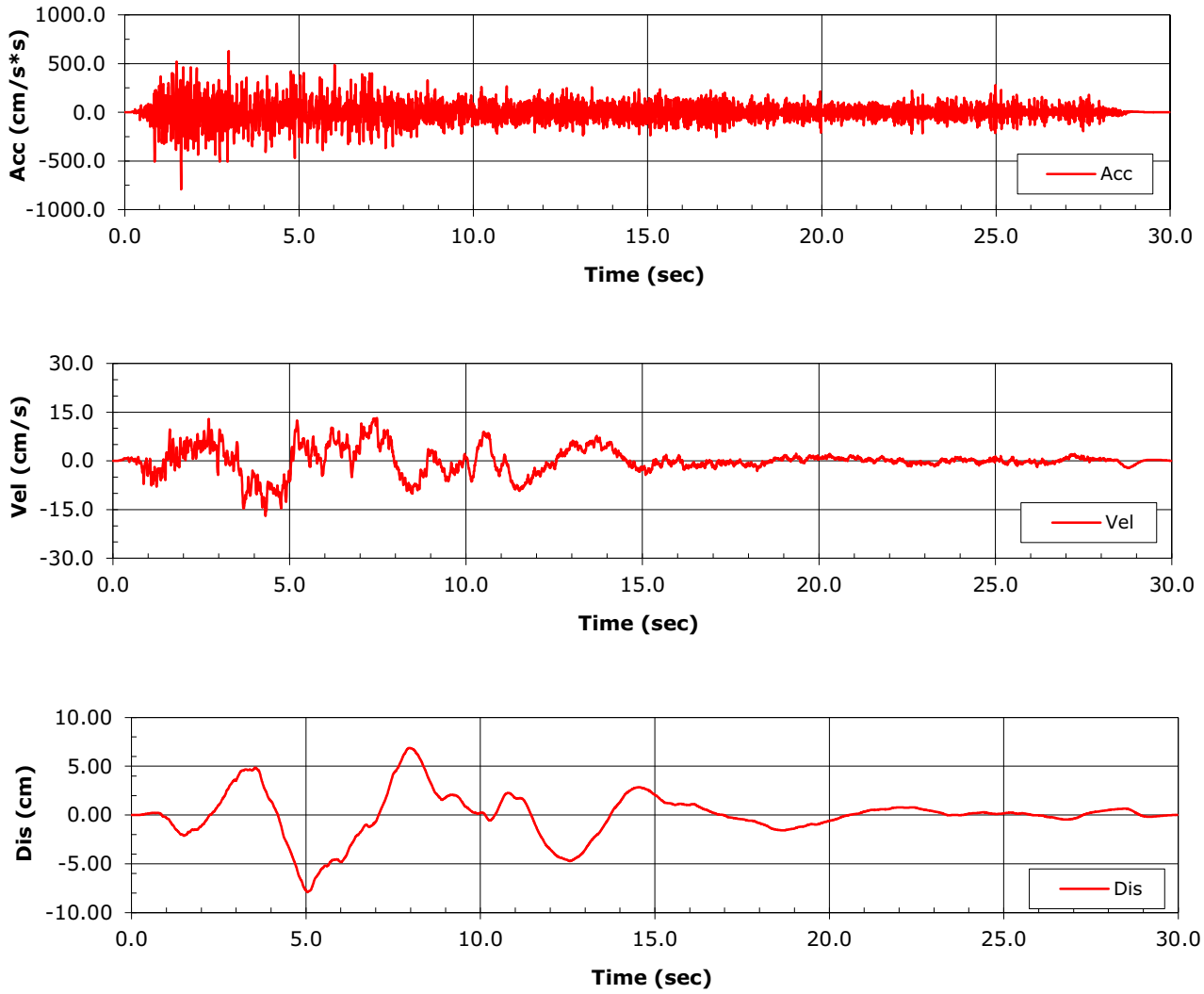

NAPS SUP 3.7-2 **Figure 3.7.1-255 Acceleration, Velocity, and Displacement Spectrally Matched Partial Column Outcrop Time-Histories for CB, UP Component**

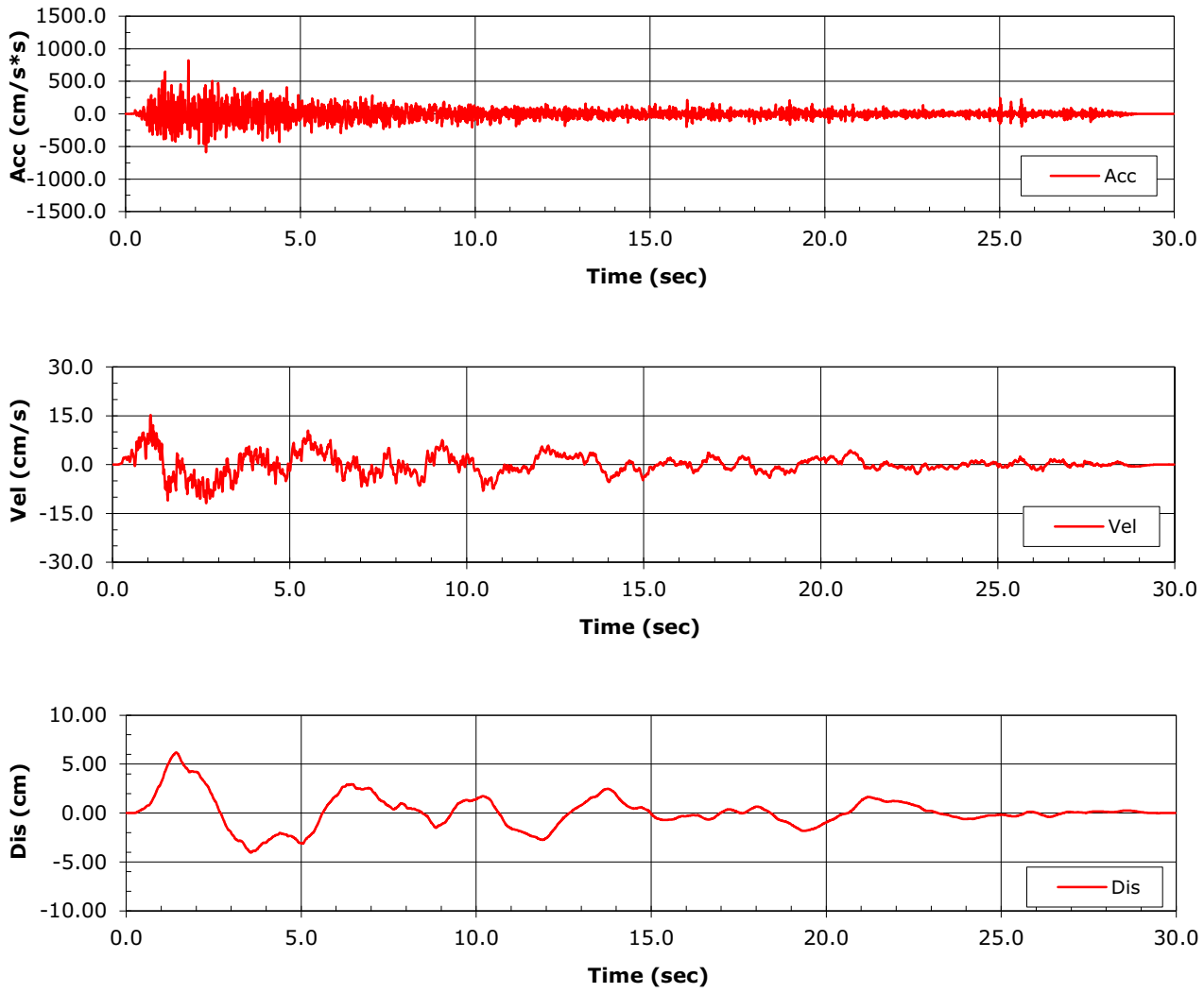

NAPS SUP 3.7-2 **Figure 3.7.1-256 Acceleration, Velocity, and Displacement Spectrally Matched Full Column Outcrop Time-Histories for CB, H1 Component**

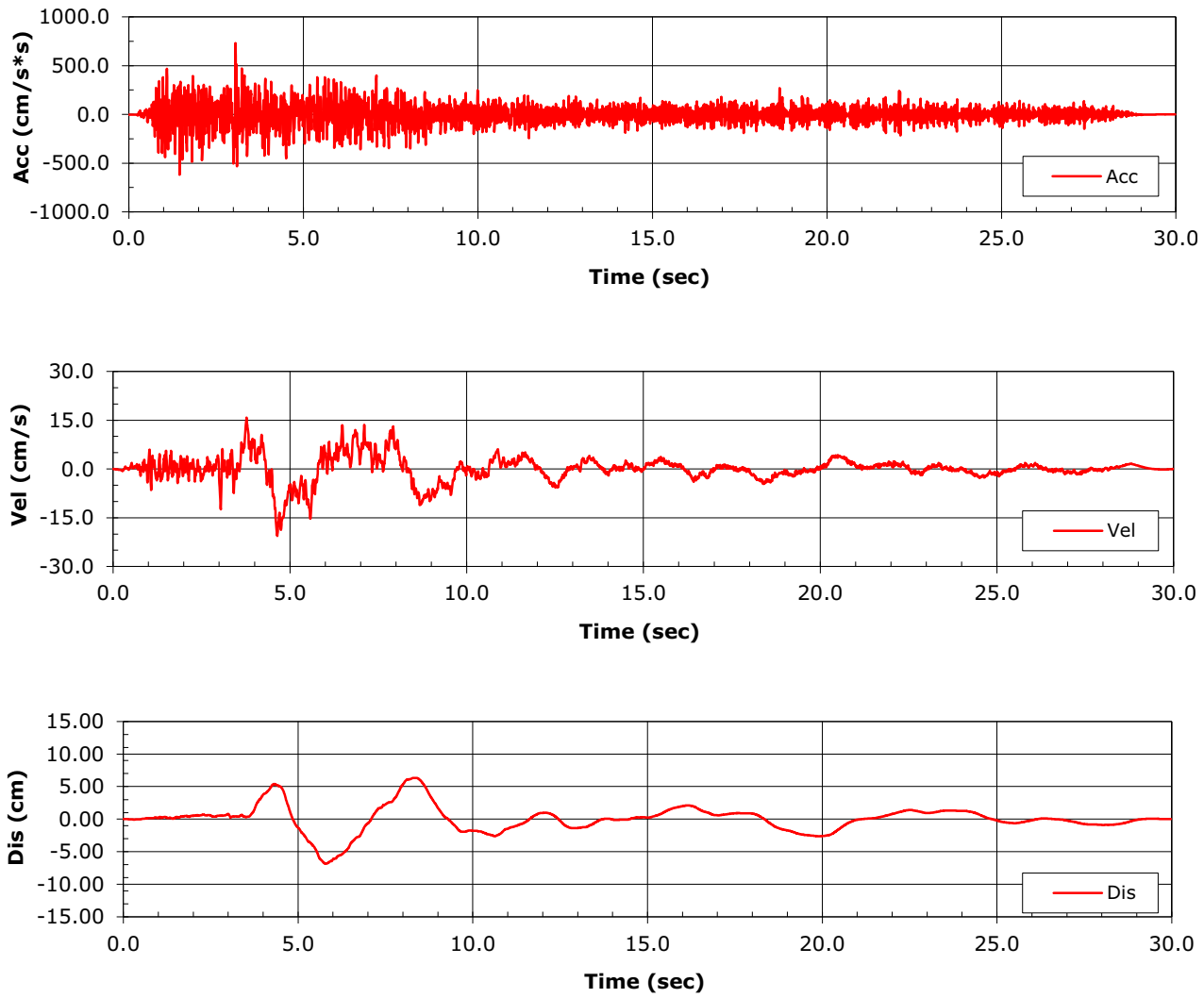

NAPS SUP 3.7-2 **Figure 3.7.1-257 Acceleration, Velocity, and Displacement Spectrally Matched Full Column Outcrop Time-Histories for CB, H2 Component**

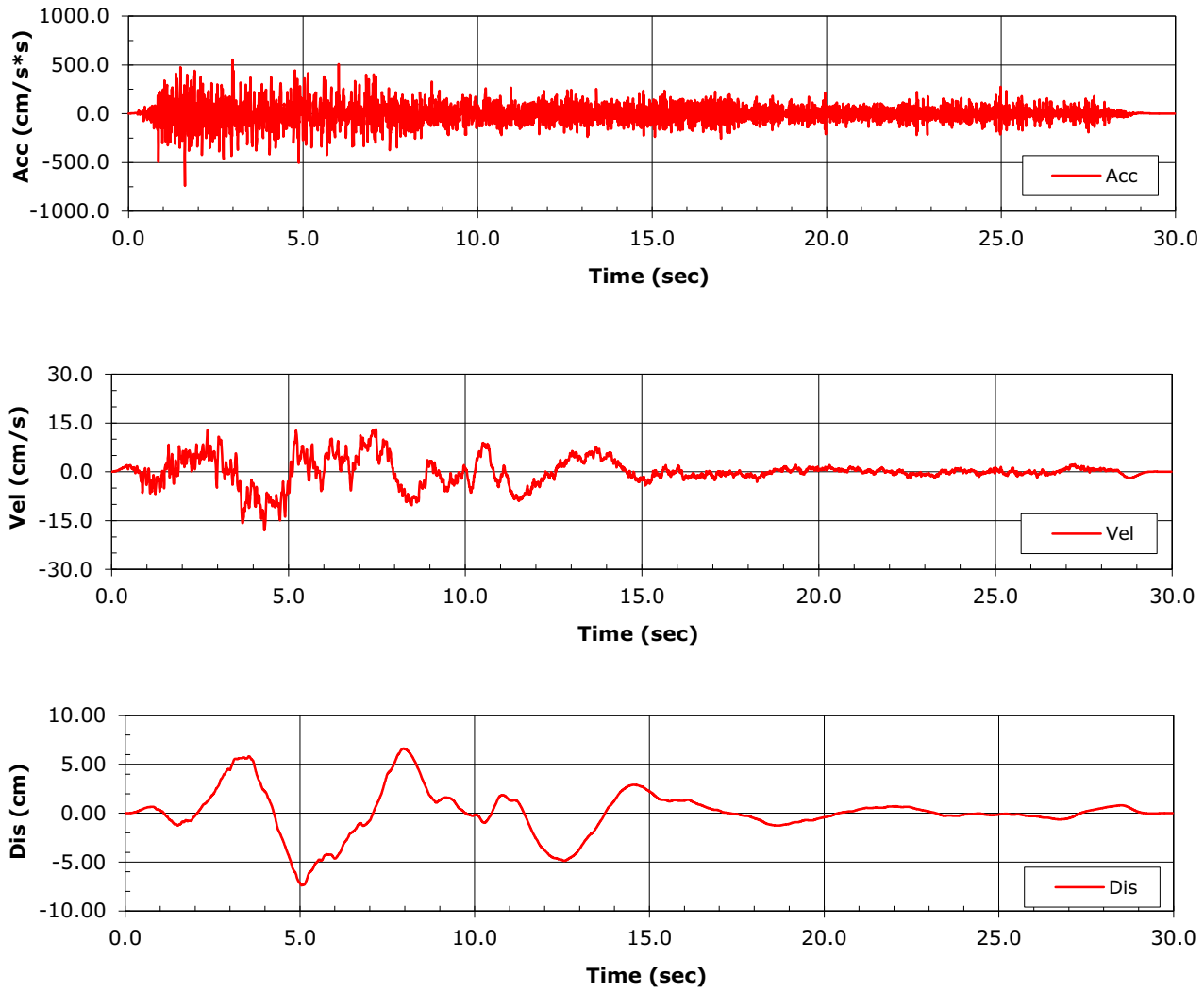

NAPS SUP 3.7-2 **Figure 3.7.1-258 Acceleration, Velocity, and Displacement Spectrally Matched Full Column Outcrop Time-Histories for CB, UP Component**

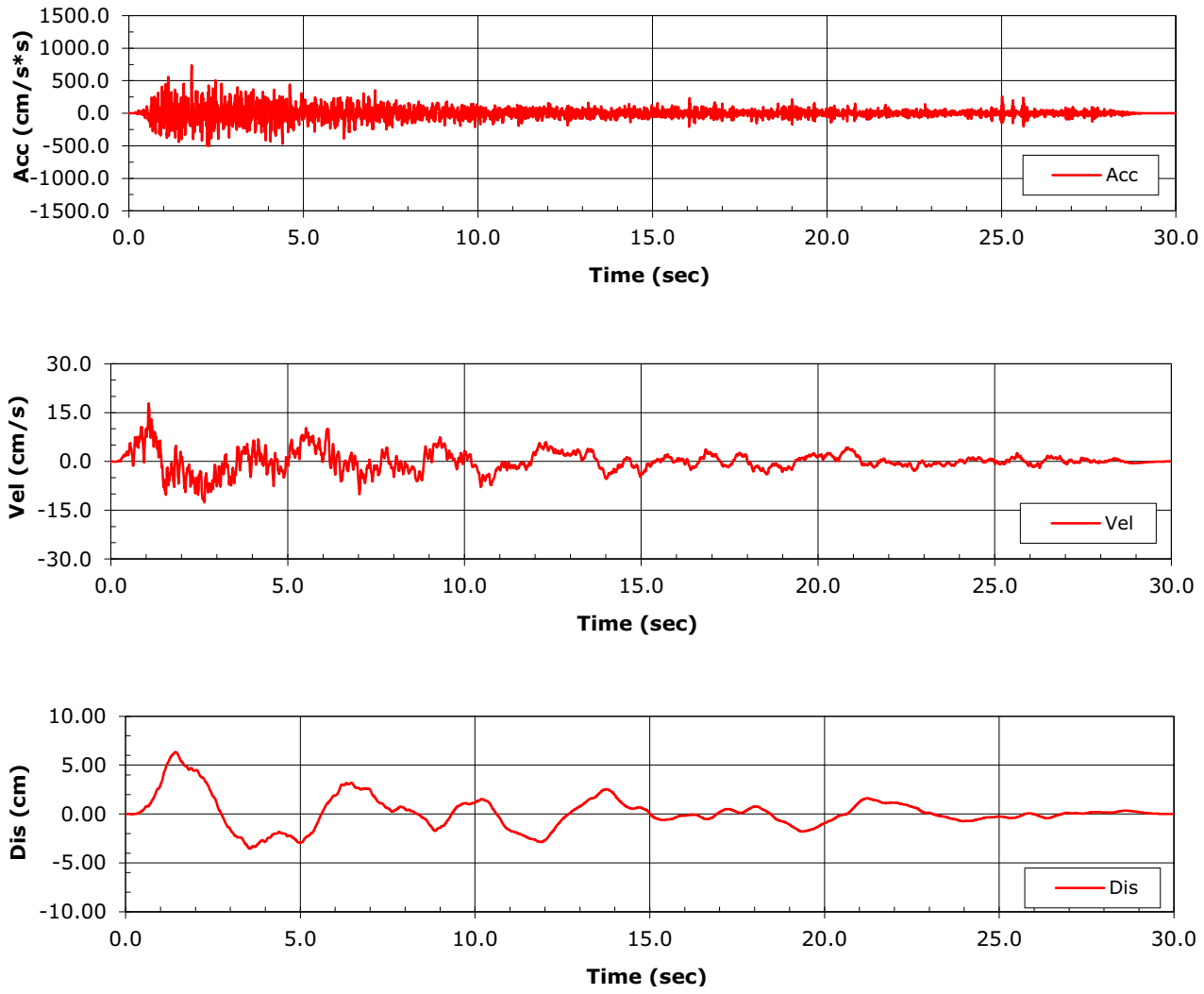

NAPS SUP 3.7-2

Figure 3.7.1-259 Comparison between the Final Scaled Spectrum Compatible Response Spectrum, the Target Spectrum, and Upper and Lower Target Spectrum Bounds for the FWSC, H1 Component at Elevation 282 ft

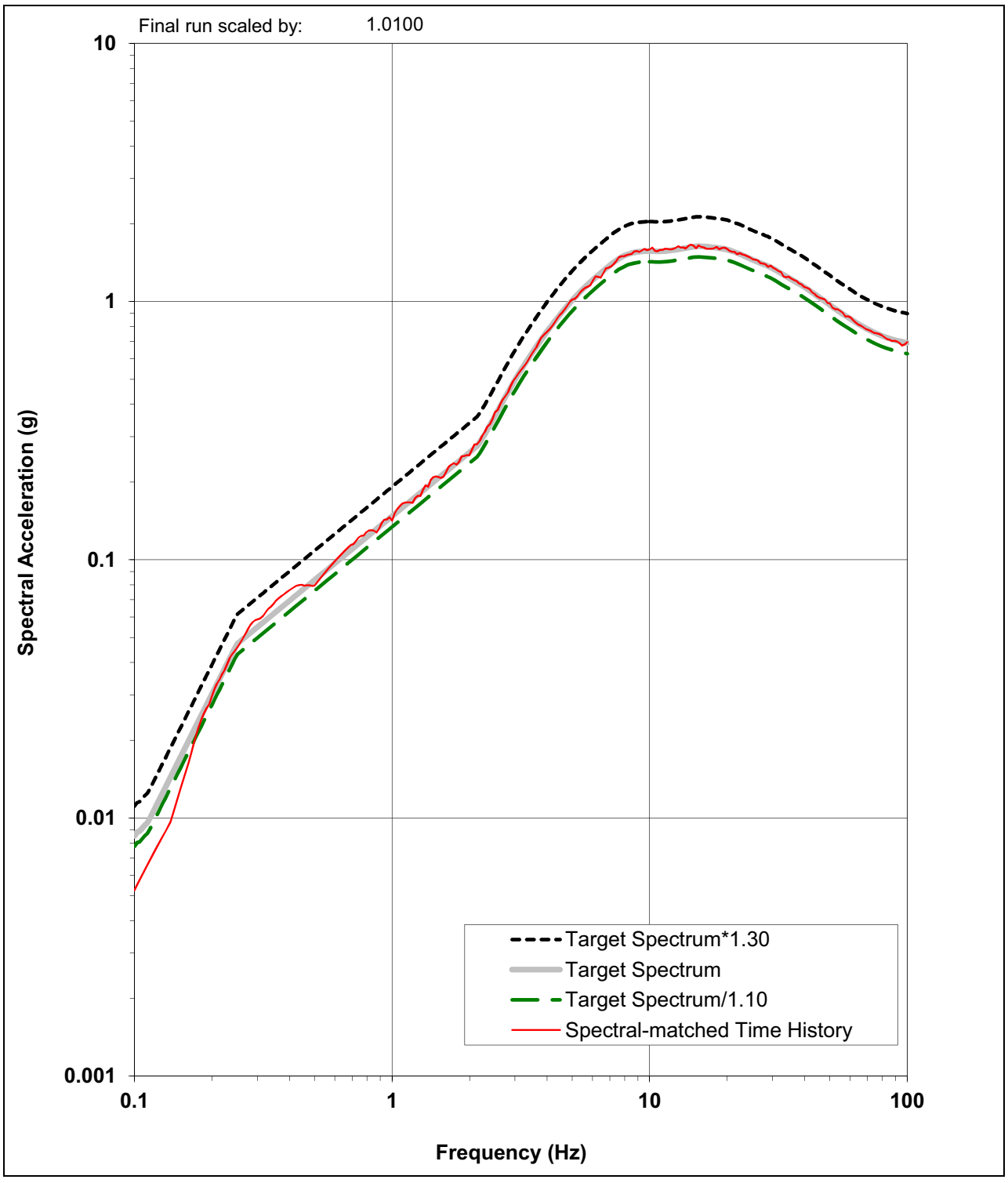

NAPS SUP 3.7-2

Figure 3.7.1-260 Comparison between the Final Scaled Spectrum Compatible Response Spectrum, the Target Spectrum, and Upper and Lower Target Spectrum Bounds for the FWSC, H2 Component at Elevation 282 ft

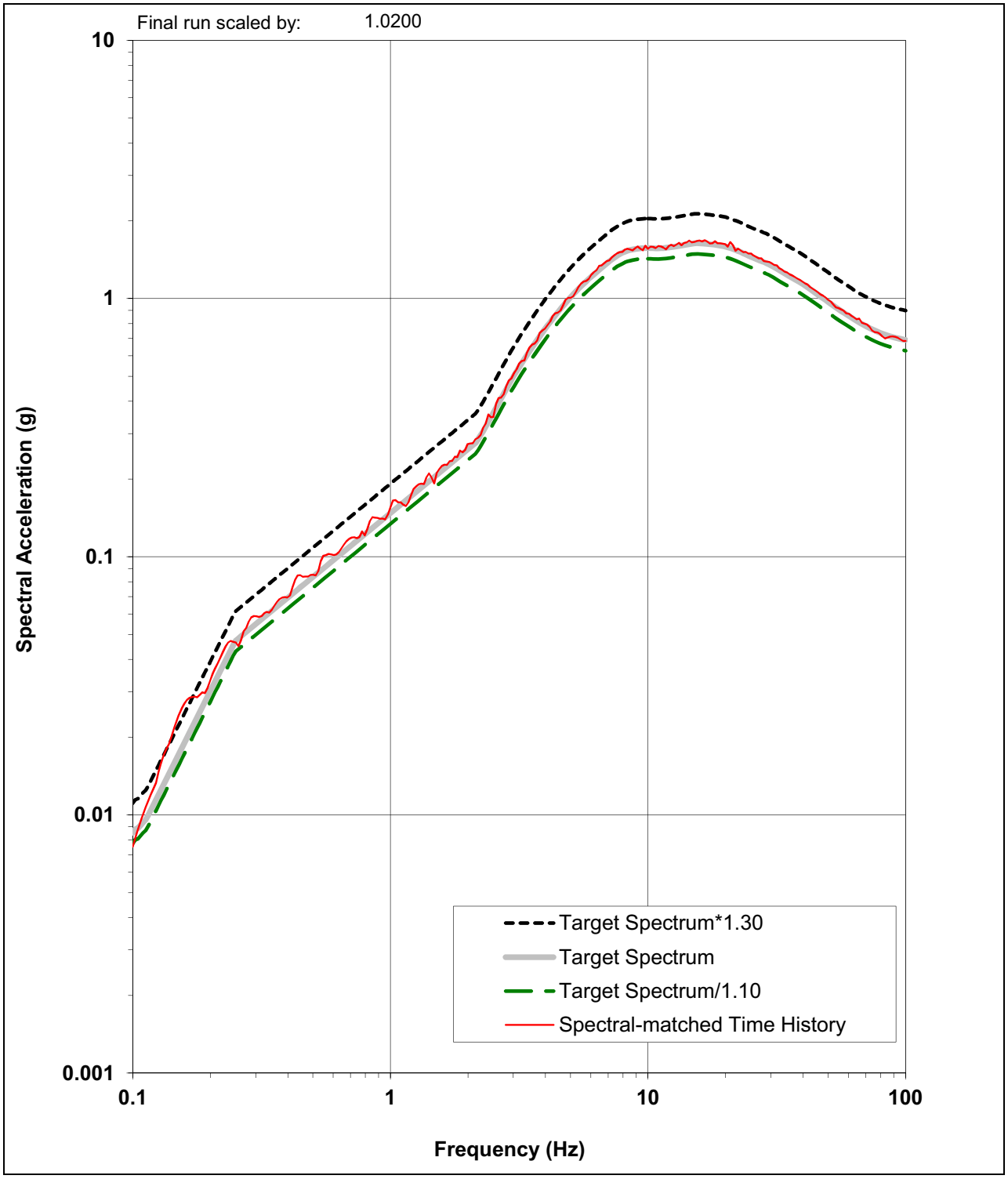

NAPS SUP 3.7-2

Figure 3.7.1-261 Comparison between the Final Scaled Spectrum Compatible Response Spectrum, the Target Spectrum, and Upper and Lower Target Spectrum Bounds for the FWSC, UP Component at Elevation 282 ft

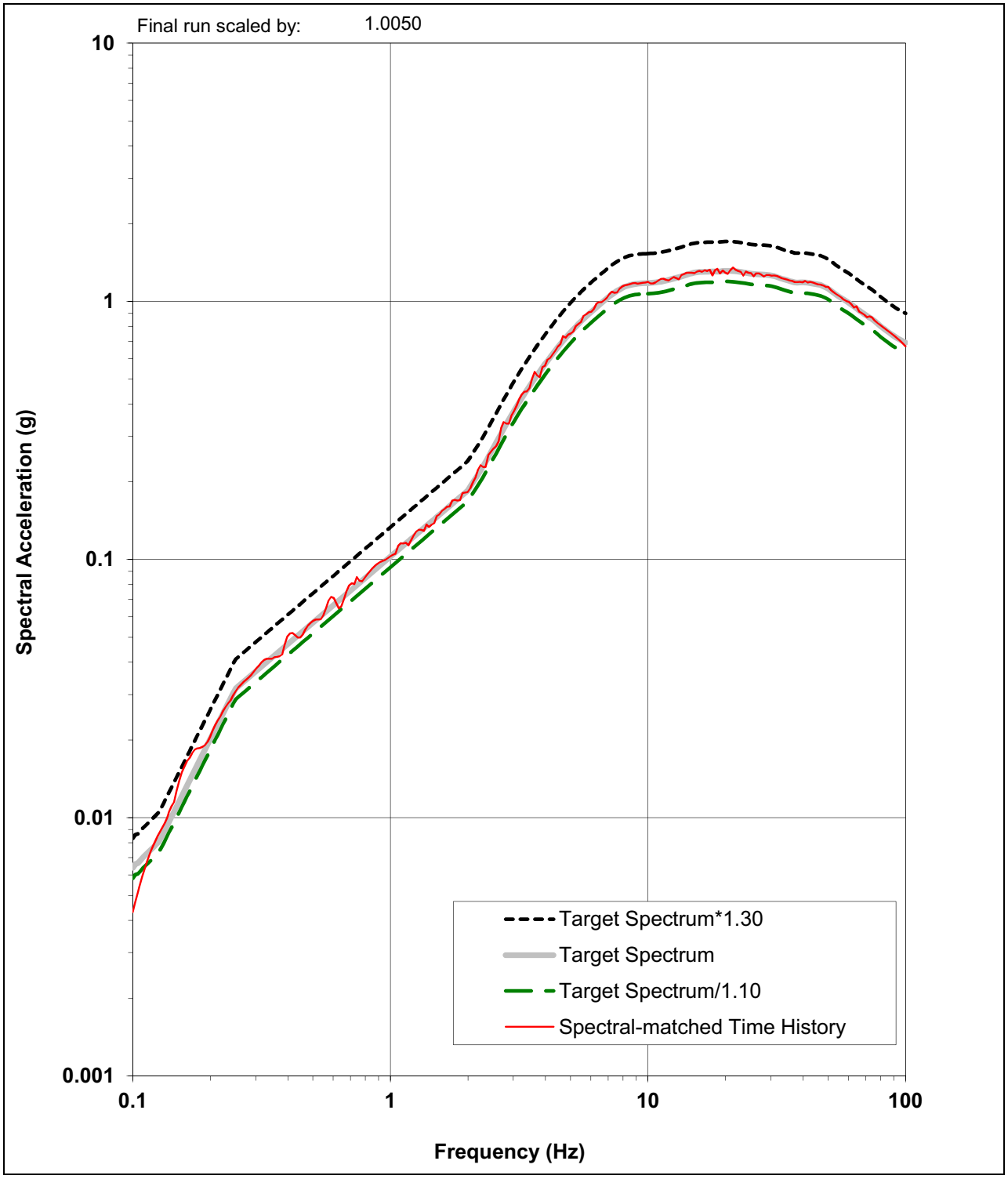

NAPS SUP 3.7-2 **Figure 3.7.1-262 Acceleration, Velocity, and Displacement Spectrally Matched Partial Column Outcrop Time Histories for the FWSC, H1 Component at Elevation 282 ft**

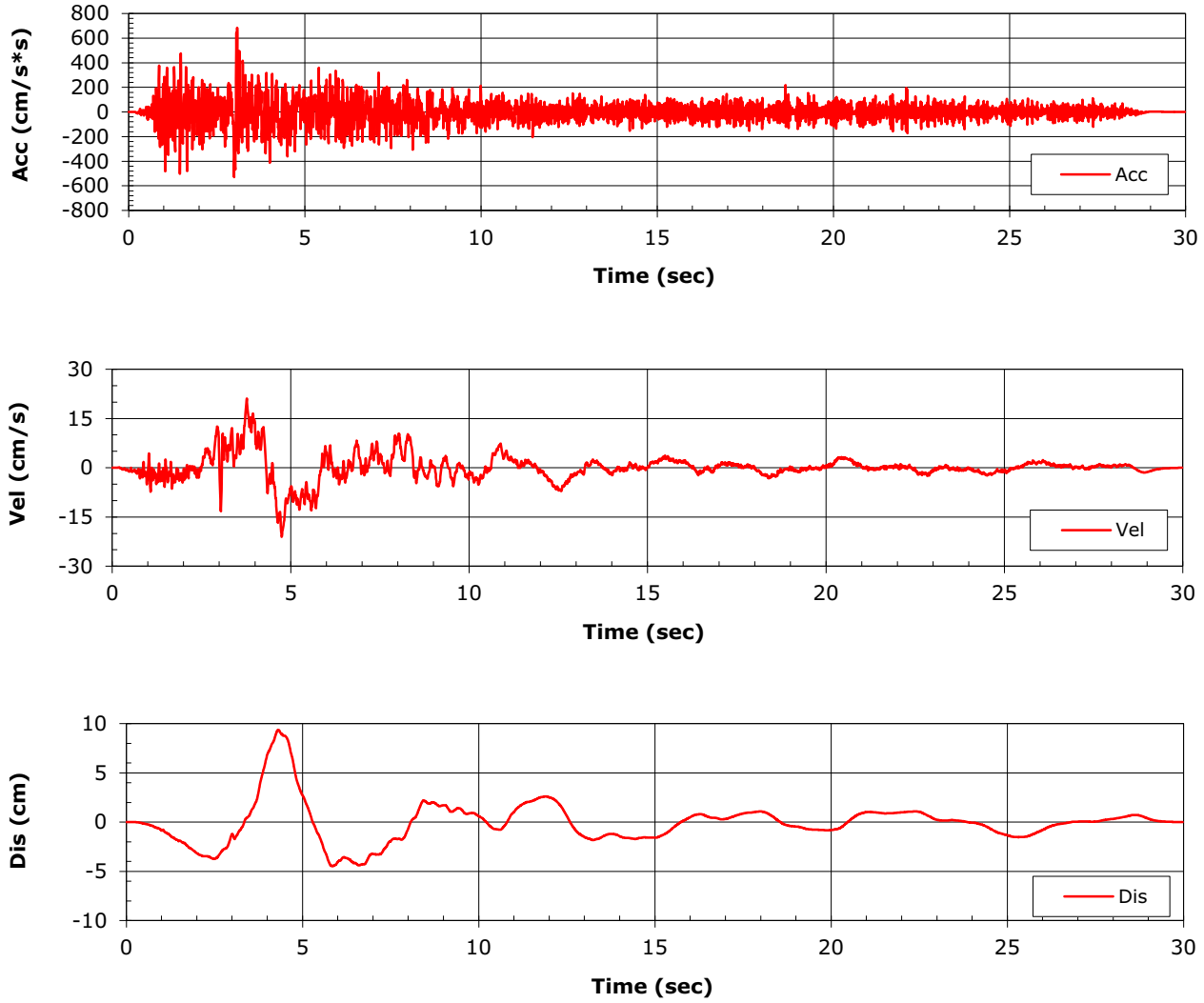

NAPS SUP 3.7-2 **Figure 3.7.1-263 Acceleration, Velocity, and Displacement Spectrally Matched Partial Column Outcrop Time Histories for the FWSC, H2 Component at Elevation 282 ft**

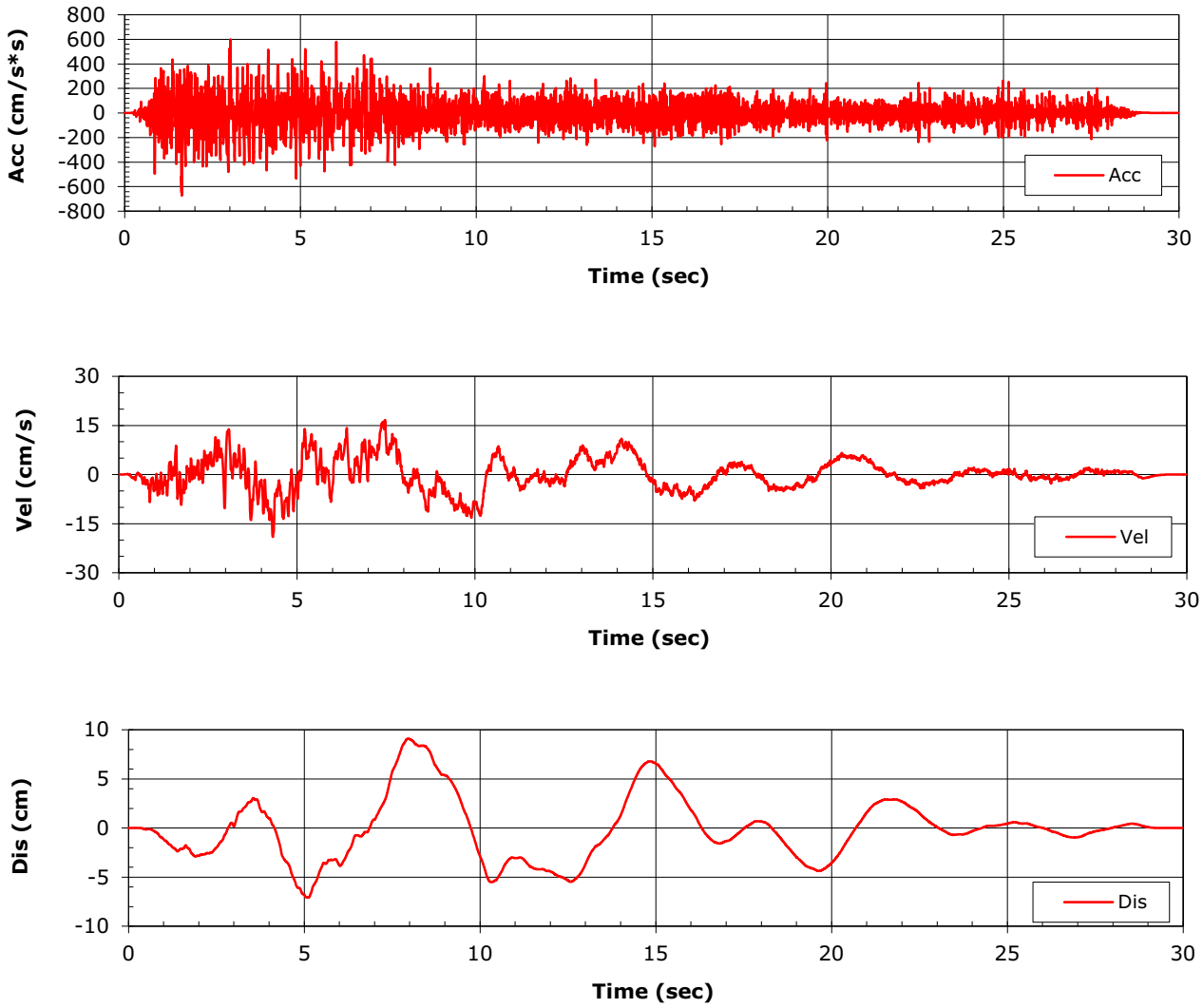

NAPS SUP 3.7-2 **Figure 3.7.1-264 Acceleration, Velocity, and Displacement Spectrally Matched Partial Column Outcrop Time Histories for the FWSC, UP Component at Elevation 282 ft**

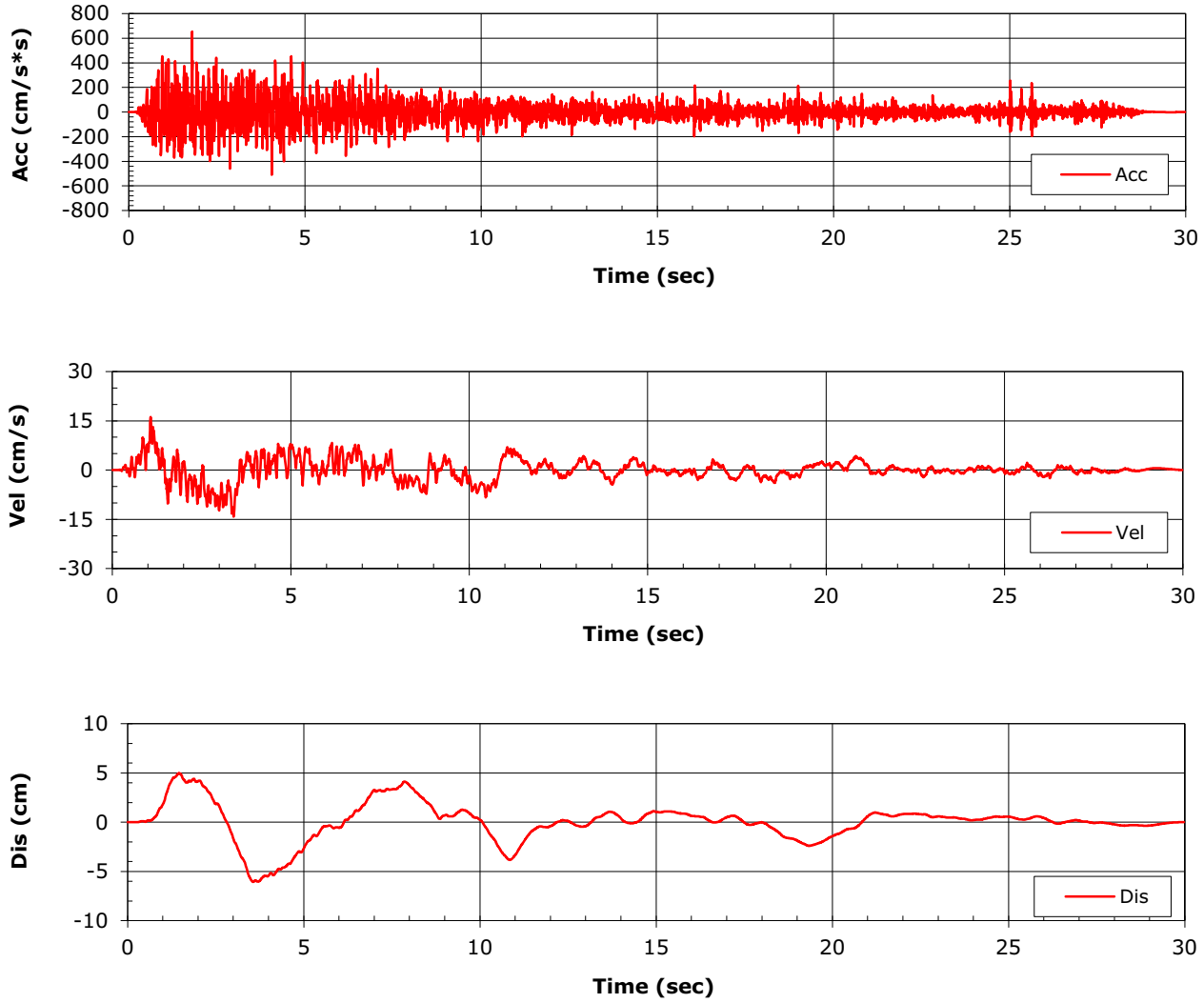

NAPS SUP 3.7-2 **Figure 3.7.1-265 Development of Horizontal Site-Dependent SSE and OBE at Grade**

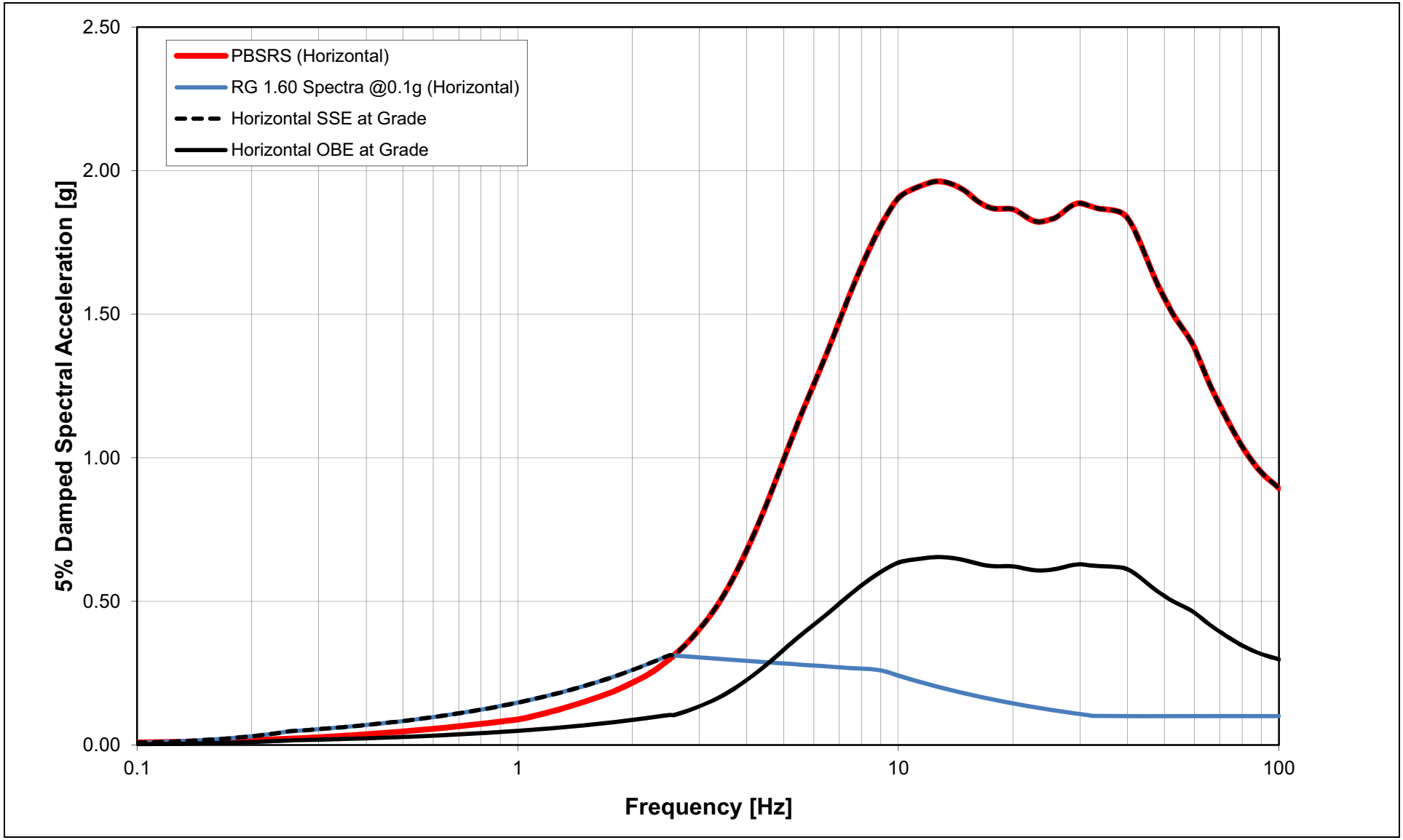

NAPS SUP 3.7-2 **Figure 3.7.1-266 Development of Vertical Site-Dependent SSE and OBE at Grade**

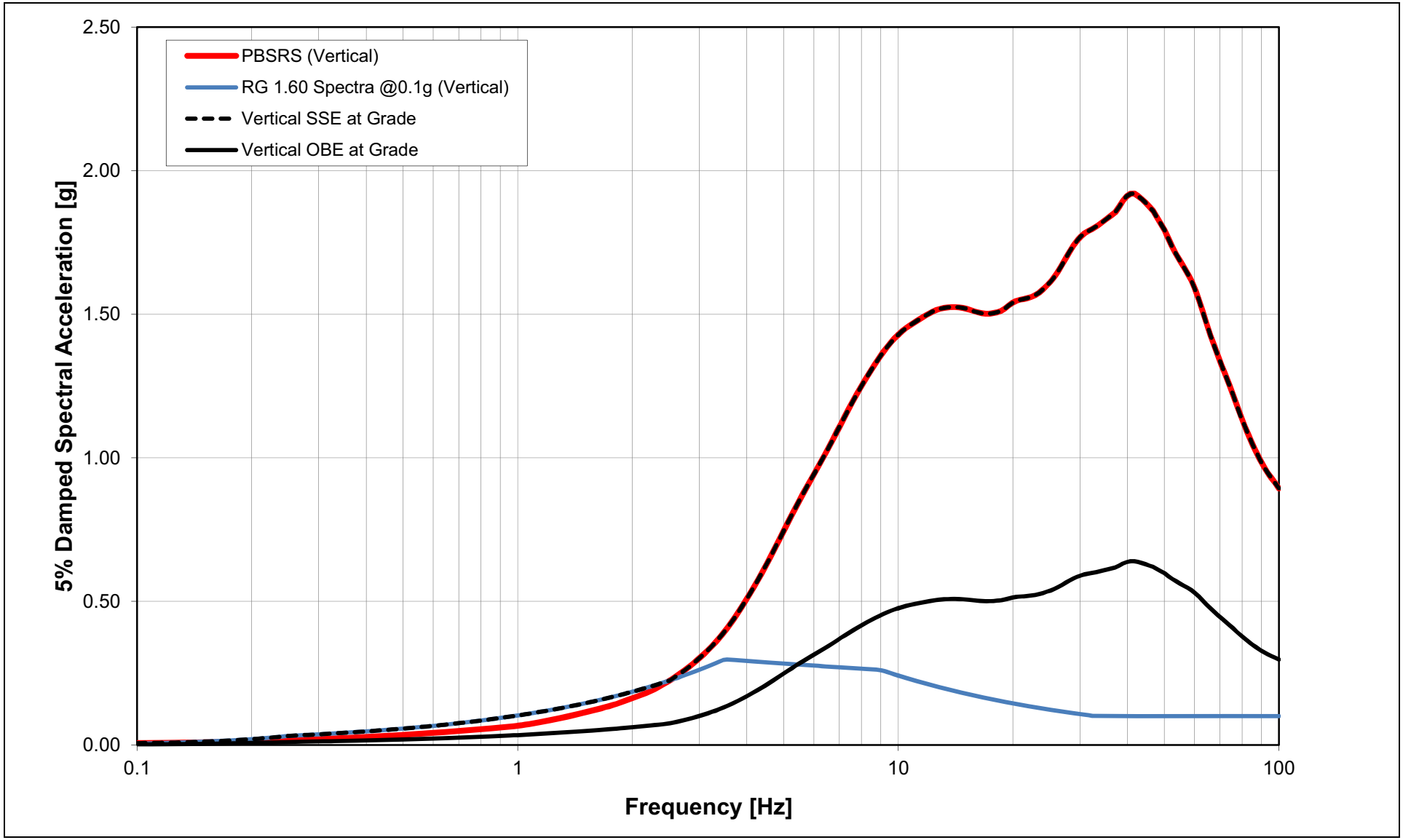

NAPS SUP 3.7-2 **Figure 3.7.1-267 Site-Dependent SSE and OBE at Grade**

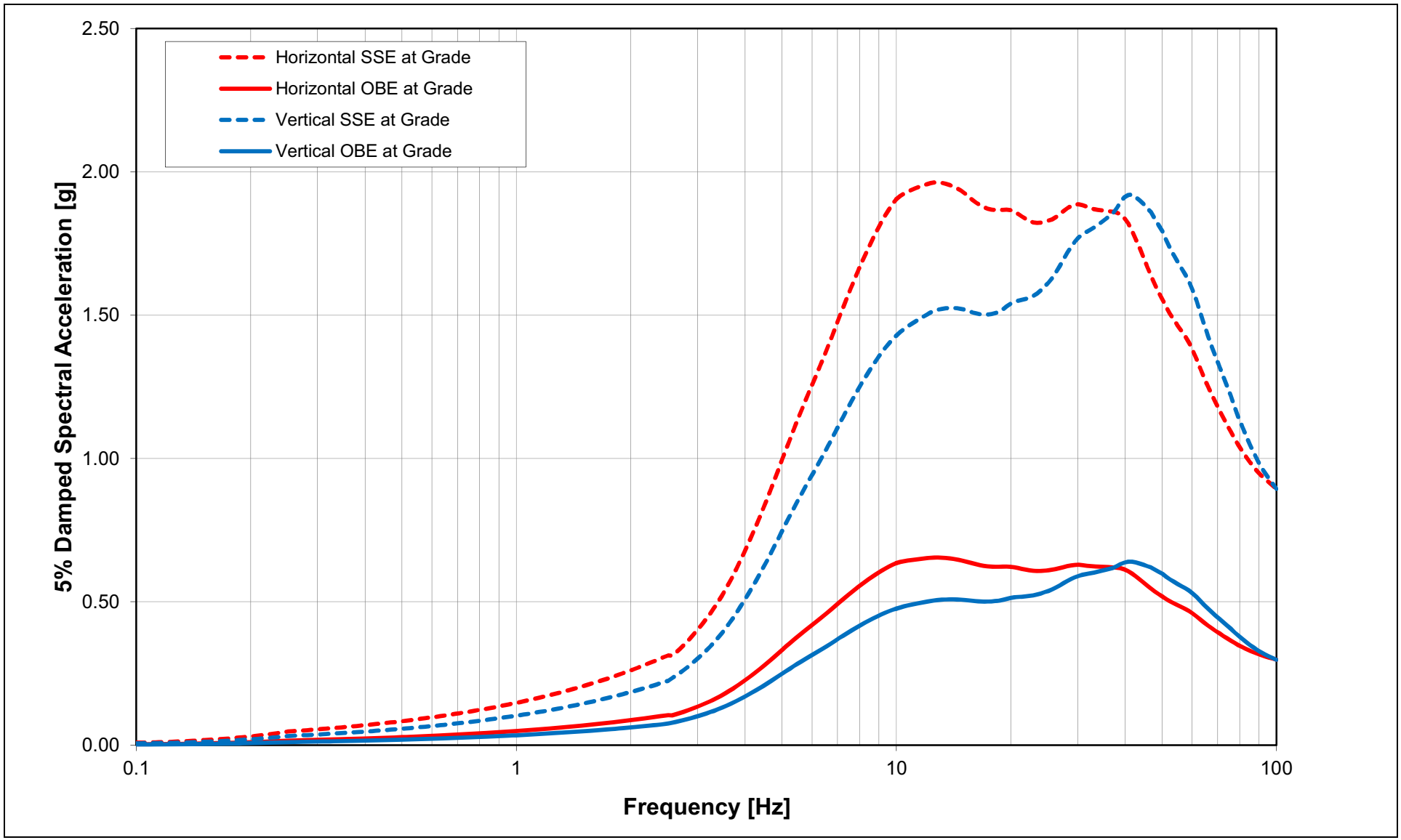

NAPS SUP 3.7-2 **Figure 3.7.1-268 PSD for the H1 Component of the RB/FB Partial Profile Spectrum Compatible Acceleration Time History**

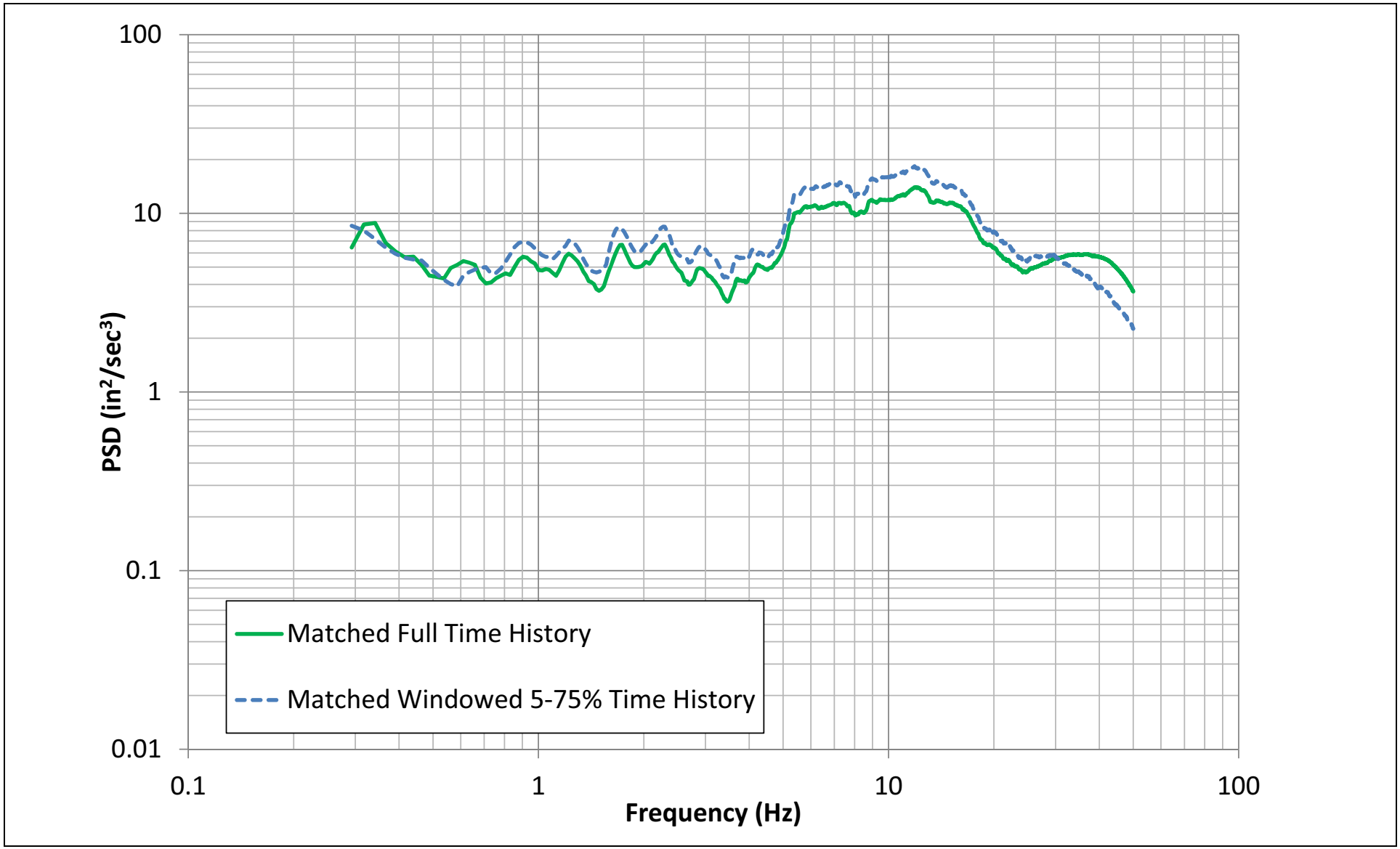

NAPS SUP 3.7-2 **Figure 3.7.1-269 PSD for the H2 Component of the RB/FB Partial Profile Spectrum Compatible Acceleration Time History**

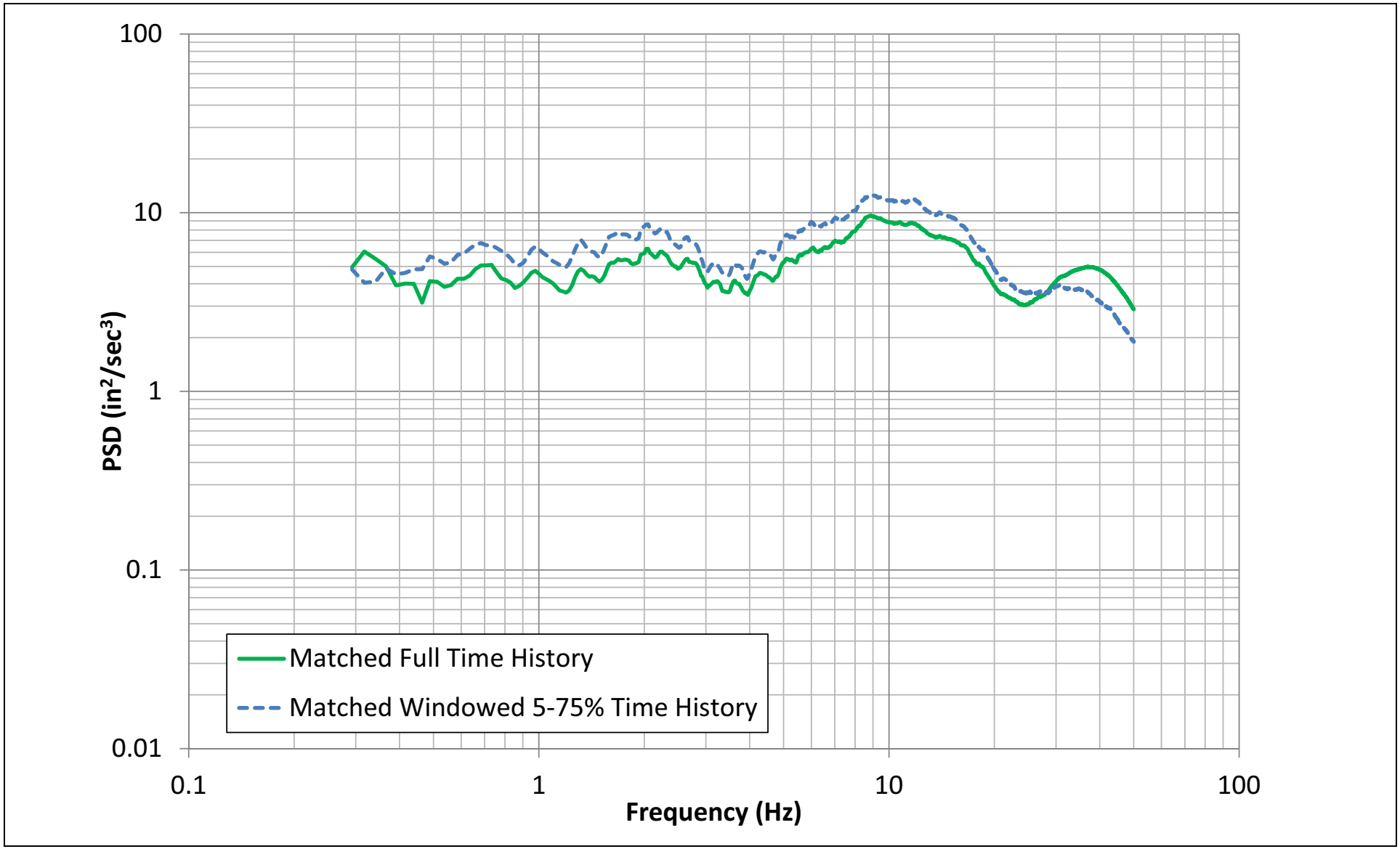

NAPS SUP 3.7-2 **Figure 3.7.1-270 PSD for the UP Component of the RB/FB Partial Profile Spectrum Compatible Acceleration Time History**

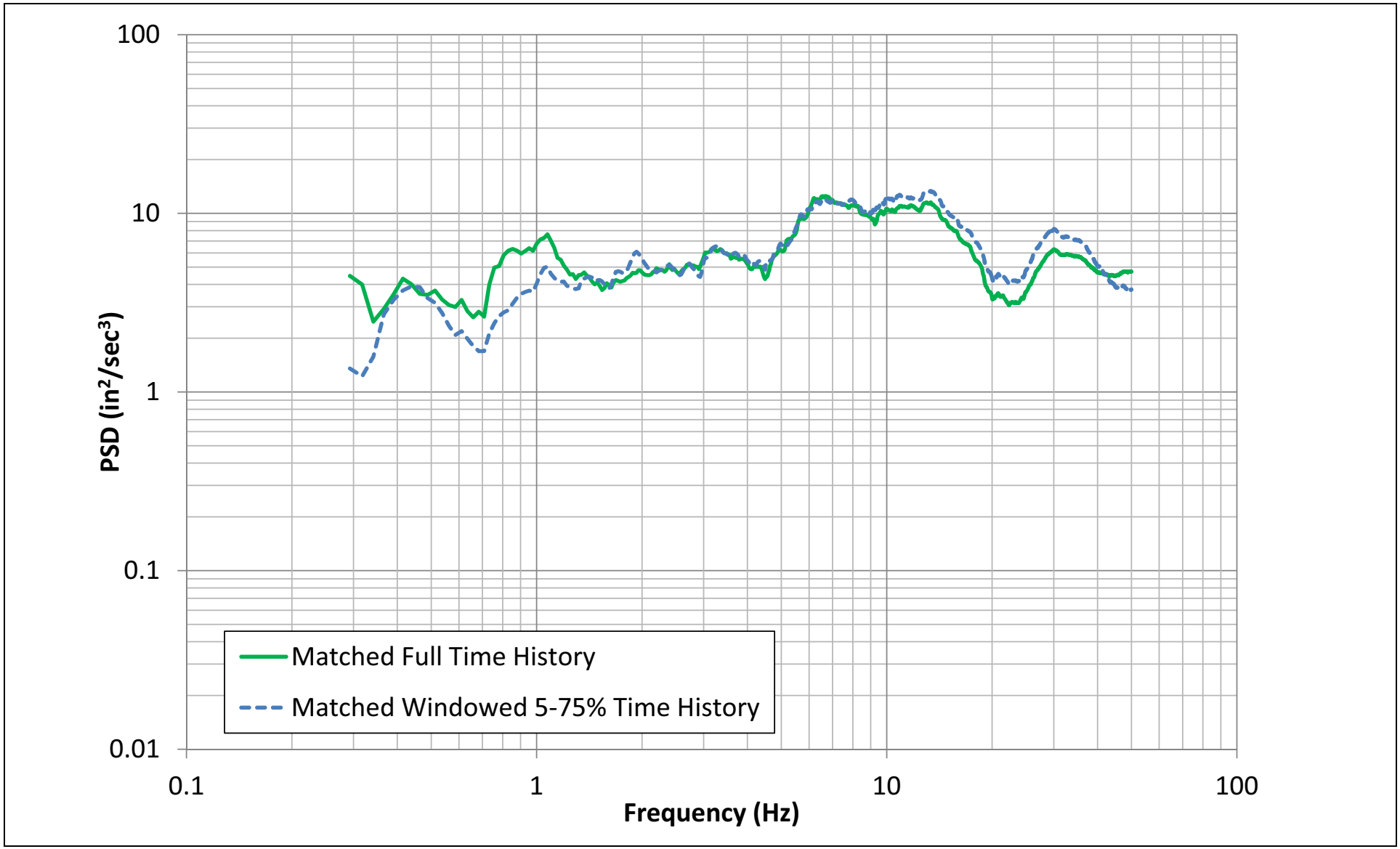

NAPS SUP 3.7-2 **Figure 3.7.1-271 PSD for the H1 Component of the RB/FB Full Profile Spectrum Compatible Acceleration Time History**

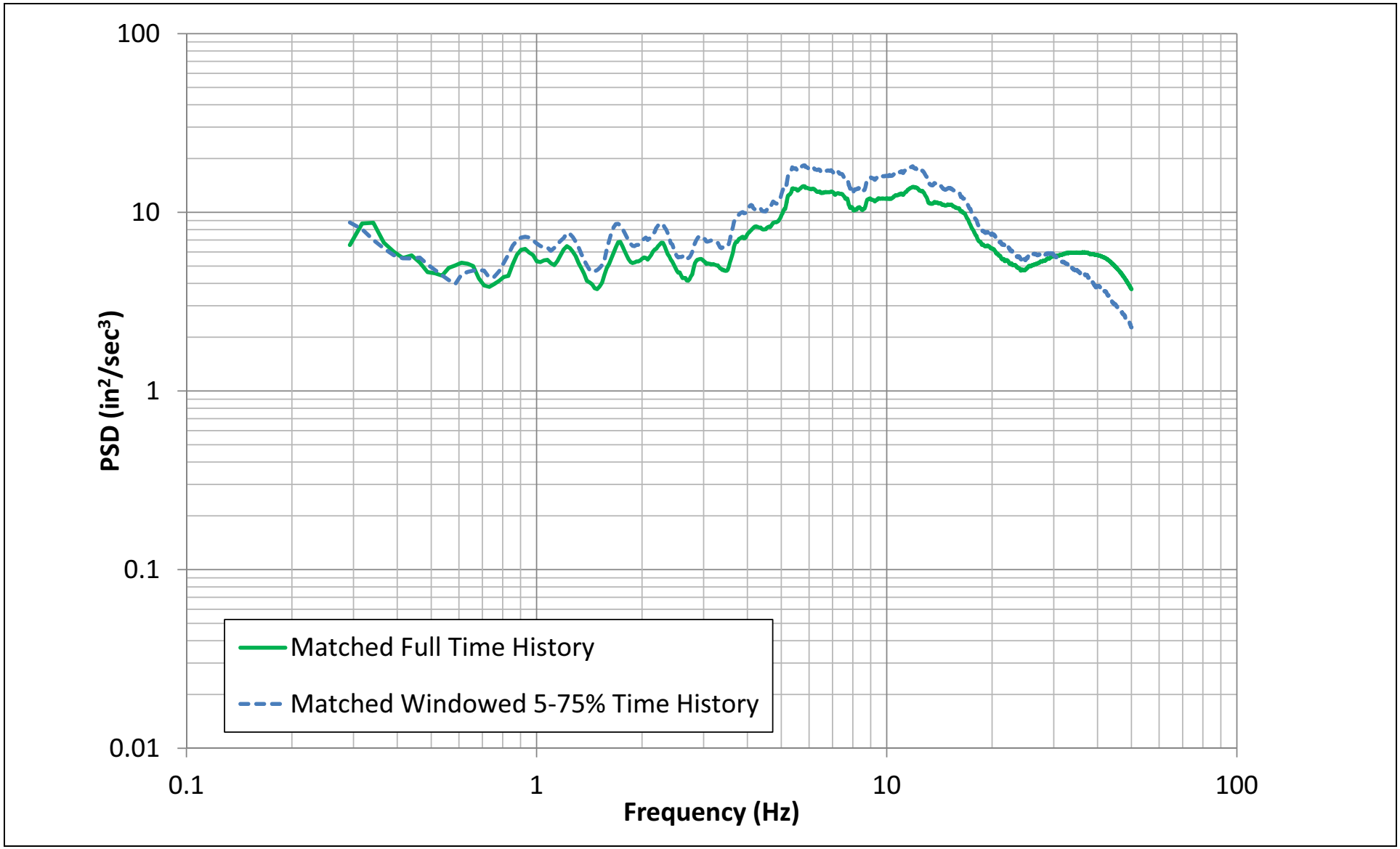

NAPS SUP 3.7-2 **Figure 3.7.1-272 PSD for the H2 Component of the RB/FB Full Profile Spectrum Compatible Acceleration Time History**

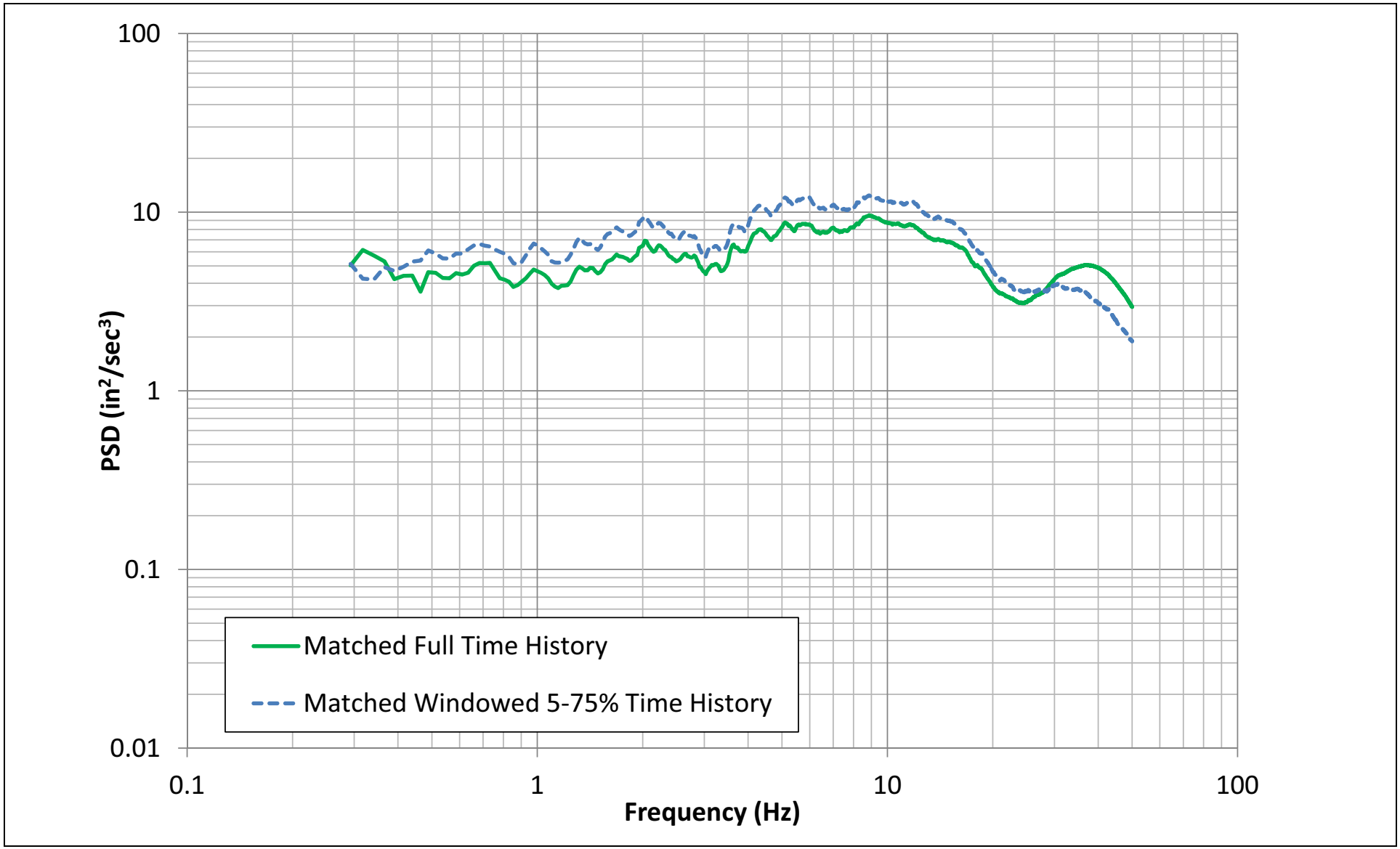

NAPS SUP 3.7-2 **Figure 3.7.1-273 PSD for the UP Component of the RB/FB Full Profile Spectrum Compatible Acceleration Time History**

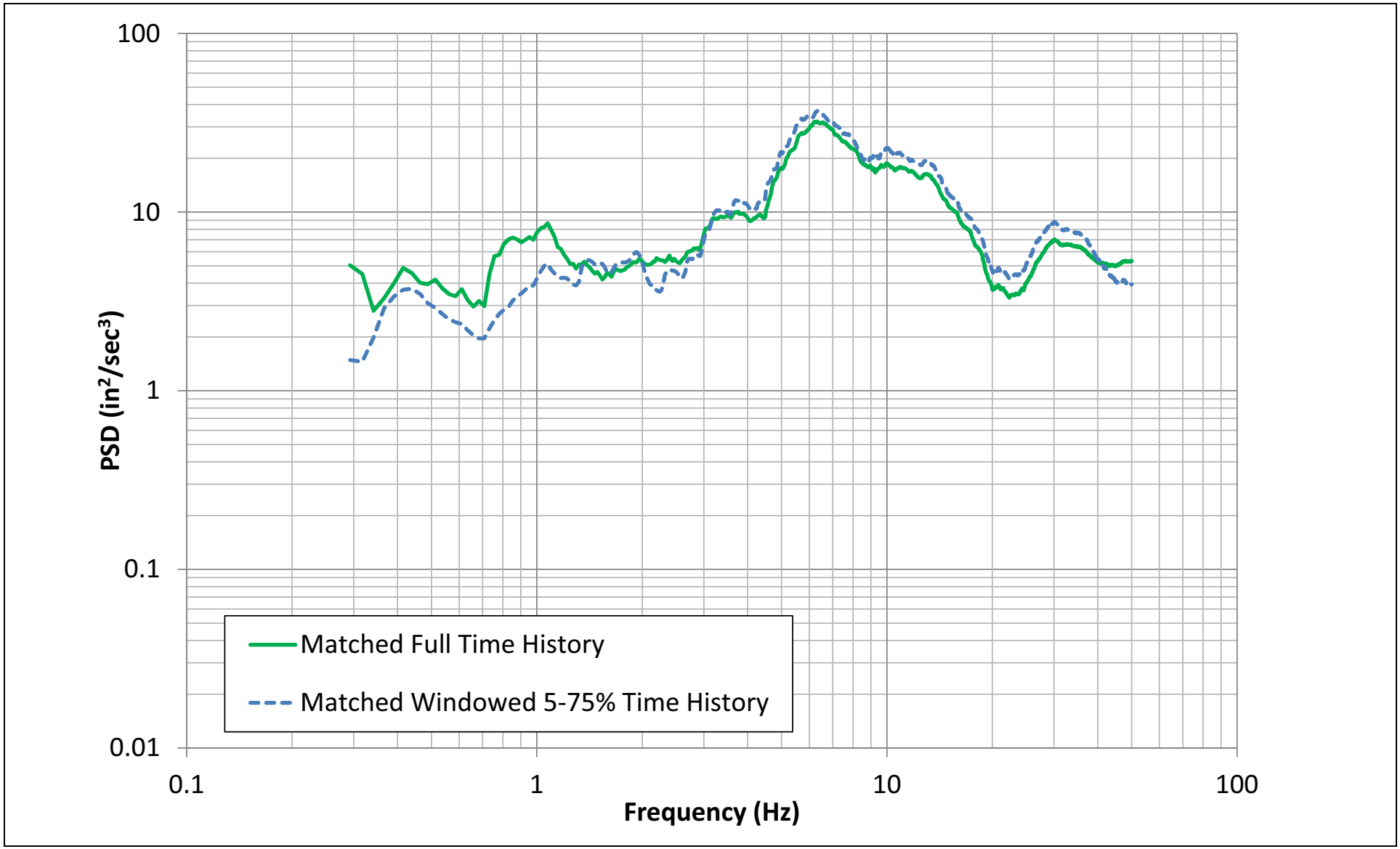

NAPS SUP 3.7-2 **Figure 3.7.1-274 PSD for the H1 Component of the CB Partial Profile Spectrum Compatible Acceleration Time History**

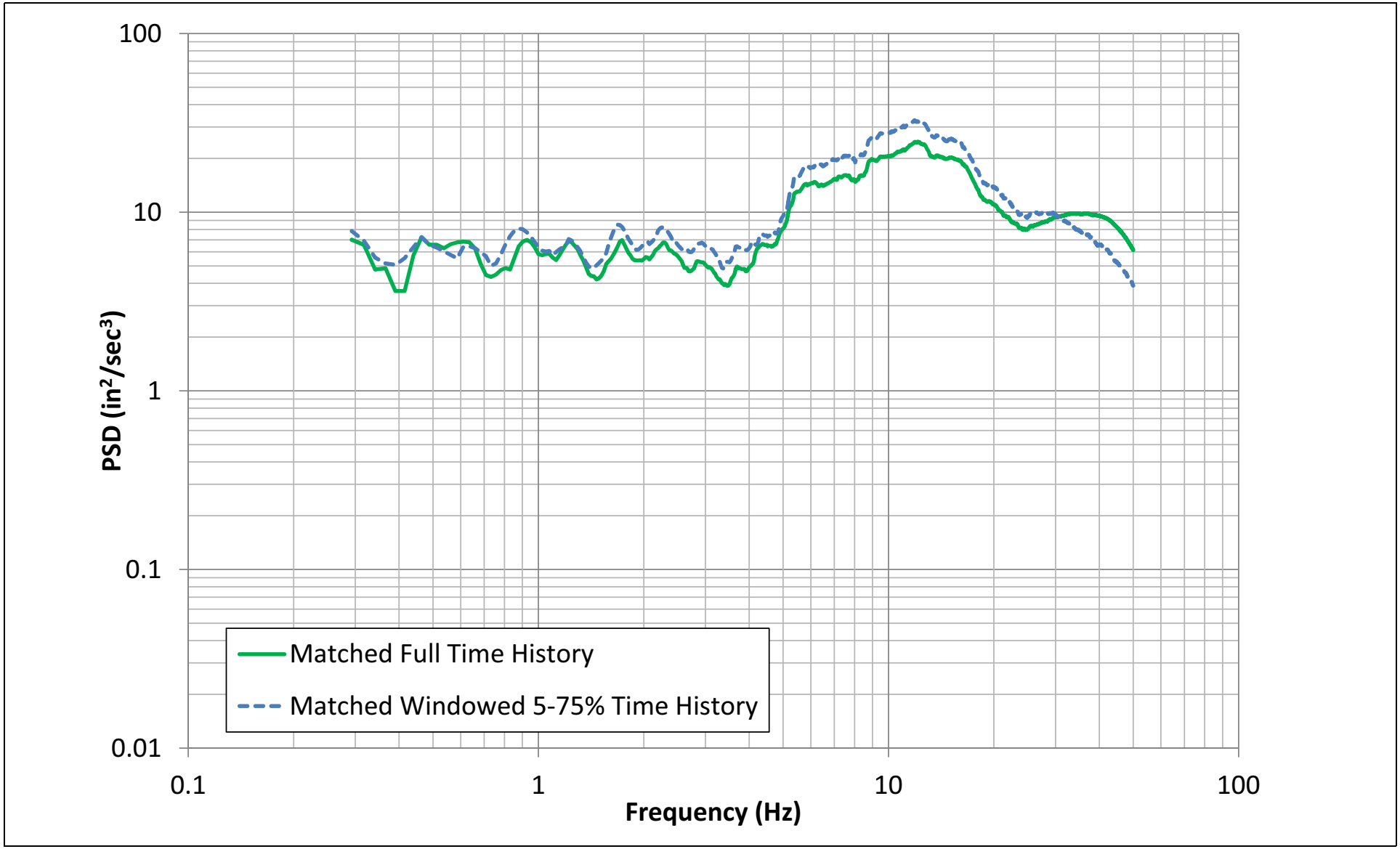

NAPS SUP 3.7-2 **Figure 3.7.1-275 PSD for the H2 Component of the CB Partial Profile Spectrum Compatible Acceleration Time History**

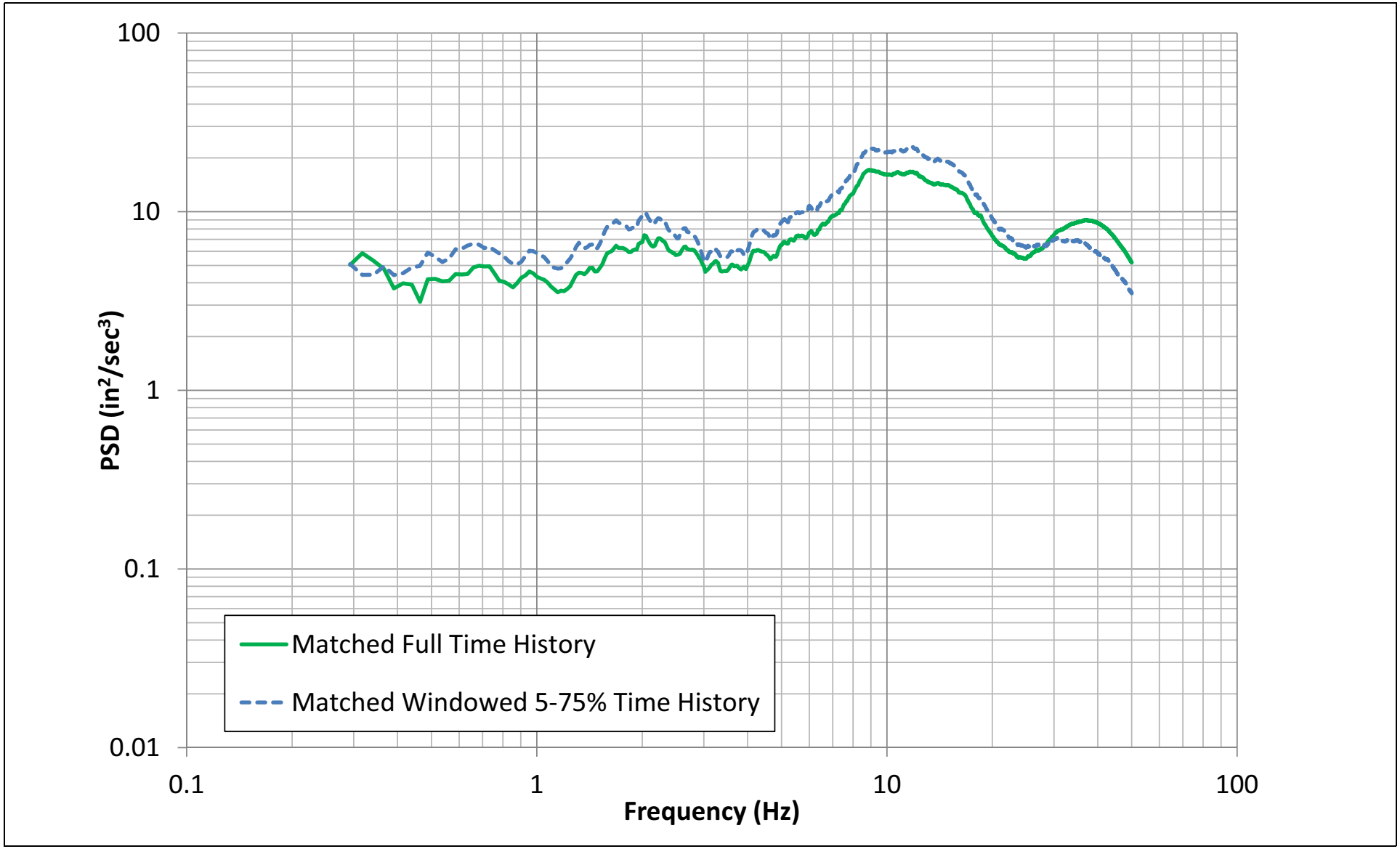

NAPS SUP 3.7-2 **Figure 3.7.1-276 PSD for the UP Component of the CB Partial Profile Spectrum Compatible Acceleration Time History**

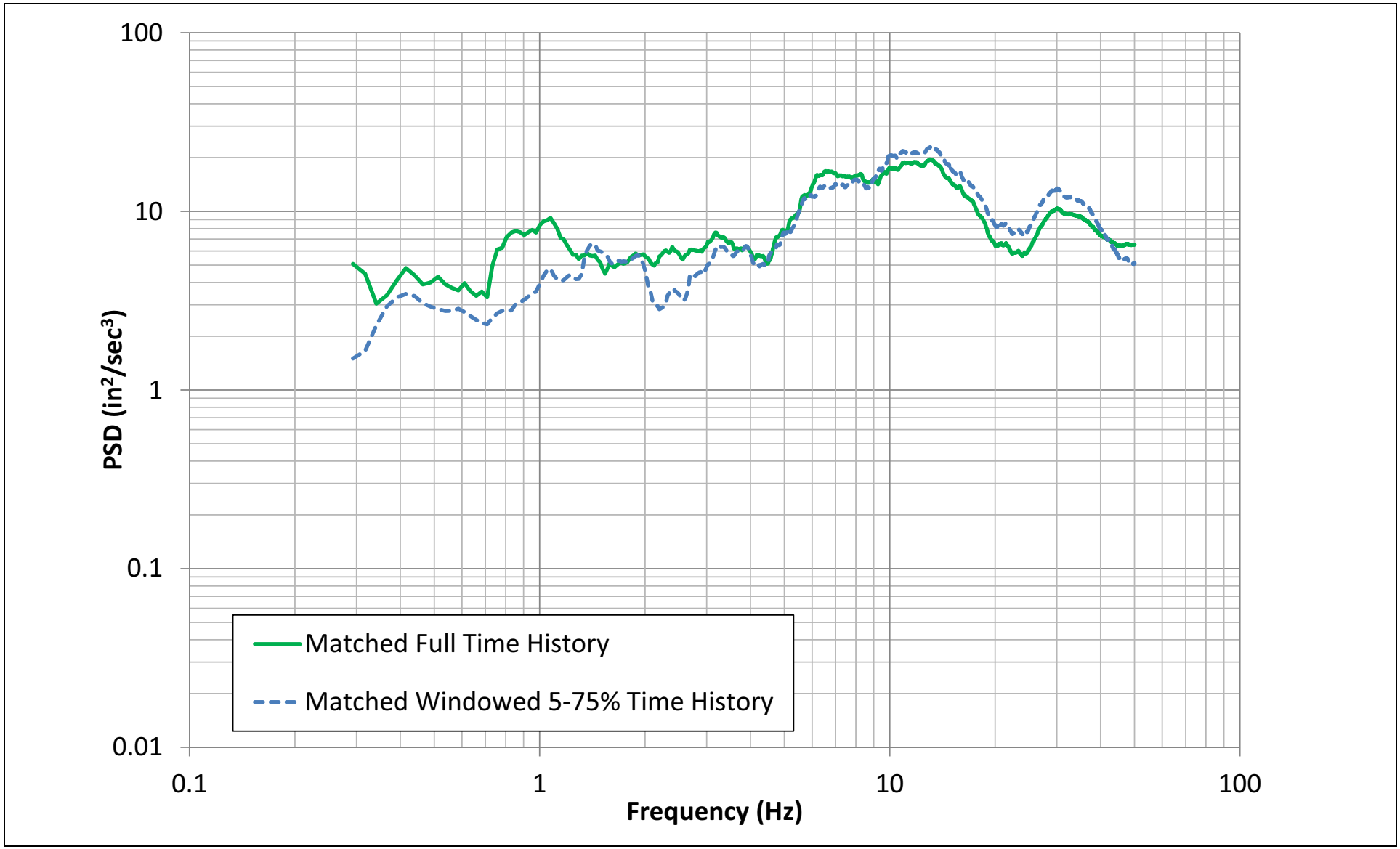

NAPS SUP 3.7-2 **Figure 3.7.1-277 PSD for the H1 Component of the CB Full Profile Spectrum Compatible Acceleration Time History**

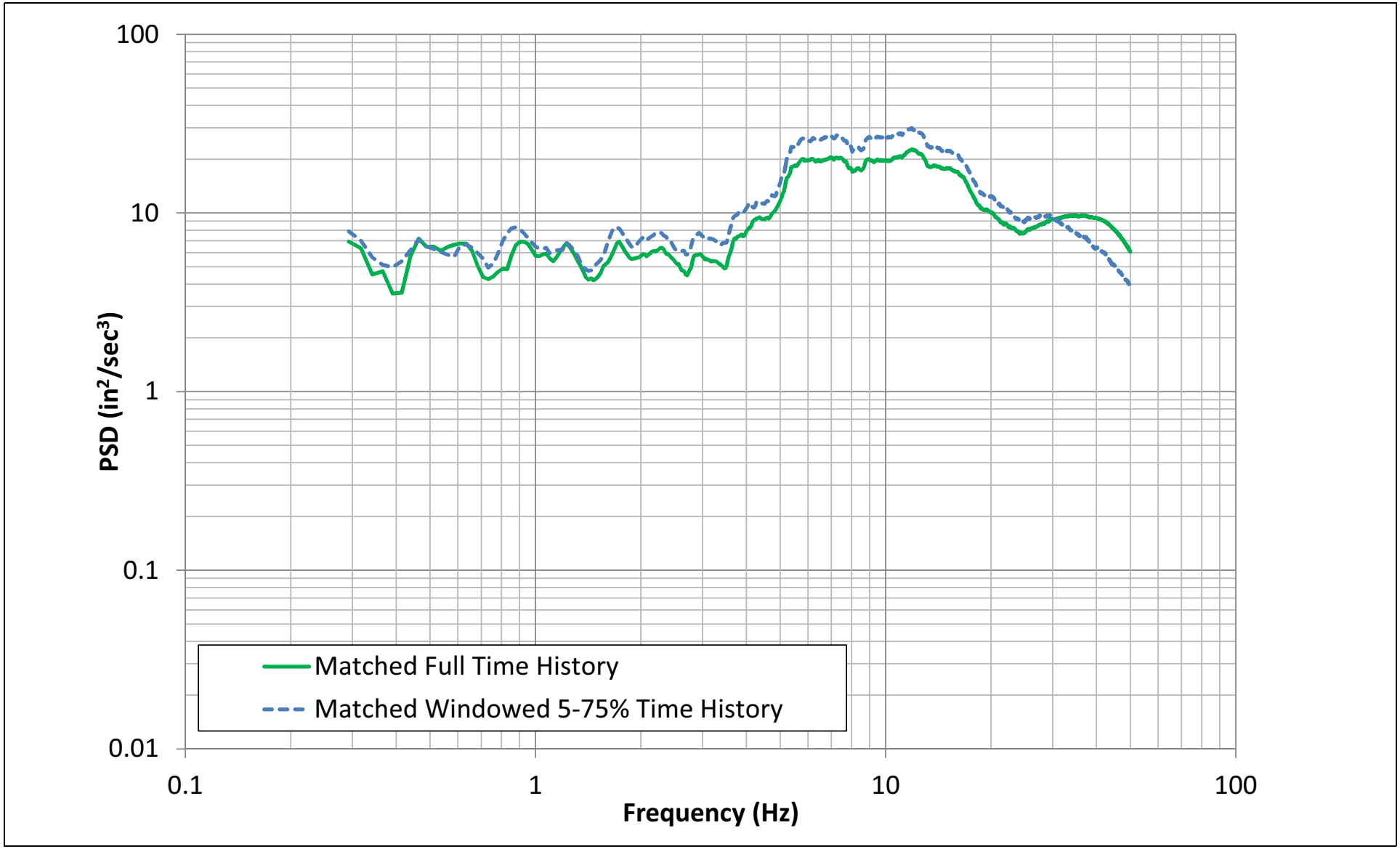

NAPS SUP 3.7-2 **Figure 3.7.1-278 PSD for the H2 Component of the CB Full Profile Spectrum Compatible Acceleration Time History**

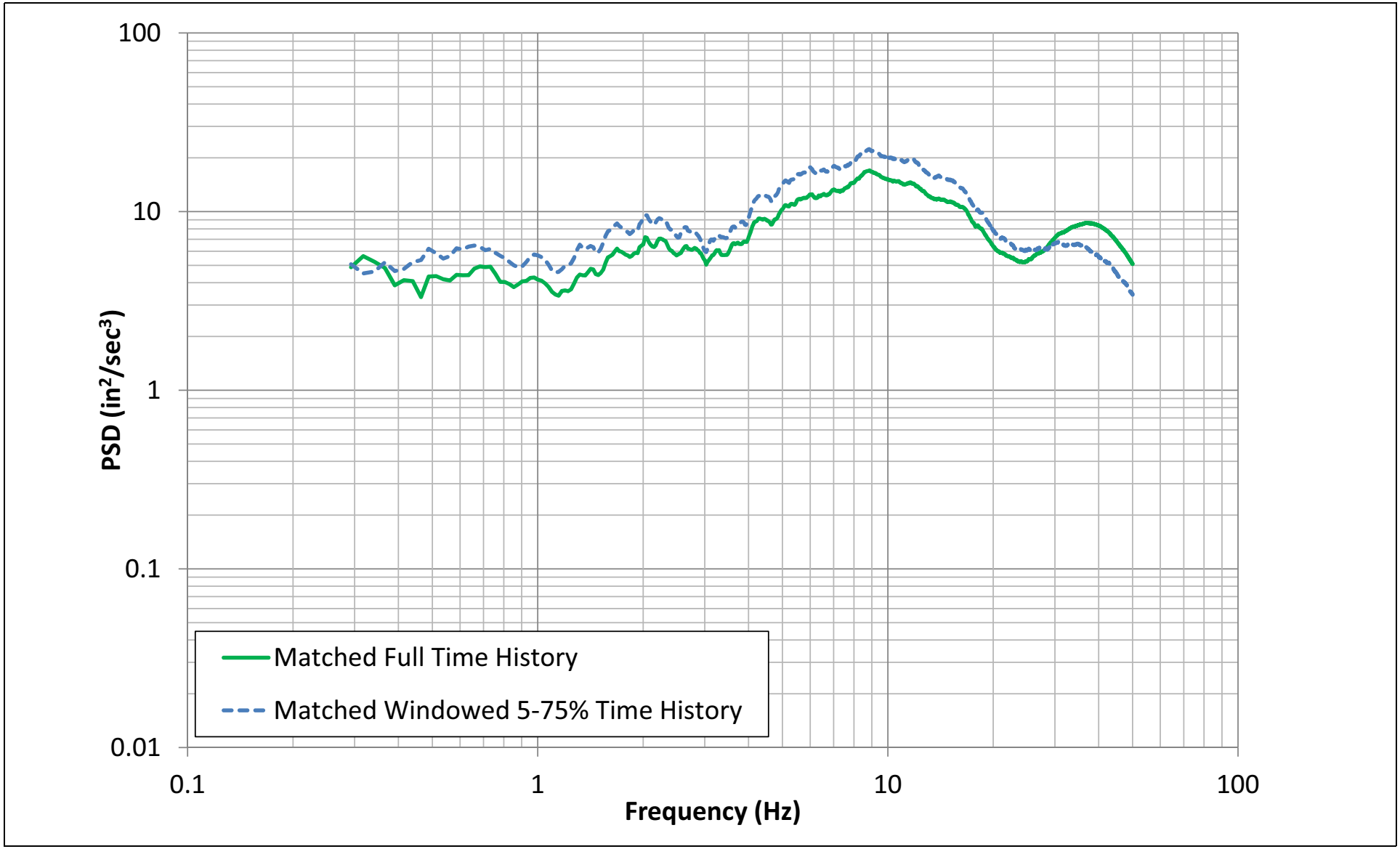

NAPS SUP 3.7-2 **Figure 3.7.1-279 PSD for the UP Component of the CB Full Profile Spectrum Compatible Acceleration Time History**

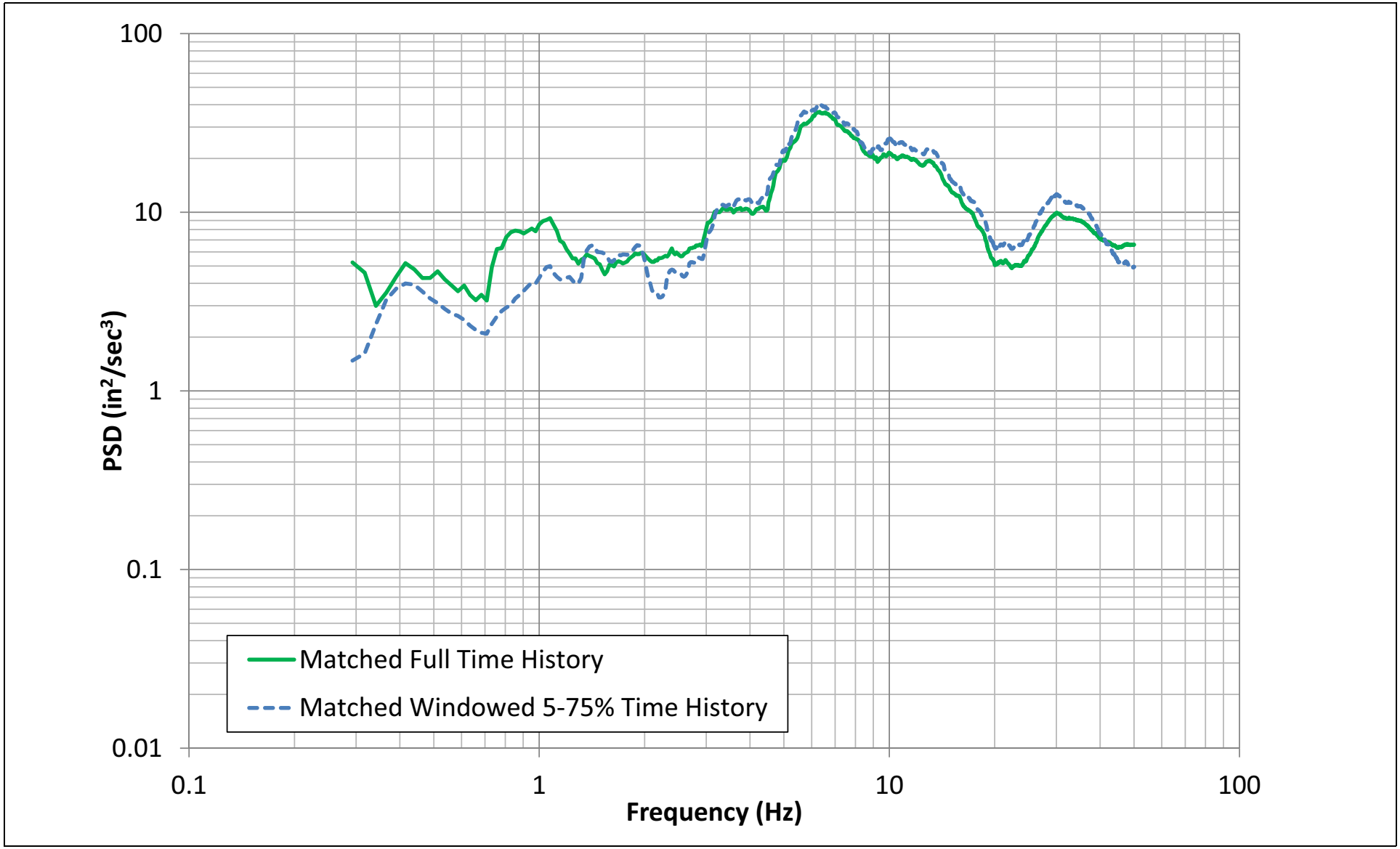

NAPS SUP 3.7-2 **Figure 3.7.1-280 PSD for the H1 Component of the FWSC Spectrum Compatible Acceleration Time History at Elevation 282 ft**

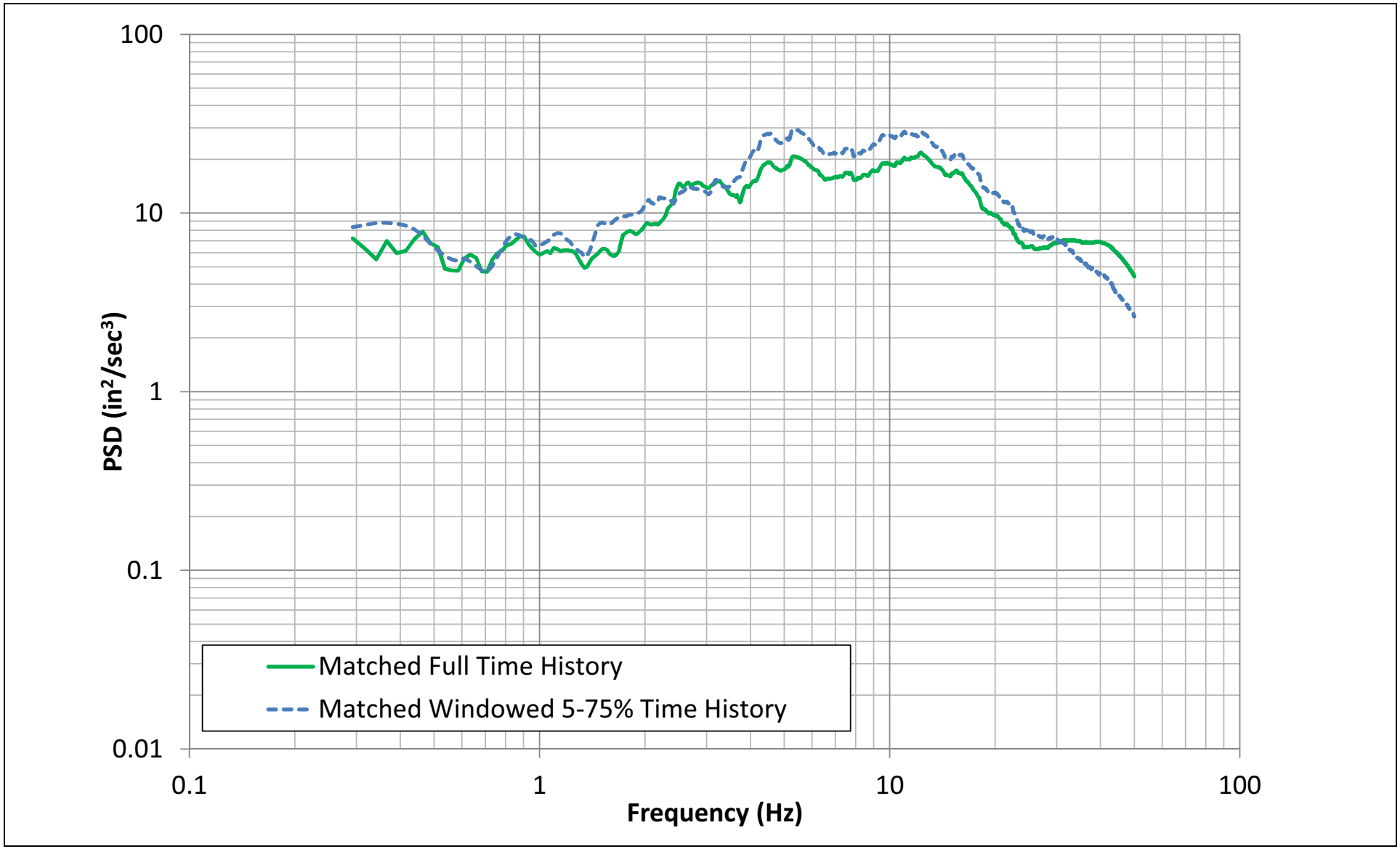

NAPS SUP 3.7-2 **Figure 3.7.1-281 PSD for the H2 Component of the FWSC Spectrum Compatible Acceleration Time History at Elevation 282 ft**

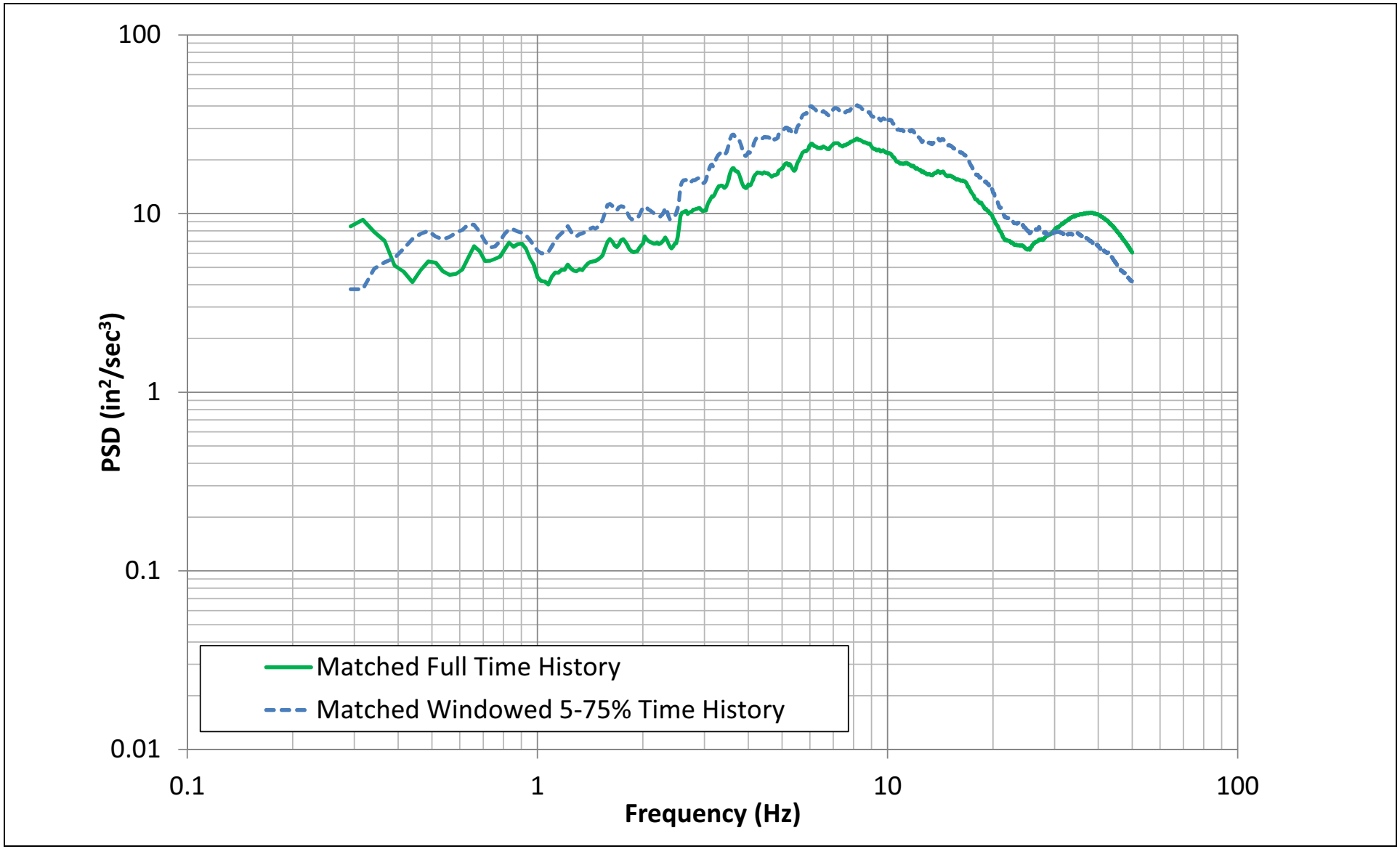

NAPS SUP 3.7-2 **Figure 3.7.1-282 PSD for the UP Component of the FWSC Spectrum Compatible Acceleration Time History at Elevation 282 ft**

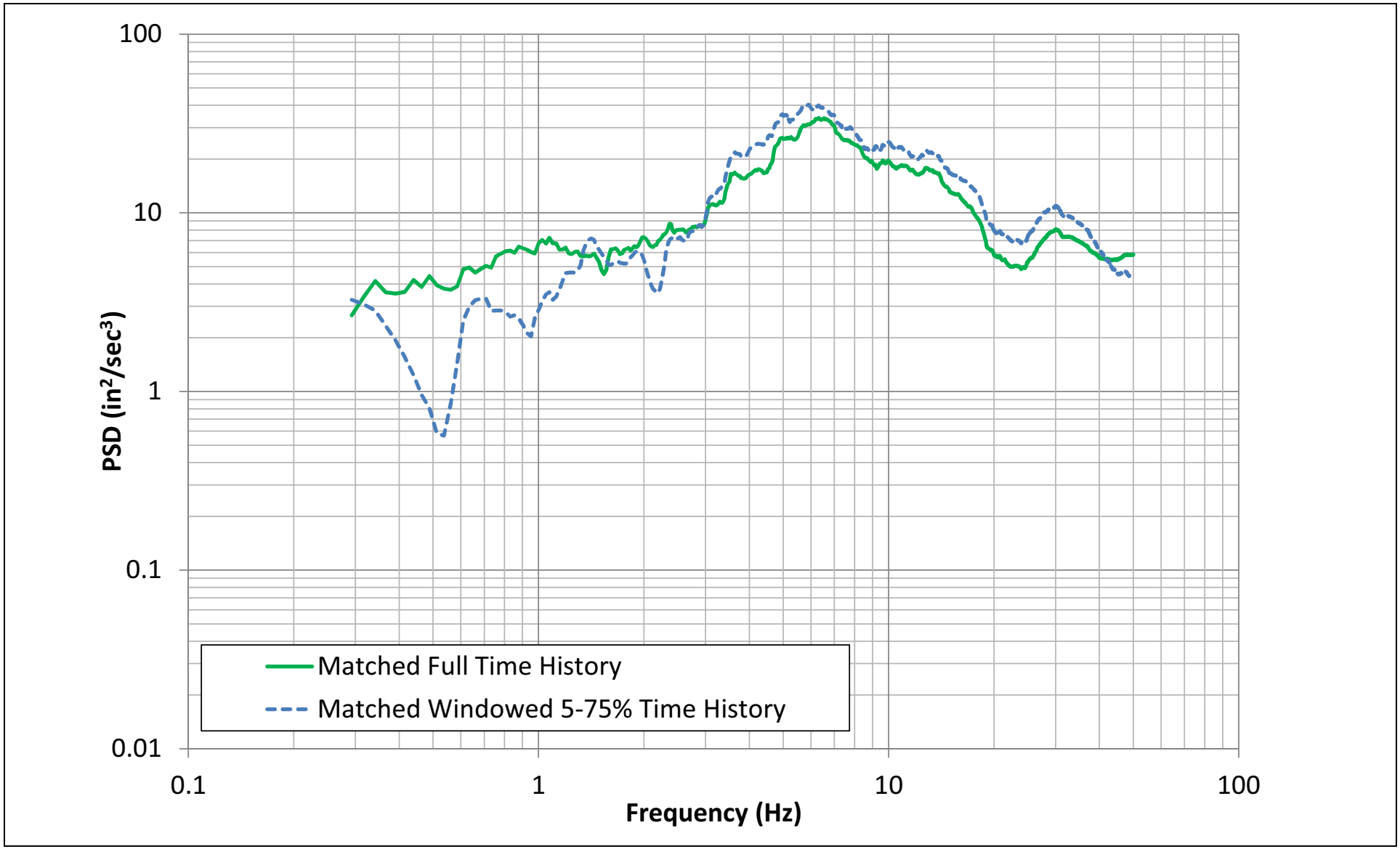

NAPS SUP 3.7-1 **Figure 3.7.1-283 Development of 5% Damped Final Horizontal SSI Input Response Spectrum at Elevation 220 ft for FWSC**

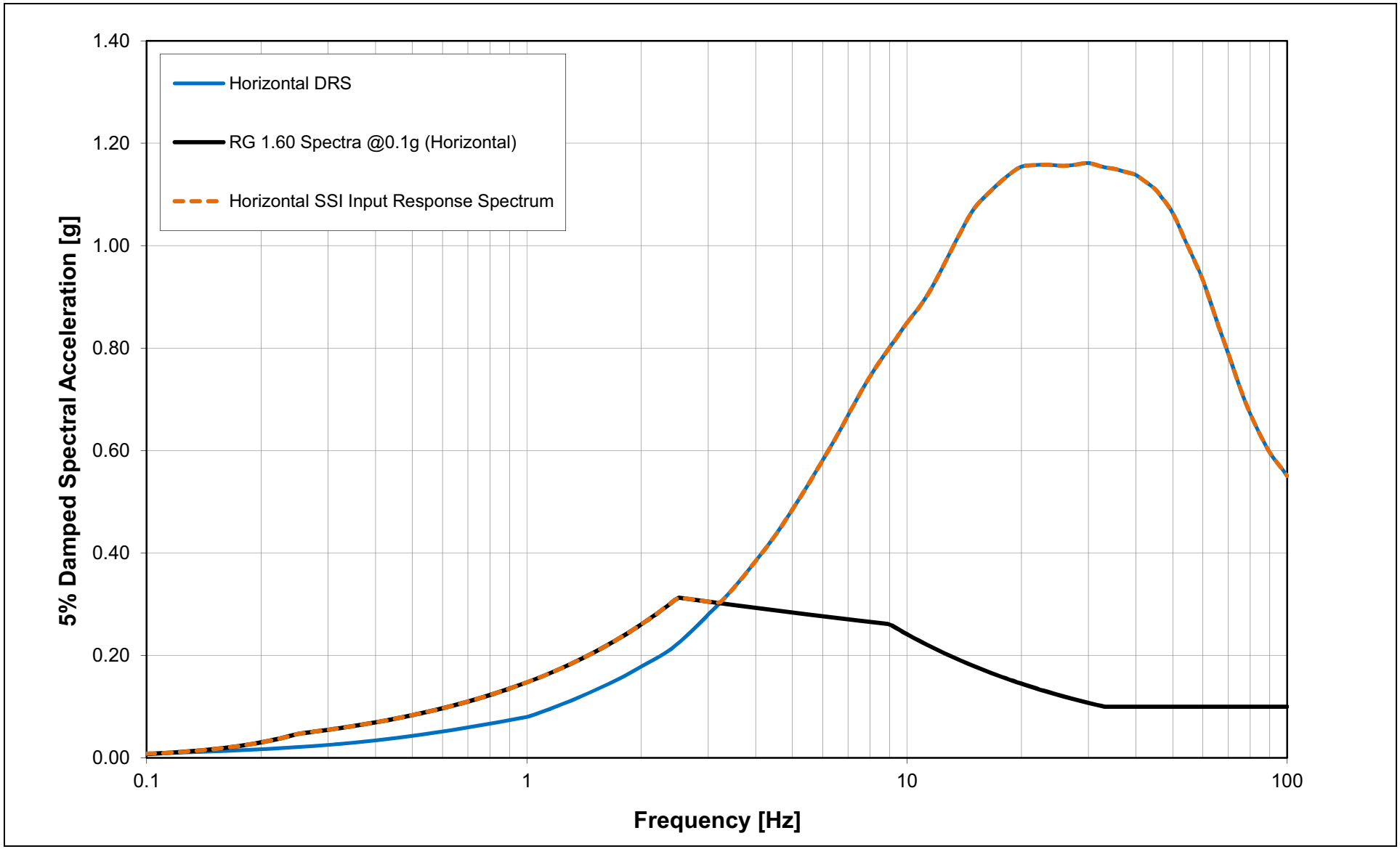

NAPS SUP 3.7-1

Figure 3.7.1-284 Development of 5% Damped Final Vertical SSI Input Response Spectrum at Elevation 220 ft for FWSC

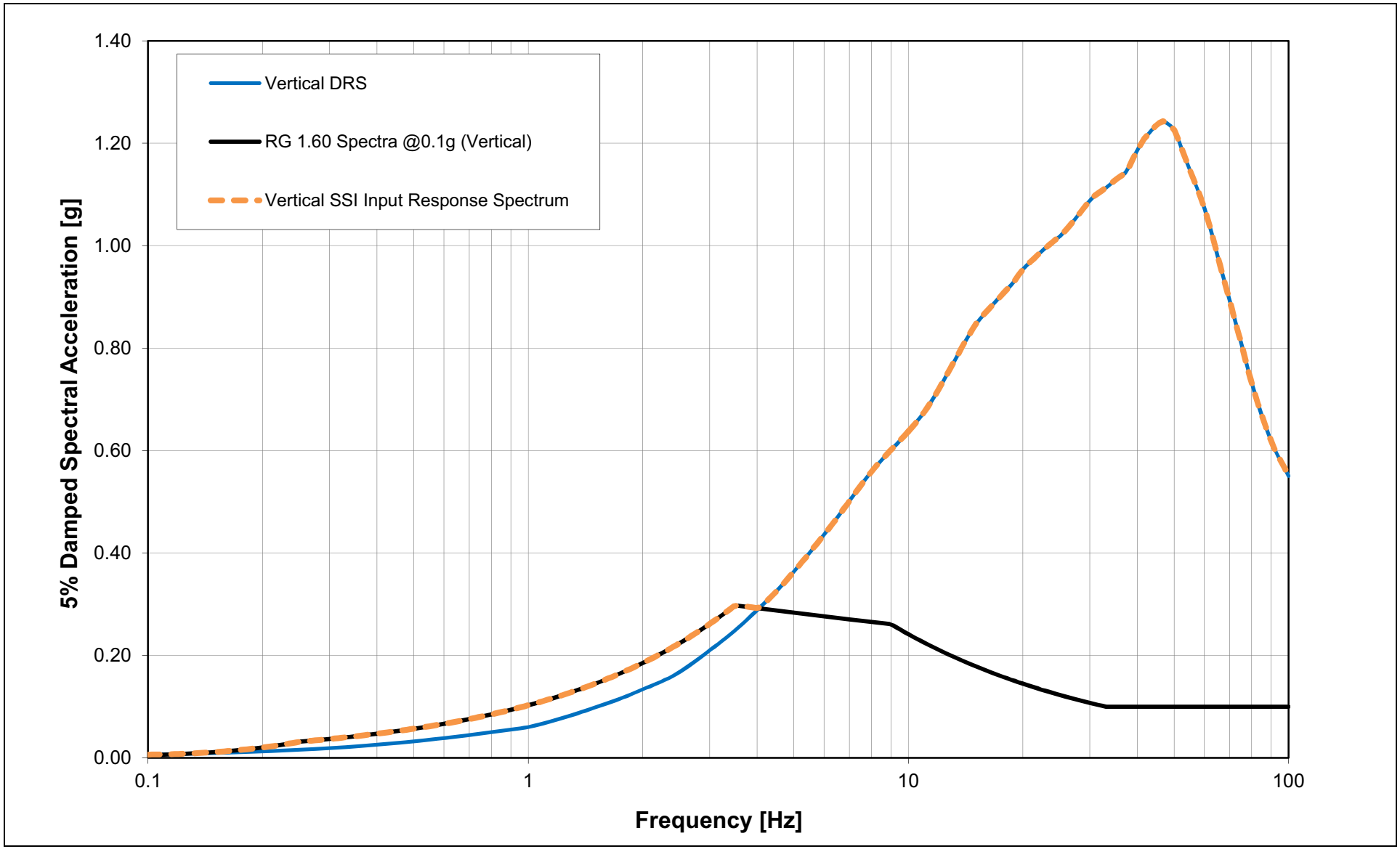

NAPS SUP 3.7-1 **Figure 3.7.1-285 5% Damped Final SSI Input Response Spectra at Elevation 220 ft for FWSC**

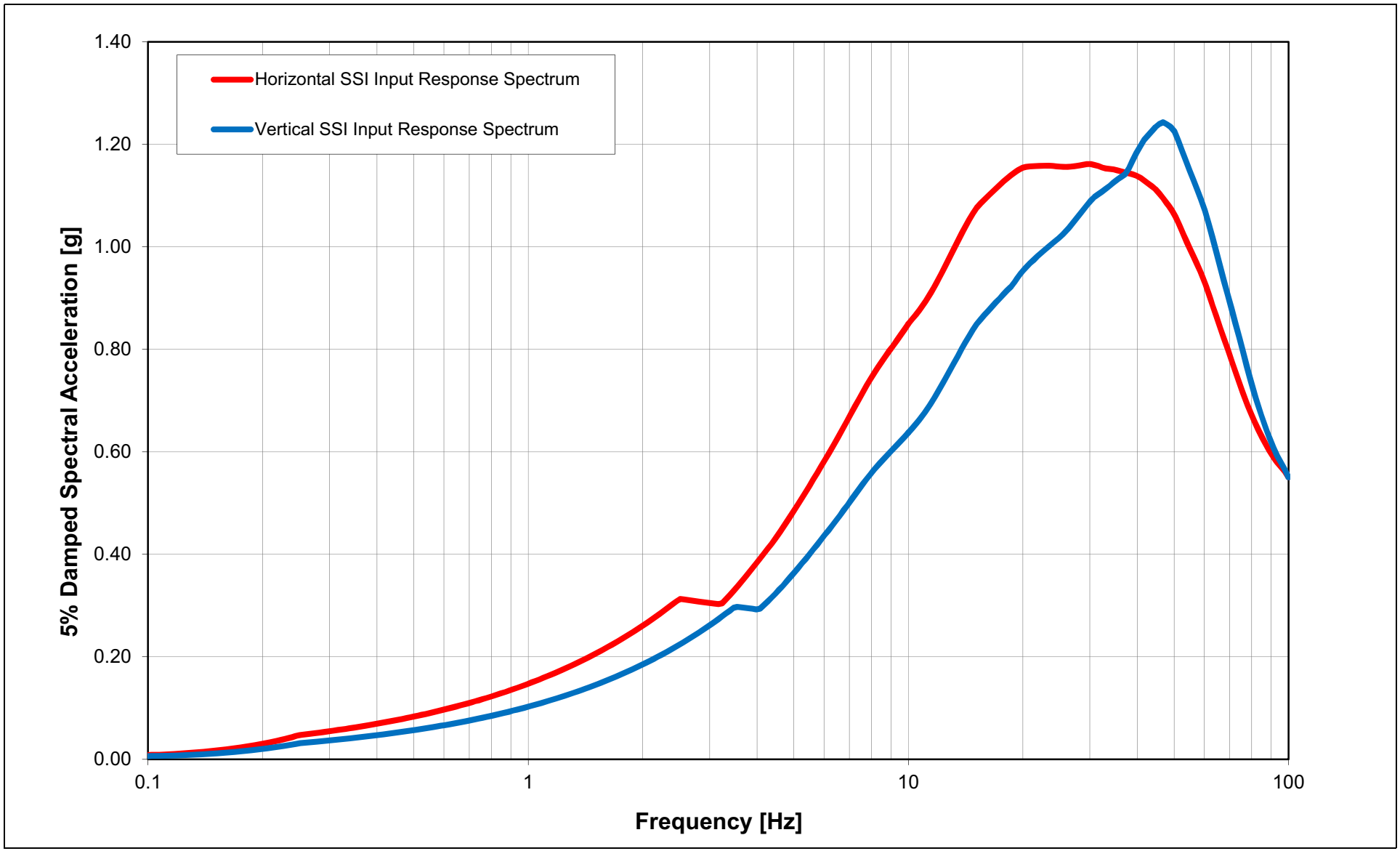

NAPS SUP 3.7-2

Figure 3.7.1-286 Comparison between the Final Scaled Spectrum Compatible Response Spectrum, the Target Spectrum, and Upper and Lower Target Spectrum Bounds for the FWSC, H1 Component at Elevation 220 ft

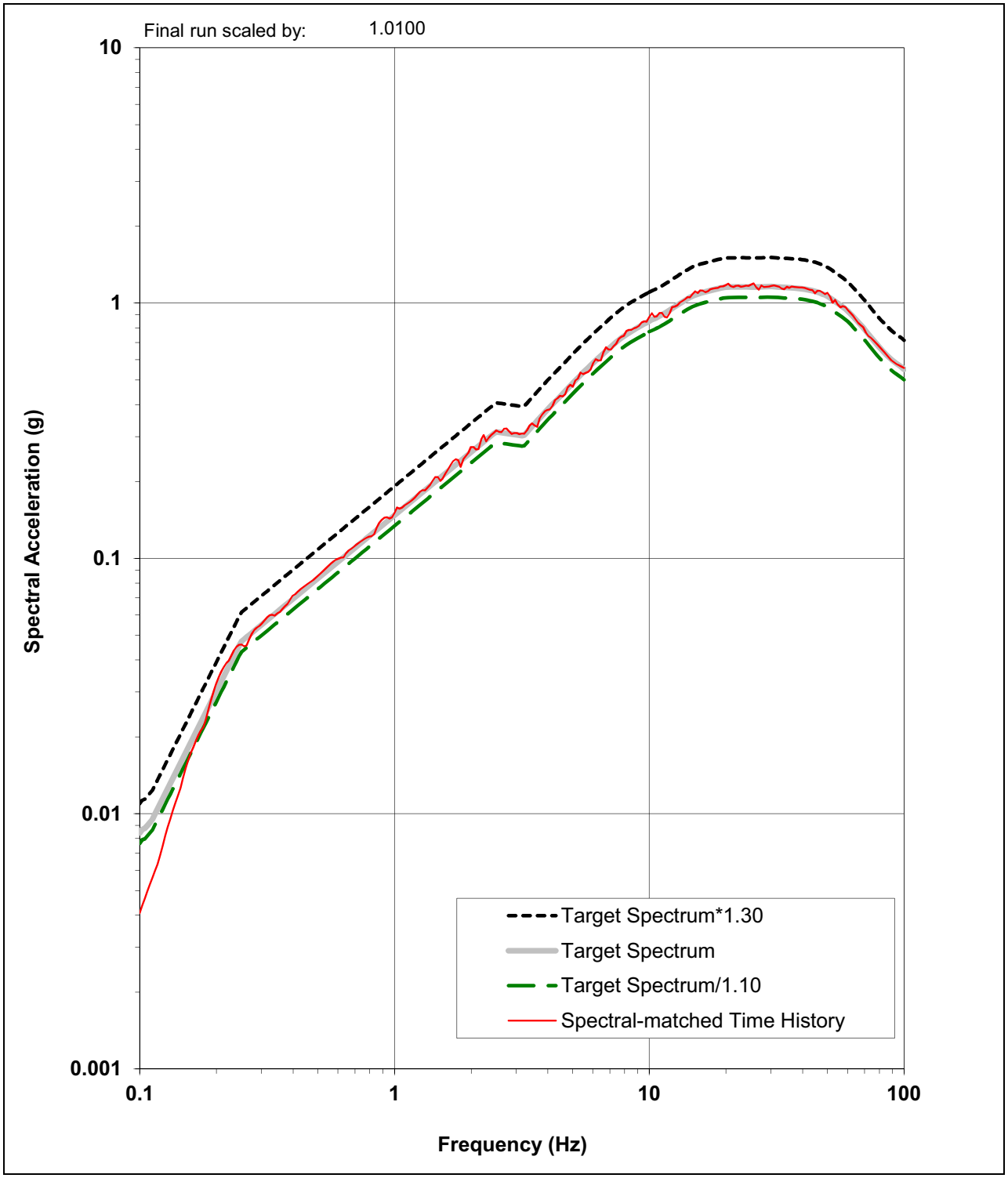

NAPS SUP 3.7-2

Figure 3.7.1-287 Comparison between the Final Scaled Spectrum Compatible Response Spectrum, the Target Spectrum, and Upper and Lower Target Spectrum Bounds for the FWSC, H2 Component at Elevation 220 ft

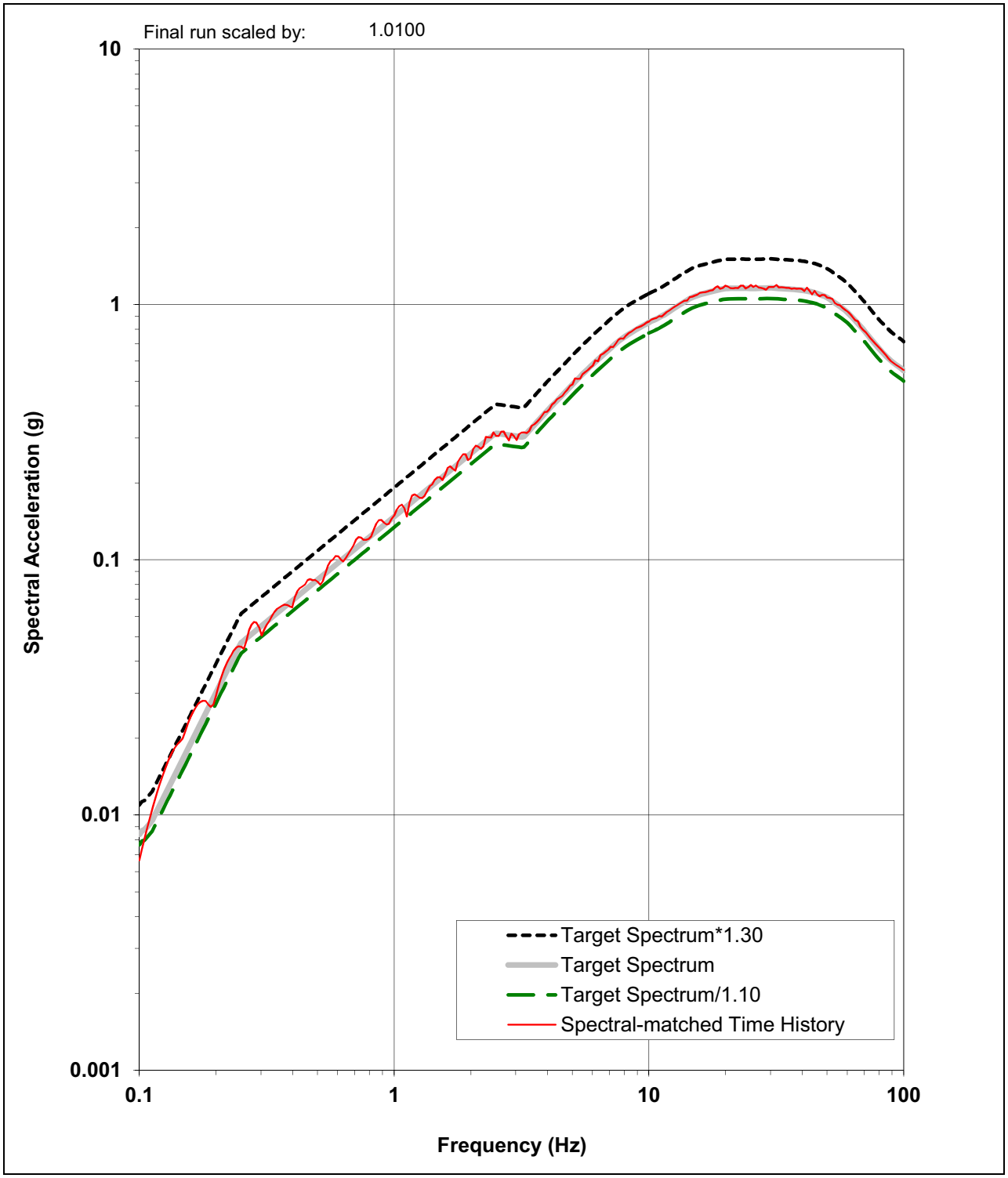

NAPS SUP 3.7-2

Figure 3.7.1-288 Comparison between the Final Scaled Spectrum Compatible Response Spectrum, the Target Spectrum, and Upper and Lower Target Spectrum Bounds for the FWSC, UP Component at Elevation 220 ft

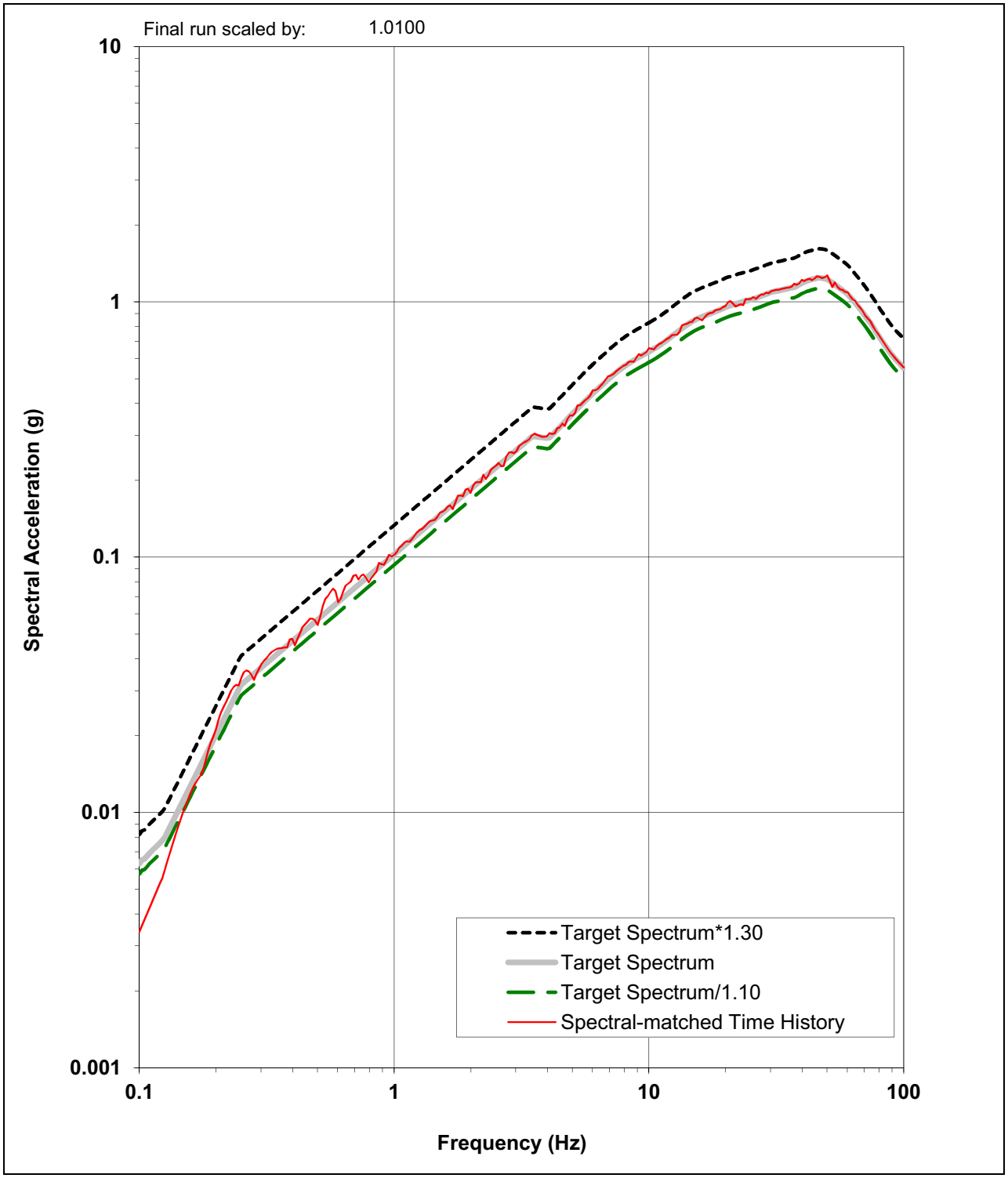

NAPS SUP 3.7-2 **Figure 3.7.1-289 Acceleration, Velocity, and Displacement Spectrally Matched Partial Column Outcrop Time Histories for the FWSC, H1 Component at Elevation 220 ft**

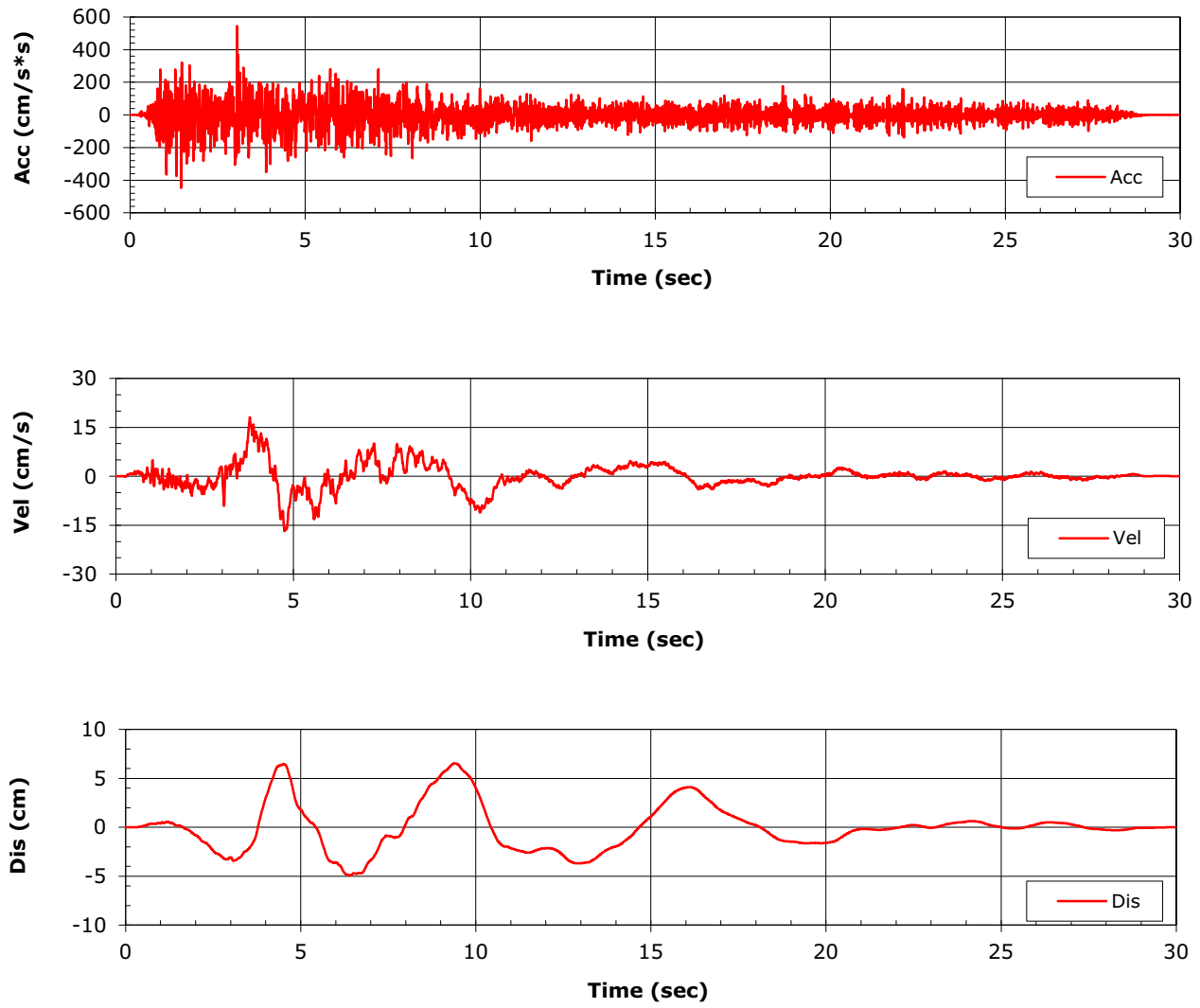

NAPS SUP 3.7-2 **Figure 3.7.1-290 Acceleration, Velocity, and Displacement Spectrally Matched Partial Column Outcrop Time Histories for the FWSC, H2 Component at Elevation 220 ft**

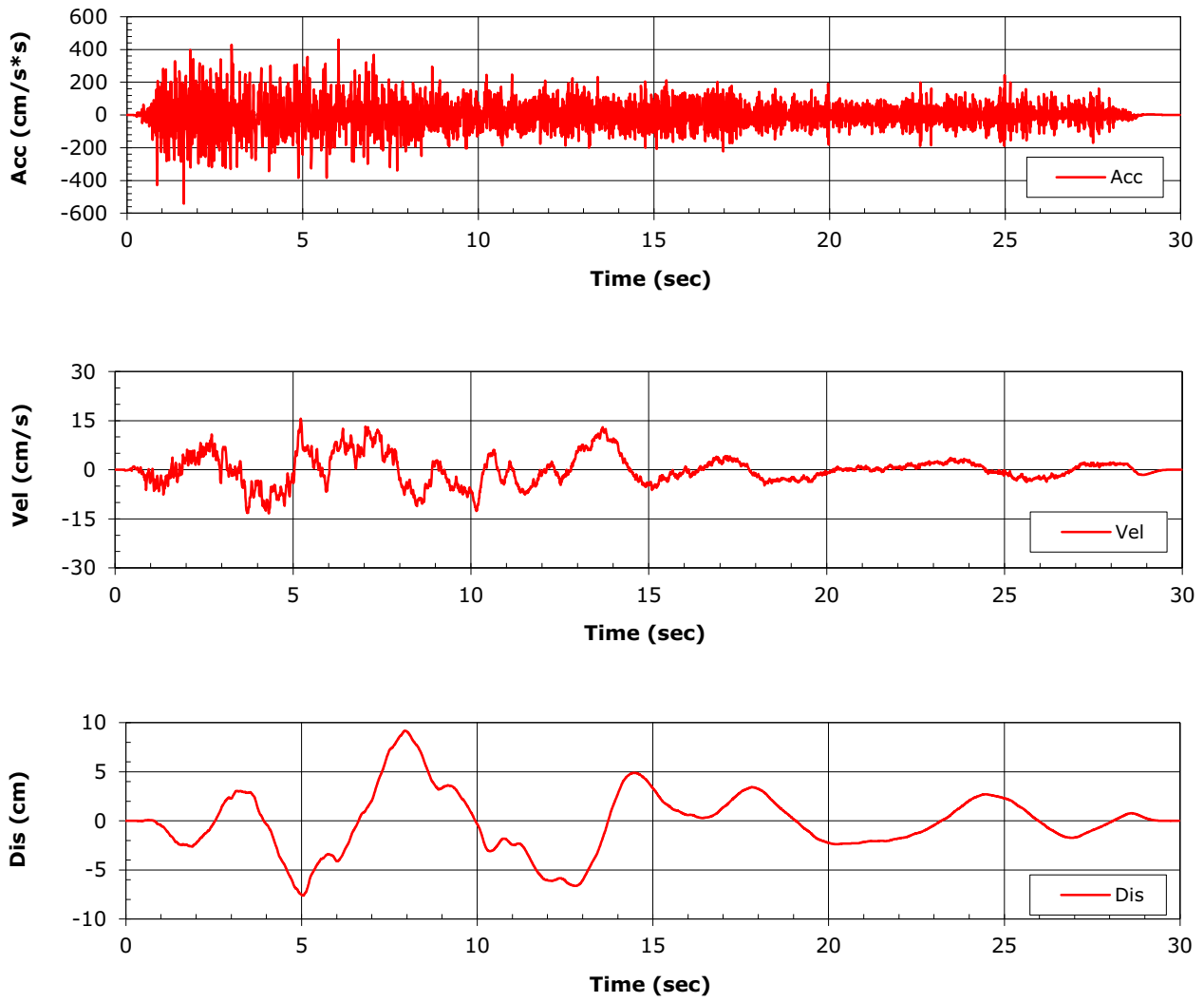

NAPS SUP 3.7-2 **Figure 3.7.1-291 Acceleration, Velocity, and Displacement Spectrally Matched Partial Column Outcrop Time Histories for the FWSC, UP Component at Elevation 220 ft**

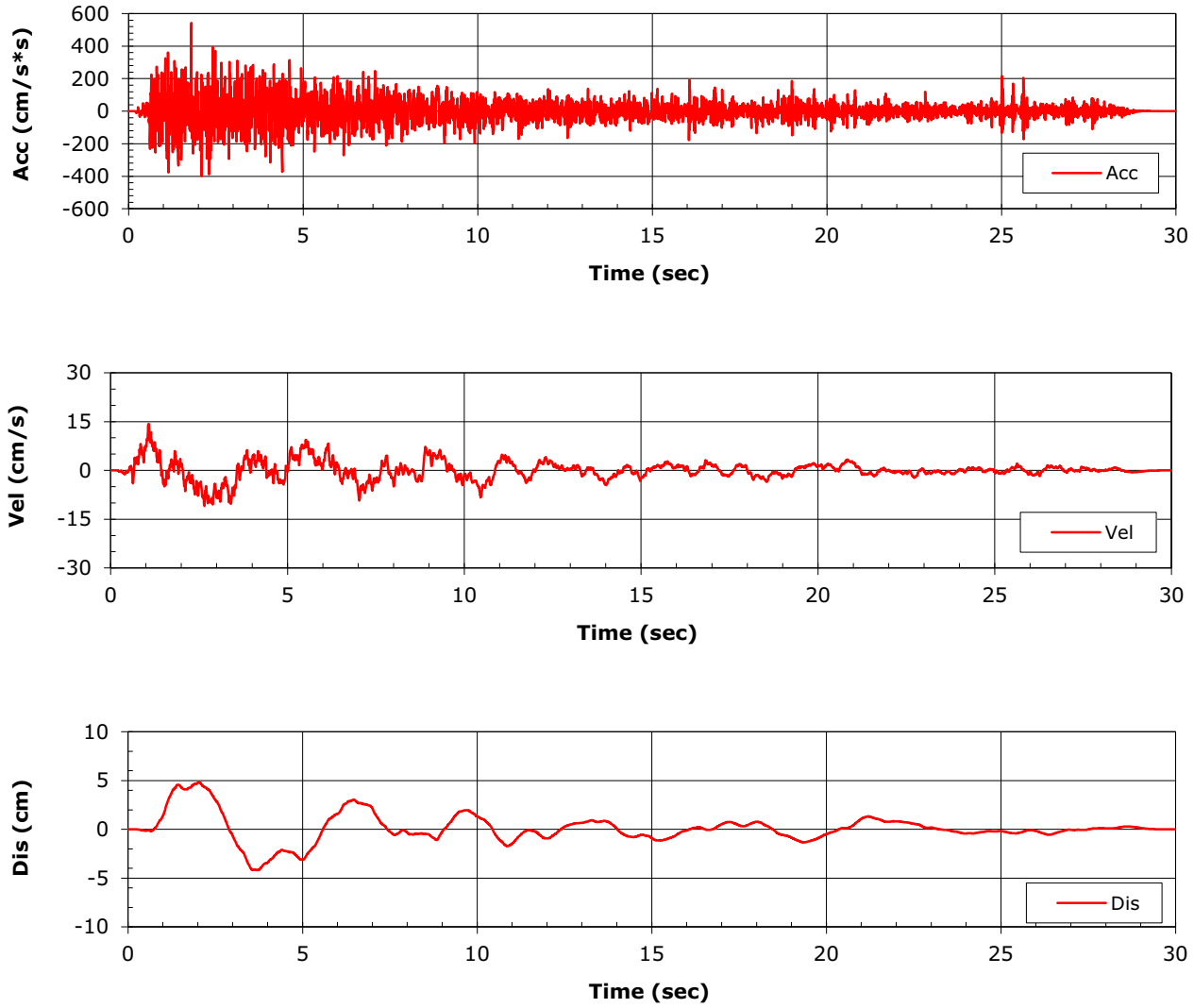

NAPS SUP 3.7-2 **Figure 3.7.1-292 PSD for the H1 Component of the FWSC Spectrum Compatible Acceleration Time History at Elevation 220 ft**

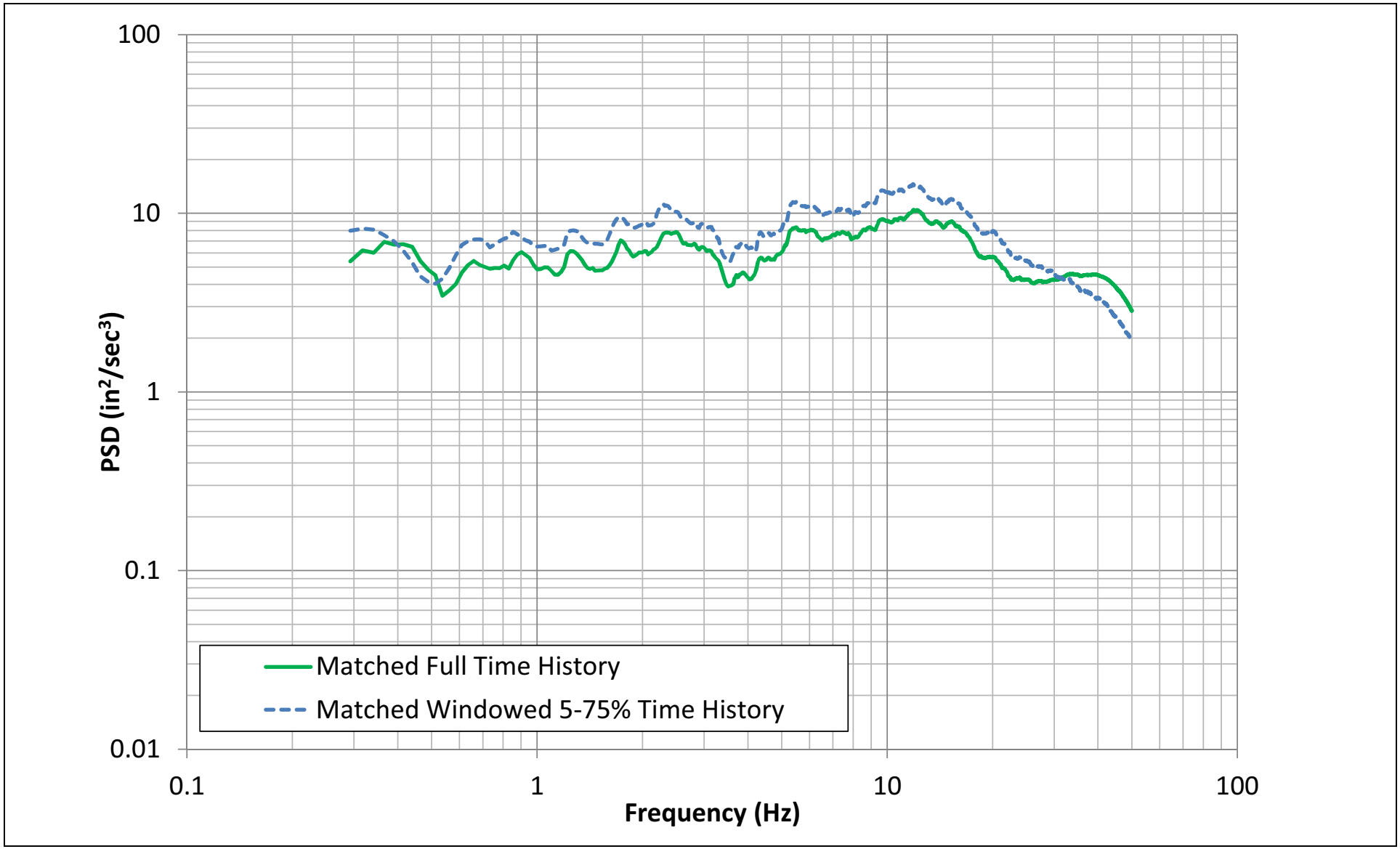

NAPS SUP 3.7-2 **Figure 3.7.1-293 PSD for the H2 Component of the FWSC Spectrum Compatible Acceleration Time History at Elevation 220 ft**

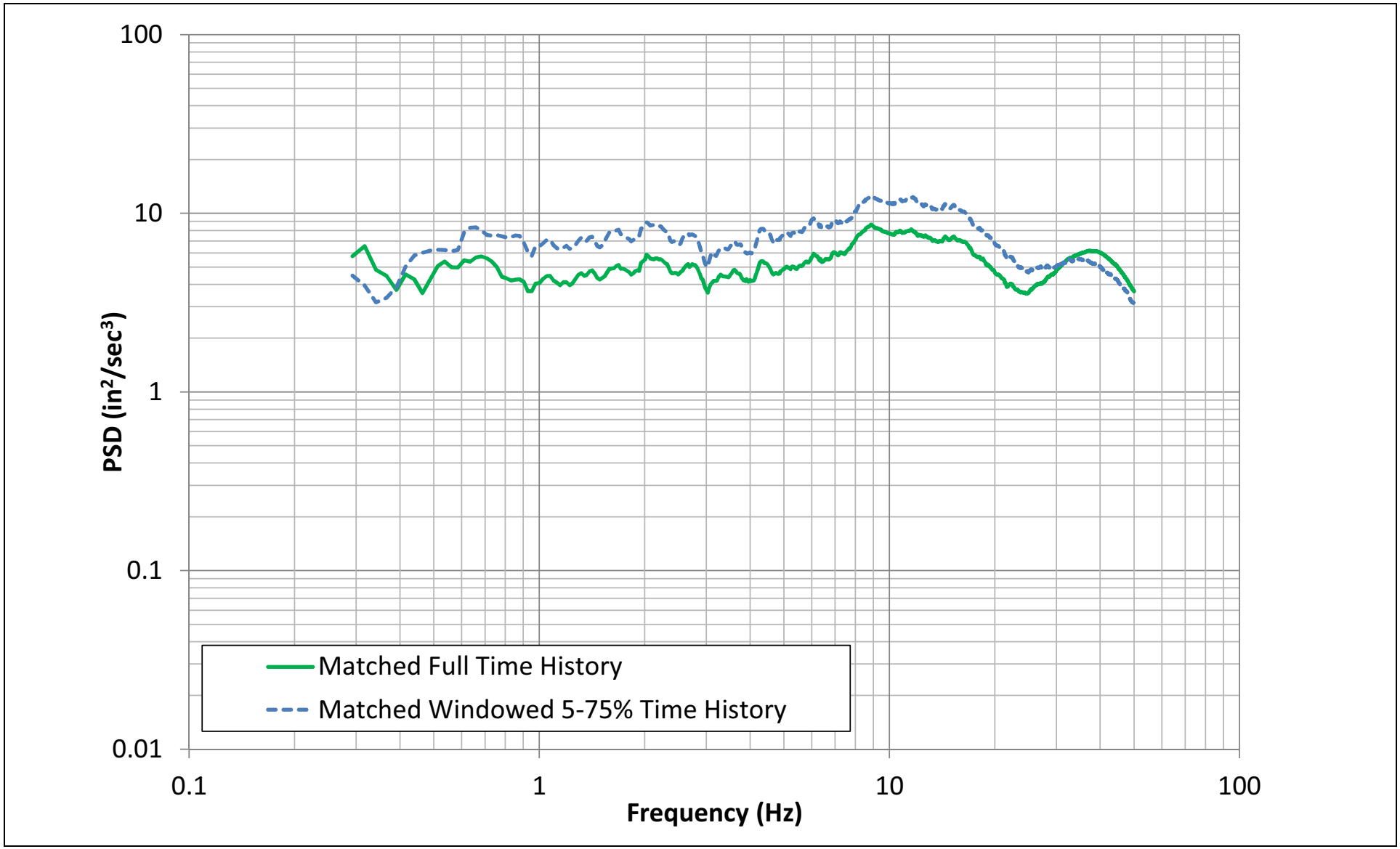

NAPS SUP 3.7-2 **Figure 3.7.1-294 PSD for the UP Component of the FWSC Spectrum Compatible Acceleration Time History at Elevation 220 ft**

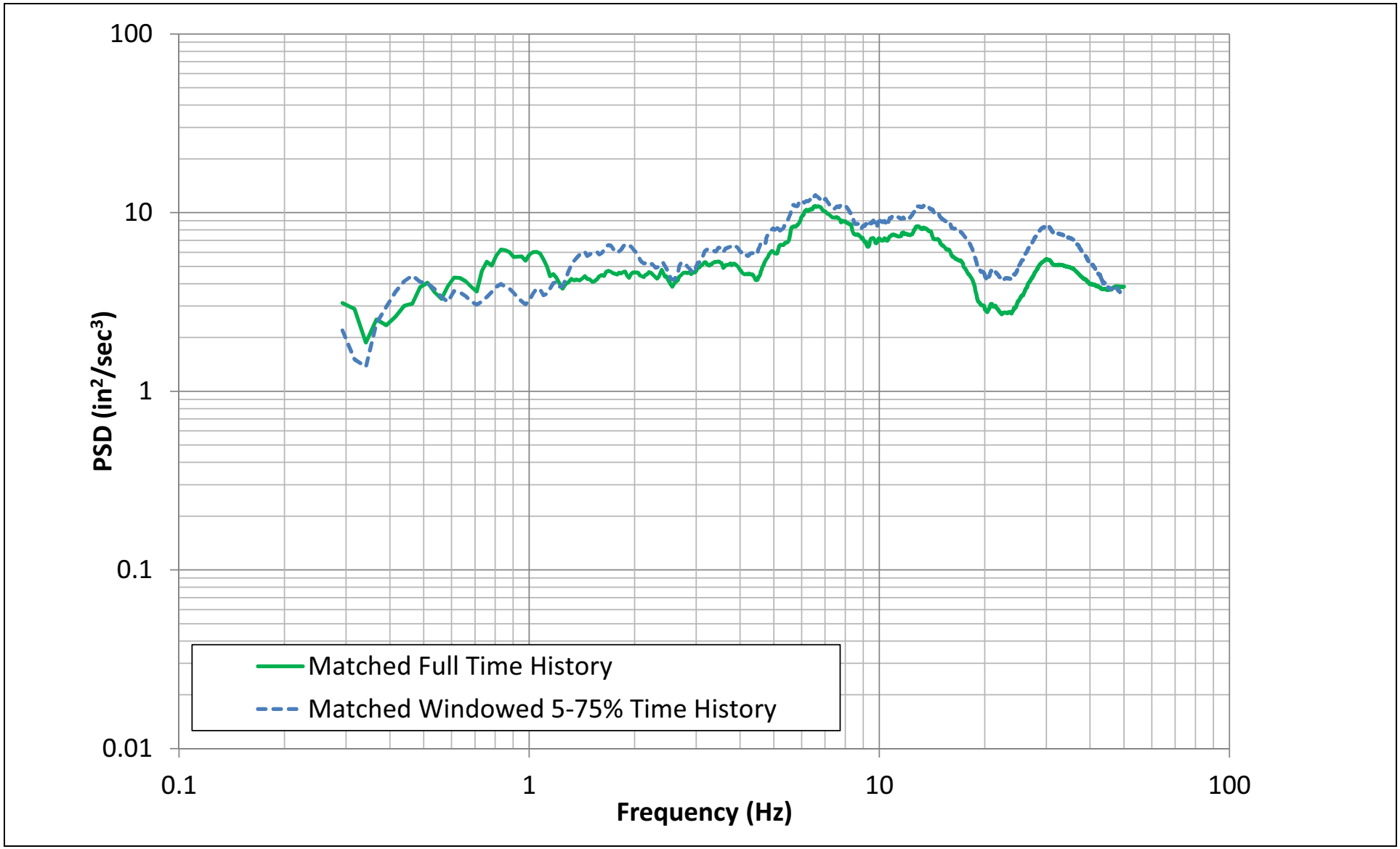

Variance: NAPS ESP VAR 2.0-3 – Hydraulic Gradient

Request

This is a request to use the Unit 3 hydraulic gradient value provided in FSAR Section 2.4.12.1.2 rather than the corresponding ESP value in FSER Supplement 1, Appendix A and in SSAR Table 1.9-1. The Unit 3 value does not fall within (is larger than) the ESP and SSAR value.

SSAR Section 2.4.12.1.2 states that there is a hydraulic gradient toward Lake Anna of about 3 ft per 100 ft. The corresponding Unit 3 hydraulic gradient in FSAR Section 2.4.12.1.2 is calculated to be 5 ft per 100 ft.

The variance in hydraulic gradient results from the use of additional groundwater data collected from the Unit 3 subsurface investigation.

Justification

The variance in hydraulic gradient is acceptable because compliance with 10 CFR 20 is demonstrated in FSAR Section 2.4.13 with the use of the higher hydraulic gradient of 5 ft per 100 ft to evaluate radionuclide concentrations and associated doses as a result of a postulated accidental release of liquid effluents in the groundwater pathways.

Variance: NAPS ESP VAR 2.0-4 – Vibratory Ground Motion

Request

This is a request to use the Unit 3 horizontal and vertical spectral acceleration (g) values for the ground motion response spectra (GMRS) at the top of a hypothetical outcrop under the reactor building/fuel building (RB/FB) common foundation (Elevation 224 ft NAVD88 (224.86 ft NGVD29)), rather than hypothetical outcrop control point safe shutdown earthquake (SSE) spectrum at the top of Zone III-IV (Elevation 249.14 ft NAVD88 (250 ft NGVD29)), as presented in the ESP and SSAR. The Unit 3 values do not fall within (are larger than) the ESP and SSAR values at ~~almost all~~ some frequencies.

The Unit 3 GMRS horizontal and vertical spectra at Elevation 224 ft NAVD88 (224.86 ft NGVD29) are plotted in FSAR Figure 2.5.2-313. The corresponding ESP spectra at Elevation 249.14 ft NAVD88 (250 ft NGVD29) are provided in ESP FSER NUREG-1835, Supplement 1, Appendix A, Figure 2, and in SSAR Figure 2.5-48A. FSAR Figure 2.0-206 and Table 2.0-202 compare the Unit 3 and ESP horizontal response spectra. FSAR Figure 2.0-207 and Table 2.0-203 compare the Unit 3 and ESP vertical response spectra. There are 38 frequencies used for the Unit 3 spectra, ~~while 21 frequencies were used for the ESP spectra~~ however, the comparison with the ESP spectra is shown for the 21 frequencies which were used for the ESP spectra.

Besides the difference in elevation at which the SSE and GMRS are defined in the SSAR and FSAR, there are additional differences in models, data, and methodologies that contribute to the differences of the resulting SSE and GMRS.

A significant change in the FSAR is the replacement of the starting EPRI-SOG models and databases used in the SSAR (SSAR Section 2.5 References 1, 115, 120, and 121) by the starting models and databases of the Central and Eastern US Seismic Source Characterization (CEUS SSC) report by EPRI et al. (FSAR Reference 2.5-223). The new CEUS SSC models and databases included a new earthquake catalog, different characterization of the seismic sources, and state-of-the-knowledge evaluation of maximum magnitudes.

Unlike the EPRI-SOG earthquake catalog, the CEUS SSC earthquake catalog does not include a specific tabulation of Modified Mercalli intensities (MMI). Measures of MMI were considered in the development of the CEUS SSC earthquake catalog in estimating a uniform measure of magnitude; however, their exclusion in the final catalog tabulation is reflected in the earthquake tabulation in FSAR Table 2.5.2-202.

~~While the EPRI (2004) model of ground motion prediction equations (FSAR Reference 2.5-224) was used to determine median ground motions for both the SSAR and the FSAR, and the EPRI (2004) model of ground motion aleatory uncertainties was used in the PSHA for the SSAR, the model of ground motion aleatory uncertainties used for the FSAR was taken from EPRI (2006) (FSAR Reference 2.5-225).~~

While the EPRI (2004) model of prediction equations for median ground motions and their aleatory uncertainties (FSAR Reference 2.5-224) was used in the PSHA for the SSAR, the EPRI (2013) model of prediction equations for median ground motions and their aleatory uncertainties (FSAR Reference 2.5-407) was used in the PSHA for the FSAR.

The procedures by which the rock ground motions are developed and used as input to the site response analyses in the SSAR and FSAR are different in two notable ways because the FSAR follows RG 1.208; the SSAR was based on earlier guidance. First, in the SSAR, the hard rock SSE was developed as a hybrid envelope of two methods: a modified reference probability approach from then-active RG 1.165 and a “pre-RG 1.208” performance-based approach. In the FSAR, only the published RG 1.208 performance-based approach was used. Second, in the SSAR, the rock motions used for input to the site response were high frequency (HF) and low frequency (LF) components of the hard rock SSE. In the FSAR, the performance-based methodology in RG 1.208 was applied not to rock motions (as in the SSAR), but to the GMRS-horizon motions resulting from the site response analyses. That is, for the FSAR, the HF and LF rock motions corresponding to uniform hazard response spectra (UHRS) at mean annual frequencies (MAFE) of 10^{-4} and 10^{-5} were used as rock motion inputs to the site response analyses, resulting in GMRS-horizon UHRS at MAFEs of 10^{-4} and 10^{-5}. The RG 1.208 performance-based methodology is then applied to the GMRS-horizon UHRS to obtain the GMRS ground motions. Another input to the site response

analyses was the additional FSAR data from the Unit 3 subsurface investigation, which provided the seismic wave transmission characteristics of the materials specifically applied to the Unit 3 Seismic Category I RB/FB.

In the FSAR's development of the Unit 3 horizontal spectral acceleration (g) values for the GMRS at a hypothetical outcrop at Elevation 224 ft NAVD88 (224.86 ft NGVD29), the site response analysis program P-SHAKE was used, rather than SHAKE2000, which was used in the SSAR evaluations. Operating exclusively in the frequency domain, P-SHAKE uses power spectral density functions derived from input rock response spectra, in lieu of earthquake time histories matched to those same rock response spectra, and then used as input to SHAKE2000, as was the approach used in the SSAR analysis. Simulating the effect of numerous input spectrally-matched time histories, the methodology used in P-SHAKE derives a more robust consideration of the variability of input ground motions. The resulting smooth output ground motions from P-SHAKE do not require a post-process fitting function, as was used to smooth the ground motions for the top of Zone III-IV SSE in the SSAR analysis.

In the SSAR, the subsurface soil/rock column characterization was represented by 50 simulated profiles, while for the FSAR, 60 simulated profiles were used.

This variance also includes moving the definition of the operating basis earthquake (OBE) from SSAR Section 2.5.2 to FSAR Section 3.7 in order to facilitate compatibility with OBE instrumentation that records free-field ground motions at grade.

Justification

The variance in the GMRS control point location is justified because its location at a hypothetical outcrop under the RB/FB foundation is representative of the Unit 3 site below the foundations for the Seismic Category I structures in the power block area. This location is also consistent with NUREG-0800, SRP 2.5.2, which specifies that the GMRS be defined on an outcrop or a hypothetical outcrop that will exist after excavation.

The variance in the horizontal and vertical spectral acceleration values results from and is justified not only by the change in control point location but also from application of updated methodology and data, consistent with current NRC guidance. The GMRS was derived using the performance-based approach endorsed in RG 1.208, and the new CEUS SSC models and databases. To evaluate the potential significance of any reinterpretation of past earthquakes and to consider the impact of more recent seismicity, including the 2011 **M** 5.8 Mineral, Virginia earthquake, the CEUS SSC earthquake catalog was reviewed and updated for the period 2009 through mid-December 2011. Therefore, by using RG 1.208 and updating the CEUS, the Unit 3 GMRS is acceptable.

EPRI (2013) reviewed the model of prediction equations for median ground motions given in EPRI (2004) and the subsequently updated aleatory uncertainties given in EPRI (2006) (FSAR Reference 2.5-225). EPRI (2013), which presented an updated version of the EPRI (2004, 2006)

ground motion models, was endorsed by the NRC (2013) (FSAR Reference 2.5-408) as an "acceptable ground motion attenuation model for use by CEUS plants in developing plant-specific ground motion response spectra until such time as the NGA-East project is completed and has been reviewed and approved by NRC staff." As of mid-2014, the NGA-East project, which is a SSHAC Level 3 study on a new CEUS ground motion model, has not been completed.

The number of frequencies was increased to 38 frequencies based on the minimum number of points specified in RG 1.206 and RG 1.208. The SSAR, which presents 21 points, was written before these documents were issued. Therefore, the FSAR was updated to conform to the existing guidance.

The specification of OBE in SSAR Section 2.5.2.7 is moved to FSAR Section 3.7 because neither SRP 2.5.2 nor the DCD requests the OBE information to be described in FSAR Section 2.5.2. Further, given that OBE instrumentation is likely to be at a surface location, the definition of the OBE ground motions should consider the site response of multiple possible surface or at grade locations, which is not assessed in FSAR Section 2.5.2, but is in FSAR Section 3.7. Therefore, the OBE is defined in FSAR Section 3.7.

Variance: NAPS ESP VAR 2.0-5 – Distribution Coefficients (K_d)

Request

This is a request to use the Unit 3 distribution coefficient (K_d) values provided in FSAR Table 2.4-206 rather than the corresponding values in SSAR Table 1.9-1 and SSAR Table 2.4-20. Some of the values provided in FSAR Table 2.4-206 do not fall within (are smaller than) the SSAR values and therefore would predict higher doses than the K_d values in the SSAR.

A variance for several K_d values results from using the minimum site-specific K_d values from FSAR Table 2.4-207 for estimating the radionuclide migration to surface waters via groundwater pathways. The SSAR K_d values were assigned using literature values. The measured Unit 3 K_d values were obtained by laboratory testing and are provided in FSAR Table 2.4-207.

Justification

The variance in K_d values is acceptable because compliance with 10 CFR 20 is demonstrated in FSAR Section 2.4.13 with the use of the minimum site-specific K_d values to evaluate radionuclide concentrations and associated doses as a result of a postulated accident release of liquid effluents in the groundwater pathways.